1995

Genome Organization, Replication And Movement Of Foxtail Mosaic Virus

Michele Rouleau

GENOME ORGANIZATION, REPLICATION AND MOVEMENT OF FOXTAIL MOSAIC VIRUS

by

Michèle Rouleau

Department of Biochemistry

Submitted in partial fulfilment
of the requirements for the degree of
Doctor of Philosophy

Faculty of Graduate Studies
The University of Western Ontario
London, Ontario
September 1994

ISBN 0-315-99276-X

ABSTRACT

Foxtail mosaic virus (FMV) is a member of the potexvirus family which infects primarily monocotyledonous plants. Its flexuous filamentous particles are 500 nm long and consist of a messenger sense RNA encapsidated by a single type of coat protein. We have determined the nucleotide sequence of the FMV gRNA as well as the organization of its coding sequences. The gRNA is 6151 nucleotides long and contains five major open reading frames (ORF). The amino acid sequences of the putative proteins are closely related to homologous proteins of other sequenced potexviruses.

A procedure for the partial purification of the RNA-dependent RNA polymerase (RdRp) complex of FMV from infected leaves of *Chenopodium quinoa* was established. The products synthesized *in vitro* by the enzyme were double-stranded RNA molecules. The RdRp preparations obtained could copy RNA templates endogenous to the preparation but were unable to copy added RNA templates. Moreover, potexviral gRNAs specifically inhibited the RNA synthesis activity on endogenous templates. The regions of the genome responsible for the inhibition were identified. Both 5' and 3' terminal regions of the viral genome were necessary to interfere with RNA synthesis suggesting that this inhibition resulted from a competition for the binding of component(s) of the RdRp complex.

The proteins encoded by ORFs 2, 3, and 4 as well as the coat protein (encoded by ORF5) are believed to play some role in the cell-to-cell movement of potexviruses. We have used a bacterial expression system to produce and purify p26, the protein encoded by ORF2 of FMV, and have determined some *in vitro* properties of p26. It is

an ATP, CTP and RNA binding protein with apparent ATPase activity. An analysis of infected *C. quinoa* leaves by immunogold electron microscopy using an anti-serum produced against p26 revealed that it is exclusively associated with cytoplasmic inclusions adjacent to aggregates of virus particles. These results suggest that p26 could be involved in the processing of viral RNA or particles prior to their transport rather than being directly involved in their translocation through plasmodesmata.

The distribution of the coat protein in infected *C. quinoa* was also investigated by immunocytochemistry. Most of the coat protein was localized in the cytoplasm, polymerized into viral particles, but significant amounts were also associated with plasmodesmata. This suggests that the coat protein plays a role in the cell-to-cell movement of potexviruses.

ACKNOWLEDGEMENTS

None of this work could have been done alone. I would like to express my gratitude to all of those who have made this project possible, through their technical and/or moral support.

First and foremost, I would like to sincerely thank my supervisors Dr George Mackie and Dr John Bancroft for their generous support and exceptional guidance. It has been a learning experience beyond all expectations.

I am especially grateful to Ron Smith, not only for his excellent and extensive technical support at all time, but also for his enthusiasm and patience in teaching me electron microscopy techniques and for numerous stimulating discussions and helpful suggestions. Special thanks also go to Ron for his tremendous help with the mounting and printing of the electron micrographs presented in this thesis.

I would like to acknowledge the technical support of the greenhouse staff, Daphne Boyce and Theresa Donworth, and Walter Chung for amino acid analyses.

I would like to thank Jennifer Bender for her excellent work regarding protein analyses and particularly with the expression of p152 and the immunocytochemical analysis of p26 in *E. coli*.

Very special thanks go to past and present members of the "Mackie Lab", for their help on many occasions, their friendship and for keeping the everyday life so much more interesting: Lesley Rapaport, Andy White, Rob Cormack, Tina Spencer, Leena Mansihna, Julie Genereaux, Glen Coburn, Jennifer Bender, Kris Cunningham, Xin Miao, Ken Niguma and Anand Rampersaud. Special thanks also go to Andy for stimulating discussions and helpful suggestions during the course of this work and to Lottie Koeniger for keeping things in perfect shape in the lab. I would also like to thank students and friends from the department, Amanda Cockshutt, Laurie Baggio, Kathy Hamilton, Brigitte Lavoie and Donna Goldhawk. Your presence and support were appreciated.

Je tiens à remercier très sincèrement mes parents, pour tout. Et merci à François, pour son constant support moral, ses encouragements, sa compréhension et sa patience à toute épreuve qui furent indispensables à l'accomplissement de ce projet.

I would also like to acknowledge the financial support from the Medical Research Council of Canada.

TABLE OF CONTENTS

LIST OF FIGURES

LIST OF TABLES

LIST OF APPENDICES

LIST OF ABBREVIATIONS

°C	degree Celsius
Ala	alanine
AlMV	alfalfa mosaic virus
Arg	arginine
Asn	asparagine
Asp	aspartic acid
ATP	adenosine triphosphate
BaMV	bamboo mosaic virus
BMV	brome mosaic virus
BNYVV	beet necrotic yellow vein virus
BSA	bovine serum albumin
BSMV	barley stripe mosaic virus
CaMV	cauliflower mosaic virus
cDNA	complementary DNA
CP	coat protein
CPMV	cowpea mosaic virus
C-terminus	carboxyl-terminus
CTP	cytidine triphosphate
CVX	cactus virus X
CW	cell wall
CyMV	cymbidium mosaic virus
CYMV	clover yellow mosaic virus
Cys	cysteine
ddNTP	dideoxyribonucleotide triphosphate
DEPC	diethyl pyrocarbonate
dNTP	deoxyribonucleotide triphosphate
DMSO	dimethylsulfoxide
DNA	deoxyribonucleic acid
D RNA	defective RNA
dsDNA	double-stranded DNA
dsRNA	double-stranded RNA
DTT	dithiothreitol
DVX	daphne virus X
EDTA	ethylenediaminetetraacetate
FMV	foxtail mosaic virus
g	gram
GGP	glycerol gradient pool
Gln	glutamine
Glu	glutamic acid
Gly	glycine
gRNA	genomic RNA
GTP	guanosine triphosphate
HEPES	N-2-hydroxy ethylpiperazine-N'-2-ethanesulfonic acid

His	histidine
HMW	high molecular weight
hr	hour
Ile	isoleucine
IPTG	isopropyl-ß-thiogalactopyranoside
kb	kilobase
kDa	kilodalton
LB	Luria-Bertani broth
Leu	leucine
LIC	laminated inclusion component
LMW	low molecular weight
LVX	lily virus X
Lys	lysine
μCi	microcurie
μg	microgram
μl	microliter
μm	micrometer
M	molar
Met	methionine
mg	milligram
min	minute
ml	millilitre
mM	millimolar
M-MuLV	Moloney-murine leukemia virus
mRNA	messenger RNA
MW	molecular weight
nm	nanometer
NMV	narcissus mosaic virus
NP-40	nonidet P-40
N-terminus	amino-terminus
NTP	nucleotide triphosphate
OD	optical density
ORF	open reading frame
PAGE	polyacrylamide gel electrophoresis
PaMV	potato aucuba mosaic virus
P/C/I	phenol/chloroform/isoamyl alcohol
PCR	polymerase chain reaction
PEG	polyethylene glycol
Phe	phenylalanine
p.i.	post-inoculation
PlAMV	*plantago asiatica* mosaic virus
pmole	picomole
PMSF	phenylmethylsulfonyl fluoride
PMV	papaya mosaic virus
poly(A)	polyadenylate
Pro	proline

PVDF	polyvinyldifluoride
PVX	potato virus X
RCNMV	red clover necrotic mosaic virus
RdRp	RNA-dependent RNA polymerase
RNA	ribonucleic acid
RNAse	ribonuclease
rpm	rotation per minute
RT	reverse transcription
SD	Shine-Dalgarno
SDS	sodium dodecyl sulfate
sec	second
Ser	serine
sgRNA	subgenomic messenger RNA
SMYEAV	strawberry mild yellow edge-associated virus
ssDNA	single-stranded DNA
SSC	standard saline citrate
ssRNA	single-stranded RNA
TBE	tris-borate-EDTA
TEV	tobacco etch virus
Thr	threonine
TLC	thin layer chromatography
TMV	tobacco mosaic virus
TomRSV	tomato ringspot virus
Tris	tri(hydroxymethyl)aminomethane
Trp	tryptophane
TRV	tobacco rattle virus
TYMV	turnip yellow mosaic virus
Tyr	tyrosine
UTP	uridine triphosphate
UV	ultraviolet
U	unit
v	volume
V_o	void volume
Val	valine
VPg	virus protein genome-linked
w	weight
WClMV	white clover mosaic virus

CHAPTER 1

GENERAL INTRODUCTION

Viruses constitute an important group of plant pathogens. Over 600 distinct viruses have so far been identified (Zaitlin and Hull, 1987), some of which may cause serious damage to economically important crops (Bos, 1982). Indeed, it is generally accepted that of the various plant pathogens, viruses come second only to fungi with respect to crop losses they cause (Matthews, 1991). Therefore, in the hope of developing improved control methods, plant viruses have been the subject of a large number of studies. Applications of acquired knowledge have indeed been emerging in the past decade, such as the development of lines of genetically-engineered crops which exhibit increased resistance to specific viral infections (Tumer *et al.*, 1993; reviewed by Wilson, 1993). Since plant viruses are relatively simple entities made of only proteins and a nucleic acid, they have also been valuable in the study of fundamental cellular processes such as replication, transcription and translation as well as protein-protein and protein-nucleic acid interactions. Finally, the use of plant viruses as vectors for the introduction of foreign genetic material into plants is now feasible (Joshi *et al.*, 1990; Chapman *et al.*, 1992b) and their potential for permitting the commercial production of valuable pharmaceutical and industrial proteins in plants is being evaluated currently (Simon Moffat, 1992).

The simplicity of the composition of plant viruses contrasts remarkably with the complexity of their functions and the damage they may cause. Usually, the nucleic acid genome is encapsidated by a single type of protein although a bilayer of lipoproteins envelops the nucleocapsid particles of a few plant viruses. In more than 75% of plant viruses the nucleic acid genome consists of a single-stranded (ss) RNA molecule of messenger [(+) sense] encapsidated in a helical or in an icosahedral particle (Zaitlin and

Hull, 1987). However, the genetic material can also consist of negative (—) sense ssRNA, double-stranded (ds) RNA, ssDNA or dsDNA. The genome may consist of a single nucleic acid molecule (monopartite genome) or may be separated among up to four different molecules (multipartite genome), each of which is separately encapsidated by the coat protein. Figure 1.1 summarizes the characteristics of the viral particles of a number of plant viruses.

1.1 POSITIVE-STRAND RNA PLANT VIRUSES

The (+) sense RNA plant viruses have been classified in various families (Fig. 1.1) based on particle morphology, serology as well as characteristics of the genome, i.e. end groups on the RNA, sequence, organization and expression of the coding regions. By comparing these features of the gRNAs, it has become clear that plant viruses from different families actually share common properties and that plant viruses can be related to families of (+) sense RNA animal viruses (Franssen *et al.*, 1984; Haseloff *et al.*, 1984). Based on the common properties of their (+) sense RNA genomes, plant and animal viruses have been grouped in two superfamilies, the picorna-like and sindbis-like viruses (Goldbach, 1990). Comparisons among members of each superfamily have established parallels between coding sequences and have led to the identification of putative functions of coding regions of the plant virus genomes. Features characteristic of the RNA of viruses belonging to each superfamily are described below (reviewed by Matthews, 1991).

1. Structure of the genomic RNA.

The genomic ssRNAs (gRNA) of many plant viruses exhibit characteristic

Figure 1.1 Particle morphology and genome strategy of the groups of plant viruses. (Drawn approximately to scale; from Matthews (1991), with permission).

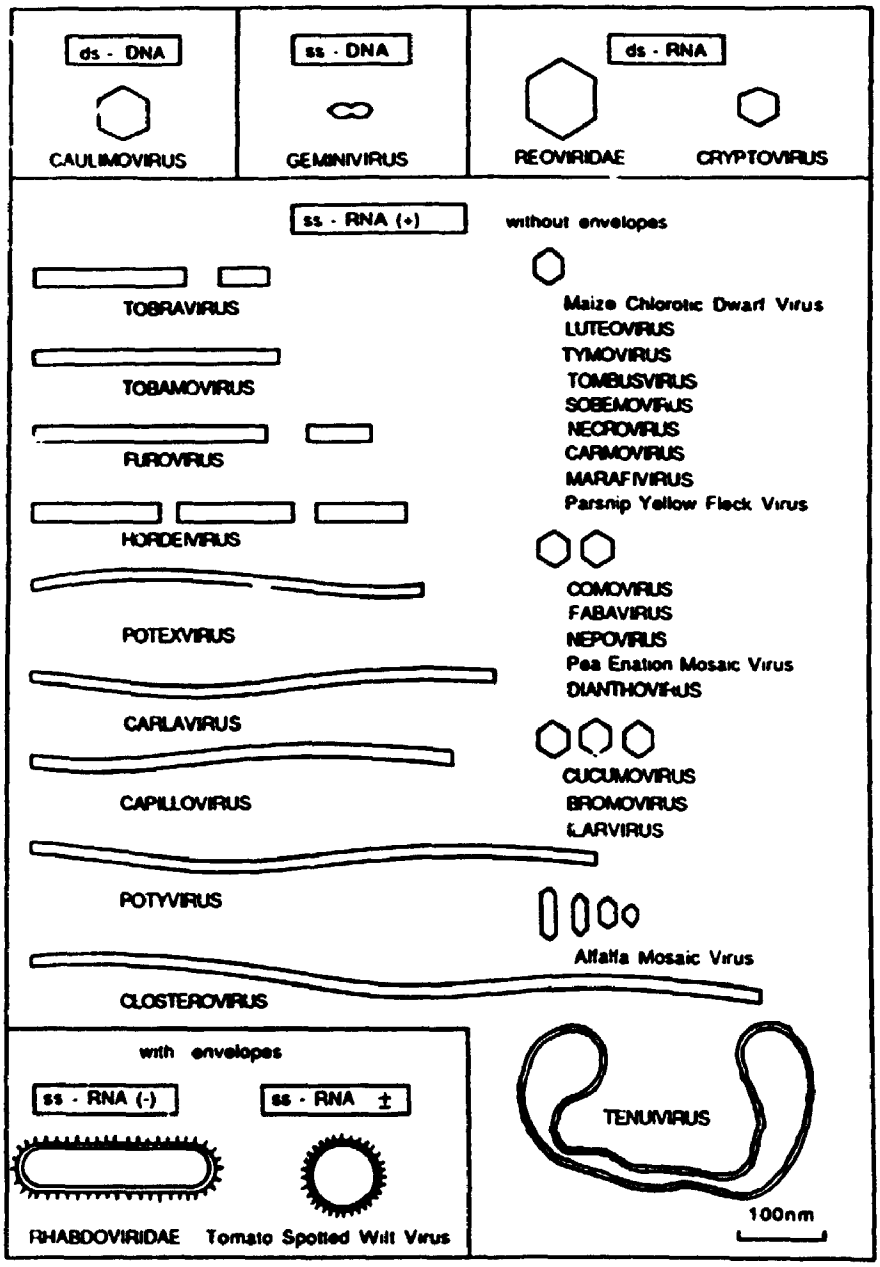
ds - DNA
CAULIMOVIRUS
ss - DNA
GEMINIVIRUS
ds - RNA
REOVIRIDAE
CRYPTOVIRUS
ss - RNA (+)
without envelopes
TOBRAVIRUS
TOBAMOVIRUS
FUROVIRUS
HORDEIVIRUS
POTEXVIRUS
CARLAVIRUS
CAPILLOVIRUS
POTYVIRUS
CLOSTEROVIRUS
Maize Chlorotic Dwarf Virus
LUTEOVIRUS
TYMOVIRUS
TOMBUSVIRUS
SOBEMOVIRUS
NECROVIRUS
CARMOVIRUS
MARAFIVIRUS
Parsnip Yellow Fleck Virus
COMOVIRUS
FABAVIRUS
NEPOVIRUS
Pea Enation Mosaic Virus
DIANTHOVIRUS
CUCUMOVIRUS
BROMOVIRUS
ILARVIRUS
Alfalfa Mosaic Virus
with envelopes
ss - RNA (-)
ss - RNA ±
RHABDOVIRIDAE
Tomato Spotted Wilt Virus
TENUIVIRUS
100nm

structures at their 5' and 3' termini which play various roles in their infectivity and accumulation in their hosts. The 5' end may carry a "virus protein genome-linked" (VPg) covalently attached to the first nucleotide of the gRNA. VPg is virally encoded and is of relatively small size (3.5-24 kDa). Alternatively, the 5' end may consist of a methylated guanine connected to the first base of the gRNA by a 5'-5' triphosphate linkage, in the form m^7Gppp... This structure, also referred to as a "cap" structure, is similar to that at the 5' terminus of eucaryotic messenger RNAs (mRNA). The 3' end of ssRNA genomes may consist of a poly(A) tract as is present at the 3' end of eucaryotic mRNA or may be folded into a tRNA-like structure. In the latter case, the 3' end of certain gRNAs can be aminoacylated with a specific amino acid (e.g. tobacco mosaic virus (TMV) RNA: histidine; brome mosaic virus (BMV) RNA: tyrosine).

Members of the picornavirus-like family (poty-, como-, and nepoviruses) all appear to possess similar terminal structures, a 5'-VPg and a 3'-poly(A) tail. In contrast, members of the sindbisvirus-like family, such as tobamo-, bromo-, hordei-, furo- and potexviruses, are not as uniformly structured. Most have a cap structure but a few have a VPg (e.g. luteoviruses) at the 5' end. Similarly, the 3' end may consist of a poly(A) tail (e.g. potex- and furoviruses) or a tRNA-like structure (e.g. tobamo-, bromo- and hordeiviruses).

2. Expression strategies.

The size of plant viral genomes varies between ~4.0 kb (carmoviruses) and ~13.1 kb (furoviruses) and can code for up to 12 proteins. However, a major constraint of the eucaryotic translational machinery (with only a few exceptions), is its ability to recognize only the open reading frame (ORF) closest to the 5' end of a mRNA. The

scanning model best reconciles the known events in the initiation of mRNA translation (Kozak, 1989). It proposes that following the assembly of an initiation complex at the 5' end of a mRNA, the mRNA sequence will be scanned towards the 3' end until the complex reaches a start codon in a favorable context, at which it will bind the large subunit of the ribosome and will start translation. Once a stop codon is reached, the ribosomal subunits usually dissociate from the mRNA and ORFs beyond this point remain untranslated. The various strategies employed by plant viruses to express their genome have likely evolved to fit this constraint. The seven main strategies used by plant viruses to express their ssRNA genomes are described below and are illustrated in Figure 1.2 (Matthews, 1991). They are not mutually exclusive. Indeed, most plant viruses combine two or three different strategies to express the potential ORFs in their own genome.

(1) Subgenomic RNAs. RNA molecules smaller than gRNA, but 3' co-terminal with it, termed subgenomic RNAs (sgRNA), can be synthesized to include at their 5' end an ORF which is internal in the gRNA (e.g. potexviruses).

(2) Multipartite genomes. A number of plant viruses segment their genome into several RNA molecules, each containing at least one ORF (e.g. furo- and bromoviruses). These RNAs are not 5' or 3' co-terminal and are essentially unique.

(3) Polyproteins. A single ORF encodes the viral proteins. This ORF is translated into a polyprotein which is subsequently cleaved at specific locations (usually by virally encoded proteases) to generate a number of separate polypeptides (e.g. potyviruses).

(4) Readthrough. Two ORFs may be separated by a "leaky" stop codon which can be by-passed in some rounds of translation, allowing the synthesis of two nested proteins which

Figure 1.2 Seven strategies used by plant viruses to express their (+) sense ssRNA genome in the plant eucaryotic translation system. The bold and wavy lines represent the gRNA and proteins, respectively. (Modified from Matthews (1991), with permission).

1 Subgenomic RNAs

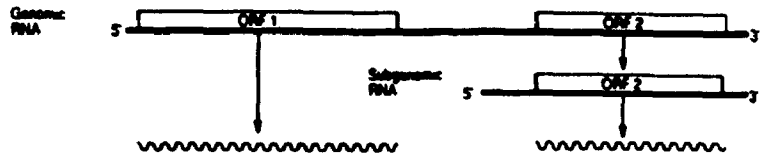

2 Multipartite genome

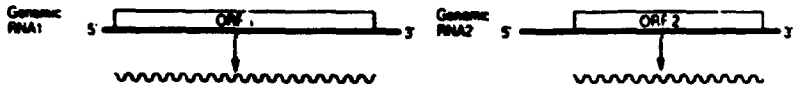

3 Polyprotein

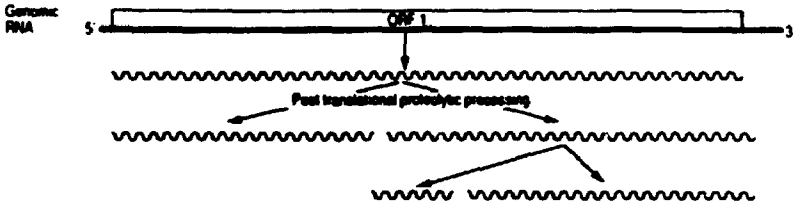

4 Read through protein

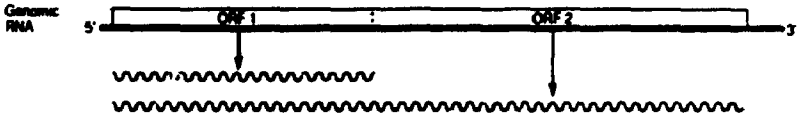

5 Translational frameshift

The ribosome bypasses a stop codon in Frame 0 by switching back one nucleotide to Frame -1 at a UUUAG sequence before continuing to read triplets in Frame -1 to give a fusion or transframe protein

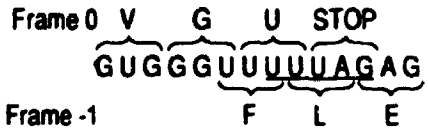

6. Overlapping ORFs

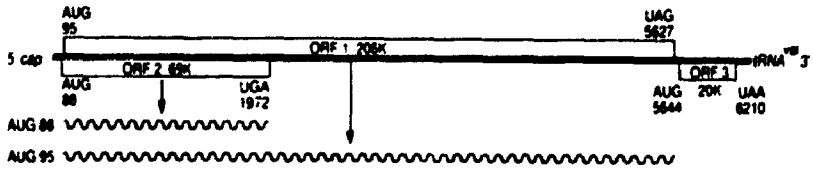

7. Internal Initiation

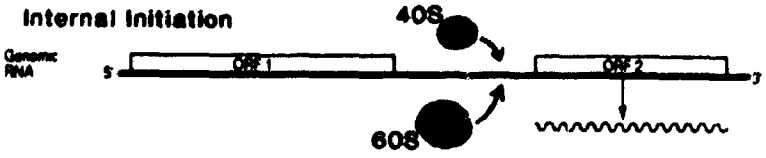

have a common N-terminal sequence but differ at their C-termini (e.g. tobamoviruses).

(5) Frameshifting. In a particular sequence context (Fig. 1.2), ribosomes have been found to "slide" to a different frame near the stop codon of a first ORF to generate a second, larger protein (e.g. luteoviruses).

6) Overlapping ORFs. Closely spaced start codons which specify two ORFs in different frames are used by tymoviruses, thereby maximizing the coding capacity of the genome (Weiland and Dreher, 1989).

7) Internal initiation. In a particular primary and secondary structure context, ribosomal subunits bind to an internal region of the viral RNA from which scanning to a start codon in a favorable context takes place. This mechanism has been documented for the translation of the animal poliovirus genome and it appears that some plant viruses may employ such a strategy (luteo-, como- and potexviruses; Matthews, 1991; Hefferon *et al.*, 1994).

Picorna-like viruses have the common characteristic of expressing their genome as a polyprotein which is subsequently cleaved to generate functional proteins. In contrast, various combinations of the strategies described above are used by sindbis-like viruses. However, a common characteristic of this latter group is the production of their capsid protein from a sgRNA (Goldbach, 1990).

3. Conserved coding regions.

Plant viruses with ssRNA genomes usually encode from four to seven polypeptides which are involved in the various processes such as replication, movement, encapsidation and proteolysis leading to the accumulation of the virus in host plants. In some cases, there can also be a protein involved in insect transmission. No specific

function has been clearly assigned to a large proportion of these proteins. A comparison of the predicted amino acid sequences of the encoded proteins has provided clues for possible function(s) as well as to relationships among the various plant virus groups.

The most conserved open reading frame (ORF) among (+) sense RNA viruses is that encoding the putative viral component of the RNA-dependent RNA polymerase (RdRp) complex responsible for the replication of the viral nucleic acid. This ORF includes a conserved amino acid motif which forms the "polymerase domain", centered around the sequences ..(S/T)GXXXTXXXN(S/T)X_{21-37}.. followed by ..GDD.. surrounded by hydrophobic amino acids (where X is any amino acid) (Kamer and Argos, 1984). This motif is conserved not only among the viral component(s) of the RdRp of animal, plant, yeast and bacterial viruses but also among DNA-dependent DNA and RNA polymerases and reverse transcriptases (Argos, 1988). Evidence for the importance of the GDD domain in the polymerase function has been provided by the mutagenesis of this motif in the viral RdRp component of a few viruses [e.g. Qß bacteriophage (Inokuchi and Hirashima, 1987); BMV (Traynor *et al.*, 1991); yeast dsRNA L-A virus (Ribas and Wickner, 1992)]. A second conserved amino acid pattern has been associated with the polymerase function. It is centered around the motif ..GXXGXGK(S/T).. (Gorbalenya *et al.*, 1988, 1989). This domain is also characteristic of a large number of demonstrated and putative NTP-binding proteins with, in some cases, an associated helicase activity (Gorbalenya *et al.*, 1988; Gorbalenya and Koonin, 1989). This domain may confer a similar activity to the RdRp complex. The helicase and polymerase domains may be located on a single polypeptide (e.g. potexviruses) or on two distinct viral products (e.g. bromoviruses). In the latter case, the two proteins encoded by BMV have been shown

to interact to form the active RdRp complex (Kao *et al.*, 1992; section 3.1.2). The putative viral components encoded by members of the sindbisvirus-like superfamily share an additional conserved region which is likely involved in the capping functions of the polymerase. This putative methyltransferase domain, centered around the motif ..DXXR.., is not found in the sequences of picorna-like viruses (Rozanov *et al.*, 1992). Evidence for the role of this domain in the methyltransferase activity has been obtained by mutagenesis of the sindbis virus genome (Niesters and Strauss, 1990). Generally, the polymerase coding region of members of the sindbis virus superfamily is located at the 5' end of their genome while it is located at the 3' end of the genome of members of the picornavirus superfamily.

Other proteins encoded by the viral gRNA of picorna-like and sindbis-like viruses do not share any obvious sequence similarities although they are involved in processes common to all plant viruses, such as in movement and encapsidation (coat protein(s)). Rather, smaller groups of viruses can be formed within each superfamily, and particularly within the sindbis-like superfamily which is large and heterogeneous. Bromo-, alfalfa- and cucumoviruses are often referred to as the tricornaviridae, having a tripartite genome with similar coding sequence organization and expression strategies (van Vloten-Doting *et al.*, 1981). Hordei-, furo-, carla- and potexviruses can be grouped on the basis of their comparable organization of 3 slightly overlapping coding regions, often referred to as the "triple gene block" (Morozov *et al.*, 1989). Sequences characteristic of picorna-like viruses include those encoding proteases responsible for generating the separate viral polypeptides as well as those encoding the genome-linked protein (VPg) attached at the 5' end of the viral gRNA (Goldbach, 1986).

1.2 POTEXVIRUSES

The potexvirus group has been named after its type member, potato virus X (PVX). The members of this group are characterized by flexuous, rod-shaped particles with lengths of 470-580 nm and a diameter of 14 nm (Table 1.1). The particles consist of a single species of coat protein which encapsidates a single-stranded RNA molecule of coding (+) sense. The research presented in this thesis focuses on members of the potexvirus family. For this reason, a more detailed description of the members of this group is presented below.

1. Transmission and economic significance.

Virus members of the potexvirus family collectively infect a large number of mono- and dicotyledonous plant species although each member has a rather narrow host range (Short and Davies, 1987). They are easily transmitted mechanically and usually propagate by this mean within fields. However, low levels of transmission by fungi and grasshopers has been reported for PVX (Koenig and Lesemann, 1989). As well, a low degree of transmission by aphids has been noted for white clover mosaic virus (WClMV; Goth, 1962). Some potexviral infections can be of economical significance. Yields from cultures of potatoes can be reduced 10-20% by PVX infections (Koenig and Lesemann, 1989). Crop losses due to cassava common mosaic virus infections may reach 30% (Costa and Kitajima, 1972). Moreover, mixed infections of a potexvirus and other plant viruses can result in synergism, such as with co-infections of PVX and potato virus Y, a potyvirus (Damirdagh and Ross, 1967).

2. Symptoms and cytopathology.

The severity of potexviral symptoms ranges from undetectable to moderate.

Table 1.1 Characteristics of completely or partially sequenced potexviruses.

Member[a]	Particle length (nm)	gRNA[b] (nt)	coat protein[c] (kDa)
BaMV	490	6366	25.0
CYMV	540	7015	23.5
CyMV	475	6800-7500[d]	23.6
FMV	500	6151	23.7
LVX	550	-	21.6
NMV	550	6955	26.1
PMV	530	6656	23.0
PaMV	580	8000[d]	26.0
PlAMV	510	6128	21.8
PVX	515	6435	25.1
SMYEAV	480	5966	25.7
WClMV	480	5845	20.7

[a] Full name described in the list of abbreviations.

[b] Size of genome determined from sequenced cloned cDNAs.

[c] Molecular weight predicted from deduced amino acid sequence.

[d] Size of genome estimated from mobility in gel electrophoresis.

Infections may be localized to infected leaves (local lesions; see example in Appendix II) or spread systemically throughout the plant. The most prevalent symptoms induced by potexviruses are chlorotic mottle and mosaic patterns. Stunting of plants is also common.

Within infected cells, potexviruses generally accumulate to high levels, i.e. approximately 10^6 particles per cell (Lesemann and Koenig, 1977). The particles are often aggregated in inclusion bodies, usually in the cytoplasm but sometimes in the nucleus [e.g. narcissus mosaic virus (NMV) and papaya mosaic virus (PMV)]. Viral particles may be organized in fibrous aggregates (i.e. without specific organization) or may be stacked in a parallel array, forming banded inclusions. For some potexviruses (e.g. NMV and cactus virus X), arrangement of the particles may also be spindle-shaped (Lesemann, 1985).

In addition to the aggregates of virus particles, other virus-induced structures may be observed. Several potexviruses induce the proliferation of the endoplasmic reticulum [e.g. clover yellow mosaic virus (CYMV), PMV and WClMV (Lesemann, 1985)]. During PVX infections, characteristic and unique proteinaceous sheets termed laminated inclusion components can be observed predominantly in the cytoplasm of infected cells (Shalla and Shepard, 1972) and sometimes in the nucleus (Davies *et al.*, 1993). These structures are antigenically unrelated to the coat protein (Shalla and Shepard, 1972) and, therefore, do not consist of viral particles. However, they contain another virally-encoded protein, the product of ORF2. The function of laminated inclusion components is unknown, but a role in cell-to-cell movement has been assigned to the ORF2-encoded product (see below; Beck *et al.*, 1991). In cells infected by bamboo mosaic virus (BaMV), electron dense crystalline bodies serologically unrelated to the coat protein can

be detected. These are structurally unrelated to the laminated inclusion components of PVX (Lin and Chen, 1991). In early stages of CYMV infections, amorphous inclusions which contain viral antigen have been noted in the cytoplasm and vacuoles (Schlegel and Delisle, 1971). The relationship between the formation of inclusions and viral replication as well as virally induced pathology is still only poorly understood.

3. Potexviral genome organization.

Members of the potexvirus group share several properties with other members of the sindbisvirus-like superfamily. The presence of a cap (m^7Gppp) at the 5' end of the genomic RNA (gRNA) has been demonstrated for PMV (AbouHaidar and Bancroft, 1978), CYMV (AbouHaidar, 1983) and PVX (Sonenberg *et al.*, 1978), suggesting that all potexviruses have a similar structure at the 5' end of their genomic RNA. A poly(A) tail of variable length (PVX: 75-100, Morozov *et al.*, 1981; CYMV: 75-100, AbouHaidar, 1983; PMV: 50-125, AbouHaidar, 1988; WClMV: 100-300, Guilford *et al.*, 1991) is present at the 3' end of the RNA.

The complete nucleotide sequence of the gRNA of most of the potexviruses listed in Table 1.1 has been determined. Comparisons of the nucleotide sequences have been valuable in identifying conserved residues in untranslated and coding regions which are likely important for the accumulation of the virus during an infection. Cloned cDNAs corresponding to the full length sequence of PMV (Sit and AbouHaidar, 1993), PVX (Hemenway *et al.*, 1990; Longstaff *et al.*, 1993), WClMV (Beck *et al.*, 1990) and CYMV (Holy and AbouHaidar, 1993) from which infectious transcripts can be synthesized have been constructed and have allowed an assessment of the role of conserved sequences in the infectivity and viability of potexviruses.

The 5' untranslated region varies in length between 80-107 nucleotides and is rich in adenosine residues. Only the 5' first 6 residues (5' GAAAAC..) are well conserved among the sequenced members. The 5' untranslated region plays several roles in the accumulation of the virus in plant hosts, namely replication (section 1.3.1) and encapsidation (Sit *et al.*, 1994; section 1.3.2) of the gRNA and enhancement of the translation of the first ORF (Smirnyagina *et al.*, 1991). The 3' untranslated region varies in length from 43-138 nucleotides, excluding the poly(A) tail. In most but not all potexviruses, it includes the polyadenylation signal AAUAAA (Chapter 2; Bancroft *et al.*, 1991). The importance of this motif in polyadenylation as well as of the poly(A) tail in infectivity has been demonstrated by mutagenesis of infectious WClMV transcripts (Guilford *et al.*, 1991). A hexanucleotide motif 5'..ACUUAA, located 32 to 80 nucleotides from the poly(A) tail, is also present in the genome of most sequenced potexviral RNAs (Chapter 2; Bancroft *et al.*, 1991) and is probably involved in the replication of the gRNA (White *et al.*, 1992b; section 1.3.1.3).

The potexviral genome comprises 5 well conserved open reading frames (ORFs) from which the amino acid sequences of the putative products were deduced. This genomic organization is presented in Figure 1.3A. The 5' open reading frame (ORF1) codes for a 147-191 kDa protein which is likely the viral component of the RdRp complex. It contains the polymerase motif .. GDD.., an NTP-binding/helicase motif centered around the sequence ..GXXXGXGK(S/T).. and the methyltransferase domain centered around the sequence ..DXXR.. (Fig. 1.3A). In support of a role for ORF1 in replication, the infectivity of transcripts corresponding to the PVX gRNA was abolished after introduction of point mutations in the GDD coding region (Longstaff *et al.*, 1993).

Figure 1.3 Potexviral genome organization.

(A) The general coding organization of the capped (m^7Gppp) and polyadenylated (A_n) gRNA which ranges from 5.8-8 kb. The relative position of the open reading frames (ORF; open boxes) are shown. ORF1 encodes the putative viral component of the polymerase. The positions of methyltransferase (✱), NTP-binding (■) and polymerase (▲) domains are indicated. ORFs 2, 3 and 4 slightly overlap to form the triple gene block (TGB), involved in cell-to-cell movement. The position of the NTP binding domain is shown in ORF2. ORF5 codes for the coat protein (CP).

The two most abundant sgRNAs produced during the potexviral infection range from 1.9-2.1 kb and 0.9-1.0 kb and serve as templates for the expression of the ORF2 and the CP, respectively.

(B) Regions likely to be important for the encapsidation of the gRNA (origin of assembly; approximately the 5' 50 nucleotides), for polyadenylation (5'AAUAAA) and for replication ($m^7GpppGAAAAC$; 5'GGUUAAGU; 5'ACUUAA). [Redrawn from White (1992)].

A

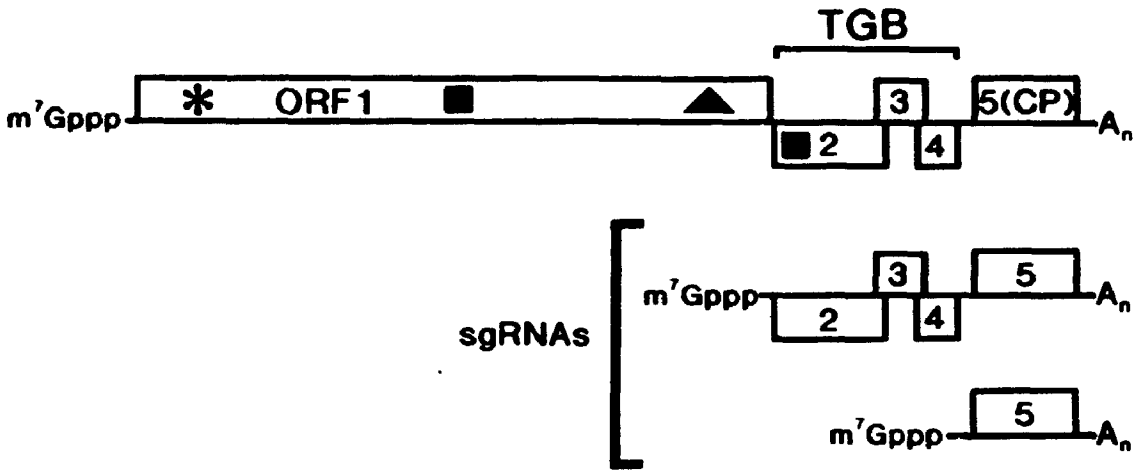
TGB
m7Gppp
ORF1
3
5(CP)
2
4
An
sgRNAs
m7Gppp
3
5
2
4
An
m7Gppp
5
An

B

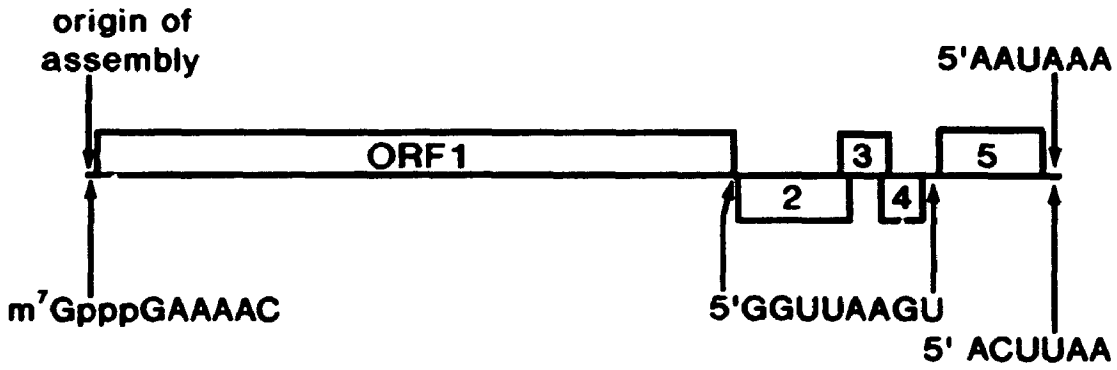
origin of
assembly
5'AAUAAA
ORF1
3
5
2
4
m7GpppGAAAAC
5'GGUUAAGU
5' ACUUAA

The central ORFs (2, 3 and 4) overlap slightly, in different frames, and for this reason are often termed the "triple gene block" (Fig. 1.3A). These ORFs are required for the movement functions of potexviruses (Beck *et al.*, 1991) and perhaps for other functions. ORF2 codes for a 24-26 kDa protein which also carries a NTP-binding motif at its N-terminal region (Fig. 1.3A; Skryabin *et al.*, 1988b). In cells infected by PVX, this product is confined to the laminated inclusion components, as shown by immunocytochemical methods (Davies *et al.*, 1993). ORF3 and ORF4 code for small proteins of 11-14 kDa and 6-13 kDa, respectively. Each putative protein contains a conserved stretch of hydrophobic amino acids (Skryabin *et al.*, 1988b). Exceptions to this arrangement of the central coding sequences have been found with the foxtail mosaic virus (FMV) genome, for which the ORF3 and ORF4 sequences do not overlap (Chapter 2; Bancroft *et al.*, 1991). Also, although sequences resembling the triple gene block region are present within the genomes of strawberry yellow edge-associated virus (SMYEAV) and lily virus X (LVX), start codons which could specify the translation of ORF2 (SMYEAV; Jelkmann *et al.*, 1992) or ORF4 (LVX; Memelink *et al.*, 1990) are lacking. Interestingly, SMYEAV has only been detected in phloem parenchyma cells (Jelkmann *et al.*, 1990) while LVX accumulates to very low concentrations in infected tissues and is poorly sap transmissible (Stone, 1980).

The 3' ORF encodes the 21-26 kDa coat protein (CP) (Fig. 1.3A). In addition to its structural role, the CP likely plays a role in short and long distance transport of the virus in host plants (Chapman *et al.*, 1992a, 1992b; Forster *et al.*, 1992; section 1.3.3). In the genomes of FMV, CYMV, *Plantago asiatica* mosaic virus (PlAMV) and SMYEAV, the ORF5 is preceded by an upstream start codon (ORF5A), which could

code for an extended CP. The longer coat protein is probably expressed during PlAMV infections (Solovyev *et al.*, 1994) but not during FMV and CYMV infections (Bancroft *et al.*, 1991; White and Mackie, 1990, section 1.2.4).

Comparison of the coding sequences of potexviruses with those of other virus families indicates that carlaviruses are the most closely related to potexviruses. The genome organization, size and conserved motifs of the coding regions are very similar, with the exception of an additional ORF (3' of the coat protein sequence) in the genome of carlaviruses (Foster, 1992). Furo- and hordeiviruses are also related to potex- and carlaviruses. The RNA2 of their multipartite genomes comprises 3 ORFs with sequences and organization similar to the potexviral triple gene block (Morozov *et al.*, 1989).

4. Expression of the potexviral genome.

In an *in vitro* translation system prepared from wheat germ or rabbit reticulocyte lysate programmed with the gRNA obtained from purified preparations of a number of potexviruses [e.g. FMV, CYMV, PMV, PVX and BaMV], a large protein of 155-182 kDa is the predominant product (Bendena and Mackie, 1986 and references therein; Lin *et al.*, 1992). This polypeptide corresponds to the translation of the 5' open reading frame, ORF1. This suggests that during an infection, the gRNA serves mostly as a template for the expression of ORF1. For some of the potexviruses, a small amount of coat protein may also be produced. The synthesis of coat protein may arise from the translation of smaller RNAs resulting from the degradation of the gRNA in the translation extract (Bendena *et al.*, 1985) or from the translation of subgenomic RNAs (sgRNAs) which had been encapsidated. It has also been suggested that internal ribosome entry can promote a small level of CP synthesis (Hefferon *et al.*, 1994). During an

infection, at least two sgRNAs (of ~1.0 and ~2.0 kb) can be detected in extracts from plants infected with BaMV (Lin *et al.*, 1992), CYMV (Bendena *et al.*, 1987), daphne virus X (DVX; Guilford and Forster, 1986), FMV (Bancroft *et al.*, 1991), NMV (Short and Davies, 1983; Mackie and Bancroft, 1986) and PVX (Dolja *et al.*, 1987). These sgRNAs are co-terminal with the 3' end of the gRNA but have their 5' end internal to the sequence of the gRNA (Fig. 1.3A). Mapping of the 5' end of the ~2.0 kb sgRNA of CYMV indicated that it lies a few nucleotides upstream of the ORF2 (White and Mackie, 1990). Likewise, the 5' end of the ~1.0 kb sgRNA of some potexviruses has been mapped to a few nucleotides upstream of the coat protein reading frame (White and Mackie, 1990; Bancroft *et al.*, 1991; Solovy *et al.*, 1994). This suggests that the sgRNAs serve as templates for the expression of these ORFs, a notion strongly supported by an *in vitro* study of the coding capacity of synthetic RNA transcripts of CYMV sequences (White and Mackie, 1990).

The sgRNAs are, like the gRNA, capped at the 5' end (White and Mackie, 1990) and polyadenylated at the 3' end (Guilford and Forster, 1986; Dolja *et al.*, 1987). Most sgRNAs have not been detected in their encapsidated form, with the exception of CYMV sgRNAs (White and Mackie, 1990), NMV CP sgRNA (Short and Davies, 1983) and possibly others.

With the exception of the ORF4 product of PVX which has been detected in very low amounts in PVX infected tobacco but not in infected potato (Hefferon *et al.*, 1994; Hefferon and AbouHaidar, personal communication), the expression of ORFs 3 and 4 during an infection remains to be convincingly demonstrated (Price, 1992). Indirect evidence, nonetheless, suggests that they are expressed: introduction of point mutations

at the start codons specifying ORF3 and ORF4 destroyed the ability of WClMV to spread in host plants, while replication in protoplasts was not impaired (Beck *et al.*, 1991). This result would imply that synthesis of the products encoded by ORF3 and ORF4 would occur, by an as yet unknown mechanism. For PVX and DVX, additional sgRNAs with sizes intermediate between the ~2.0 and ~1.0 sgRNAs have been detected in infected tissues (Guilford and Forster, 1986; Dolja *et al.*, 1987) and may be the templates for expression of ORF3 and ORF4 (Morozov *et al.*, 1991). Alternatively, evidence for the expression of the WClMV proteins by internal ribosome binding on a synthetic 2.1 kb sgRNA has been obtained *in vitro*, using a wheat germ translation system (Forster *et al.*, 1993) but not with rabbit reticulocyte lysates. Internal ribosome binding on the larger sgRNA and possibly on the gRNA may be a common mechanism employed by potexviruses to express ORF3, ORF4 and possibly a small amount of the CP (Hefferon *et al.*, 1994). Even if inefficient, this mechanism may supply all the ORF3- and ORF4-encoded protein(s) needed during the infection.

1.3 BIOLOGY OF THE ssRNA PLANT VIRUS INFECTION

Upon entry of the virus into the plant cell, a series of events takes place that will lead to the accumulation of the virus in the host and the development of disease. The general events that lead to the accumulation of the virus can be subdivided into (1) replication, (2) encapsidation and (3) movement. Many viruses have been studied to various extents to elucidate the molecular mechanism of each of these processes and a summary of this knowledge is presented in this section.

1. Replication.

1.1 General model.

Studies which have contributed to our understanding of the replication process include: (1) identification of viral RNA species isolated from infected tissues; (2) *in vitro* translation of viral RNAs; (3) demonstration of infectivity of *in vitro* synthesized viral RNA transcripts in plants and protoplasts; and (4) purification and characterization of RNA-dependent RNA polymerase (RdRp) complexes.

Following entry in the plant cell, the gRNA must be released from the virions. Evidence from both *in vitro* and *in vivo* studies with tobacco mosaic virus (TMV) and other filamentous plant RNA viruses including potexviruses suggests that stripping of coat proteins occurs simultaneously (in the 5' to 3' direction) with the translation of the gRNA by 80S ribosomes (Wilson, 1985; Wilson and Shaw, 1987). Translation of the viral gRNA is obviously essential for the subsequent replication of the gRNA since it will result in the expression of the viral component of the polymerase complex.

A general outline of the replication cycle of a (+) sense gRNA is presented in Figure 1.4 (reviewed by Palukaitis and Zaitlin, 1986). The RdRp complex binds to the 3' end of the gRNA (Fig. 1.4A) and synthesizes its complementary copy [(—) sense] (Fig. 1.4B). Although the "replicative form" generated is represented as a dsRNA molecule (Fig. 1.4C), its state *in vivo* is not clear. Viral dsRNA molecules have been isolated from plants infected by TMV (Jackson *et al.*, 1971) and by some potexviruses (Guilford and Forster, 1986; Dolja *et al.*, 1987; Mackie *et al.*, 1988). However, in the replication of turnip yellow mosaic virus, this intermediate is thought to be single-stranded (Garnier *et al.*, 1980). Subsequently, the RdRp complex or a modified form of

it synthesizes multiple copies of (+) sense gRNA from a (—) strand RNA template (Fig. 1.4D (1)). This replicative intermediate has been proposed to contain a number of (+) sense gRNAs associated with fewer (—) sense RNA molecules, based on the isolation of RNA molecules which contain both ss and ds regions but where nearly the entire (—) sense RNA template is base-paired (Nilsson-Tillgren, 1970; Jackson *et al.*, 1971; Kamen, 1975). This mechanism of (+) sense RNA synthesis is also consistent with the asymmetry in (+) versus (—) strand synthesis, which favors the production of (+) strands (Nassuth and Boi, 1983; French and Ahlquist, 1987).

The mechanism by which the RdRp complex is able to bind initially to the 3'end of the newly synthesized (—) strand (assuming it is double-stranded) may involve the formation of a transient secondary structure within the 5' end of the gRNA, which would free a small portion of the (—) strand. This model was proposed for BMV replication (Pogue and Hall, 1992). However, similar structures have not been reported for other plant virus RNAs.

Cis-acting elements involved in the recognition of the viral RNA by the polymerase complex have been mapped for a number of viruses (e.g alfalfa mosaic virus, van der Kuyl *et al.*, 1991; beet necrotic yellow vein virus, Jupin *et al.*, 1990; BMV, Pogue *et al.*, 1990). These sequences may carry signals in their primary, secondary or tertiary structures. The tRNA-like structure at the 3' end of BMV RNAs is necessary for replication although aminoacylation is not required (Dreher *et al.*, 1989). Other modifications at the ends of the gRNA [i.e. covalently bound VPg, cap structure and poly(A)] also appear to play a role in the replication of some but not all viruses (Matthews, 1991).

Figure 1.4 General model for the replication of a (+) sense RNA genome.

(A, B) The RNA polymerase complex (RdRp) binds a promoter element near the 3' end of the gRNA (A) and synthesizes a complementary [(—) sense] copy of the gRNA (B).

(C, D, E) The RdRp complex then binds the 3' end (C1) or the sgRNA promoter (C2) of the (—) sense RNA which serves as the template for the synthesis of multiple copies of the gRNA (D1) or of sgRNAs (D2).

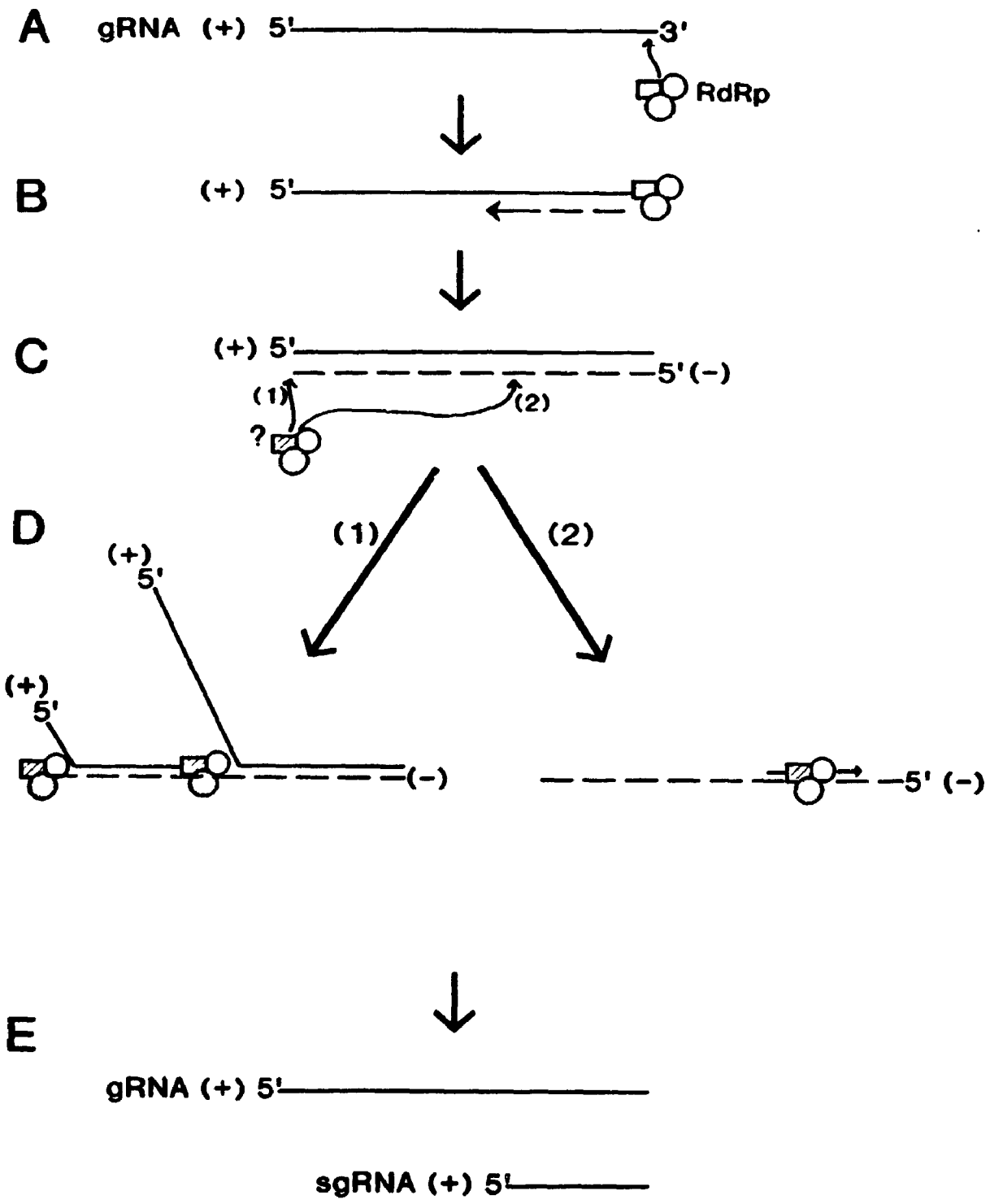
A
gRNA (+) 5'
3'
RdRp
B
(+) 5'
C
(+) 5'
5' (-)
(1)
(2)
?
D
(1)
(2)
(+)
5'
(+)
5'
(-)
5' (-)
E
gRNA (+) 5'
sgRNA (+) 5'

The synthesis of sgRNAs is likely to occur by internal binding of the RdRp complex to the (—) sense RNA (Fig. 1.4D (2)). An alternative model would invoke formation of truncated (—) strand species as templates. However, double-stranded sgRNAs which would be expected if this mechanism were operative, have not been isolated from infected tissues (Mackie *et al.*, 1988). In support of the first model, synthesis of a BMV sgRNA by internal binding of the polymerase complex to a (—) sense RNA has been demonstrated (Miller *et al.*, 1985). Moreover, putative sgRNA promoter sequences which could direct the binding of the polymerase complex to internal sites on the (—) strand have been identified for a number of viruses (Marsh *et al.* 1988; French and Ahlquist, 1988; Skryabin *et al.*, 1988b).

1.2 Proteins involved in viral replication.

The isolation and purification to various extents of the RdRp complex of a number of viruses has shed some light on the replication process (Miller *et al.*, 1985) as well as identified proteins involved in replication (Blumenthal, 1980; Hayes and Buck, 1990; Quadt *et al.*, 1993). In general, this approach has proven challenging and has not yielded large amounts of information. It has been difficult, for example, to obtain an enzyme preparation which can complete a full cycle of replication (reviewed by Quadt and Jaspars, 1989). In fact, many preparations of RdRp are unable to initiate RNA synthesis on a new template and can only complete RNA synthesis initiated *in vivo* (template-independent RdRp). Moreover, the template-dependent enzymes isolated, which can copy an exogenous RNA template, often synthesize only the complementary copy of the added template. For both template-dependent and template-independent enzymes, the products usually consist of double-stranded viral RNA molecules. Only one preparation of an

RdRp has been described which can complete a full cycle of replication *in vitro*, including the synthesis of a sgRNA, from a (+) sense gRNA template (Hayes and Buck, 1990). In this case, the enzyme complex of cucumber mosaic virus consists of three polypeptides: two viral products, carrying the polymerase, the NTP binding, and the methyltransferase domains, and a 60-kDa host component of unknown identity and function (Hayes and Buck, 1990). Unfortunately, this preparation is highly unstable, even in purified form, and has not yielded much mechanistic information.

The most purified template-dependent RdRp complex preparation of BMV consists of two viral proteins homologous to the CMV viral components of the polymerase as well as at least five host proteins (Quadt and Jaspars, 1990). A physical interaction between the two viral proteins is essential to the formation of an active RdRp complex (Kao *et al.*, 1992). Moreover, a homologue of the p41 subunit of the translation initiation factor eIF-3 of wheat germ has been identified as one of the host components which directly interacts with one of the viral component of the RdRp. This p41-like protein is required for the BMV RdRp activity *in vitro* (Quadt *et al.*, 1993). These findings correlate with the association of the translation elongation factors EF-Tu and EF-Ts with the polymerase complex of the bacteriophage Qß (Blumenthal, 1980) and suggest that translation factor(s) may comprise at least one of the host components generally involved in the replication of viral (+) sense RNAs. Moreover, Janda and Ahlquist (1993) have demonstrated that the replication of BMV viral RNAs can occur in yeast cells, indicating the ubiquitous nature of the host components of the RdRp complex.

Replication of the (+) sense RNA of a large number of plant viruses is believed to occur in the cytoplasm of infected cells (Matthews, 1991). The viral components of

TMV involved in replication have been localized by immunocytochemical means to areas of the cytoplasm termed "viroplasm", where replication and virus assembly are believed to take place (Hills *et al.*, 1987). In contrast, in TYMV-infected tissues, viral RNA synthesis and the viral polymerase were both shown to be located in invaginations of the chloroplast envelope (Garnier *et al.*, 1980; 1986). Interestingly, most RdRp complexes isolated from infected plant tissues are associated with a membrane fraction (reviewed by Quadt and Jaspars, 1989).

1.3 Replication of potexviruses.

Replication of the potexviral genome is believed to generally occur as described in Figure 1.4. Each step in this cycle involves the recognition of the viral template, either (+) or (—) strand, by the RdRp complex. In the potexvirus genome, several well conserved sequence motifs appear to act in *cis* as the RNA component of this recognition event. The first of these is the hexanucleotide sequence 5'..ACUUAA.., in the 3' end sequence of the gRNA, which is well conserved among potexviruses and may be part of the RdRp recognition element for (—) strand synthesis. A defective RNA (D-RNA) associated with some CYMV infections has been used to test the importance of the hexanucleotide sequence in the accumulation of potexviral RNAs. The CYMV D-RNA prototype consists of the 5' terminal 757 nucleotides linked to the 415 3' nucleotides of the CYMV genomic RNA. Since it is strictly dependent on its helper virus (CYMV) for its replication and encapsidation, it can serve as a reporter to identify cis-acting elements involved in these processes. Indeed, point mutations of the hexanucleotide motif in CYMV D-RNA destroyed its ability to accumulate in plants when co-inoculated with helper virus, supporting the hypothesis that this conserved sequence is important in the

viability of the viral RNA (White *et al.*, 1992b). A second motif is the sequence 5' GAAAAC.., at the 5' end of the potexviral gRNA, which is well conserved and is probably involved in the recognition of the 3' end of the (—) sense RNA template by the RdRp.

sgRNAs likely result from the internal initiation of (+) sense RNA synthesis on the (—) sense RNA. The sequence 5'..GGUUAAGU.., which is complementary to the hexanucleotide motif (underlined sequence) and which is well conserved among potexviruses, has been identified upstream of the ORF2 and CP coding regions (Skryabin *et al.*, 1988b; White *et al.*, 1992b; Fig. 1.3B). This conserved sequence may serve as a promoter for the synthesis of sgRNAs. In support of this hypothesis, the 5' end of the sgRNAs of CYMV (White and Mackie, 1990) and of the CP sgRNAs of FMV (Bancroft *et al.*, 1991) and PlAMV (Solovyev *et al.*, 1994) have been mapped and lie downstream of the putative promoter sequence. Figure 1.3B summarizes sequences important for the accumulation of potexviruses.

The terminal structures of potexviral gRNAs play a role in the infectivity of the viral RNAs, as shown by the use of mutants of infectious synthetic transcripts. In the absence of the cap structure, very low levels of infectivity are observed for WClMV and PMV (Beck *et al.*, 1990; Sit and AbouHaidar, 1993) while the infectivity of CYMV transcripts is abolished (Holy and AbouHaidar, 1993). The absence of a poly(A) tail on a synthetic transcript of WClMV drastically decreases its infectivity. However, the infectivity of the transcript is abolished only if the poly(A) tail is absent and the polyadenylation signal is mutated to a non-functional sequence (Guilford *et al.*, 1991). Detection of a poly(A)-poly(U) hybrid at the end of the ds form of the gRNA isolated

from PVX infected plants further suggests the involvement of the poly(A) tail as part of the template for the synthesis of the (—) strand (Dolja *et al.*, 1987).

2. Encapsidation.

The potexviral particles are flexuous and rod-shaped, in contrast to the rigid particles of TMV. The potexviral particles consist of 1000-1500 coat protein subunits, distributed in a helical fashion along the RNA genome, with about 9 subunits per turn of the helix (Richardson *et al.*, 1981). Much of our knowledge about the assembly of the potexvirus particle has been generated from *in vitro* studies of the self-assembly of PMV and has been reviewed by AbouHaidar and Erickson (1985). It occurs in a biphasic and polar fashion. The formation of the initiation complex (protohelix) is very rapid (less than 20 sec) and involves the interaction of a double disk of coat proteins (2 layers of 9 subunits) with 38-47 nucleotides located at the 5' end of the PMV gRNA (Sit *et al.*, 1994), unlike TMV where encapsidation is initiated internally about 1,000 nucleotides from the 3'-terminus of its gRNA. At pH 8.0 and low ionic strength, the coat protein interacts with PMV gRNA and the closely related CYMV gRNA, but not with other RNAs, suggesting that a specific recognition of the RNA is involved. The nucleation region is rich in adenosines and cytidines and secondary structures are unlikely to be necessary for nucleation (Sit *et al.*, 1994). The slower elongation phase consists of the progressive addition of coat protein subunits to the protohelix in a 5' to 3' direction. Unlike the nucleation event, this step is not sequence specific at pH 8.0.

Little is known about the regions of the coat protein involved in the formation of viral particles. A prediction of the organization of the coat protein residues in the virus helix has been proposed on the basis of immunological data as well as tritium

planigraphy (Baratova *et al.*, 1992a, 1992b). These results suggest that while the C-terminal region is buried in the interior of the virus particle, the N-terminus is exposed at the surface. This contrasts with the organization of other tubular plant viruses (e.g. tobamoviruses and potyviruses) where both N and C termini of the coat protein are exposed at the surface of the virus particle.

Mutational analysis of the coat protein sequence in infectious synthetic RNAs of PVX and WClMV has defined some important residues in the formation of viral particles. The dispensibility of the 31 residues of the N-terminus (PVX, Chapman *et al.*, 1992a) and of the 31 residues of the C-terminus (WClMV, Forster *et al.*, 1992) for the polymerization of CP to form viral particles was demonstrated. However, the resulting mutant particles displayed an atypical morphology.

Post-translational modifications of the PVX coat protein have been reported. The N-terminal residue is acetylated (Miki and Knight, 1968) and the presence of O-linked sugars at either or both terminal regions of the PVX coat protein has been described only very recently (Tozzini *et al.*, 1994). These modifications may play a role in the structure of the coat protein as well as in protein-protein interactions within viral particles.

3. Movement.

The systemic spread of plant viruses in hosts occurs at two different levels. First, the virus will spread slowly from the primary infected cell into neighboring ones (short distance movement) until it reaches the vascular system. The virus will then travel rapidly, usually through the phloem, to different parts of the plant (long distance movement), where it will cross the vascular cell wall and subsequently spread cell-to-cell into the healthy tissues.

It has now been clearly established that plant viruses move between cells through plasmodesmata (reviewed by Maule, 1991; Deom *et al.*, 1992). These intercellular connections span the width of the plant cell wall, making a channel through which only cellular nutrients can usually be exchanged. The complex structure of plasmodesmata has been well studied (reviewed by Robards and Lucas, 1990). Observations by electron microscopy can be interpreted in the schematic representation of a simple plasmodesma shown in Figure 1.5. The interior of the channel is lined by desmotubules which consist of a modified extension of the endoplasmic reticulum. The space between the plasma membrane and the desmotubules is the cytoplasmic sleeve, where the passage of molecules probably occurs. At the neck regions of the plasmodesma, the cytoplasmic sleeve is partially occluded. The sleeve is further divided into small channels by globular subunits closely packed around the desmotubules (Fig. 1.5B). The effective diameter of the channels is about 3 nm (Terry and Robards, 1987). The size exclusion limit of the plasmodesmatal channels is 10-fold smaller than the size of plant viruses (average for a spherical virus: 30 nm; Matthews, 1991). It is also smaller than the average diameter of free folded viral RNA (~10 nm; Gibbs, 1976). These findings suggest that plasmodesmata must be modified during infection to allow cell-to-cell movement of the virus progeny.

A small number of movement proteins encoded by plant viruses have been characterized partially and two distinct mechanisms by which they may facilitate viral movement have been described (Maule, 1991; Deom *et al.*, 1992). A common feature of these two mechanisms, however, is the interaction of the viral proteins with components of the plasmodesmata. The tobacco mosaic virus P30 protein is among the

Figure 1.5 Schematic representation of a plasmodesma.

(A) Longitudinal view of the plasmodesmatal channel, which is traversed by an extension of the endoplasmic reticulum (ER), termed desmotubule (DT). The cytoplasmic sleeve (CS) is bordered by the plasma membrane (PM) and the cell wall (CW).

(B) View in cross-section of the plasmodesma in the neck region. The globular subunits (GS) are located within the cytoplasmic sleeve. [Redrawn from Deom *et al.* (1992)].

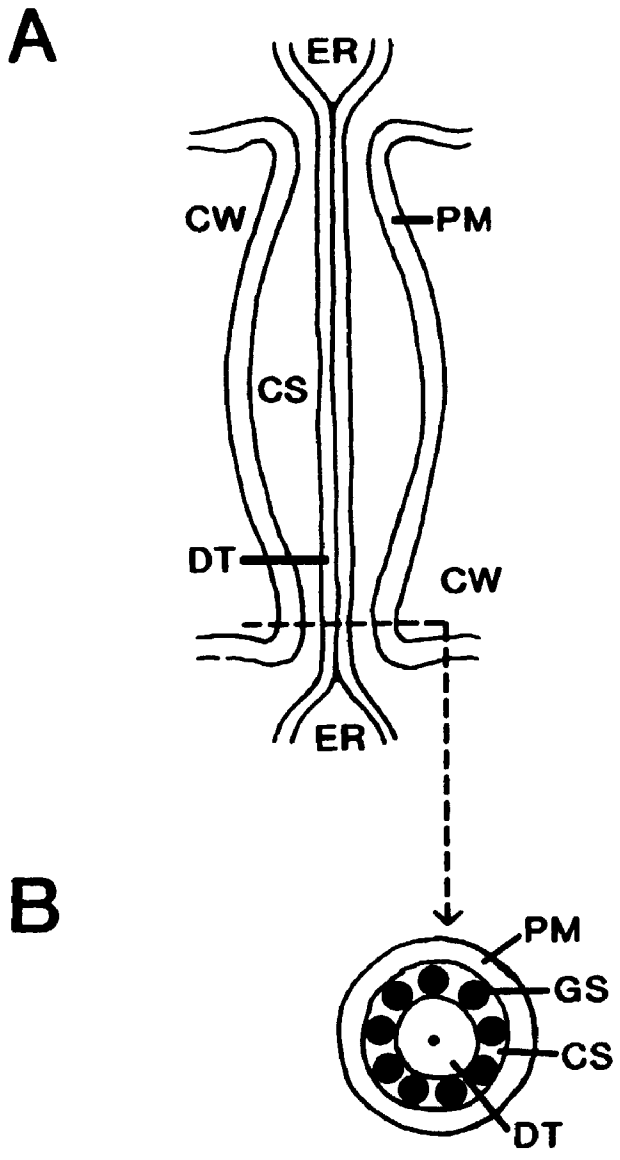
A
ER
CW
PM
CS
DT
CW
ER
B
PM
GS
CS
DT

best characterized movement proteins. It binds to and induces the formation of an elongated structure in the bound ssRNA molecules (Citovsky *et al.*, 1990; 1992). In infected plants, P30 is localized in plasmodesmata (Tomenius *et al.*, 1987). Moreover, its ability to modify the size of the plasmodesmatal permeable space was demonstrated using transgenic plants expressing P30 (Wolf *et al.*, 1989). The movement protein of red clover necrotic mosaic virus (RCNMV, a dianthovirus) is likely to function in a manner similar to the TMV protein (Osman *et al.*, 1992; Lommel *et al.*, 1994). In contrast, the movement proteins of cowpea mosaic comovirus (CPMV; Shanks *et al.*, 1989; van Lent *et al.*, 1990), cauliflower mosaic caulimovirus (CaMV; Linstead *et al.*, 1988) and tomato ringspot nepovirus (TomRSV; Wieczorek and Sanfaçon, 1993) participate in the formation of tubular structures which extend from plasmodesmata within the cytoplasm and in which virus-like particles have been detected. Encapsidation of the viral RNA is required prior to cell-to-cell movement of CPMV, CaMV and TRSV, but not for TMV and RCNMV (Dawson *et al.*, 1988; Xiong *et al.*, 1993).

Additional mechanisms by which viral proteins facilitate cell-to-cell movement of viruses are likely to be described in the future. The alfalfa mosaic virus movement protein P3 is not localized in the plasmodesmata but is found into the middle lamellae of the cell walls of cells just reached by the infection (Stussi-Garaud *et al.*, 1987). Moreover, transgenic plants expressing P3 had a significant but insufficient increase in the size exclusion limit of plasmodesmata to allow the movement of the virus (Poirson *et al.*, 1993), suggesting that additional unknown function(s) are required for the efficient movement of AlMV. Indeed, the requirement for the coat protein in the short distance movement of AlMV was recently demonstrated (van der Vossen *et al.*, 1994).

Potexviruses encode three proteins required for cell-to-cell movement (encoded by ORFs 2, 3 and 4), but the role played by each protein in movement is unknown. It is not clear whether these proteins function directly (e.g. modification of plasmodesmata) or indirectly (e.g. in viral assembly). The potexviral proteins do not share an obvious sequence similarity with previously characterized movement proteins. Moreover, although the requirement for the encapsidation of the viral RNA for its short distance transport has not been clearly established, the coat protein is likely to play an additional role in the transport process (Chapman *et al.*, 1992a, 1992b; Forster *et al.*, 1992). Similar observations for the requirement of the coat protein in the movement of potyviruses were also reported (Dolja *et al.*, 1994).

Little is known about the long distance transport of plant viruses. Short and long distance movement probably occur by distinct mechanisms although they are likely to be mutually dependent (Hull, 1989; Atabekov and Taliansky, 1990; Xiong *et al.*, 1993). Although a number of viruses do not require the expression of the coat protein for their cell-to-cell transport, the coat protein may (TMV and tobacco rattle tobravirus) or may not (barley stripe mosaic hordeivirus and tomato bushy stunt tombusvirus) be necessary for rapid long distance movement (Harrison and Robinson, 1986; Petty and Jackson, 1990; Saito *et al.*, 1990; Scholthof *et al.*, 1993). Moreover, the requirement of the coat protein for this process may be dependent on additional factors, such as the host genotype and the temperature (e.g. RCNMV; Xiong *et al.*, 1993). The role of the coat protein in long distance movement is difficult to establish for viruses which require the protein for short distance movement. In a structure-function analysis of the tobacco etch potyvirus coat protein, Dolja and coworkers (1994) demonstrated that this protein possesses 3

distinct and separable activities which are required for virion assembly, cell-to-cell movement and long distance transport.

1.4 GOAL OF THE RESEARCH

This introduction described basic functions exhibited by plant viruses which are central to the establishment of an infection in plants. Our knowledge of these functions is limited to a small number of viruses which have been selectively characterized. This knowledge has been extrapolated to hypothesize how other, less studied viruses may function. However, as data accumulate, it becomes clear that plant viruses have evolved many different mechanisms to invade the plant kingdom.

This thesis research was undertaken to gain more insight into the molecular biology of potexviruses, using foxtail mosaic virus (FMV) as a model system. FMV was first identified in the foxtails *Setaria viridis* and *S. italica* by Paulsen and Niblett (1977). Although it can infect a number of mono-and dicotyledonous plants, it has not been isolated from crop plants and presumably causes no known economic loss. However, FMV primarily infects Gramineae such as barley (*Hordeum vulgare*), wheat (*Triticum aestivum*) and oat (*avena sativa*) (Paulsen and Niblett, 1977) where it spreads systemically. FMV is considered a possible member of the potexvirus group. It is serologically related to some members of the potexvirus group (Short, 1983) and is structurally related to all potexviruses examined. Its flexuous filamentous particles have a length of 500 nm (Short, 1983) and the number of coat protein subunits per turn of the helical particle is about 9, with a true repeat of 44 subunits in 5 turns of the helix (Richardson *et al.*, 1981). FMV also resembles other potexviruses in that it produces two

sgRNAs during infection of approximately 1.9 kb and 0.9 kb (Mackie *et al.*, 1988). Because FMV is one of the few potexviruses that attack monocotyledonous plants, reaches high concentrations in barley and good yields of virus can be obtained from it, FMV appears to be a good model for the study of potexviruses.

The research presented in this thesis contributed to the determination of the genomic sequence and organization of FMV RNA. Moreover, we have sought to obtain a better understanding of two important aspects of the potexviral infection, i.e. replication and movement, and the role played by proteins encoded by FMV in these processes.

CHAPTER 2

THE ENTIRE NUCLEOTIDE SEQUENCE OF FMV RNA

2.1 INTRODUCTION

The elucidation of the sequence of a viral genome is of considerable value since it permits 1) defining the coding capacity of the genome; 2) deducing the amino acid sequence of the encoded products which can be informative for the specification of putative functions of the viral proteins; 3) identifying evolutionary relationships among various viruses and families of viruses by comparing their nucleotide sequences and the organization of the coding regions; 4) comparing the viral nucleotide sequence with that of related viruses to define cis-acting elements which may play a role in the life cycle of the virus, such as replication and encapsidation.

Nucleotide sequences of the gRNA of some members of the potexvirus group have been determined over the past six years. Complete sequences are now known for white clover mosaic virus (WClMV) (strain M: Forster *et al.*, 1988; strain O: Beck *et al.*, 1990), potato virus X (PVX) (Russian strain: Skryabin *et al.*, 1988a; strain X3: Huisman *et al.*, 1988; Andean strain: Orman *et al.*, 1990; HB strain: Querci *et al.*, 1993), narcissus mosaic virus (NMV) (Zuidema *et al.*, 1989), papaya mosaic virus (PMV) (Sit *et al.*, 1989), clover yellow mosaic virus (CYMV) (Sit *et al.*, 1990), strawberry mild yellow edge-associated virus (SMYEAV) (Jelkmann *et al.*, 1992), *Plantago asiatica* mosaic virus (PlAMV) (Solovyev *et al.*, 1994) and bamboo mosaic virus (BaMV) (Lin *et al.*, 1994). Partial sequences have been determined for potato aucuba mosaic virus (PaMV) (Bundin *et al.*, 1986), lily virus X (LVX) (Memelink *et al.*, 1990) and cymbidium mosaic virus (CyMV) (Neo *et al.*, 1993). The organization of potential coding sequences in these viruses is generally well-conserved and supports a model for gene organization proposed by Bendena and Mackie (1986).

In order to extend the description of foxtail mosaic virus (FMV) and establish it as a definitive member of the potexvirus group, the nucleotide sequence of the FMV genomic RNA (gRNA) was determined and compared to that of other potexviruses. The findings presented in this chapter have been published elsewhere (Bancroft *et al.*, 1991). Comparisons of potexviral sequences have been updated, however, to include sequences which have since been reported.

2.2 MATERIALS AND METHODS

1. Enzymes and chemicals.

All chemicals were of reagent grade. Acrylamide was from BDH (Toronto) and agarose from Bio-Rad Inc. (California). Chemicals used in the purification of virus and RNA were from either BDH or Sigma (St-Louis). ^{35}S-dATP was purchased from New England Nuclear (Mississauga) and Amersham (Oakville). 7-deaza GTP, T4 DNA ligase, T7 DNA polymerase, avian myeloblastosis virus reverse transcriptase and restriction endonucleases were obtained from Pharmacia. Oligonucleotides used in this study were synthesized using an Applied Biosystems model 380A DNA synthesizer and are listed in Appendix I.

2. Strains and plasmids.

Escherichia coli strain MV1190 (Δ(*lac-pro*), *thi*, *sup* E, Δ(*sr*1-*rec* A)306::Tn10 (*tet*^{r}) [F': *tra* D36, *pro* AB, *lac* IqZΔM15]) and plasmid pTZ18U (Mead *et al.*, 1986) were purchased from Bio-Rad. A cDNA library corresponding to the FMV genome was constructed by Dr J. B. Bancroft as described (Bancroft *et al.*, 1991). A number of cloned cDNAs were mapped by J. B. Bancroft and chosen to determine almost the

complete nucleotide sequence of the FMV genome.

3. Preparation of subclones of p105X.

Clone p105X was used to determine the sequence of the 5' third of the genome. Restriction digests of p105X were carried out using 3-5 U of enzyme per μg of DNA under conditions recommended by the manufacturer. Reactions were stopped by the addition of 1/4 volume of gel loading buffer (50 % (w/v) glycerol, 50 mM EDTA, 0.075 % (w/v) xylene cyanol and bromophenol blue). DNA fragments were separated by electrophoresis in a 6 % (w/v) polyacrylamide gel (29:1, acrylamide:bisacrylamide) in TBE running buffer (90 mM Tris, 90 mM boric acid, 2 mM EDTA) (Sambrook *et al.*, 1989). Gels were subsequently stained with a 0.5 μg/ml ethidium bromide solution.

DNA fragments were localized by a brief exposure of the gel to UV light and excised from the gel. The DNA fragments were eluted by incubation of the crushed acrylamide gel slice in elution buffer (500 mM ammonium acetate, 10 mM magnesium acetate, 1 mM EDTA, 0.1 % (w/v) SDS, 10 μg/ml yeast RNA) at 37°C overnight. The acrylamide pieces were removed by passing the elution buffer through siliconized glass wool. The DNA was extracted with phenol/chloroform/isoamyl alcohol (P/C/I, 25:24:1) and subsequently with 2-butanol and was precipitated twice with ethanol. The quality and recovery of the gel-purified DNA fragments were verified by electrophoresis in 6 % polyacrylamide gels.

The vector pTZ18U was cut with various restriction enzyme(s) and treated with alkaline phosphatase. Ligation mixtures contained plasmid vector (60 ng) and DNA fragment resulting in a molar fragment:vector ratio of 5:1, 60 mM Tris-Cl (pH 7.5), 6 mM $MgCl_2$, 10 mM DTT, 0.5 mM ATP, 0.025 % (w/v) gelatin and 0.5 U/μl T4 DNA

ligase in a final volume of 10 μl. The reaction was incubated at 15°C overnight.

E. coli transformations were carried out following essentially the procedure suggested by Bio-Rad (Inc.). *E. coli* strain MV1190 was grown in 250 ml Luria-Bertani medium (LB: 10 % bactotryptone, 5 % yeast extract, 5 % NaCl, 0.2 % (w/v) glucose, 1 mM $MgSO_4$) to an $OD_{600} \sim 0.9$. Cells were harvested by centrifugation at 5 000 rpm in a JA-14 rotor (Beckman) at 4°C for 5 min. Cells were gently washed in 50 ml of 100 mM $MgCl_2$ and collected by centrifugation. They were then resuspended in 110 ml of 100 mM $CaCl_2$, stored on ice for 60 min, collected by centrifugation and resuspended in 12.5 ml of 85 mM $CaCl_2$ containing 15 % (v/v) glycerol. Cells were stored at -70°C until their transformation. Competent cells (300 μl) were mixed with the ligation mixture (10 μl) and stored on ice for 60 min. Cells were then heated at 42°C for 3 min and stored on ice for a further 5 min. One ml of LB was added to the cells which were then incubated at 37°C for 1 hr. Subsequently, cells were spread onto LB agar plates containing 20 μg/ml of carbenicillin, an ampicillin analog.

Colonies exhibiting ampicillin resistance were streaked on fresh LB plates containing carbenicillin and single colonies obtained were used to inoculate 2.5 ml LB supplemented with carbenicillin. Cultures were grown with shaking at 37°C overnight and plasmids were isolated by the alkaline lysis method of Birnboim and Doly (1979). Recombinant plasmids were identified by restriction digests. Plasmids to be sequenced were further purified by precipitation with polyethylene glycol (PEG). The mixture (5 μg plasmid in 50 μl ddH_2O, 30 μl of 20 % (w/v) PEG in 2.5 M NaCl) was incubated on ice for 60 min and the DNA was recovered by centrifugation.

4. cDNA sequencing.

The method of Sanger *et al.* (1977) which relies on base-specific termination of enzyme-catalyzed primer extension, was used to determine the DNA sequence. Reactions were performed using the Pharmacia T7 sequencing Kit according to the protocol provided by the manufacturer. Each [^{35}S]-labeling reaction contained approximately 2 μg of double-stranded plasmid DNA template and 20 ng of primer. [^{35}S]-labeled products were denatured by heating at 90°C for 3 min in 8 mM EDTA and 40 % formamide. They were resolved in 5-8 % polyacrylamide gels (19:1, acrylamide:bisacrylamide) containing 8 M urea. Electrophoresis was carried out in TBE running buffer.

To resolve the sequence in regions rich in G and C residues, reaction mixtures were prepared where the dGTP was replaced with the analog 7-deaza GTP.

5. Dideoxysequencing of RNA templates.

FMV was grown in barley and purified by differential centrifugation as described for clover yellow mosaic virus (Bancroft *et al.*, 1979). The viral RNA was then extracted with 2.5 M guanidine-HCl and 5 mM EDTA, pH 8.0, at 4°C and quantified spectrophotometrically.

An adaptation of the dideoxynucleotide method used for cDNA sequencing described by Fichot and Girard (1990) was used. The oligonucleotides GM-40 (Appendix I) was used to determine the 5' terminal nucleotides while oligonucleotides MR-413 and MR-418 (Appendix I) were used to verify the sequence obtained from cDNA clones. For the sequencing reaction, the synthetic primer (5-15 pmol) was annealed to 1.5 μg of purified viral RNA in a buffer containing 60 mM Tris-Cl, pH 8.3, 75 mM NaCl, 7.5 mM $MgCl_2$ and 5 mM DTT by heating for 3 min at 90°C followed by incubations at

45°C for 30 min, 37°C for 15 min and room temperature for 10 min. The elongation and termination reactions were exactly as described (Fichot and Girard, 1990) using avian myeloblastosis virus reverse transcriptase. Analysis of the labeled products was performed as described in the preceding section.

6. Analysis of the nucleotide sequence data.

Sequences obtained were assembled and analyzed with the PC Gene programs (Intelligenetics) or with the University of Wisconsin Genetics Computing Group (UWGCG) programs mounted on a VAX computer (Devereux *et al.*, 1984).

2.3 RESULTS AND DISCUSSION

1. Nucleotide sequence and genome organization.

1.1 Strategy.

The sequence of the 5' terminal 2200 nucleotides of FMV gRNA was almost entirely determined using the plasmid p105X and subclones generated from it. Approximately 90 % of the sequence was determined from both DNA strands, using synthetic primers specific for the vector or for viral sequences already determined. The sequence of the last 5' terminal nucleotides of the genome were determined by dideoxynucleotide sequencing of the gRNA since plasmid p105X lacked this region. The first five residues are 5'-NGAAA. The first "residue" (N) is likely an artifact of reverse transcription caused by a cap structure (Ahlquist and Janda, 1984; Allison *et al.*, 1988; Sit *et al.*, 1990) whose presence is expected by analogy to other potexviruses (Sonenberg *et al.*, 1978; AbouHaidar and Bancroft, 1978; Sit *et al.*, 1990). Taking this into account, the extreme 5' terminal sequence of FMV RNA, m^7GpppGAAAACUCUUCC, is very

similar to the terminal sequence of other potexviral RNAs (Zuidema *et al.*, 1989).

The sequence of cloned and subcloned cDNAs corresponding to the remaining two thirds of the genome was determined primarily by J. B. Bancroft, R. Johnson and L. Prins. Assembly of the nucleotide sequence data revealed that the FMV gRNA is 6151 nucleotides long excluding the poly(A) tail, this size being intermediate compared to that of the other sequenced potexviruses. The complete nucleotide sequence of FMV gRNA is presented in Figure 2.1.

1.2 Organization of potential coding sequences in the FMV genome.

The organization of the FMV RNA genome, deduced from its nucleotide sequence, is depicted in Figure 2.2. The first ORF encompasses 66 % of the genome as it initiates at nucleotide 81 and terminates at nucleotide 4088, encoding a protein with a M_r of 152.3 K. The size of the latter is consistent with the 160-kDa protein produced by *in vitro* translation of FMV gRNA (Bendena and Mackie, 1986). Interestingly, the context of the initiation codon for ORF1 (AUGUC) differs from that of all other potexviruses (AUGGC) as well as from the consensus context (AUGGC) in plant mRNAs (Lütcke *et al.*, 1987). The region encompassed by ORF1 contains two smaller out-of-frame ORFs [ORF6 (26 kDa) and ORF7 (10 kDa)] designated by the dashed-line boxes in Figure 2.2. Analogous ORFs are not found in all potexviruses but are present in PMV (Sit *et al.*, 1989) and CYMV (Sit *et al.*, 1990) in which ORF6 encodes a 14-kDa protein. WClMV RNA of strain M, but not of strain O, contains an ORF within ORF1 which could code for a 10-kDa protein (Forster *et al.*, 1988). This ORF corresponds in size and position to ORF7 found in FMV RNA. The significance of these internal ORFs remains to be established.

Figure 2.1 The complete nucleotide sequence of FMV gRNA.

The variable length poly(A) tail at the 3' terminus of the sequence is designated A_n. The predicted amino acid sequences of the encoded proteins are shown above the corresponding nucleotide sequence. The sizes of the encoded proteins are shown at the 5' ends of their respective ORFs. This sequence appears in the EMBL, GenBank and DDBJ nucleotide sequence databases under the accession number M62730.

(This sequence is presented in the following two pages).

```
                                                                                                                  1320 M  S  I  E  A  V  F  D  Q  V  T  D  P  S
   1  GAAAACUCUUCCGAAACCGAAACUGACUGAAACUACCUCGACCGACCUUAGAACCCAAGAACCCAACGGGUGCGGCCACUAUGUCUAUCGAGGCAGUUUUCGACCAGGUUACCGACCAU   120

      L  R  A  V  I  Q  E  E  A  M  K  Q  I  K  D  L  F  E  E  T  T  R  C  N  P  Y  S  I  P  Q  A  G  R  K  V  L  E  K  Y  A
 121  CGCUCCGCGCUGUGAUUCAGA[illegible]AAGCGCACAAACAGAUCAAAGAUUUAUUUAAGGAAACGACGCGCUGCAAUCCCUACUCCAUACCGCAAGCUGGGCGCAAGGUUUUGGAAAAGUACG   240

      I  P  Y  N  P  Y  S  L  K  L  H  P  M  A  A  S  M  A  F  E  V  S  L  Y  E  A  A  S  N  Y  L  P  S  T  S  S  T  P  V  T
 241  CCAUCCCCUACAACCCGUACUCUCUCAAACUACACCCUCACGCAGCCUCAAAAGCGUUUGAAGUGUCGCUCUACGAGGCUGCGUCUAACUACCUCCCCUCCACCUCCUCAACUCCUGUCA   360

      F  M  F  T  K  P  G  E  L  R  F  F  R  R  R  G  M  V  D  E  F  V  M  A  D  I  V  P  R  D  L  A  R  Y  P  R  D  T  V  Y
 361  CAUUCAUGUUCACAAAACCGGGCAAGCUCAGAUUCUUUAGGCGCCGAGGUCACGUGGACAAAUUCGUUAAUGCUGACAUAGUUCCAAGAGACUUGGCUAGAUACCCACGCGACACAGUCU   480

      S  Y  L  P  E  I  T  T  M  A  F  I  G  D  T  L  H  H  F  G  E  D  F  L  V  E  V  F  S  R  S  P  R  L  E  V  L  L  A
 481  ACAGUUAUCUGCCCGAGAUCACCACCACACACGCUUUCAUUGGCGACACCCUACAUCACUUCGUGAGGACUUUCUCGUCGAGGUUUUCUCCAGGUCACCGAAACUAGAAGUGCUUCUAG   600

      T  N  V  L  P  P  E  A  F  Y  Y  M  E  S  L  H  P  S  V  Y  T  L  L  Y  R  D  D  R  F  L  Y  L  P  G  G  L  S  G  G  E
 601  CCACCAUGGUAUUACCACCCGAAGCCUUUUACAGAAUGGAGUCCCUUCAUCCCUCGGUUUACACUCUCCUCUACAGGGACGACCGAUUCCUAUACCUGCCUGGUGGCCUGUCUGGCGGUG   720

      Y  E  H  R  Y  K  D  L  H  W  L  T  F  G  T  V  T  H  G  G  I  T  I  T  G  E  R  I  E  T  H  A  A  K  H  L  F  L  F  R
 721  AGUACGAACAUCGCUAUAAGGACCUAAACUGGCUAACAUUGGCACAGUUACGCACGGCGGAUCACUAUCACAGGAGAACGCAUUGAGACUAAGGCCGCGAAACAUCUUUUCCUCUUCA   840

      R  G  R  L  A  T  P  K  F  R  S  F  D  H  P  E  P  H  V  L  L  P  K  V  F  R  P  A  K  Y  H  V  Q  K  P  I  P  R  E  R
 841  GACGAGGGCGACUAGCGACACCAAAAUUCCGCUCAUUCGACAUGCCCGAGCCUAUGGUCCUGCUUCCCAAGGUUUUCCGCCCCGCAAAGUACAAUGUACAGAAGCCAAUUCCCCGGGAGA   960

      A  H  K  W  L  M  Y  V  K  S  I  G  N  A  T  I  R  D  V  W  A  K  L  R  Q  T  I  A  N  A  D  I  G  L  F  S  P  T  E  L
 961  AAGCAAACAAAUGGUUGAUGUACGUUAAAUCCAUCGGCAAUGCCACCAUUCGUGACGUAUGGGCUAAGCUGAGCGAACCAUAGCCAAUGCAGACAUUGGACUCUUCUCGCCCACUGAGC  1080

      V  H  L  T  H  Y  F  L  L  L  C  R  L  D  S  H  N  S  F  D  Q  V  L  A  D  S  V  L  K  A  W  F  R  P  N  V  A  K  L  Q
1081  UCGUGCAUCUCACGAAUUACUUCCUGCUCCUGGGCCGGCUUGACUCACACAAUUCCUUCGACCAAGUACUGGCCGACAGUGUGCUGAAAGCAUGCUUCAGACCAAUGGUCGCAAAGCUUC  1200

      K  I  K  H  K  L  M  G  Q  T  Q  F  M  Q  L  C  Q  A  L  E  M  T  E  V  D  L  V  F  E  V  R  D  S  K  T  P  H  R  Q  A
1201  AGGACAUUAAGCACAAACUCAUGGGCAGACCCAAUUCAUGCAACUCUGCCAAGCGCUAGAGAUGACGAGGUGGACCUCGUCUUUGAGGUCCGGGACUCCAAGACUCCCCACAAACAAG  1320

      V  P  L  D  R  E  I  E  N  V  L  L  E  G  V  S  S  E  P  T  Y  T  E  T  E  G  V  A  D  G  P  L  P  P  P  M  Q  T  A  A
1321  CUGUGCCGUUGGACCGUGAAAUUGAAAACGUUUUGUUGGAAGGAGUCUCAUCGGAGCCAACUUACACUGAAACCGAAGGCGUUGCUGAUGGUCCACUUCCCCCCCCAAUGCAAACUGCAG  1440

      E  P  S  A  T  S  D  E  P  E  S  S  S  R  E  I  E  N  Q  P  A  P  E  I  T  L  D  E  E  E  P  Q  R  D  D  L  P  W  D
1441  CCGAGCCGUCCCGGACCUCAGACGAGCCCGAGAGCUCUAGCUCGCGUGAAAUUGAACAUCAACCGGCGCCUGAACUCACGAGGAAGAACCUCAGCGAGACGAUCUGCCUUGGG  1560

      A  W  R  T  Q  L  R  A  L  G  F  E  A  S  E  R  Q  Y  D  P  D  G  E  L  I  S  P  I  L  S  T  R  R  L  P  K  T  P  I  D
1561  ACGCUUGGAGAACACAAUUAAGGGCGCUUGGCUUUGAGGCCUCCGAAAGGCAGUAUGACCCGGACGGUGAACUGAUCUCUCCUAUCCUCAGCACCCGAAGGUUGCCUAAAACUCCCAUAG  1680

      T  T  L  Y  A  T  L  D  K  I  A  R  C  P  T  F  Y  K  P  C  T  D  R  A  Q  T  Y  A  R  D  V  M  A  G  K  T  G  A  I  L
1681  ACACAACACUCUACGCCACGCUACACAAGAUUGCACGCUGCCCAACUUUCUACAAGCCUGACACAGAUCGCGCGCAGACUUACGCUCGCGAUGUCAUGGCGGGGAAAACCGGUGCCAUUC  1800

      K  Q  Q  P  F  E  W  K  T  T  L  K  R  K  T  K  E  E  P  E  E  I  N  L  A  V  L  H  G  A  G  G  S  G  R  S  Y  A  L  Q
1801  UCAAGCAACAACCCUUUGAGUGGAAAACCACGCUCAAGCGCAAGACUAAAGAGGAACCGAAGGAAAUUCACCUUGCGGUGUUGCAUGGUGCGGGCGGGUCGGGCAAAUCCUACGCACUGC  1920

      E  F  M  R  M  N  S  D  T  P  I  T  V  I  L  P  T  M  E  L  R  A  D  W  K  A  R  L  P  A  M  D  E  D  T  F  M  T  Y  E
1921  AGGAAUUUAUGCCGGAACAACUCUGACACACCGAUUACGGUCAUCCUGCCGACUAACGAGCUCAGGGCCGACUGGAAGAAAAAUUGCCCCGCCCACGACAAAGACACAUUUAUGACAUACG  2040

      N  A  L  L  C  P  R  G  D  I  F  I  M  D  D  Y  T  R  L  P  R  G  Y  I  E  A  F  V  Q  M  A  P  A  L  S  L  L  I  L  T
2041  AAAACGCGCUCUUGUGCCCUCGUGGAGACAUCUUCAUUAUGGACGAUUACACAAAAUUGCCCAGGGGCUACAUUGAGCCUUUCGUGCAGAAUGCACCUGCCCUCUCACUUCUGAUACUCA  2160

      C  D  P  M  Q  A  E  M  F  E  T  T  E  D  W  E  I  M  S  L  A  P  A  S  V  V  F  G  K  F  S  R  Y  M  I  M  A  T  M  P
2161  CCGGUGACCCCAACCAAGCCGAACACUUUGACACCACGGAGGACAAUGAAAUUAACAGCUCGCCCCCGCCUCAGUGGUCUUCGGCAAGUUCUCUAC[illegible]UACCACAUAAAUGCCACACACC  2280

      M  P  R  M  L  A  M  A  L  G  V  Y  S  E  T  P  G  E  V  K  V  L  Y  T  R  M  I  E  T  G  Y  .     L  V  P  S  Q  M  E
2281  GCAACCCCAGAAACUUGGCAAACGCCCUCGCUGUUUACUCCGAGACGCCCGGGGAGGUUAAAGUGCUUUACACGAGGAACAUCAAGACCGGUUAU[illegible]UCUCGUGCCCUCACAAAUGA  2400

      M  R  M  Y  A  S  L  G  Q  R  A  S  T  Y  A  G  C  Q  G  I  T  A  P  R  V  Q  I  I  L  D  S  D  T  P  R  C  T  R  Q  V
2401  AGAUGAGAAUUACGCCUCACUCGGGCAGCGAGCGUCCACCUAUGCGGGUUGUCAGGGGAUCACCGCGCCCCGCGUUCAAAUCAUCCUAGACUCCGACACACCC[illegible]GGUGCACCAGGCAAG  2520

      M  Y  T  A  L  S  R  A  T  T  E  V  V  L  C  M  T  M  P  D  E  K  S  F  F  Q  K  V  E  A  T  P  Y  L  K  A  I  L  M  L
2521  UCAUGUACACUGCACUCUCAAGGGCCACGACGGAAGUGGGUCUCUGCAACACGAUGCCGGAUGAGAAAAGCUUUUUCCAGAAGGUUGAAGCAACACCGUACCUCAAAGCCAUCCUCAACC  2640

      M  K  E  I  K  V  T  E  C  D  L  T  E  E  P  P  R  E  P  A  P  P  T  T  M  L  P  V  E  M  R  I  I  L  M  E  A  L  V  E
2641  UCAACAAAGAGAUUAAAGUCACUGAGGGCGACUUGACAGAAGAACCGCCGAGGGAGCCCCGCUCCUCCCCACCACACACCUGCCUGUUGAAA[illegible]CAGAAUCAUUCUUAAUGAGGCCCUAGUCG  2760

      P  L  P  D  K  M  D  R  E  I  T  S  W  S  T  G  F  S  M  C  I  Q  T  Q  D  P  Y  I  Q  A  F  Q  M  Q  Q  A  K  D  E  T
2761  AACCGCUGCCCGACAAACAUGACCGCGAGAUCUACUCCAACUCCACUGGCUUUUCAAACUGCAUACAGACUCAAGACCCG[illegible]ACAUCCAAGCCUUCCAACAUCAGCAAGCCAAGGACGAGA  2880

      L  F  M  A  T  V  E  K  R  L  A  A  S  T  P  K  D  M  W  T  E  F  K  T  E  R  F  L  G  D  V  L  W  L  A  Y  K  R  A  M
2881  CAUUGUUCUGGGCAACCGUCGAGAAGAGGCUCGCAGCAUCUACGCCGAAGGACAACUGGACAGAAUUCAAGACCAAGAGACCUCUGGGUGACGUGCUUUGGCUCGCGUACAAGCGGGCGA  3000

      V  L  P  D  E  P  I  K  F  M  P  E  L  M  M  A  C  A  D  E  V  G  K  T  Y  L  S  K  F  I  M  A  L  K  M  G  I  L  R  Q
3001  UGGUGCUCCCAGAUGAGCCCAUCAAAUUUAACCCAGAGCUCUCGUGGGGCAUGUGCAGAUGACGUGCAAAAGACCUACCUCUCCAAGCCCAUACACGCGCUCAAGAACGGAAUUCUUCGGC  3120

      S  P  D  F  D  M  M  K  L  Q  I  F  L  K  S  Q  M  V  K  K  I  D  K  I  G  K  I  D  V  M  A  G  Q  T  I  A  A  F  T  Q
3121  AAUCACCCGACUUUGACUGGAACAAACUGCAGAUUUUCCUCAAGUCACAGUGGGUUAAGAAAAUUGACAAAAUCGGCAAAAUUGACGUCAACGCUGGACAGACAAUUGCCGCCUUUUACC  3240

      P  T  V  M  L  F  G  T  M  A  R  Y  M  R  R  I  R  D  T  Y  Q  F  G  E  I  L  I  M  C  E  R  M  Q  K  M  I  S  K  M  V
3241  AACCAACUGUUAUGCUGUUUGGAACCAUGGCGAGAUACAUGCGCCGCAUCCGCGACACUUAUCAACCCGGCGAAAUACUCAUCAAUUGCGAGAAGAACCAGAAGCACAUUUCGAAGUGUG  3360

      E  S  M  W  M  M  R  L  P  A  Y  T  M  D  T  T  A  Y  D  Q  S  Q  D  G  A  M  L  Q  F  E  V  L  K  A  L  M  M  D  I  P
3361  UCGAGAGCAAUUGGAACCACCGCCUACCUGCUUACACCAAUGACUUCACUGCUUACGACCAAAGCCAAGACGGGGCUAUGUUACAGUUUGAGGUACUGAAAGCCCUGCACCAUGAUAUCC  3480

      M  E  V  V  E  A  Y  V  A  L  K  L  M  S  K  M  F  L  G  T  L  A  I  M  R  L  T  G  K  G  P  T  F  D  A  M  T  E  C  M
3481  CUCAUGAGGUUGUGGAAGCUUACGUAGCCCUUAAACUCAACUCAAAAAUGUUUCUGGGCACACUGGCGAUUAUGAGAUUAACUGGUGAGGGACCCACCUUCGACGCUAACACAGAGUGCA  3600

      I  A  Y  T  M  A  R  F  E  I  P  K  M  V  A  Q  M  Y  A  G  D  D  C  A  L  M  C  R  P  V  E  R  Q  S  F  L  P  L  V  E
3601  ACAUUGCUUACACACACGCCCGGUUCGAGAUCCCAAAGAAUGUGGCGCAAAUGUACGCGGGUGACGACUGUGCGCUCAACUGCAGGCCCGUUGAACGGCAGUCCUUCCUGCCUCUUGUGG  3720

      K  F  T  L  K  S  K  P  K  V  F  E  Q  K  V  G  S  W  P  E  F  C  G  M  L  I  T  P  R  G  Y  L  R  D  P  M  R  L  Q  M
3721  AGAAAUUCACCCUGAAA[illegible]CAAAACCUAAAGUAUUUGAGCAAAAAGUUGGGUCAUGGCCUGAGUUCUGCGCAAUCUGAUCACCCCACGGGGCUACCUCAAGGAUCCCAUGAAGCUACAAC  3840

      C  L  Q  L  A  Q  R  K  K  P  S  E  P  G  S  L  K  D  V  A  E  M  Y  A  M  D  L  L  P  T  Y  E  L  G  D  A  L  Y  E  I
3841  ACUGCCUGCAACUCGCCACAGAGGAAGAAACCAUCCGAACCUCGCGUCGCUUAAAGACGUUGCUGAGAACUACGCUAUCGACUUGCUACCCACAUACGAGCUAGGUGAUGCACUCUUACGAAA  3960

      F  D  E  R  Q  M  M  A  M  Y  Q  S  V  R  T  L  I  T  C  A  M  T  K  V  L  R  V  A  Q  A  L  Q  E  D  C  T  F  F  S  S
3961  UCUUCGACGAGAGACAAAUGAACGCGCACUAUCAGUCGGUCAGGACGCUUAUCACAUGCGCCCACACCAAAGUCCUCCGAGUUGCACAGGACAUUCAGGAAGACUGCACCUUCUUUAGCU  4080

      I  *                                                  26K  M  D  S  E  I  V  E  R  L  T  K  L  C  F  V  K  T  S  M  T  M  I  A
4081  CCAUCUAACAGCUUUUGAGUUAGGCUAACUCCACUGACGAAUUAAAUAACAAUGGAUAGUGAAAUAGUUGAACGACUAACAAAGCUUGGUUUCGUCAAGACUUCACACACGCACAUCGCU  4200
```

```
      G  E  P  L  V  I  N  A  V  A  G  A  G  N  T  T  L  L  R  S  L  L  E  L  P  G  V  E  V  F  T  G  G  E  N  D  P  P  N  L
4201  GGCGAGCCCCUCGUGAUUUCACGCCGUUGCUGGGGCCGGUAAAACCACCCUCCUUCGGUCCUUACUUGAUUUACCGGGAGUGGAAGUCUUCACAGGCGGGGAGCACGAUCCUCCAAAUUUG   4320

      S  G  R  Y  I  R  C  A  A  F  P  V  A  G  A  Y  H  I  L  D  E  Y  P  A  Y  P  N  W  R  S  Q  P  W  H  V  L  I  A  D  N
4321  UCAGGGAAAUAUAUCCGCUGCGCUGCACCCCCUGUGGCCGGUGCAUACAACAUUCUUGACGAGUACCCCGCGUACCCAAAUUGGCGAUCGCAACCCUGGAACGUCCUAAUCGCCGACAAC   4440

      L  Q  Y  E  E  P  T  R  R  A  H  Y  T  C  H  R  T  H  R  L  G  Q  L  T  V  D  A  L  R  R  V  G  F  D  I  T  F  A  G  T
4441  CUACAAUACAAAGAACCCACACGUCGCGCCCACUACACAUGCAAUCGCACUCACCGCCUGGGGCAGCUCACUGUCGACGCUUUGCGUAGGGUUGGUUUCGACAUCACCUUUGCCGGCACG   4560

      Q  T  E  D  Y  G  F  Q  E  G  H  L  Y  T  S  Q  F  Y  G  Q  V  I  S  L  R  T  Q  A  H  E  I  A  V  R  H  G  L  A  P  L
4561  CAGACUGAAGACUACGGAUUCCAGGAAGGCCAUCUCUACACUAGUCAAUUUUACGGACAGGUCAUUUCACUUGACACGCAGGCCCAUAAGAUCGCUGUGCGCCACGGACUCGCACCCCUG   4680

      S  A  L  E  T  R  G  L  E  F  D  E  T  T  V  I  T  T  K  T  S  L  E  E  V  F  D  R  H  H  V  Y  V  A  L  T  R  H  R  R
                                                                                                                 11K H  S  L  S  Q  G  T  G  A
4681  UCCGCUUUAGAAACCCGGGGGCUGGAAUUUGAUGAGACCACUGUGAUAACGACUAAAACCUCGCUGGAGGAAGUGAAGGACAGGCACAUGGUCUAUGUCGCUCUCACAAGGCACAGGCGC   4800

      T  C  H  L  Y  T  A  H  F  A  P  S  A  *
       P  A  I  S  T  P  L  T  L  R  P  P  P  D  H  T  K  A  I  L  T  V  A  I  G  I  A  A  S  L  V  F  F  H  L  T  R  H  R  L
4801  ACCUGCCAUCUCUACACCGCUCACUUUGCGCCCUCCGCCUGACAACACGAAAGCCAUACUAACUGUAGCUAUAGGUAUAGCCGCCUCCCUCGUCUUUUUCAUGCUCACACGCAACAAUCU   4920

       P  H  V  G  D  N  I  H  S  L  P  H  G  G  S  Y  I  D  G  T  R  S  I  H  Y  R  P  P  A  S  R  Y  P  S  S  H  L  L  V  S
4921  GCCACACGUCGGUGAUAACAUCCACUCACUACUACCCCACGGAGGAAGUUACAUUGACGGUACCAAGUCCAUCAACUACCGCCCACCUGCGUCACGCUACCCCUCAUCUAACUUACUCGUUUC   5040

       L  H  Q  Y  S  P  Q  Y  S  F  S  S  H  S  H  I  *                                                   6K R  H  E  S  H  L  V  V
5041  GCUCCACCAAUACUCGCCGCAGUACUCUUUUUCCUCACACAGCCAUAUCUAGCUACCAGACGAUCCAGGUGCGUUCGGUGCUUCGUUGUCCACGGGGCAUGCACGAAUCACACCUAGUUG   5160

                                                                                  25K H  S  R  S  T  A  T  P  S  S  S  P  E  T  A  G  T  P
       I  L  A  L  L  L  I  A  L  W  C  L  S  T  R  P  V  Q  P  S  C  H  V  E  I  H  C  H  S  I  I  V  T  G  H  C  W  H  S  T
5161  UUAUAUUAGCGCUGUUACUUAUAGCUCUGUGGUGUCUAAGCACUCGACCCGUUCAACCAUCGUGCCAUGUCGAAAUCAACGGCCACUCCAUCAUCGUCACCGGAAACUGCUGGCACUCCA   5280

       Q  R  P  H  *                                                                  24K CP -->
      L  H  D  R  I  E  C  V  R  V  T  H  I  S  E  E  K  Q  P  T  S  S  V  T  S  S  F  Q  D  T  H  A  T  Q  H  A  D  V  T  D
5281  CUCAACGACCGCAUUGAGGGUGUUAGGCUAACCAACAUCAGUGAAGAGAAACAACCCACCUCAAGUGUGACCUCAUCAUUUCAGGACACAAUGGCAACACAAAAUGCCGACGUCACUGAU   5400

      A  T  D  Y  R  K  P  P  A  E  T  E  Q  K  A  L  T  I  Q  P  R  S  H  K  A  P  S  D  E  E  L  V  R  I  I  H  A  A  Q  K
5401  GCGACGCACUACAAGAAACCGCCUGCUGAAACUGAGCAGAAGGCACUCACCAUUCAACCACGGUCAAACAAGGCGCCCAGUGACGACGAGUUGGUACGCAUCAUCAACGCCGCGCAGAAG   5520

      R  G  L  T  P  A  A  F  V  Q  A  A  I  V  F  T  H  D  K  G  A  T  D  S  T  I  F  T  G  K  Y  H  T  F  P  H  K  S  L  A
5521  CGAGGCCUCACACCCGCGGCCUUUGUUCAAGCAGCUAUAGUCUUCACCAUGGACAAGGGCGCCACCGACUCCACGAUUUUCACGGGAAAAUACAACACUUUCCCAAUGAAAAGUCUGGCG   5640

      L  R  C  K  C  A  C  V  P  V  H  K  L  C  Y  F  Y  T  K  P  A  Y  A  H  R  R  V  A  W  Q  P  P  A  R  W  T  H  E  N  V
5641  CUACGUUGCAAAGAUGCUGGCGUGCCCGUGCACAAACUUUGCUACUUCUAUUACCAAGCCGGCUUACGCGAACCGUAGGGUCGCCAACCAGCCCGCCUGCUCGCUGGACUAACGAGAAUGUG   5760

      P  R  A  H  K  H  A  A  F  D  T  F  D  A  L  L  D  P  Y  V  V  P  S  S  V  P  Y  D  E  P  T  P  E  D  R  Q  V  H  E  I
5761  CCCAAAGCUAACAAGUGGGCGGCUUUCGACACCUUCGACGCACUUCUCGACCCAUACGUAGUCCCAUCCUCUGUACCGUACGAUGAGCCCACGCCAGAGGAUCGCCAAGUCAAUGAGAUU   5880

      F  R  K  D  N  L  S  Q  A  A  S  R  N  Q  L  L  G  T  Q  A  S  1  T  R  G  R  L  W  G  A  P  A  L  P  W  H  G  Q  Y  F
5881  UUCAAGAAGGACAAUUUGAGUCAGGCAGCAUCCAGAAACCAA UCCUAGGAACGCAAGCCUCCAUCACGCGCGGGAGACUCAACGGCGCACCAGCACUACCAAACAACGGGCAGUACUUC   6000

      I  E  A  P  Q  *
6001  AUCGAGGCACCUCAGUGAUCAGUAGUAUGAUACCAAUAAAUAAAUCGGGCGAAUCCGCGCCUCCUGACUAUGGGCAGGUUUACGGACCAAGCUCJAUCGAGAUACGACCUAACAGUAACG   6120

6121  CAGCUAAGGGGUGAAUGCACACAUCGCUUAU(A)n  6151
```

Figure 2.2 The genomic organization of FMV.

ORFs 1 to 5 are shown by numbered boxes, with the corresponding M_r values of their encoded proteins. The coding frame of each ORF is indicated by the position of boxes relative to the baseline. The dashed-line boxes represent internal ORFs within ORF1. The asterisks in ORFs 1 and 2 locates the NTP-binding helicase domain. The triangle in ORF1 designates the position of the RNA-dependent RNA polymerase consensus sequence. The arrows correspond to the relative locations of the large (1.9 kb) and small (0.9 kb) sgRNAs.

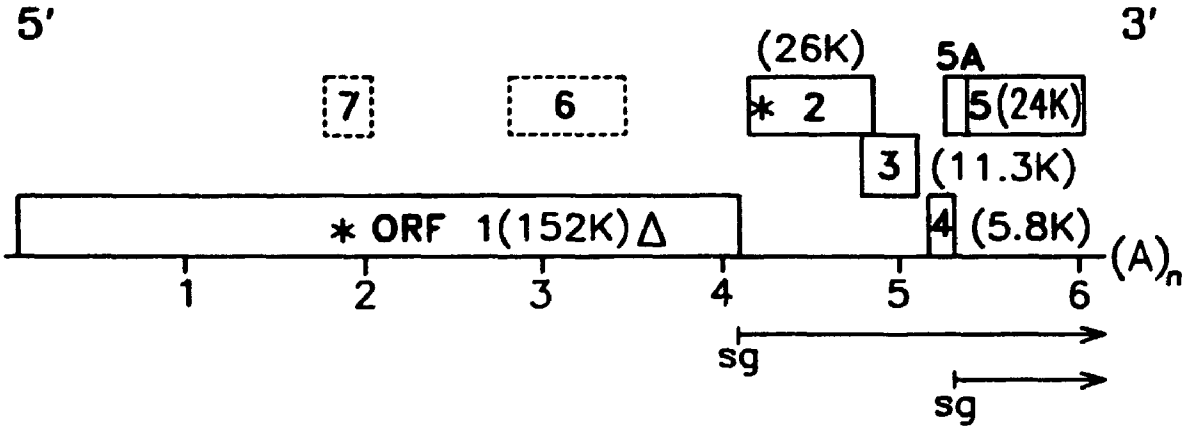
5'
3'
(26K)
5A
7
6
* 2
5(24K)
3
(11.3K)
* ORF 1(152K)Δ
4
(5.8K)
(A)n
1
2
3
4
5
6
sg
sg

The remaining third of the FMV genome is occupied by a minimum of four ORFs. ORF2 spans nucleotides 4132 to 4842 and could encode a protein with a predicted M_r of 26.4 K. ORF2 shares its last 68 nucleotides with ORF3 which begins at nucleotide 4775 and finishes at nucleotide 5092, encoding a protein with a M_r of 11.3 K. ORF4 encompasses nucleotides 5139 to 5297 and would encode a protein with a M_r of 5.8 K. The latter overlaps ORF5A, which encodes a readthrough protein (Mackie *et al.*, 1988) which is translated *in vitro* from FMV gRNA although probably not *in vivo*. ORF5A starts at nucleotide 5227 and leads into the 23.7 kDa coat protein cistron (ORF5) which initiates at nucleotide 5371 and terminates at nucleotide 6018. The identity of ORF5 as encoding the coat protein was established unambiguously by a direct comparison with the amino acid sequence of 18 residues of an internal peptide from purified FMV coat protein generated by CNBr cleavage (Bancroft *et al.*, 1991). The size of the coat protein as well as the amino acid composition predicted from the nucleotide sequence also corresponds to that estimated by Short and Davies (1987) from amino acid analyses. It is, however, approximately 7 kDa smaller than that previously established by electrophoresis (Mackie *et al.*, 1988). The anomalous mobility of the coat protein in SDS-polyacrylamide gel has also been reported for PVX and cactus virus X coat proteins (Koenig, 1972). Presumably, it reflects the possible glycosylation state of the subunits (Tozzini *et al.*, 1994) and non-ideal binding of detergent.

Several ORFs which might encode proteins of 6.4 to 9.6 kDa are found in the negative RNA strand of FMV, as is also the case for PMV, PVX, and WClMV (strain M) minus-strand RNAs. Their significance is unknown.

The sizes of the anhydrous proteins predicted from the FMV ORFs are generally

within the range found for other potexviruses. FMV, however, possesses the smallest ORF3 (11.3 kDa) and ORF4 (5.8 kDa) of all potexviruses (11.9 to 14 kDa and 6.5 to 13 kDa for ORF3 and ORF4, respectively, for other members).

1.3 The 3' non-coding sequence.

The 3' non-coding region of FMV RNA is 133 nucleotides long and is followed by a poly(A) tail of variable length. A putative polyadenylation signal (AAUAAA) is found in the non-coding region of FMV, 107 nucleotides from the poly(A) tail, as well as in most but not all 3'-end sequences of potexviruses (Table 2.1). This signal was recognized independently by Guilford *et al.* (1991) who also demonstrated its importance in polyadenylation of WClMV RNA. Polyadenylation of eucaryotic mRNAs generally occurs in the nucleus, directed by the polyadenylation motif AAUAAA which is usually located 15-25 nucleotides upstream of the polyadenylation start site (reviewed by Wickens, 1990). In contrast, the potexviral motif is located 7-119 nucleotides upstream of the poly(A) tail. Nonetheless, the putative polyadenylation signal of most potexviral RNAs exactly matches the higher eucaryotic poly(A) signal while only 39% of the mRNAs examined from plants contain a precise match (Joshi, 1987). Assuming that potexviral infections take place in the cytoplasm of cells, a cytoplasmic poly(A) polymerase activity would be required. Such activity has not been described for plants but has been found in the cytoplasm of oocytes and HeLa cells (Wickens, 1990).

A common six-nucleotide sequence, ACUUAA, was also identified 30 to 80 nucleotides from the 3'-terminus of all potexviral sequences (Table 2.2). It is conceivable that this consensus sequence may be involved in the production of the minus-strand gRNA during viral replication by acting as a recognition sequence for the replicase

Table 2.1 Putative polyadenylation signals in potexviral RNAs.

Virus[a]	Putative Signal	
CyMV	**AAUAA**c	- 75nt - $(A)_n$
PlAMV	**AAUAA**g	- 29nt - $(A)_n$
SMYEAV	absent	
NMV	**AAUAAAAUAAA**	- 11nt - $(A)_n$
WClMV (M)	**AAUAAA**	- 7nt - $(A)_n$
PVX (X3)	absent	
CYMV	**AAUAAA**	-104nt - $(A)_n$
PMV	**AAUAAA**	-119nt - $(A)_n$
LVX	**AAUAA**c	- 97nt - $(A)_n$
PaMV	**A[illegible]UAAA**	- 11nt - $(A)_n$
FMV	**AAUAAAUAAA**	-107nt - $(A)_n$

[a] The complete name of the viruses is given in the text and in the list of abbreviations.

Table 2.2 Conserved sequences near the 3'-termini of potexviral RNAs.

Virus	Sequence
CyMV	**ACUUAA** - 64nt - $(A)_n$
PlAMV	**ACUUAA** - 80nt - $(A)_n$
SMYEAV	**ACUUAA** - 34nt - $(A)_n$
NMV	**ACUUAA** - 59nt - $(A)_n$
WClMV (M)	**ACUUAA** - 33nt - $(A)_n$
PVX (X3)	**ACaUAA** - 58nt - $(A)_n$
CYMV	**ACUUAA** - 35nt - $(A)_n$
PMV	**ACUUAc** - 32nt - $(A)_n$
LVX	**ACUUAA** - 32nt - $(A)_n$
PaMV	**ACUUAA** - 60nt - $(A)_n$
FMV	**ACcUAA** - 39nt - $(A)_n$

complex. White and coworkers (1992b) have provided further support for this hypothesis. The mutagenesis of this hexamer motif in the sequence of a defective RNA of CYMV abolished its ability to accumulate in host plants when co-inoculated with the helper virus. Another partially conserved sequence near the 3' terminus of some potexvirus RNAs has been identified (Orman *et al.*, 1990) but is matched poorly by FMV gRNA (13/23 residues).

2. Similarity of the putative proteins encoded by the FMV genome to corresponding proteins of other potexviruses.

The predicted protein sequences of all potexviruses (including FMV) were compared using the GAP alignment program (UWGCG) with a gap weight of 3.0 and a length weight of 0.1. The percentage of identity and similarity of residues encoded by each ORF with the corresponding ORF of other members of the potexvirus family were obtained and are summarized in Table 2.3.

2.1 Non-structural proteins.

The ORF1 product from FMV is closely related to that of the other potexviruses, since the percentage of similarity of both the amino and carboxyl ends is in a constant range for all comparisons (Table 2.3). The N-terminal region of FMV ORF1 contains the putative methyltransferase domain which is well conserved among the sindbis-like viruses (Rozanov *et al.*, 1992). The C-terminal domain of ORF1 contains both the NTP-binding helicase consensus sequence (Gorbalenya *et al.*, 1988; Hodgman, 1988) and the RNA-dependent RNA polymerase consensus motif (Argos, 1988) (Fig. 2.2), as reported for other potexviruses (Skryabin *et al.*, 1988b). The NTP-binding and polymerase motifs are not only well conserved in potexviruses but also in most positive-strand RNA plant

Table 2.3 Similarities of FMV ORFs to ORFs in other sequenced potexviruses compared to similarities among all other potexviruses[a].

Protein encoded by		FMV			OTHERS		
		range %sim.[b]	average %sim.	%id.	range %sim.	average %sim.	%id.
ORF1	N-term[c]	60-67	62	41	60-72	65	46
	C-term[d]	63-68	66	49	66-73	69	54
ORF2[e]		48-57	52	32	46-63	53	34
ORF3		57-64	60	44	47-72	56	39
ORF4		36-60	50	27	36-59	47	26
ORF5 (CP)		40-47	43	26	47-65	55	38

[a] Data for ORF1 and ORF4 were obtained from an eight-member comparison, data for ORF2 and ORF3 from a nine-member comparison and for ORF5, eleven potexviral sequences were compared.
[b] % similarity represents the sum of the % identical (id.) and similar (sim.) residues.
[c] First 400 residues of the ORF1 encoded product.
[d] Last 800 residues of the ORF1 encoded product.
[e] Includes the putative ORF2 of SMYEAV although it lacks a start codon for this ORF (Jelkmann *et al.*, 1992).

viruses (Habili and Symons, 1989). The 26-kDa protein (ORF2) of FMV also contains a NTP-binding helicase motif, located at the N-terminus as in other potexviruses (Skryabin *et al.*, 1988b). The remaining ORF2 sequences from all other potexviruses are less related to each other than are ORF1 and ORF3 (11-kDa protein) sequences (Table 2.3; see also Zuidema *et al.*, 1989). FMV ORF3 and ORF4 are related to that of other potexviruses in that they contain stretches of hydrophobic residues predicted to form transmembrane helices (Morozov *et al.*, 1987; Forster *et al.*, 1988; Skryabin *et al.*, 1988b) bordered by charged residues. Although FMV has the smallest ORF4 of all potexviruses, the common N-terminal hydrophobic region is conserved. Frequent conservative exchanges among hydrophobic amino acids have occurred suggesting that the function of the product of ORF4, if any, is not impaired by such replacements. Two sequenced potexviruses lack one of the ORF described. Although open reading frames appear to be present, SMYEAV and LVX lack a start codon which could specify ORF2 and ORF4, respectively. Nonetheless, it remains possible that the translation of these reading frames involves an unusual initiation codon.

2.2 Capsid protein.

The coat proteins (ORF5) of potexviruses are the only translation products with a defined function which may be used to help interpret their amino acid sequences. The amino acid sequence of FMV coat protein is not as similar to the coat protein sequences of the other potexviruses as these are amongst themselves (Table 2.3) but maintains consensus regions (Fig. 2.3). In the optimal alignment in Figure 2.3, only 9 residues are absolutely conserved and are predominantly found between amino acids 121 to 145 (on the FMV sequence). The most striking feature in this region is the 11-residue amphipa-

Figure 2.3 Comparison of the amino acid sequence of the coat protein of 11 potexviruses.

A multiple alignment of the sequences was created using the program GAP (UWGCG) and was manually optimized. Conserved residues are in uppercase. Underlined residues in the consensus line are strictly conserved. The numbering is that of the FMV coat protein sequence. The sequences of strain M of WClMV and of strain X3 of PVX were used to perform the comparison. SMYE refers to the sequence of the potexvirus associated strain SMYEAV.

```
CyMV                                   mgeptptpaatysaadptsaPkladLaaikyspvtssiATpeEikaItqlwvnnlglPADtvgtaAiDLAray
PlAMV                                                  malntaPtadaLaamafpvsSpsVpTaqEldtIts.glttlgvPtDsllshAlaLvnaC
SMYE  mgdqprppvppapgsnplpmgstppvlpgrtpnpnanvanqvgdpfrvltpeeL.aapisaaSnkVATr.Eqilgivadlnalgfvgd.palglfDLAfhC
NMV                                matpstqttdpkpanadlsdpnraPsledLkkikyestttaVATpaEiqllgdlfkklgl.dAnsvapamwDLAray
WClMV                                            matttattpPsltdiralkytsstvsVAspaEieaItktwaetfkiPnDvlplacwDLAraf
PVX                msapasttqatgsttstttktagatpatasglftiPdgdffstaraivaSnaVAT.nEdlskieaiwkdmkvPtDtmaqaAwDLvrhC
CYMV                                            mtdtkktlfsaPtdeqLdtltltieSnlVpsisEleaIakdwktlglqeADfta.nAikiAwfC
PMV                                          mskssmstpniafpaitqeqmssikvdptSnllps.qEqlksvstlmvaakvPAasvttvAleLvnfC
LVX                                                     mttfvPdaktwadtaytaqSesVATaeElqsIatlwegigipaAnffd.vAfqLAmrC
PaMV   mvdskktetpqvvdaskkaensktsqagriqflsapkqfsasdvrssPsladLdeiayevrttsiAspaEieavcqlwirnteiPADkvaliAiDmAray
FMV                                       matgnadvtdatdykkpPaeteqkaltiqprSnkapsdeElvrIinaaqkrgltPAafvq.aAivftm..
                                          1
Cons  ----- ----------------------------------------P----L--------S--VAT--E---I----------PAD-----A-DLA--C

CyMV  aDvGASksatLlGfcptkPdvrraaLAaqifvanvTpRQFCaYYAKvVWNlmLatNdPPANWAkaGfqedtrFAAFDFFDaVdstAALePaecngR.PTdr
PlAMV fDaGsSsfvtLsGpspt.PtislaqiAgvvKv.ttTLRkFCrfYAKiiWNarLarNlPPAgfAraniKfehrwAgFDFFDGllnPAALePpgGLsRtPTpd
SMYE  yDiGsSpsaqpvGpspfgcsr.mqvaAvvrn..hcTLRQlCmfYApsVWNkavrdNrPPgNWsnlqftpetKFAAFDFFDGVlnPAsqevp..LwRqPTpq
NMV   aDvqASrsavLsGttpsnPaitrqaLArqfyviniTpRQFCmYfAKvVWNllLdsNvPPAgWAkqGlpddcKFAgFDFFeGVlsPAALdPadGLIRpPsqr
WClMV aDvGASskseLtGdsaalagvsrkqLAqaiK.ihcTiRQFCmY...niVWNimLdtktPPAsWsklGyKeesKFAgFDFFDGVnhPAALmPadGLIRgPsda
PVX   aDvGsSaqtemidtgpysngisrarLAaaiKe.vcTLRQFCmkYApvVWNwmLtnNsPPANWqaqGfKpehKFAAFDFFnGVtnPAAimPkeGLIRpPsea
CYMV  yhsGsSesvqvqGn.stsdkiplyqLAgvvrqhs.TLRrFCrYfAKviWNyaLrkNqPPANWAsqnyKeadrFAAFDFFeGVsssAALsPpgGLIRePspn
PMV   yDnGsSayttvtGp.ssiPeislaqLAsivKasgtsLRkFCrYfApiiWN.lrtdkmaPANWeasGyKpsaKFAAFDFFDGVenPAAmqPpsGLIRsPTqe
LVX   sDghASsltvLsGnctvaPtvtlkaaAglvK.avlpLRQFCrYYAKfVWNwrLshdlPPANWAdsqfpaearFAAFDFFDGVtnsAApqPpdGLIRpPTel
PaMV  aDvGASrkavLldaptlaPtvarsrLAqlkagagispRQFCsYYAKiVWNlmLhkNePPANWAniGfKedyKFAAFDFFDaVdsPAALePsqwv.RhPTdk
FMV   .DkGAtdstiftGkyn...tfpmksLAlrcKdagvpvhklCyfYtKpayanrrvaNqPPArWtnenvpkanKwAAFDtFDalldPyvv.PssvpydePTpe
     71
Cons  -D-GAS----L-G-----P------LA---K----TLRQFC-YYAK-VWN--L--N-PPANWA--G-K---KFAAFDFFDGV--PAAL-P--GLIR-PT--

CyMV  EraAhsigKygaLaRqriqngnlitni.AevTkGhlgstntlyalpappte
PlAMV EvtAneTarslnLfearasys.nlaststqfTrGqlsntapqvqflpapsd
SMYE  EiyAsaThKdvatyRaaskahdrisns.tllTkGasrstppallpgpda
NMV   EiqAhsTaKygaLaRqryrmetsfppwlkslTvGsavstpctplkhlqncnrntsklklvcgl
WClMV EilAhqTaKqvaLhRdakptwhkrcqlc
PVX   EmnAaqTaafvkitkaraqsnd.fasldAavTrGritgtttaeavvtlppp
CYMV  ErmAneTnKnvhLyqtasrgsn...stva.TkGaystnasnagfpyhrpe
PMV   EriAnaTnKqvhLfqaaaqdnnftsns.AfiTkGqisgstptiqflpppe
LVX   ElsAaqTaKfaaLaR..vrgsgfvt.taAeiThGr...vsrtmllspp
PaMV  EraAhgvvnwasLsRerlqeg.tsittvAelnkGhlygynnlpalmapps
FMV   drqvneifKkdnLsqaasrnqll..gtqAsiTrGrlngapalpnngqyfieapq
    164
Cons  E--A--T-K---L-R-------------A--T-G----------------------------
```

thic "core" consensus KFAAFDFFDGV. In contrast to the relative divergence of potexviral coat proteins, 25 of 158 residues in 7 different tobamovirus coat proteins are absolutely conserved (Altshuh *et al.*, 1987). This relatively high number of conserved residues may be related to the fact that tobamovirus members are rigid helical viruses and all strains may require fairly uniform properties encompassed in a rigid structure. Although all potexviruses have the same general size and shape, they are flexuous, relatively "loose" structures with variable true repeats (Richardson *et al.*, 1981). Consequently, structural options not available to TMV may exist with flexuous viruses and may be reflected in a greater permissible amino acid sequence variation than found among tobamoviruses, or those of other rigid viruses. In addition, the 11-residue core consensus described above is not only well conserved among potexvirus coat proteins but also among the other filamentous viruses, i.e. carla-, poty-, clostero- and bymoviruses. However, it is not present in the rigid helical tobamo-, tobra-, hordei- and furoviruses (Dolja *et al.*, 1991). Therefore, this region may be structurally important for the flexible properties of these viral particles.

3. Subgenomic termini and "promoters".

3.1 Abundant sgRNAs.

Bancroft and co-workers (1991) have determined the exact 5' terminus of the ~0.9 kb sgRNA of FMV by S1 nuclease mapping. It is located 43 nucleotides upstream of the start codon for ORF5 (encoding the coat protein), at position 5323 (Fig. 2.4(2)). The 5' terminal nucleotides of this sgRNA are 5'GAAGA[1]. A putative promoter sequence

[1]By analogy to other potexvirus sgRNAs, the coat protein sgRNA of FMV is likely capped, giving the sequence m^7GpppGAAGA. However, capping was not tested.

Figure 2.4 Initiation of the synthesis of FMV sgRNAs.

Top: The synthesis of sgRNAs likely involves the recognition of a cis-acting element on the (—) strand RNA template by the polymerase. The position of the start sites for the synthesis of the 2.0 kb sgRNA (1) and the 0.9 kb sgRNA (2) are indicated.

(1) The proposed promoter sequence for the synthesis of the 2.0 kb sgRNA (3'CCgAUUgA) is shown on the (—) strand template. It is located 5 nucleotides (nt) upstream of the putative sgRNA synthesis start site. The 5' end of the sgRNA (5'GAcGA) would be located 17 nucleotides upstream of the ORF2 start codon.

(2) The proposed promoter sequence for the synthesis of the 0.9 kb sgRNA (3'aCAAUcCc) is shown on the (—) strand template. It is located 14 nucleotides upstream of the demonstrated 5' end of the sgRNA (5' GAAGA) which lies 43 nucleotides upstream of the coat protein start codon.

The uppercase letters in the promoter and 5' end of sgRNA sequences indicate a match with the consensus motifs proposed by Skryabin *et al.* (1988b) and White *et al.* (1992b).

(1) 2.0 kb sgRNA:

(2) 0.9 kb sgRNA:

for the synthesis of sgRNAs of potexviruses has been identified by Skryabin and coworkers (1988b). It is centered around the usually conserved nucleotides:

5' .GGUUAAGU..
3' .CCAAUUCA..

upstream of the presumed or demonstrated 5' end of sgRNAs of potexviruses. The complementary sequence of this putative sgRNA promoter (underlined) (as it would be present on the (—) strand, i.e. the template for the sgRNA synthesis; Fig. 2.4) resembles the hexanucleotide motif 5'..ACUUAA (Table 2.2), as noticed by White *et al.* (1992b). The sequence 5'..uGUUAgGg.. ((+) strand sequence; nucleotides 5301-5308), 14 nucleotides upstream of the demonstrated 5' end of the coat protein sgRNA of FMV best matches the proposed promoter sequence (capital letters indicate a match) (Fig. 2.4(2)).

Although the exact 5' end of the 1.9 kb sgRNA of FMV has not been determined, the sequence 5'..GAcGA (nucleotides 4116-4120), 10 nucleotides upstream of the start codon specifying ORF2, may denote the terminus of the 1.9 kb sgRNA (Fig. 2.4(1)). It resembles the coat protein sgRNA 5' terminal sequence and a subgenomic message initiating at this location would have a size of 2.0 kb, which corresponds to the experimental value of 1.9 kb (Mackie *et al.*, 1988). Moreover, the sequence 5'..GGcUAAcU ((+) strand sequence; nucleotides 4103-4110), 5 nucleotides upstream of the proposed 5' end of the 1.9 kb sgRNA, resembles the putative sgRNA promoter of potexviruses (Fig. 2.4(1)). Therefore, the cis-acting elements suspected to direct the synthesis of the sgRNAs of FMV generally conform to those proposed for other potexviruses. The similarities of these putative promoter sequences among potexviruses suggest that a common mechanism ay be employed by potexviruses for the synthesis of their sgRNAs and gRNAs by the RNA-dependent RNA polymerase.

3.2 Minor ORFs.

No sgRNAs have been detected for the 11 kDa (ORF3) and 6 kDa (ORF4) cistrons of FMV (Mackie *et al.*, 1988). The predicted size of a sgRNA for ORF4 would be close to that encoding ORF5 (1.0 kb versus 0.83 kb without a poly(A) tail) and may have escaped detection. A sgRNA for ORF3 would be about 1.4 kb and should be resolved from other viral RNA species. However, no messages other than those of ORF2 and ORF5 have been noted for most potexviruses including FMV (Mackie *et al.*, 1988). The presence of a series of additional sgRNAs has been reported in two cases, those of PVX (Dolja *et al.*, 1987) and of daphne virus X (Guilford & Forster, 1986). The lack of sgRNAs for ORF3 and ORF4 of FMV is consistent with the absence of a potential "promoter" sequence or of any other shared motif upstream of the coding regions of the two ORFs. The mechanism by which these ORFs are expressed, assuming that they are, is not understood. It could involve internal ribosome binding on the larger sgRNA or on the gRNA near the start codons for ORF3 and ORF4 (Forster *et al.*, 1993; Hefferon *et al.*, 1994). The p13 product encoded by beet necrotic yellow vein virus, which shares sequence similarity with the product encoded by ORF3 of FMV and of other potexviruses, is expressed *in vivo* (Niesbach-Klösgen *et al.*, 1990) despite the apparent absence of a corresponding sgRNA. This may also be the case for the FMV ORF3 product. Despite these ambiguities, ORFs 2, 3 and 4 have been demonstrated to play a role in the cell-to-cell movement of potexviruses (Beck *et al.*, 1991). Interestingly, SMYEAV which lacks a start codon specifying ORF2, has only been detected in phloem parenchyma cells (Jelkmann *et al.*, 1990). LVX, which lacks the start codon for ORF4, accumulates to very low concentrations in infected tissues and is poorly sap transmissible

(Stone, 1980).

The nucleotide sequence of FMV, and indeed of other potexviruses, offers few clues regarding the function or mode of expression of the putative products of ORFs 3 and 4. Nonetheless, these sequences will serve as a basis for the design of approaches to elucidate their functions, such as by mutagenesis (Beck *et al.*, 1991) and immunological means (Price, 1992).

CHAPTER 3

PARTIAL PURIFICATION AND CHARACTERIZATION OF FMV RNA-DEPENDENT RNA POLYMERASE

3.1 INTRODUCTION

Replication of positive sense RNA virus genomes is achieved by RNA-dependent RNA polymerases (RdRp). Using genomic RNA (gRNA) as template, this enzyme catalyzes the synthesis of a complementary (—) sense RNA which in turn serves as a template for the production of progeny gRNA (see Fig. 1.4). RdRps of a number of plant viruses have been isolated and purified to various extents (reviewed in Quadt and Jaspars, 1989). It has been a difficult task to obtain template-dependent RdRp preparations (enzymes which are able to copy exogenously added template *in vitro*), rather than template-independent RdRps (enzymes which copy RNAs endogenous to the enzyme preparation). Nevertheless, specific template-dependent enzymes have been obtained in a few cases, such as for cucumber mosaic virus (CMV) (Hayes and Buck, 1990), brome mosaic virus (BMV) (Quadt and Jaspars, 1990), turnip yellow mosaic virus (TYMV) (Mouchès *et al.*, 1974) and alfalfa mosaic virus (AlMV) (Houwing and Jaspars, 1986; Quadt *et al.*, 1991) but not for tobacco mosaic virus (TMV) (Young and Zaitlin, 1986), cowpea mosaic virus (Dorssers *et al.*, 1984) and velvet tobacco mottle virus (Rohozinski *et al.*, 1986).

Although several members of the potexvirus group have been well characterized at the molecular level, their replication is poorly understood. The first open reading frame (ORF1) of the potexviral genome likely encodes the viral component of the RNA-dependent RNA polymerase because it contains the helicase-like and polymerase-like motifs found in the amino acid sequences of non-structural proteins of most (+) strand RNA viruses (Habili and Symons, 1989). The importance of the polymerase-like motif for replication of potexviruses has been demonstrated with mutants of potato virus X

(type member of the potexvirus group) which failed to accumulate in protoplasts because of point mutations in this motif (Longstaff *et al.*, 1993). As a first step in elucidating the replication process and in identifying polypeptides which participate in potexviral replication, we have undertaken the purification of the RdRp complex of foxtail mosaic virus (FMV). This chapter describes a procedure for the partial purification of FMV RdRp and the characterization of the products it synthesizes *in vitro*. Most of the findings presented in this chapter have been published elsewhere (Rouleau *et al.*, 1993).

3.2 MATERIALS AND METHODS

1. Enzymes and chemicals.

Miracloth and dodecyl-sucrose were purchased from Calbiochem (California). Glass beads were from Sigma (St-Louis). Glyoxal was from Kodak (Rochester). [α^{32}P]CTP was obtained from Amersham or New England Nuclear. The Protein Assay Kit was purchased from Bio-Rad Inc. Micrococcal nuclease, T4 DNA polymerase, SP6 and T7 RNA polymerases, DNase I and RNAguard were from Pharmacia. *Taq* DNA polymerase and pGEM-4 were obtained from Promega Biotech Inc. (Madison). Moloney murine leukaemia virus reverse transcriptase (M-MuLV RT) was from Bethesda Research Laboratories (Burlington, Ont.). Plasmid pET-3c and *Escherichia coli* strain BL21(DE3) (Studier *et al.*, 1990) were purchased from Novagen (Madison). Isopropyl-ß-thiogalactopyranoside (IPTG) was from Boehringer Mannheim (Laval, Qué). Nonidet P-40 (NP-40) was from Particle Data Laboratories Ltd. (Illinois) and Tween-20 was from Sigma. Alkaline phophatase-conjugated goat anti-rabbit antibodies were obtained from Sigma Immunochemicals. 5-bromo-4-chloro-3-indoyl phosphate p-toluidine salt and p-

nitro-blue tetrazolium chloride were purchased from Bio-Rad Inc. Nitrocellulose and polyvinyldifluoride (PVDF) membranes were purchased from Bio-Rad Inc. and Millipore (Bedford, MA), respectively. All other reagents were obtained as described in Chapter 2.

2. Inoculation of plants.

Inocula were prepared by grinding leaves systemically infected with the appropriate virus in H_2O in a mortar. Leaves of the plants to be inoculated were dusted with aluminum oxide (Grit 600), which served as an abrasive. Leaves were then gently rubbed with the sap inoculum.

3. Viral infections, RNAs and coat protein.

FMV and clover yellow mosaic virus (CYMV) virions were propagated in barley (*Hordeum vulgare*) and broad bean (*Vicia faba*), respectively. Virions and gRNAs were prepared as described by Bancroft *et al.* (1979) and Erickson and Bancroft (1978), respectively (see also section 2.2.5). The FMV coat protein was prepared from purified virions using 4M LiCl. One volume of virus solution was mixed with an equal volume of 4M LiCl containing 10 mM EDTA, pH 8.0. Prior to its use, the LiCl solution was treated overnight with 0.1 % diethylpyrocarbonate (DEPC) and autoclaved, to destroy any ribonucleases which may be present. The virus-LiCl mixture was kept frozen at -20°C for approximately 48 hrs, thawed on ice and centrifuged at 10,000 rpm for 10 min (JA-20 rotor, Beckman) to pellet the viral RNA. To remove remaining virion particles, the solution was subsequently centrifuged at 40,000 rpm for 1 hr (Ti 70.1 rotor, Beckman). The supernatant solution, containing the coat protein, was dialyzed for 12-24 hrs against 50 mM Tris-HCl, pH 8.0. BMV virions were grown in barley and BMV gRNAs were prepared according to Bancroft *et al.* (1968). Virus titres in the sap of

infected plants were measured by a standard half-leaf technique (Matthews, 1991) using *Chenopodium quinoa* as the local lesion assay host. Five to eight leaves were used per assay. All plants were raised in a greenhouse at 26-28°C. For trial purifications, FMV was grown in *C. quinoa* kept at higher temperatures (30-32°C) necessary for good lesion formation, and in barley (a systemic host) at ~26°C. *C. quinoa* leaves were usually harvested 4-6 days following inoculation, when lesions were well developed. The mid-rib of harvested *C. quinoa* leaves was removed prior to homogenization. For barley, only systemically infected leaves were harvested, around 2 weeks following inoculation, when systemic symptoms were evident.

4. Extraction of RNA-dependent RNA polymerase (RdRp) from FMV infected plants.

The procedure used to isolate an active RdRp membrane fraction is based on that developed by Bradley and Zaitlin (1971) for TMV. All steps were carried out at 4°C. Leaf tissue (5 g) was homogenized in a mortar, using 14 ml of buffer A (0.4 M sucrose; 10 mM KCl; 5 mM $MgCl_2$; 50 mM Tris-HCl, pH 8.2; 20% glycerol; 10 mM β-mercaptoethanol). For barley leaves, glass beads were also included in the homogenization mixture. The homogenate was filtered through a single layer of Miracloth prior to centrifugation at 1,000 x *g* for 10 min (JA-20 rotor) to remove cell debris. The resulting supernatant solution was centrifuged at 30,000 x *g* for 30 min in a JA-20 rotor, in order to separate the soluble material (S30K) from the membrane fraction (P30K). The P30K fraction was resuspended in 1 ml of buffer B (0.75 M KCl; 25 mM NH_4Cl; 50 mM Tris-HCl, pH 8.2; 7.5% glycerol; 2.5% dodecyl-sucrose; 10 mM β-mercaptoethanol; 0.1 mM phenylmethylsulfonyl fluoride (PMSF); 10 mM EDTA).

The suspension was stirred for 1.5 hr and then centrifuged at 120,000 x *g* for 1 hr (70.1 Ti rotor) to separate the solubilized RdRp activity (S120K) from the membrane fraction. A number of detergents were tested for their ability to solubilize the RdRp activity, such as CHAPS, Triton X-100, NP-40, ß-dodecyl maltoside and dodecyl sucrose, in various concentrations, in the presence of 0.1-1 M KCl. ß-dodecyl maltoside and dodecyl sucrose in the presence of 0.75 M KCl gave optimal solubilization of the activity. The volume of the S120K fraction was reduced to 0.25 ml using an Amicon ultrafiltration unit equipped with a YM-10 membrane and was subsequently diluted to 0.5 ml in buffer B devoid of KCl and glycerol. This step allowed a reduction in the density of the S120K fraction prior to loading it onto a 25-45% linear glycerol gradient (11.5 ml) prepared in buffer B containing 100 mM KCl and 2.0% dodecyl-sucrose. Gradients were centrifuged at 33,000 x *g* in a SW 41 Ti rotor (Beckman) for 20 hr at 2°C. Fractions (0.5 ml) were collected from the bottom of the tube using a peristaltic pump and assayed for RdRp activity. A flow diagram of this purification procedure is shown in Appendix III.

5. RNA-dependent RNA polymerase assays.

RdRp activity was tested in a 100 μl reaction mixture containing 50 μl of the fraction to be tested, 5 mM $MgCl_2$, 20 mM $(NH_4)_2SO_4$, 100 mM Tris-HCl, pH 8.0, 0.5 mM each of ATP, GTP, UTP, 5 μM CTP, 4 μCi [α-^{32}P]CTP (3000 Ci/mmol) and 7.5 mM dithiothreitol (DTT). Reactions were incubated at 30°C for 60 min, then terminated by the addition of 50 μl of a stop mixture (30 mM EDTA; 6 M ammonium acetate; 100 ng/μl yeast RNA). In some assays, actinomycin D was added to the reaction mixture, in concentrations described in the text. A stock solution of actinomycin D (2 μg/μl) was prepared in 95 % ethanol (Sambrook *et al.* 1989). Control reactions containing 95 %

ethanol in proportions similar to the reactions containing the drug were prepared. RNA products were extracted twice with P/C/I and precipitated with ethanol.

6. Micrococcal nuclease treatment of RdRp fractions.

Fifty μl of a RdRp fraction was supplemented with calcium chloride (final concentration of 1 mM) prior to the addition of 4 to 20 units of micrococcal nuclease. The final volume of the mixture was brought to 70 μl with ddH_2O prior to incubation for 30 min at 30°C. Nuclease activity was subsequently stopped by the addition of EGTA to a final concentration of 5 mM and the treated fraction was assayed for polymerase activity in conditions similar to those described above.

7. Analysis of RdRp reaction products.

RNA products were resuspended in 8 μl DEPC treated-H_2O, mixed with 2 μl of gel loading buffer and electrophoresed in 1.2% agarose gels using 1 mM sodium phosphate (pH 7.0) running buffer (McMaster and Carmichael, 1977). The buffer was recirculated during electrophoresis. The gel was subsequently placed onto a piece of Whatman paper, dried for 60 min in a 43°C oven and then for an additional 1.5 hr in a gel drier at 80°C. Products were detected by autoradiography of the dried gel at -70°C. The bands corresponding to high molecular weight products were cut out of the gel and counted for Cerenkov radiation in order to quantify the RdRp activity of each fraction. Alternatively, relative RdRp activity was estimated by densitometric analysis of autoradiographs using a Gel Print system (BioPhotonics corporation) equipped with the Gel Print Toolbox software.

8. Nuclease treatment of RdRp products.

i) <u>S1 nuclease</u>. RdRp products generated by a P30K fraction were resuspended

in S1 buffer (280 mM NaCl; 50 mM sodium acetate, pH 4.5; 4.5 mM $ZnSO_4$; 20 μg/ml denatured salmon sperm DNA). S1 nuclease was added to a final concentration of 5-1000 U/ml. Samples were incubated at room temperature for 30 min.

ii) Ribonuclease A. RdRp products generated by a S120K fraction were resuspended in either 2X or 0.1X SSC (2X SSC: 300 mM NaCl, 30 mM sodium citrate, pH 7.0). RNase A was added to a final concentration of 0.1 or 1 μg/ml and samples were incubated at 37°C for 15 min. Both nuclease treatments were subsequently terminated by the addition of a stop mixture (250 μg/ml yeast RNA; 25 mM EDTA; 2 M ammonium acetate), products were extracted once with P/C/I, precipitated with ethanol and subsequently analyzed by electrophoresis in non-denaturing conditions as described above.

9. Plasmid constructions.

Plasmids p133X [1430-6151(A_{13})], p124X [17-1194], p133XS [4696-6151(A_{13})], p107X [1-2007] and p90X [1863-6151(A_7)] consist of cDNA fragments spanning different regions of FMV genome described by the coordinates indicated between brackets, inserted in the vector pSP65 (Melton *et al.*, 1984) as described previously (Bancroft *et al.*, 1991).

Plasmid pMR1, which contains sequences from the 5' and 3' extremities of FMV gRNA, was constructed as follows. First, a cDNA fragment containing the 5' terminal 604 nucleotides of FMV gRNA was prepared by reverse transcription (RT) followed by polymerase chain reaction (PCR). The synthesis of the first cDNA strand was initiated by annealing 100 pmoles of oligonucleotide MR-8 (Appendix I) to 0.5 μg of purified FMV gRNA in a volume of approximately 13 μl. The mixture was heated at 95°C for

2 min, then incubated sequentially at 45°C and room temperature, each for 10 min. Extension of the primer was carried out at 50°C for 40 min in a reaction volume of 25 μl containing 50 mM Tris-HCl, pH 8.3, 75 mM KCl, 3 mM $MgCl_2$, 0.8 mM each of the four deoxyribonucleoside triphosphate and 200 U of M-MuLV RT. The cDNA produced was then used as a template for PCR amplification. The cDNA synthesis mixture was supplemented with 100 pmoles of a second primer, MR-2 (Appendix I), which contains the sequence of an *Eco*RI restriction site, followed by a T7 RNA polymerase promoter sequence and nucleotides 1-25 of FMV gRNA sequence. Amplification buffer (to give final concentrations of 50 mM KCl, 10 mM Tris-HCl, pH 9.0, 1.5 mM $MgCl_2$, 0.01 % gelatin and 0.1 % Triton X-100), 2.5 U *Taq* polymerase and ddH_2O to a final volume of 100 μl were then added and the reaction mixture was overlayed with 100 μl paraffin oil to prevent evaporation during the PCR. The amplification was carried out for 30 cycles. The first cycle consisted of a denaturation step at 95°C for 5 min, annealing step at 50°C for 2 min and an elongation step at 72°C for 5 min. The 28 subsequent cycles had a denaturation of 1 min, annealing of 2 min and elongation of 4 min. The last cycle had an extended elongation step of 10 min. The products of the PCR reaction were analyzed in a non-denaturing polyacrylamide gel in TBE buffer and eluted from the gel as described in section 2.2.3. The PCR-derived cDNA was subsequently restricted with *Nco*I (at nucleotide 604) and blunt-end repaired. For this reaction, the mixture consisted of 33 mM Tris-acetate, pH 7.9, 66 mM potassium acetate, 10 mM magnesium acetate, 0.5 mM DTT, 100 μg/ml bovine serum albumin (BSA), 0.125 mM each of dATP, dCTP, dGTP and dTTP, and 0.25 U/μl of T4 DNA polymerase in a final volume of 50 μl. It was incubated for 15 min at ambient temperature. The reaction mixture was

subsequently extracted once with P/C/I and precipitated with ethanol. The recovered cDNA fragment was then restricted with *Eco*RI and ligated to *Eco*RI/*Sma*I digested pSP64 (Melton *et al.*, 1984). The recombinant plasmid was subsequently restricted with *Nco*I and *Xba*I and ligated to a *Nco*I/*Xba*I fragment from p133XS, corresponding to the 3' terminal 584 nucleotides of FMV genome followed by 13 adenines, to generate pMR1. The *Nco*I/*Xba*I DNA fragment was prepared by restriction of p133XS with the enzymes *Nco*I and *Xba*I. Analysis and elution of the fragment from a polyacrylamide gel were as described above.

Plasmid pAW1, containing a full-length cDNA fragment of CYMV defective RNA (D-RNA), has been described previously (White *et al.*, 1991). Plasmid $pAWA_{14}$, which consists of the 3' terminal 250 nucleotides of CYMV genome and a poly(A) tract of 14 residues cloned between *Eco*RI and *Sal*I sites in pGEM-4, was a gift from Dr K.A. White.

10. Synthesis of RNA transcripts.

Transcripts used in this study are schematically represented in Table 3.1 (p.107). Plasmids p133X and p90X were linearized with *Pvu*II and served as templates for FM(+) and FM(—) transcript synthesis, respectively; p124X was linearized with *Hin*dIII and directed the synthesis of I·M5(+) transcript; p133XS and pMR1 were linearized with *Xba*I and were templates for FM3(+) and FMV mini-RNA(+) transcript synthesis, respectively; p107X was linearized with *Acc*I to direct FM5(—) synthesis; *Sal*I linearized p90X served as template for FM3(—); $pAWA_{14}$ was linearized with *Eco*RI or with *Hin*dIII and directed the synthesis of CY3(+) and CY3(—), respectively; pAW1 was linearized with *Sal*I to direct the synthesis of CYMV D-RNA(+).

Transcription reactions contained 50 ng/μl of linearized plasmid, 10 mM DTT, 1 U/μl RNAguard, 0.5 mM each of ATP, CTP, GTP and UTP, 40 mM Tris-HCl, pH 7.5, 6 mM $MgCl_2$, 2 mM spermidine, 10 mM NaCl and 0.6 U/μl RNA polymerase in a 100 μl reaction volume. Transcription was catalyzed by SP6 RNA polymerase, except for the synthesis of FMV mini-RNA(+), CY3(+) and CYMV D-RNA(+), for which T7 RNA polymerase was used. Reactions were incubated for 1 hr at 37°C, the concentration of the polymerase was raised to 1.2 U/μl and incubation at 37°C was continued for an additional hour. Ten units of DNase I were added to the reaction mixtures and incubated at 37°C for 15 min. Final transcription mixtures were extracted once with P/C/I and precipitated twice with ethanol. The resulting RNA transcripts were resuspended in 50 μl H_2O and were quantified by measuring their A_{260} or by assessing their quality and quantity from ethidium bromide-stained polyacrylamide gels in which the transcripts were electrophoresed. The vector pSP65 linearized with *Pvu*II served as a template for SP6 RNA polymerase to prepare control transcripts. The synthesis of ^{32}P-labeled RNA transcripts was in conditions similar to those described above with the following exceptions. The concentration of CTP was 5 μM and 50 μCi of [α-^{32}P]CTP (3000 Ci/mmol) was added to the reaction mixture.

11. Characterization of RdRp products.

i) <u>Isolation of RdRp products</u>. Products generated by forty 100 μl reactions catalyzed by the P30K fraction were fractionated by centrifugation through 5-20% sucrose gradients prepared in 10 mM Tris-HCl, 100 mM LiCl, 1 mM EDTA, 0.1% SDS, pH 7.4. Fractions containing high molecular weight products were combined, the

RNA was precipitated with ethanol and resuspended in 10 μl DEPC-H_2O.

ii) Slot blots and hybridization. RNA transcripts and purified FMV gRNA were denatured in 1 M deionized glyoxal, 50 % (v/v) dimethyl sulfoxide and 10 mM Na phosphate, pH 7, at 50°C for 60 min, in a final volume of 30 μl (McMaster and Carmichael, 1977). Twenty X SSC (60 μl) was added to each RNA sample prior to blotting onto nitrocellulose according to Sambrook *et al.* (1989) using a slot blot apparatus (Schleicher and Schuell). The nitrocellulose membrane was baked for 2 hrs at 80°C. The membrane was then prehybridized in a standard hybridization buffer (50 % formamide, 5X SSC, 5X Denhardt's solution, 0.1 % SDS, 250 μg/ml yeast RNA) at 47°C for 12-24 hrs. The ^{32}P-labeled RNA products were denatured by heating at 95°C for 3 min, cooled on ice and added to 12 ml of hybridization buffer (~ 4 x 10^4 cpm/ml) in which the membrane was incubated at 47°C for 12 hrs. The membrane was washed twice for 10 min in 2X SSC, air dried and autoradiographed. In control experiments, the labeled RNA product probe was replaced by ^{32}P-labeled FM(+) or FM(—) transcripts (~ 1 x 10^5 cpm/ml) to verify the specificity of hybridization.

12. Generation of an anti-serum against p152, the ORF1-encoded product of FMV.

i) Construction of a p152 expression plasmid. Plasmid p105X (section 2.2.3) was restricted with *Eco*RI and served as a template for the amplification of a portion of the ORF1 coding region (nucleotides 1511-2120) by PCR. Primers used in the PCR reaction, FMV1-1 and FMV1-2 (Appendix I), were designed to introduce *Bam*HI restriction sites flanking the coding regions. Primers were also designed to introduce a C→T change at position 1519 to create a start codon (FMV1-1) and a C→G change at position 2111 to

introduce a stop codon (FMV1-2). The amplification was carried out as described in section 3.2.9 using 100 pmoles of each primer and 100 ng of p105X. The PCR-amplified cDNA was restricted with *Bam*HI, analyzed in and eluted from a non denaturing polyacrylamide gel as described in section 2.2.3. It was then ligated to *Bam*HI-linearized pET-3c vector. *E. coli* strain MV1190 was transformed with the ligation mixture and recombinant plasmids were prepared as described in section 2.2.3. Recombinant plasmids were identified by digestion with *Bam*HI. The nucleotide sequence of the FMV-derived insert in the recombinant plasmid was verified by the dideoxynucleotide chain termination method as described in section 2.2.4.

ii) Expression of a portion of p152 (p152s) in *E. coli*. *E. coli* strain BL21(DE3) was transformed with the recombinant vector, grown at 30°C in 100 ml M9ZB (1% casitone, 0.5% NaCl, 0.1% NH_4Cl, 0.3% KH_2PO_4, 0.6% Na_2HPO_4, 0.2% glucose, 1 mM $MgSO_4$) until an OD_{600} of 0.5 was reached. Expression of T7 RNA polymerase and p152s were induced by dilution of the culture with 100 ml of M9ZB containing 1 mM isopropyl-ß-thiogalactopyranoside (IPTG) followed by incubation for 3 hrs at 30°C. Cells were pelleted by centrifugation in a JA-14 rotor (Beckman) at 10,000 *x g* for 10 min, resuspended in an ice-cold lysis buffer (20 mM Tris-HCl pH 7.4; 500 mM NaCl; 10% glycerol; 1 mM EDTA; 1 mM PMSF; 5 μg/ml leupeptin; 0.1% NP-40) and frozen in a dry ice/ethanol bath. Cells were stored overnight at -70°C. All subsequent steps were carried out at 4°C. Cells were thawed and lysed by two passages in a French pressure cell at 12,000 psi. The cell paste was centrifuged in a JA-20 rotor at 10,000 *x g* for 10 min. The pellet, which contained most of the overexpressed p152s, was washed three times in lysis buffer containing 3 % NP-40 and 0.5 M NaCl.

iii) Generation of antibodies. Proteins in the washed pellet fraction were electrophoresed in 6 % polyacrylamide preparative gels in conditions described in the following section. Gels were stained with a 0.05% Coomassie Blue R-250 solution for 20 min and destained in water. The region of the gel containing p152s was excised. Polyacrylamide gel pieces were lyophilized and pulverized with a mortar and pestle. Approximately 100 mg of dehydrated ground gel powder (containing approximately 200 μg of p152s) was hydrated in 1 ml of 0.85% NaCl for 30 min at room temperature. The mixture was emulsified with 1 ml of Freund's incomplete adjuvant using a drill press fitted with a stainless steel spatula with a twisted blade prior to multiple intramuscular injections into a rabbit. A pre-immune serum was obtained prior to the first injection and subsequently, six series of injections were performed at three week intervals. The rabbit was then exanguinated by heart puncture.

13. Protein analysis.

The concentration of proteins in the various fractions obtained during the RdRp purification was determined by the Bradford dye-binding procedure (Bradford, 1976) using the Bio-Rad Protein Assay Kit.

Analysis of proteins on gels was as follows. Protein samples were prepared in 1X SDS-sample buffer (120 mM Tris-Cl, pH 6.8; 3% SDS; 50 mM dithiothreitol; 10% glycerol; 0.1% bromophenol blue), boiled for 3 min and electrophoresed in 6 % polyacrylamide gels (36:1 acrylamide:bisacrylamide) containing 0.1% SDS in Laemmli running buffer (25 mM Tris; 192 mM glycine; 0.1% SDS) (Laemmli, 1970). Gels were soaked for 30 min in transfer buffer at room temperature prior to blotting. Proteins were then transferred to a polyvinyldifluoride (PVDF) membrane using a carbonate transfer

buffer (10 mM $NaHCO_3$; 3 mM Na_2CO_3; pH 9.9; 20% CH_3OH) (Dunn, 1986) in a Bio-Rad mini-transblot system. Transfer was for 1 hr at a constant current of 0.25 A (voltage was approximately 30-40 V). The protein blots were subsequently reacted with the anti-p152s serum [diluted 1:100 in PTBN buffer (20 mM Na phosphate, pH 7.0; 0.1 mM bovine serum albumin; 0.85% NaCl; 0.05% Tween-20; 1 mM NaN_3; pH 7.4) containing 5% casein] at room temperature, for 2 hrs with shaking. Blots were washed in three changes of PTBN for 15 min and were then incubated for 1.5 hrs with alkaline phosphatase-conjugated goat anti-rabbit IgG antibodies (diluted 1:3000 in PTBN) and washed as described above. The bound antibodies were detected using 5-bromo-4-chloro-3-indoyl phosphate p-toluidine salt and p-nitro-blue tetrazolium chloride as substrates as described by the manufacturer (Bio-Rad Inc.).

3.3 RESULTS AND DISCUSSION

1. Partial purification of FMV RdRp.

We designed a procedure for the isolation and partial purification of FMV RdRp from infected *C. quinoa*, a local lesion host of FMV. Infected tissue was homogenized and fractionated by differential centrifugation. The membrane fraction (P30K) contained a polymerizing activity capable of synthesizing products of various sizes when incubated in the presence of ribonucleotides (Fig. 3.1A, lane 2). In contrast, the supernatant fraction (S30K) contained little of this activity (not shown). Heterogeneous products of low molecular weight (< 2.2 kb; LMW) as well as a relatively discrete higher molecular weight product with an apparent size of approximately 9.4 kb were generated by a P30K fraction prepared from infected *C. quinoa* (Fig. 3.1A, lane 2). In contrast, the P30K

Figure 3.1 FMV RdRp activity during the course of its partial purification from *C. quinoa*. A flow diagram of the purification procedure is shown in Appendix III.

(A) Products generated by P30K (lanes 1, 2), S120K (lanes 3, 4) and P120K (lanes 5, 6) fractions prepared from either healthy (lanes 1, 3, 5) or FMV-infected (lanes 2, 4, 6) plants (as in section 3.2.4) were analyzed by electrophoresis in non-denaturing conditions and detected by autoradiography (section 3.2.7). HMW: high molecular weight products; LMW: low molecular weight products. In the right margin, the arrow indicates the mobility of FMV gRNA and the mobility of λ-*Hin*dIII DNA markers (kbp) is shown.

(B) Solubilized RdRp was centrifuged through a glycerol gradient and fractions were collected from the bottom of the tube, as in section 3.2.4. The relative RdRp activity was determined by counting the radioactivity of the products generated by 50 μl of each fraction. The protein concentration of each fraction was also assayed (section 3.2.13).

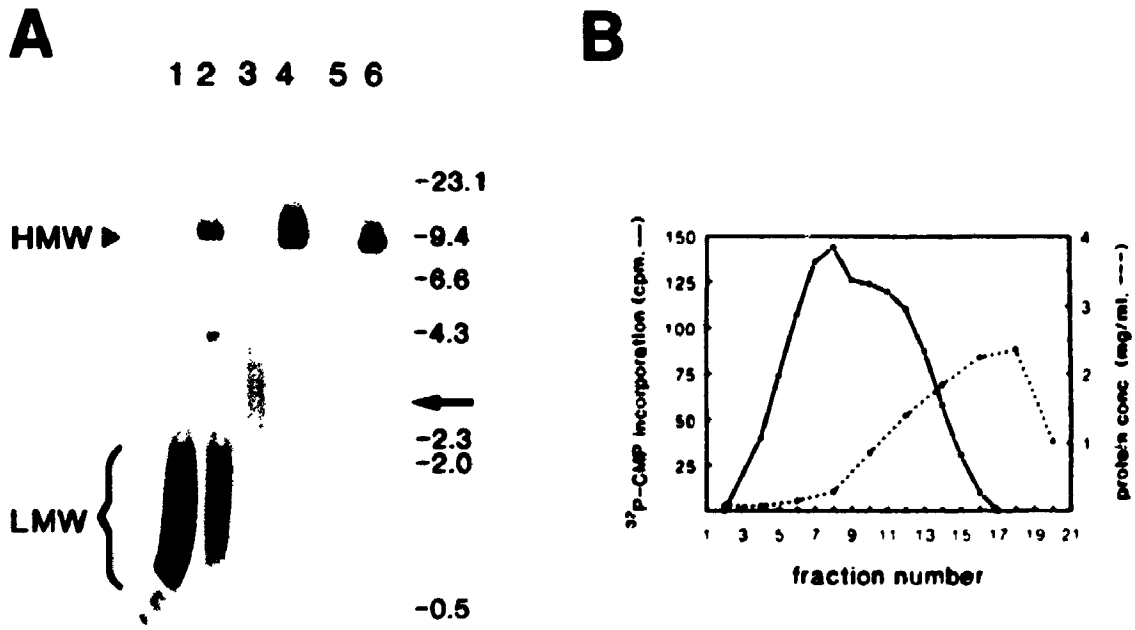
A
1 2 3 4 5 6
HMW
LMW
-23.1
-9.4
-6.6
-4.3
-2.3
-2.0
-0.5
B
^{32}P-CMP incorporation (cpm, —)
protein conc (mg/ml, ---)
150
125
100
75
50
25
4
3
2
1
1 3 5 7 9 11 13 15 17 19 21
fraction number

fraction obtained from healthy plants only catalyzed the synthesis of LMW products (Fig. 3.1A, lane 1), suggesting that synthesis of the high molecular weight (HMW) product is the result of FMV infection. The synthesis of both types of products required the presence of all four ribonucleotides, indicating that the labeled products do not arise from a terminal transferase-like activity (Fig. 3.2, lane 2). Moreover, actinomycin D partially inhibited the synthesis of LMW products, while synthesis of HMW product was not affected by this inhibitor of DNA-dependent RNA synthesis (Fig. 3.2, lanes 3-6).

In order to define the time of harvest post-inoculation (p.i.) which would be most suitable for obtaining maximum yields of enzyme, we monitored the appearance of the polymerizing activity following the inoculation of *C. quinoa* and of the systemic host barley. P30K fractions were prepared from infected leaves and were assayed for RdRp activity. In *C. quinoa*, the membrane-associated activity was detectable as early as two days following inoculation (Fig. 3.3A, lane 2) and peaked between days 3 and 4 (Fig. 3.3A, lane 4), when lesions were developing. The RdRp activity was maintained for at least 12 days p.i. (Fig. 3.3A, lane 12), by which time the necrotic lesions were well developed. The virus titres (Fig. 3.3B), measured from the sap of the same leaf homogenates prepared for measurements of RdRp activity, were determined using *C. quinoa* for local lesion assays. In general, the increase in RdRp activity paralleled the increase in virus titre. These observations are summarized in Figure 6.1A (Chapter 6). The kinetics of accumulation of FMV RdRp were slower in barley than in *C. quinoa* (Fig. 3.3C). Using only non-inoculated leaves as starting material, the RdRp activity was first detected on day 8 p.i. (Fig. 3.3C, lane 8), when symptoms were just developing, peaked between days 12 and 13 (Fig. 3.3C, lanes 12 and 13) and remained detectable for

Figure 3.2 Characterization of RdRp activity in P30K fraction from infected *C. quinoa*.

Terminal transferase activity. Products were synthesized in normal conditions (lane 1) or in a reaction mixture lacking ATP, GTP and UTP and containing only [α^{32}P]CTP (lane 2) as in section 3.2.5.

Effect of actinomycin D. Reactions mixtures were supplemented with 0.5 % (lane 3) or 5 % (lane 5) of ethanol or with 10 μg/ml (lane 4) or 100 μg/ml (lane 6) of actinomycin D as described in section 3.2.5.

Products generated were electrophoresed in non-denaturing conditions and detected by autoradiography (section 3.2.7). The arrow in the right margin indicates the HMW products.


1 2 3 4 5 6

Figure 3.3 FMV RdRp activity and virus titres following inoculation of plants.

Products generated by FMV RdRp activity in P30K fractions prepared from *C. quinoa* (A) or barley (C) on the days post-inoculation indicated above the lanes or from a mock-inoculated (M) plant were separated by electrophoresis and detected by autoradiography. The arrowhead in the right margin indicates HMW products. The infectivity of sap from *C. quinoa* (B) or barley (D) at times of harvest was measured by a standard half-leaf technique and is expressed relative to the infectivity of the sap at the last day of the respective experiment.

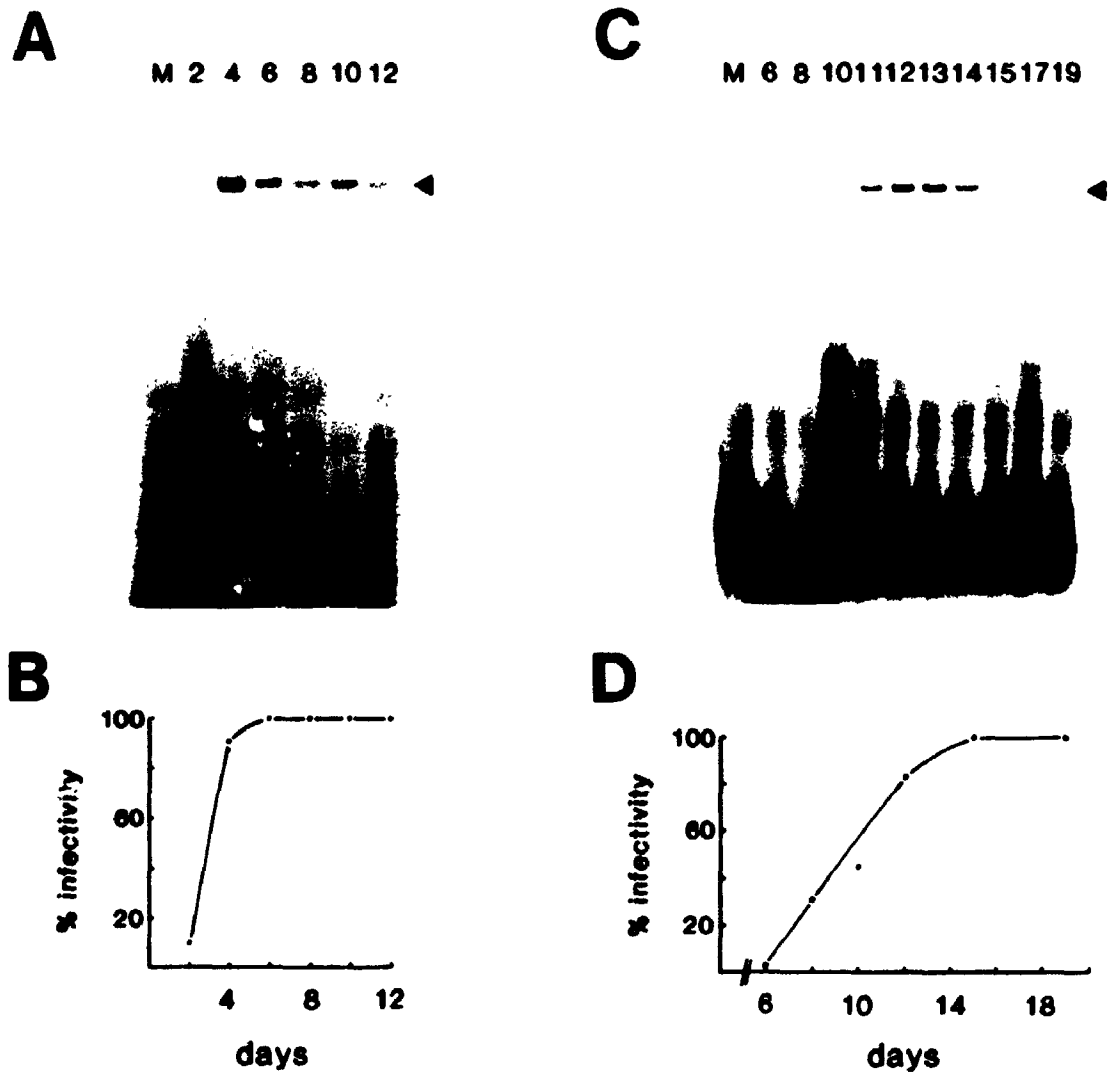
A
M 2 4 6 8 10 12
C
M 6 8 10 11 12 13 14 15 17 19
B
100
60
20
% infectivity
4
8
12
days
D
100
60
20
% infectivity
6
10
14
18
days

at least 6 additional days (Fig. 3.3C, lane 19). In barley, the continuous spread of the virus to growing leaves likely contributes to the maintenance of the observed stable levels of RdRp activity. The increase in virus titre measured in barley extracts also coincided with the increase in RdRp activity (Fig. 3.3D). These data are correlated with several other parameters of the infection in Figure 6.1B. Several varieties of barley were tested for the propagation and the extraction of the RdRp activity. There was no significant difference in terms of yields of enzyme among the varieties, and these yields were lower than those obtained with *C. quinoa* (data not shown). Since the local lesion host *C. quinoa* produced the highest yields of enzyme per gram of wet weight with a shorter lag after inoculation, it was chosen as the preferred host for investigating the further purification of FMV RdRp.

As is the case for virtually all RdRps of plant viruses examined, FMV RdRp activity is associated with a membrane fraction (P30K). Optimal solubilization of the RdRp complex from the membranes was achieved by treating the P30K fraction with the detergent dodecyl-sucrose in the presence of KCl as described in section 3.2.4. Soluble and membrane fractions were subsequently resolved by centrifugation at 120,000 x *g*. This treatment resulted in the solubilization of approximately 60-75% of the total activity contained in the P30K fraction (Fig. 3.1A, compare lanes 4 and 6). Optimal solubilization was obtained at a concentration of 0.75 M KCl and 2.5% dodecyl-sucrose. In contrast, dodecyl-sucrose or KCl alone did not release any of the RdRp activity from the membranes (not shown). The solubilized RdRp fraction (S120K) was further purified by fractionation in a 25-45% glycerol gradient, allowing a significant separation of FMV RdRp from the bulk of the contaminating proteins (Fig. 3.1B). The wide distribution of

RdRp activity in the gradient suggests that the enzymatic complex is heterogeneous. This observation was not investigated further, however. P30K, S120K and pooled active glycerol gradient (GGP) fractions generated by this purification procedure were stored at -70°C for several months without any detectable loss of activity and withstood several freeze-thaw cycles. FMV RdRp activity is strictly dependent on the presence of Mg^{2+} ions and exhibits optimal activity in the presence of 5 mM $MgCl_2$ (data not shown). Further fractionation of FMV RdRp by chromatography of the GGP on DEAE-Sepharose CL-6B in buffer B lacking KCl (section 3.2.4) resulted in the complete loss of RdRp activity (data not shown).

2. Distribution of p152 in fractions from the RdRp purification.

It has been previously proposed that the protein encoded by ORF1 (p152) is the viral component of the RdRp complex of potexviruses. To obtain further support for this hypothesis, we have raised antibodies against p152 and analyzed the distribution of p152 in the fractions generated during the purification of the RdRp activity. The anti-serum detected p152 in P30K, S120K and P120K fractions prepared from infected tissues (Fig. 3.4A, FMV lanes) but not in samples from mock-inoculated plants (Fig. 3.4A, MOCK lanes). Similarly, p152 was present in active RdRp fractions from glycerol density gradients of infected tissues (Fig. 3.4B, FMV lanes) while protein bands with a mobility similar to p152 were not detected in equivalent fractions from the gradients of mock-inoculated plant samples (Fig. 3.4B, MOCK lanes). Proteins with smaller molecular weights were also detected in samples from infected plants by the p152 anti-serum (Fig. 3.4A and B, FMV lanes). These are likely degradation products of p152 since the majority is not present in the mock-inoculated samples (Fig. 3.4A and B, MOCK lanes).

Figure 3.4 Distribution of p152 in fractions from FMV-infected *C. quinoa* and barley.

(A) Protein samples prepared from the fractions P30K, S120K, and P120K (3rd and 7th lanes from left) equivalent to 2 or 25 mg (P120K, 4th and 8th lanes from left) of leaves from mock-inoculated (MOCK) or FMV-infected (FMV) *C. quinoa*. They were separated by SDS-PAGE, electroblotted onto PVDF membrane and immunoreacted with the p152 anti-serum as described in section 3.2.13. The fractions from which the samples were prepared are indicated above the lane ("K" was omitted for reasons of space). The mobility of molecular weight markers (kDa) is indicated in the left margin.

(B) p152 in glycerol gradient fractions. S120K fractions from mock-inoculated (MOCK) or FMV-infected (FMV) leaves were separated through glycerol gradients (see section 3.2.4). Fractions #2, #6, #12 and #18 from each gradient were then analyzed, using protein samples equivalent to 5 mg of leaves.

(C) Time-course of appearance of p152 in *C. quinoa*. P30K fractions from mock-inoculated plants (M) or from plants infected with FMV for 2, 4, 6, 8, 10 or 12 days were analyzed using protein samples corresponding to 2 mg of fresh tissue for each lane. The mobility of molecular weight markers (kDa) is indicated in the left margin.

(D) Time course of appearance of p152 in barley. P30K fractions from mock-inoculated plants (M) or from plants infected with FMV for 6, 8, 10, 11, 12 13, 14, 15, 17 or 19 days were analyzed using protein samples corresponding to 2 mg of fresh tissue for each lane.

Arrowheads point at p152.

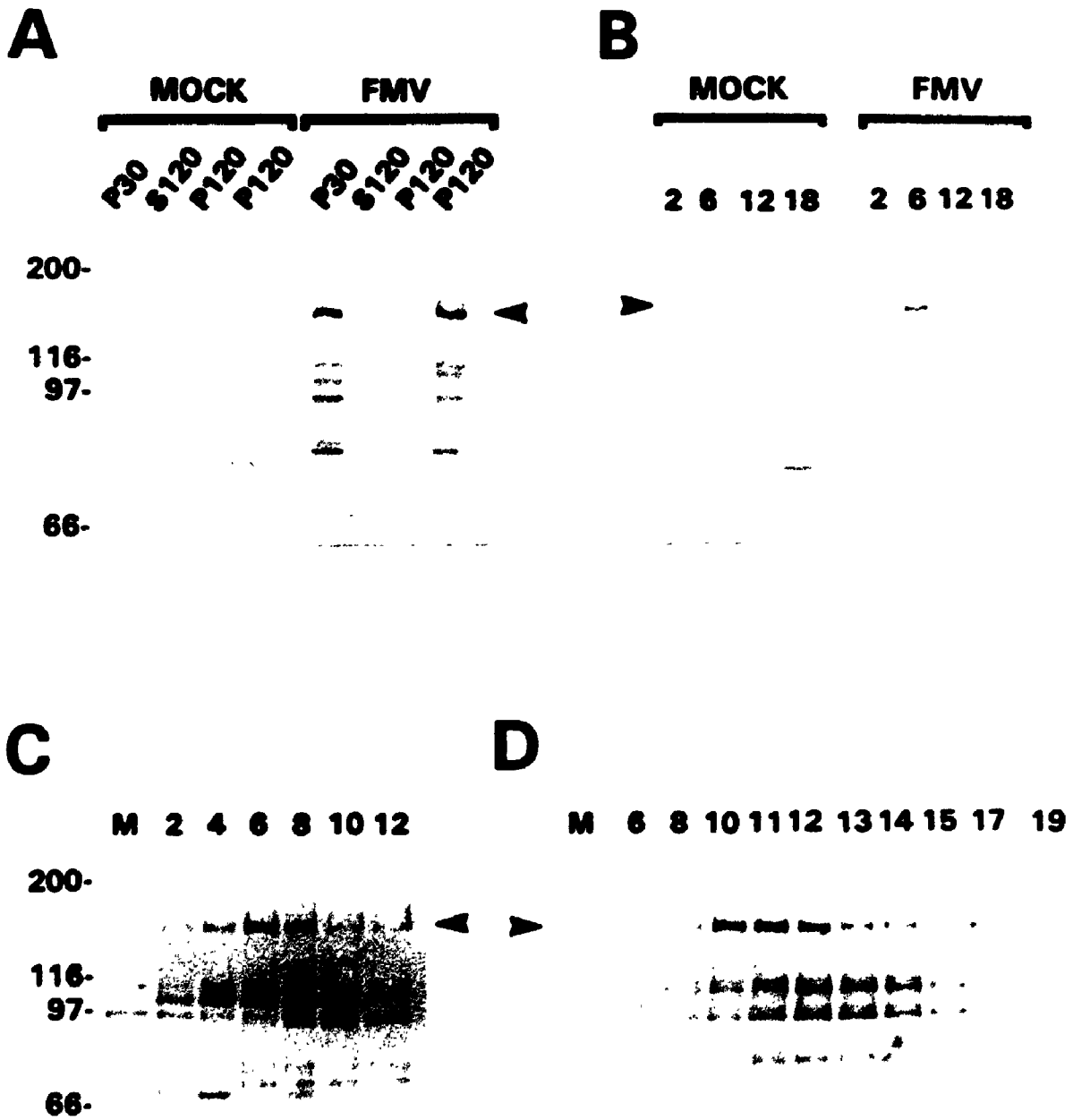
A
MOCK
FMV
P30
S120
P120
P120
P30
S120
P120
P120
200-
116-
97-
66-
B
MOCK
FMV
2 6 12 18
2 6 12 18
C
M 2 4 6 8 10 12
200-
116-
97-
66-
D
M 6 8 10 11 12 13 14 15 17 19

The level of RdRp activity, evaluated by the amount of radioactive products synthesized, generally correlated well with the levels of p152 detected serologically in the various fractions. The relative amounts of p152 in the glycerol gradient fractions (Fig. 3.4B, FMV lanes) paralleled the level of RdRp activity in the same fractions (Fig. 3.1B). Similarly, the S120K fraction contained more RdRp activity (Fig. 3.1A, lane 4) and p152 (Fig. 3.4A, FMV S120 lane) than the P120K fraction (Fig. 3.1A, lane 6; Fig. 3.4A, 7th lane). This was also the case between P30K and S30K fractions (data not shown). These observations strengthen the idea that p152 is associated with the RdRp activity.

However, the kinetics of appearance of p152 protein in *C. quinoa* and barley did not strictly parallel the accumulation of RdRp activity. In *C. quinoa*, p152 was first detected at day 2 p.i., levels peaked between days 5 and 6 p.i. (Fig. 3.3C, lane 6) and subsequently declined although p152 was detected for at least 12 days p.i. (Fig. 3.3C, lanes 8-12). The peak of p152 was therefore delayed by 1 to 2 days relative to that of the RdRp. These results are also compared in Figure 6.1A. In contrast, in barley, p152 was first detected on day 6 p.i. but its peak level preceded that of the RdRp activity by 1 day, occuring at day 11 (Fig. 3.3D, lanes 6 and 11), and then slowly declined although it remained detectable until at least day 19 p.i. (Fig. 3.3D, lane 19). These results are also correlated in Figure 6.1B. Despite the apparent delay between peak levels of p152 and RdRp activity, both generally followed a similar trend in that their levels peaked and subsequently declined, in contrast to levels of p26 (the ORF2-encoded protein of FMV) and coat protein which remain at high levels subsequent to their peak (see below; section 4.3.5; Fig. 6.1). Moreover, since the RdRp consists of a complex of proteins, maximal

activity levels should only be reached in the presence of the optimal concentration of each of the components forming the complex (one of which would be p152) as well as optimal concentration of the substrate. Therefore, the general trend of the expression of p152 and RdRp, as well as the correlation between the presence of p152 and the RdRp activity in the purified fractions described above, generally agree with the hypothesis that p152 is associated with the RdRp activity.

3. Characterization of FMV RdRp products.

In order to obtain a definitive proof that HMW products generated *in vitro* by the partially purified enzyme consist of FMV RNA molecules, we tested their ability to hybridize to FMV gRNA sequences. HMW products generated by the P30K fraction were separated from LMW products by centrifugation through a sucrose gradient. The HMW products were then used to probe slot blots (Fig. 3.5A) containing either FMV gRNA isolated from purified virions or *in vitro* synthesized RNA transcripts corresponding to viral sequence of (+) and (—) polarities (i.e. FM(+) and FM(—) respectively; see Table 3.1 for a description of these transcripts, p.107). The HMW products hybridized to FMV gRNA (Fig. 3.5A, slots 1 and 2) and RNA transcripts of both polarities (Fig. 3.5A, slots 3 and 4). In contrast, HMW products did not hybridize to an RNA transcript consisting of plasmid pSP65 sequences (Fig. 3.5A, slot 5). Moreover, the specificity of hybridization was controlled by probing similar slot blots with either labeled FM(+) or FM(—) transcripts (Fig. 3.5B). Each probe hybridized to its complementary blotted transcript (Fig. 3.5B, slots 3 and 5) but not to itself (Fig. 3.5B, slots 2 and 6). Likewise, only FM(—) hybridized to the gRNA (Fig. 3.5B, slot 4). Therefore, we conclude that each probe is displaying the expected specificity and that

Figure 3.5 Characterization of FMV RdRp products.

(A) HMW RNA products isolated by sucrose gradient centrifugation (see section 3.2.11i) were used to probe slot blots containing 2.5 pmoles (slot 1) or 12.5 pmoles (slot 2) of purified FMV gRNA or 2.5 pmoles of the following transcripts (prepared as described in section 3.2.10): FM(+) (slot 3), FM(—) (slot 4), pSP65 (slot 5).

(B) Control hybridizations. Blots consisting of 0.2-0.4 pmoles FMV gRNA (slots 1, 4), FM(+) (slots 2, 5) or FM(—) (slots 3, 6) were probed with [^{32}P]-labeled transcripts FM(+) (slots 1-3) or FM(—) (slots 4-6).

(C) Nuclease treatment of RdRp products.

Nuclease S1 was used in the following concentrations (U/ml): 0 (lane 1), 50 (lane 2), 100 (lane 3), 500 (lane 4), or 1000 (lane 5).

Prior to treatment with ribonuclease A, RdRp products were resuspended in 2X SSC (lanes 6, 7, 9) or in 0.1X SSC (lanes 8, 10). They were then treated with 0 (lane 6), 0.1 (lanes 7, 8) or 1 (lanes 9, 10) μg/ml ribonuclease A (see section 3.2.8).

Products were then electrophoresed in non-denaturing conditions and detected by autoradiography (section 3.2.7). The arrowhead indicates HMW products.

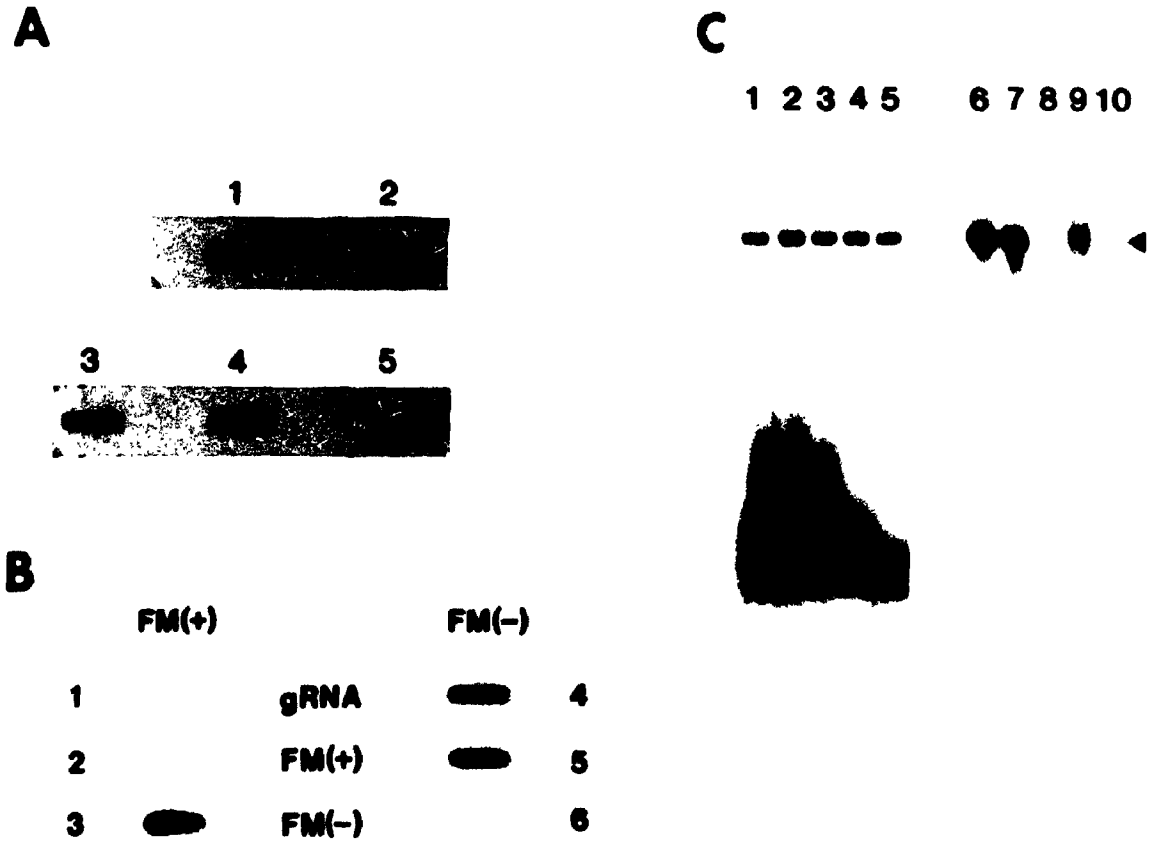
A
1
2
3
4
5
B
FM(+)
FM(-)
1
gRNA
4
2
FM(+)
5
3
FM(-)
6
C
1 2 3 4 5
6 7 8 9 10

HMW products consist of FMV sequences of both messenger and complementary senses, supporting the idea that they arise from FMV RdRp activity.

The mobility of HMW products in non-denaturing conditions is significantly slower than that of FMV gRNA (Fig. 3.1A), suggesting that the HMW products consist of double-stranded RNA molecules. To test this observation, RdRp products were treated with increasing concentrations of nuclease S1 or ribonuclease A (Fig. 3.5C). LMW products generated by a P30K RdRp fraction were sensitive to S1 at a concentration of 100 U/ml or higher (Fig. 3.5C, lanes 3-5), indicating that they consist mainly of single-stranded RNA molecules. In contrast, the abundance and mobility of the HMW products was not affected by this nuclease, even at a concentration of 1000 U/ml (Fig. 3.5C, lane 5), supporting the idea that HMW products consist of double-stranded RNA molecules. Further evidence for this conclusion was obtained by exposing products generated by a S120K fraction to ribonuclease A, in conditions favouring double-stranded (2X SSC) or single-stranded (0.1X SSC) states of the RNA molecules. HMW products were highly susceptible to degradation by ribonuclease A in 0.1X SSC (Fig. 3.5C, lanes 8 and 10) while they were resistant to or only moderately degraded by increasing concentrations of the ribonuclease in 2X SSC (Fig. 3.5C, lanes 7 and 9, respectively) .

4. FMV RdRp does not copy exogenous gRNA template.

The RNA polymerase isolated by the procedure described above must use endogenous RNA as template, since no exogenous FMV gRNA is added to the RdRp assay. In order to characterize the template specificity of the RdRp activity, we attempted to remove the endogenous template RNA from active fractions using micrococcal nuclease. Interestingly, the template RNA in the P30K and S120K fractions was

completely resistant to micrococcal nuclease, even at concentrations as high as 20 U/μl, since HMW products were generated by both intact and nuclease-treated fractions (Fig. 3.6, lanes 1-3). Nuclease treatment, though, resulted in a considerable decrease in the synthesis of LMW products, indicating that the nuclease was active in the conditions used since it could presumably degrade endogenous mRNAs (Fig. 3.6, compare lanes 1 and 3). The resistance of the FMV-induced RdRp activity to micrococcal nuclease in crude fractions contrasts strongly to RdRp preparations of BMV and CMV (Bujarski *et al.*, 1982; Hayes and Buck, 1990) where the RNA template is readily removed by micrococcal nuclease treatment of the P30K fraction or by solubilization of the BMV RdRp complex with detergent and salt (Quadt and Jaspars, 1990). The endogenous template in the purer GGP fraction was, however, susceptible to micrococcal nuclease. A concentration of 4 U/μl of nuclease was sufficient to abolish RNA synthesis completely (Fig. 3.6, compare lanes 4 and 5). This suggests that fractionation of the S120K in glycerol gradients induces a change in the RdRp complex, such as reorganization and/or loss of component(s) which may result in the exposure of RNA templates to the nuclease. Samples of the GGP fraction previously treated with micrococcal nuclease were incubated with increasing amounts of purified FMV gRNA. However, the polymerizing activity was not restored upon addition of template RNA to the assay (Fig. 3.6, lane 6). We do not believe that exogenous template was rapidly degraded by residual nuclease activity since incubation of labeled RNA transcripts of unrelated sequences in a micrococcal nuclease-treated GGP sample for 60 min did not result in significant degradation of this RNA (data not shown). Therefore, the absence of HMW products in lane 6 (Fig. 3.6) suggests that the enzymatic complex cannot initiate RNA synthesis on new templates. For

Figure 3.6 Products synthesized by micrococcal nuclease-treated RdRp fractions.

Samples of the S120K fraction (lanes 1, 2, 3) or the GGP fraction (lanes 4, 5, 6) were treated with 0 (lanes 1, 4), 4 (lanes 2, 5) or 20 (lane 3) U/μl of micrococcal nuclease and were subsequently assayed for RdRp activity following the chelation of Ca^{2+} by EGTA (section 3.2.6). The GGP fraction in lane 6 was treated with 4 U/μl of micrococcal nuclease and was assayed for RdRp activity in the presence of purified FMV gRNA (0.1 μg/μl). The arrowhead indicates HMW products.

1 2 3 4 5 6

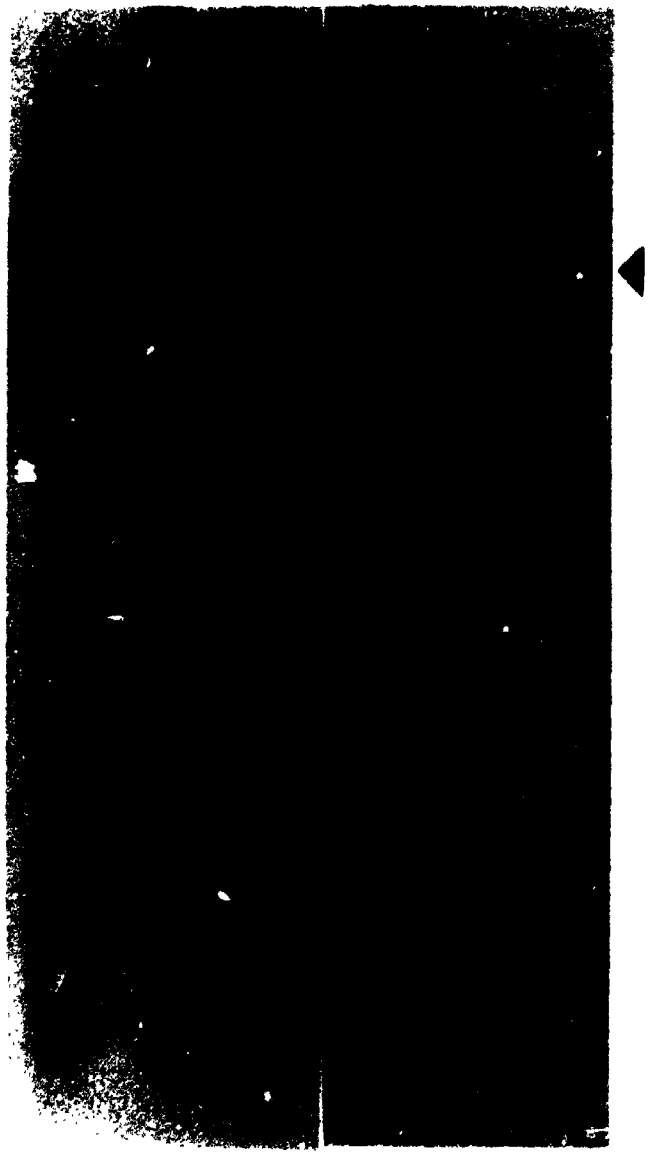

this reason, we believe that products synthesized *in vitro* arise from RdRp elongating and terminating the synthesis of RNA copies of endogenous templates previously initiated *in vivo*. This conclusion is also supported by the observation that accumulation of HMW products ceased after 60 min in a RdRp assay (data not shown), suggesting that all nascent chains have been completed by that time and that the RdRp can only complete the synthesis of one strand *in vitro*. The failure of nuclease-treated RdRp to copy an exogenous template may result from the loss during the purification procedure of one or more subunits of the polymerase complex required for initiation of replication and/or elongation. Alternatively, reinitiation of RNA synthesis may be inhibited by contaminating proteins present in the GGP fraction.

5. Potexviral gRNAs interfere with RNA synthesis on endogenous template.

5.1 Specificity of the inhibition to potexviral RNAs.

As a second means of investigating the ability of RdRp to initiate RNA synthesis on exogenously added template, we supplemented an untreated sample of the GGP fraction with various amounts of purified FMV gRNA and investigated its effect on the levels of RNA products generated in RdRp assays. Surprisingly, the presence of increasing amounts of exogenous templates in the assays caused a gradual reduction in the yield of labeled products (Fig. 3.7, lanes 1-4). To quantify this inhibition, the labeled products separated by electrophoresis were excised from the dried gel and their radioactivity determined. RNA synthesis was reduced by as much as two thirds in the presence of 0.2 $\mu g/\mu l$ FMV gRNA (Fig. 3.7, lane 4). This concentration-dependent inhibition of RNA synthesis by FMV gRNA was consistently observed with various GGP preparations. In order to determine the specificity of this inhibition, RdRp activity in the

Figure 3.7 Effect of added RNA on RNA synthesis on endogenous template.

RdRp activity in the GGP fraction was assayed in the presence of: lane 1, no RNA added; lane 2, 0.05 $\mu g/\mu l$ FMV gRNA; lane 3, 0.1 $\mu g/\mu l$ FMV gRNA; lane 4, 0.2 $\mu g/\mu l$ FMV gRNA; lane 5, 0.1 $\mu g/\mu l$ CYMV gRNA; lane 6, 0.1 $\mu g/\mu l$ BMV gRNAs; lane 7, 0.1 $\mu g/\mu l$ yeast RNA. Products were subjected to autoradiography following electrophoresis. The inhibition of RNA synthesis was quantified by measuring the radioactivity of the labeled products generated by each reaction and is expressed relative to the amount of labeled products generated in a normal assay (i.e. no RNA added, lane 1). The arrowhead indicates HMW products.

1 2 3 4 5 6 7

0	47	50	66	55	2	0

% inhibition of replication

GGP was assayed in the presence of yeast RNA or of virion RNA purified from CYMV, another member of the potexvirus family, or from BMV, a bromovirus. Interestingly, the inhibitory effect of CYMV gRNA (55%; Fig. 3.7, lane 5) was similar to that obtained with RNA purified from FMV virions (50%; Fig. 3.7, lane 3) while RNA from BMV virions or from yeast did not change the yield of FMV RNA products (Fig. 3.7, lanes 6 and 7, respectively). Clearly, potexviral RNAs specifically interfere with the synthesis of RNA copies of endogenous templates. This finding contrasts with results obtained with several other RdRps where addition of exogenous templates to template-independent RdRp preparations had no effect on their activity (Mouchès *et al.*, 1974; Dorssers *et al.*, 1984; Houwing and Jaspars, 1986; Rohozinski *et al.*, 1986; Young and Zaitlin, 1986). The inhibitory effect of potexviral RNAs was not caused by trace amounts of contaminating coat protein since addition of coat protein purified from FMV virions (50 ng/μl) had no detectable effect on the levels of FMV RdRp products generated (data not shown).

5.2 Identification of inhibitory regions.

In an attempt to identify region(s) of the potexviral genome responsible for the inhibition of RNA synthesis, transcripts of cloned cDNAs spanning the FMV gRNA sequence were generated (Table 3.1) and added to *in vitro* assays programmed by the GGP fraction. Transcripts of genomic polarity FM(+), FM5(+), and FM3(+), which collectively span most of the genome (with the exception of the seventeen 5' terminal nucleotides and 235 nucleotides at coordinates 1195-1429) did not interfere with RNA synthesis (Table 3.1). Similarly, CY3(+) transcripts, corresponding to the 3' terminal 250 nucleotide region of the CYMV genome, did not inhibit RNA synthesis (Table 3.1).

Table 3.1 Effect of RNAs corresponding to various regions of the potexviral genome on RNA synthesis on endogenous templates.

RNA[a,b,c]	relative molar amount	relative inhibition[d]
FMV gRNA	1	+++
FM(+)	1	–
FM5(+)	1	–
FM3(+)	1	–
FMV mini (+)	1	+
	3	++
FM(-)	1	++
FM5(-)	1	+
FM3(-)	1	+
CYMV gRNA	1	++
D-RNA (+)	1	–
	3	+
CY3(+)	1	–
	5	–
CY3(-)	1	–
	5	++

1 kb

[a] The gRNAs were purified from virions.
[b] The polarity of each transcript is indicated in parentheses. Transcripts FM(+) and FM(-) contain a 204 nucleotide extension at their 3' and 5' ends, respectively. This extension corresponds to pSP65 sequences between the *Xba*I and *Pvu*II restriction sites. An extension of 34 non-viral nucleotides is also present at the 5' end of transcript FM(+) and at the 3' end of transcripts FM(-), FM5(-) and FM3(-).
[c] Transcript FM5(+) lacks the first 17 nucleotides of the FMV genome.
[d] The relative inhibition was estimated by densitometric scanning of autoradiographs of RdRp products separated by electrophoresis. For each RNA tested, the relative inhibition was estimated from 1 to 4 assays, by comparison with inhibition obtained with FMV gRNA. Maximal inhibition, represented by "+++", corresponds to 36-60% inhibition, "++" corresponds to 21-35% inhibition and "+" corresponds to 10-20% inhibition.

In contrast, FMV mini-RNA(+) transcripts, which contain 604 and 584 nucleotides from the 5' and 3' ends of the genome, respectively, as well as transcripts of CYMV D-RNA(+), which also contain 5' and 3' segments of the CYMV genome (757 and 415 nucleotides, respectively; White *et al.*, 1991), did inhibit RNA synthesis (Table 3.1). A common feature of the inhibitory (+) sense transcripts is the presence of both termini of the potexviral genome, suggesting that these regions are simultaneously necessary for inhibition of RNA synthesis. The inhibitory effect of the 5' and 3' terminal regions of the RNA may be enhanced by the presence of internal sequences since none of the synthetic RNAs tested could produce the same extent of inhibition obtained with FMV gRNA, even in molar amounts 3 times that of the viral RNA (Table 3.1). The presence of a cap structure on transcripts of FMV mini-RNA(+) or CYMV D-RNA(+) did not modify the level of inhibition produced. Moreover, a longer poly(A) tail on CY3(+) transcripts (up to 40 A residues) did not improve its ability to inhibit RNA synthesis (data not shown). It is unlikely that the non-viral nucleotide extension of some synthetic RNAs reduced their inhibitory potential since other RNAs with this feature did interfere with RNA synthesis (e.g. FM(—); Table 3.1). Moreover, others have shown that full-length RNA transcripts of white clover mosaic potexvirus carrying 198 non-viral nucleotides at their 3' end are still infectious, suggesting that the non-viral nucleotides do not interfere with replication (Beck *et al.*, 1990).

Transcripts complementary [(—) sense] to various regions of the potexviral genome also produced some interference with RNA synthesis on endogenous template [Table 3.1, FM(—), FM5(—), FM3(—), CY3(—)]. The FM(—) transcript, which spans two thirds of the genome, was the most effective inhibitor among the negative sense

transcripts tested (Table 3.1). However, some inhibition was also produced by shorter FMV transcripts and by high concentrations of transcript CY3(—), which is complementary to the 3' terminal 250 nucleotides of CYMV gRNA (Table 3.1). Unlike the inhibition by (+) sense transcripts, which requires sequences of both extremities of the viral RNA, the inhibitory effect of (—) sense transcripts was exerted by RNAs which contained sequences of only one [FM(—), FM3(—), CY3(—)] or no [FM5(—)] terminal region.

The inhibition of RNA synthesis on endogenous templates, which is specifically produced by potexviral RNAs, could result from the interaction of the added RNA with 1) endogenous RNA templates and/or 2) component(s) of FMV RdRp. In regard to the former, it is conceivable that added RNA may anneal to RNA templates of the complementary strand, preventing the RdRp from moving along its substrate. This is unlikely because various (+) sense transcripts of FMV sequence added to the RdRp assays did not cause inhibition whereas CYMV gRNA and CY3(—) did, even though their sequences differ significantly from that of FMV gRNA (CY3(—) shares 39% complementarity with the corresponding region of the FMV genome). Therefore, the anti-sense mechanism, if occuring, cannot explain all cases of inhibition of RNA synthesis observed. The alternative, whereby added RNA molecules compete with endogenous RNA for binding to component(s) of the replication machinery, is more plausible. Previous reports have shown that purified RdRps can respond to the gRNAs of related viruses (Quadt and Jaspars, 1990; Quadt *et al.*, 1991) and it is conceivable that FMV RdRp does also. The signals recognized by the RdRp would probably be terminally located. This observation is consistent with the *in vivo* multiplication of CYMV D-RNA

(White *et al.*, 1992a), which lacks ~80% of the internal nucleotides of CYMV gRNA, and with its inhibitory effect along with that of FMV gRNA and FMV mini-RNA(+). Thus, the simultaneous interaction of 5' and 3' termini of added (+) sense RNA molecules may displace endogenous template but not be copied itself because partially purified RdRp may lack essential co-factors to initiate the replicative process. Alternatively, the terminal regions may associate with one (or more) components of the RdRp leading to its dissociation from the RdRp complex. This type of inhibition, produced by the interaction of small (+) sense transcripts with a purified RdRp, has been observed previously with TYMV RdRp (Morch *et al.*, 1987).

6. Summary.

We have established a procedure to partially purify a potexviral RNA-dependent RNA polymerase from infected tissues. Although the purified enzyme is not template-dependent, RNA synthesis on endogenous template is sensitive to the presence of RNA of potexviral sequences. Delineation of segments of the genome which interfere with RNA synthesis may help identify the template regions recognized by potexviral RdRps. Moreover, a search for factors which apparently interact with the added inhibitory RNAs may lead to the identification of structural components of potexviral RdRps.

CHAPTER 4

PURIFICATION, PROPERTIES AND SUBCELLULAR LOCALIZATION OF FMV 26-kDa PROTEIN

4.1 INTRODUCTION

Intercellular movement of plant viruses appears to occur by passage through plasmodesmata. A few viral proteins which facilitate movement have been characterized and appear to function in one of two general modes (Maule, 1991; Deom *et al.*, 1992). The tobacco mosaic virus (TMV) P30 protein induces an increase in the size of the plasmodesmatal permeable space (Wolf *et al.*, 1989) and possesses non-specific single-stranded RNA binding activity (Citovsky *et al.*, 1990; 1992). In contrast, the movement proteins of the comoviruses (Shanks *et al.*, 1989; van Lent *et al.*, 1990), caulimoviruses (Linstead *et al.*, 1988) and nepoviruses (Wieczorek and Sanfaçon, 1993) participate in the formation of tubular structures which extend from plasmodesmata and in which virus-like particles have been detected.

An analysis of mutants of the genome of white clover mosaic potexvirus revealed a requirement for the central three ORFs (ORFs 2, 3 and 4) for systemic spread in whole plants but not for replication in protoplasts, suggesting their involvement in cell-to-cell movement of the virus (Chapter 1; Beck *et al.*, 1991). These ORFs, often referred to as the "triple gene block" (see Fig. 1.3A), have counterparts in the genomes of carla-, furo- and hordeiviruses. They are related both in sequence (Foster, 1992; Huisman *et al.*, 1988) and in function since they are essential not only for the movement of potexviruses, but also of beet necrotic yellow vein furovirus (BNYVV; Gilmer *et al.*, 1992) and barley stripe mosaic hordeivirus (BSMV; Petty and Jackson, 1990). It is not understood what role each of these proteins plays in movement.

The 24-26 kDa protein encoded by the potexviral ORF2 does not share significant sequence similarity with the movement proteins described above. It does contain,

however, a motif common to proteins possessing nucleoside triphosphate binding and hydrolysis as well as, in some cases, helicase activities (Gorbalenya *et al.*, 1989; Habili and Symons, 1989). This motif is characteristic of a growing family of demonstrated or putative NTP binding helicases of prokaryotic, eukaryotic and viral origins which play roles in various cellular processes such as translation, splicing, replication, transcription, recombination and repair (Gorbalenya *et al.*, 1989). Among positive-sense RNA viruses, a number of putative NTP-binding/helicase proteins have recently been demonstrated to exhibit NTP hydrolysis activity (Laín *et al.*, 1991; Wengler and Wengler, 1991; Rodriguez and Carrasco, 1993; Tamura *et al.*, 1993; Warrener *et al.*, 1993) and nucleic acid unwinding activity (Laín *et al.*, 1990).

In view of the diverse properties of viral proteins implicated in cell-to-cell movement, we have sought to define the functional properties, kinetics of expression and subcellular localization of the potexviral ORF2-encoded protein using foxtail mosaic virus 26-kDa protein (p26) as a model. Most of the findings presented in this chapter have been accepted for publication (Rouleau *et al.*, 1994).

4.2 MATERIALS AND METHODS

1. Enzymes and chemicals.

Ammonium sulfate of Ultrapure grade was obtained from Gibco/BRL. Reagents for the embedding of tissues for electron microscopy were from E.F. Fullam (Latham, New-York). Lead citrate was from Fluka. [α^{32}P]-ATP, -CTP and -GTP were purchased from Amersham. Bio-Gel A0.5m and hydroxylapatite were purchased from Bio-Rad Inc. Blue dextran 2000 was obtained from Sigma. Polyethyleneimine-cellulose plates were

from Macherey-Nagel (distributed by Mandel Scientific Ltd, Guelph). The plasmid pET-11 (Studier *et al.*, 1990) was obtained from Novagen. Triton X-100 was purchased from Boehringer Mannheim. 10 nm and 30 nm gold-conjugated goat anti-rabbit antibodies were obtained from British Biocell International (distributed by Cedarlane Laboratories Ltd, Hornby, Ont.). Plasmids used for the *in vitro* transcription as well as other reagents and enzymes were described in Chapters 2 and 3.

2. Construction of the p26 expression plasmid pET-ORF2.

Plasmid p133X, which contains a cDNA fragment corresponding to the FMV sequence at coordinates 1430-6151(A_{13}) in the vector pSP65 (Bancroft *et al.*, 1991; described in section 3.2.9), was linearized at its unique *Bam*HI site and served as a template for the amplification of the ORF2 region by the polymerase chain reaction (PCR). Primers used in the PCR reaction, FMV2-1 and FMV2-2 (Appendix I), were designed to introduce a ribosome binding sequence (5' AGGAGGT) upstream of the ORF2 start codon and *Bam*HI restriction sites flanking the ORF2 region. The amplification was carried out for 30 cycles as described in section 3.2.9 using 100 pmol each of primers FMV2-1 and FMV 2-2 and 100 ng of *Bam*HI-linearized p133X. The PCR-amplified ORF2 cDNA fragment was restricted with *Bam*HI, electrophoresed in a non-denaturing polyacrylamide gel in TBE buffer, eluted from the gel and ligated to *Bam*HI-linearized pET-11 vector. *Escherichia coli* strain MV1190 was transformed with the ligation mixture and recombinant plasmids were prepared as described in section 2.2.3. Recombinant plasmids were identified by digestion with *Bam*HI. The nucleotide sequence of the FMV-derived insert in the recombinant plasmid pET-ORF2 was verified by the dideoxynucleotide chain termination method as described in section 2.2.4.

3. Expression and purification of p26.

The growth of *E. coli* BL21(DE3) transformed with the parental vector pET-11 (strain MR1) or with the recombinant vector pET-ORF2 (strain MR2) and the induction of the expression of p26 (in cultures of MR2) was performed as described in section 3.2.12ii. Induction with IPTG was for 5 hrs. Initial steps in the purification of p26 from cultures of MR2 followed a modified version of a general procedure described by Pognonec *et al.* (1991). Cells were pelleted by centrifugation in a JA-14 rotor at 10,000 *x g* for 10 min, resuspended in ice-cold lysis buffer (section 3.2.12ii) and frozen in a dry ice/ethanol bath. Cells were stored overnight at -70°C. All subsequent steps were carried out at 4°C. Cells were thawed and lysed by two passages in a French pressure cell at 12,000 psi. The cell paste was centrifuged in a JA-20 rotor at 10,000 *x g* for 10 min. The supernatant solution, containing a large proportion of p26, was recovered, ammonium sulfate was added to 33% saturation, and salted-out proteins were collected by centrifugation at 15,000 *x g* for 15 min (JA-20 rotor). The pelleted material was resuspended in 1 ml lysis buffer containing 200 mM NaCl, centrifuged at 14,000 *x g* for 10 min in a microfuge, and the supernatant fraction (S3) was saved. The pellet was resuspended in 0.75 ml of lysis buffer lacking NaCl, recentrifuged and the supernatant fraction was combined with S3 to generate fraction I.

Fraction I (~ 1.5 ml) was cleared of any insoluble material by a 10 min centrifugation in a microfuge at 14,000 *x g* and its NaCl concentration was raised to 400 mM. It was subsequently fractionated on a Bio-Gel A0.5m column (1 cm x 40 cm) equilibrated in lysis buffer containing 200 mM NaCl. Prior to the chromatography of fraction I, the column was calibrated as follows. The void volume of the column was

determined by measuring the elution volume of blue dextran 2000. The molecular weight standards BSA, ovalbumin and lysozyme prepared in lysis buffer containing 400 mM NaCl were subsequently fractionated and their elution pattern was determined. Proteins were eluted with 50 ml of lysis buffer containing 200 mM NaCl at a flow rate of 2.8 cm/hr. Fractions (1.0 ml) were collected and analyzed by SDS-polyacrylamide gel electrophoresis (SDS-PAGE) as described below (Laemmli, 1970). Fractions containing the majority of p26 were pooled and dialyzed overnight at 4°C against lysis buffer lacking glycerol and containing 20 mM NaCl. The dialyzed material constituted fraction II.

Fraction II was loaded onto a hydroxylapatite column (1.5 cm x 3 cm) equilibrated with 1 mM NaCl/1 mM EDTA, pH 8.0. Proteins were eluted with a solution of Na phosphate (pH 7.0) containing 1 mM EDTA, in steps of increasing concentration of Na phosphate as follows: 5 mM (volume of step: 20 ml); 25 mM (10 ml); 100 mM (10 ml); 200 mM (10 ml); 300 mM (10 ml), at a flow rate of approximately 25 cm/hr. Fractions (1 ml) were collected and analyzed by SDS-PAGE. Fractions containing the peak of p26 were pooled, dialyzed overnight against 50 mM N-2-hydroxy ethylpiperazine-N'-2-ethanesulfonic acid [HEPES; pH 7.5]; 20 mM NaCl; 5% glycerol; 1 mM EDTA; 0.1 mM phenylmethylsulfonyl fluoride). This fraction, which constituted fraction III, was stored at -70°C.

4. Protein analysis.

The concentration of proteins in the various fractions obtained during the purification of p26 was determined using the Protein Assay Kit purchased from Bio-Rad.

Analysis of proteins on gels was as described in section 3.2.13. Protein samples were prepared in SDS-sample buffer, boiled and electrophoresed in 15 % polyacrylamide gels (Laemmli, 1970). For direct visualization, the proteins were stained with a Coomassie blue solution (0.05% Coomassie blue R-250, 45% CH_3OH; 10% CH_3COOH). For Western blotting, proteins were transferred to a nitrocellulose or a polyvinyl-difluoride (PVDF) membrane as described in section 3.2.13. To improve the quality of the blots containing plant extracts, gels were soaked for 30 min in transfer buffer at room temperature prior to blotting. The protein blots were subsequently reacted with anti-p26 serum [diluted 1:5000 in PTBN buffer containing 5% casein] or with FMV anti-serum (diluted 1:7500 in PTBN containing 5% casein) and processed as described in section 3.2.13.

5. Generation of anti-sera.

i) p26 antibodies. The proteins in fraction I were electrophoresed on 15 % SDS-polyacrylamide preparative gels. Gel slices containing p26 were prepared as described in section 3.2.12iii. Approximately 100 mg of dehydrated ground gel powder (containing approximately 120 μg of p26) was hydrated in 1 ml of 0.85% NaCl for 30 min at room temperature. The mixture was emulsified as described in section 3.2.12iii prior to multiple intramuscular injections into a rabbit. A pre-immune serum was obtained prior to the first injection and subsequently, four series of injections were performed at three week intervals. The rabbit was then exanguinated by heart puncture.

ii) FMV antibodies. The FMV anti-serum was obtained from J.B. Bancroft. It was prepared using FMV virions as antigen. FMV virions were isolated from systemically infected barley leaves and were purified as described (Bancroft *et al.*, 1979). Their purity

was verified by electron microscopy and analytical centrifugation. FMV anti-serum was prepared by multiple intravenous injections of the virions into a rabbit.

6. Amino acid analysis of p26 expressed in *E. coli*.

A gel slice containing p26 from fraction I was prepared from a large 15 % polyacrylamide gel as described in section 3.2.12iii. A piece of acrylamide corresponding to 4-5 μg of p26 was cut in small pieces, mixed with 1-2 ml 6 N HCl containing 0.25 % ß-mercaptoethanol and hydrolyzed under vacuum in a sealed glass tube for 72 hrs in a 110°C oven. The solution was cooled to 4°C overnight, filtered through a 0.2 μm pore size filter and amino acids were analyzed by ion exchange chromatography using a Beckman (model 119CL) single column analyzer. The elution of amino acids was performed with three sodium citrate buffers of ascending pH and concentration: 0.2 N, pH 3.25; 0.4 N, pH 3.95; 1 N, pH 6.4 according to the instructions of the manufacturer. Automated identification of amino acids consisted in the reaction of the eluate with a ninhydrin based reagent, heating at 100°C and measurement of the OD_{570}. The elution pattern generated was corrected by subtracting the elution pattern obtained by subjecting a piece of acrylamide gel devoid of proteins to similar hydrolysis and chromatography. This was necessary to correct for contaminating substances arising from the gel slice itself such as glycine. Amino acid standards (6.25 nmoles) were fractionated and analyzed as for the hydrolysate and the value of the OD_{570} reading obtained for each amino acid was used to calculate the relative amounts of the amino acids in the protein sample.

7. Photochemical crosslinking of proteins to RNA and nucleotides.

^{32}P-labeled RNA transcripts were prepared by *in vitro* transcription as described

in section 3.2.10. The vector pSP64 linearized with *Pvu*II served as a template for the synthesis of a 232-nucleotide-RNA transcript of sequence unrelated to the viral sequence. Plasmid p124X linearized with *Hin*dIII served as a template for the synthesis of a 1194-nucleotide-transcript of viral sequence (FM5(+); see section 3.2.10 and Table 3.1). Plasmid p90X (section 3.2.9) was linearized with *Sca*I and served as a template for the synthesis of a 156-nucleotide-RNA transcript of sequence complementary to the viral sequence. Transcription was directed by SP6 RNA polymerase. RNA crosslinking reaction mixtures contained 20 mM Tris-HCl (pH 7.4), 50 mM NaCl, 10% glycerol, 1 mM EDTA, 5 mM $MgCl_2$, 2.5-5 ng RNA (~ 4 x 10^7 cpm/μg) and 2.5-3 μg proteins from fraction I prepared from cultures of MR1 or MR2, in a final volume of 10 μl. Mixtures were incubated for 10 min at room temperature and subsequently irradiated for 5 min on ice in a UV Stratalinker 1800 (Stratagene; California) at 8 cm from the light source (0.78 J/cm^2). Reaction mixtures were supplemented with 5 μg RNase A and incubated for 30 min at 37°C to digest excess, uncrosslinked RNA. One volume of SDS-sample buffer was subsequently added to the mixtures. For nucleotide crosslinking, reaction mixtures were identical to those described for RNA crosslinking with the following exceptions: the labeled RNA was replaced by 1.6 pmol NTP (specific activity 3000 Ci/mmol) and 1.5 μg of proteins from fraction I were used in a final volume of 10 μl. Mixtures were incubated and irradiated as described above and one volume of SDS-sample buffer was added. Samples were boiled for 3 min and analyzed by SDS-PAGE and autoradiography of the dried gels.

8. ATP hydrolysis assays.

Reaction mixtures contained 20 mM HEPES (pH 7.5), 10% glycerol, 1 mM

EDTA, 5 mM $MgCl_2$, 0.1 mM ATP (specific activity 0.5 Ci/mmol) and proteins either from fractions I (3 μg), II (2 μg) or III (0.5 μg) in a final volume of 10 μl. Mixtures were incubated for 2 hrs at 37°C and the reaction was stopped by adding EDTA to a final concentration of 20 mM. Subsequently, 0.5 μl of each reaction mixture was spotted onto a polyethyleneimine-cellulose coated plastic sheet and developed by ascending chromatography using 0.375 M KH_2PO_4 (pH 3.5; Tamura *et al.*, 1993). Products of hydrolysis were then visualized by autoradiography of the dried sheet. To quantify the enzymatic activity, regions of the sheet corresponding to ATP and ADP were excised and Cerenkov radiation was measured in a scintillation counter to determine the conversion of ATP to ADP. In some assays, the reaction mixture was supplemented with poly(A) RNA (final concentration of nucleotide bases 0.3-0.7 mM; Sigma) or with RNA transcripts (0.3 mM) of either 9S RNA sequences (Cormack and Mackie, 1992) or of FMV sequences (FM5(+); section 3.2.10; see also Table 3.1).

9. Subcellular fractionation of plants.

The leaves of the local lesion host *Chenopodium quinoa* and the systemic host barley (variety Herta) were infected with FMV and fractionated essentially as described in section 3.2.4. Leaf tissue (5 g) was homogenized with a mortar and pestle in 10 ml homogenization buffer A (0.4 M sucrose; 10 mM KCl; 5 mM $MgCl_2$; 50 mM Tris-HCl, pH 8.2; 20 % glycerol; 10 mM ß-mercaptoethanol). The homogenate was filtered through Miracloth to obtain the cell wall (CW) fibers. The filtrate was centrifuged at 1,000 *x g* (JA-20 rotor) to recover the pellet fraction P1. The supernatant solution was centrifuged at 30,000 *x g* (JA-20 rotor) to generate a supernatant fraction (S30) and a pellet fraction (P30). P1 and P30 were washed by resuspending pellets in 1 ml of

homogenization buffer and recentrifugation at 30,000 *x g* prior to resuspension of the washed pellets in 1 ml ESB (4.5 % SDS; 9 M urea; 7.5 % ß-mercaptoethanol; 75 mM Tris-HCl, pH 6.8; Godefroy-Colburn *et al.*, 1986). The CW fibers were resuspended in 5 ml (*C. quinoa*) or 15 ml (barley) homogenization buffer containing 1% Triton X-100 and stirred for 60 min at 4°C to extract any protein loosely bound to the fibrous material. The CW fibers were recovered by filtration through Miracloth and resuspended in 1.5 ml (*C. quinoa*) or 8 ml (barley) ESB. P1, P30 and CW fractions were boiled for 10 min, centrifuged for 10 min and the supernatant solutions were saved for analysis.

10. Immunocytochemical methods.

All steps were carried out at room temperature. Leaf discs (1 mm diameter) were cut out of 4-day-infected *C. quinoa* leaves in areas showing lesions or of equivalent areas of mock-inoculated leaves. Discs were fixed for 1 hr in 100 mM cacodylate buffer, pH 6.8, containing 1.5% p-formaldehyde and 0.5% glutaraldehyde, and rinsed twice for 10 min in cacodylate buffer. Tissues were subsequently post-fixed for 1 hr with OsO_4 (2% in cacodylate buffer) to enhance preservation and visibility of organelles. Leaf discs were then rinsed twice for 10 min in ddH_2O and stained for 20 min with saturated aqueous uranyl acetate. Tissues were dehydrated by 10 min-exposures to an ascending series of 20%, 50%, 70% and 90% ethanol solutions in ddH_2O, followed by two 30 min-incubations in absolute ethanol and two 15 min-incubations in propylene oxide. Tissues were subsequently infiltrated for 1 hr intervals through a graded series of propylene oxide:Epon-Araldite resin mixtures consisting of the following proportions: 3:1, 1:1 and 1:3. This was followed by an infiltration with slow end-over-end rotation overnight in pure resin, then for 4-5 hrs in fresh, pure resin. Tissues were then placed in rectangular

molds filled with fresh resin which was then allowed to polymerize for 45-60 hrs in a 60°C oven. The Epon-Araldite resin consisted of: 4.5 ml Epon 812, 3.5 ml Araldite 502, 18 ml dodecenyl succinic anhydride and 0.5 ml tri- (dimethylaminomethyl) phenol. The last chemical was only added after good mixing of the other components of the resin.

E. coli coli cultures (10 ml) of strains MR1 and MR2, which were induced for 3 hrs with IPTG, were also used for embedding. Cells were pelleted by a 1 min centrifugation in a microfuge. The culture media was removed and cells were washed once in 0.85% NaCl solution. Cells were subsequently pre-embedded in 2% agar which was then trimmed to 1-2 mm^3 blocks. These blocks were subsequently processed for fixation, dehydration and resin infiltration as described for plant tissues.

Ultrathin sections, prepared using a Sorvall Porter-Blum MT2 ultramicrotome equipped with a diamond knife, were lifted on 400-mesh nickel grids. Grids were immunostained by floating them (section side down) onto drops of appropriate solutions as described below. Sections were first etched for 15 min with a saturated aqueous $NaIO_4$ solution. This step results in the exposure of antigenic sites at the surface of the sections by a reduction of the OsO_4 which would otherwise mask the antigens. Excess $NaIO_4$ was blotted with filter paper and sections were washed by floating them over 4 drops of ddH_2O over a period of 4 min. Sections were blocked for 10 min with PTBN and subsequently incubated overnight with the anti-p26 serum (1:5000 in PTBN) in a moisture chamber. Moisture chambers were prepared by placing a piece of parafilm on top of a filter paper soaked in ddH_2O, in glass petri dishes. Dishes were covered at all times to prevent drying of drops of sera solutions which were placed on the piece parafilm. Grids were washed with 4 drop changes of PTBN and then incubated for 30

min with gold-conjugated goat anti-rabbit antibodies (10 or 30 nm gold particles; 1:50 in PTBN lacking Tween-20) in a moisture chamber. Sections were washed by passage onto 4 drops of ddH_2O, stained with saturated aqueous uranyl acetate for 10 min and washed again. Lastly, grids were stained with lead citrate for 45 seconds in a petri dish containing a few NaOH pellets to create a CO_2-free environment in order to prevent the precipitation of lead onto tissues. The lead citrate solution was prepared by dissolving approximately 35 mg lead citrate in 10 ml ddH_2O to which 2-3 drops of freshly prepared 10 N NaOH were added. Prior to use, undissolved lead was pelleted by centrifugation in a microfuge at 14,000 rpm for 1 min. Sections were subsequently observed with a Philips CM-10 electron microscope at 60 or 80 kV.

4.3 RESULTS

1. Expression and purification of p26.

The p26 protein was expressed in *Escherichia coli* from the recombinant expression plasmid pET-ORF2 constructed by introducing the FMV ORF2 sequence into the expression vector pET-11. The design of pET-ORF2, schematically represented in Figure 4.1, is such that signals for bacterial expression would direct the synthesis of the entire p26 protein as encoded by the viral genome, without the introduction of additional amino acids at either end of the protein.

Cultures of MR1 or MR2 [strain BL21(DE3) transformed with pET-11 or pET-ORF2, respectively] were grown and induced for 5 hrs with IPTG. Total cellular proteins from each culture were analyzed by SDS-PAGE (Fig. 4.2). A prominent polypeptide with an apparent molecular weight of 26 kDa is present in the culture of MR2 (Fig. 4.2,

Figure 4.1 Schematic representation of the p26 expression plasmid pET-ORF2.

A cDNA fragment containing a Shine-Dalgarno sequence fused to the viral ORF2 sequence was generated by PCR and ligated into the *Bam*HI restriction site of the bacterial expression vector pET-11 as described in section 4.2.2. The relative position of the start (ATG) and stop (TGA) codons and of the T7lac promoter, Shine-Dalgarno (SD) and T7 terminator regulatory sequences are indicated.


ATG
TGA
T7 lac prom
S
D
ORF2
T7 term
BamHI
BamHI

Figure 4.2 Analysis of the expression and purification of p26 by 15% SDS-PAGE and Coomassie blue staining.

The expression of p26 is shown by a comparison of total protein extracted from cultures of MR1 (—; lane 2) or of MR2 (+; lane 3) following a 5 hr induction with IPTG (see section 4.2.3). An ammonium sulfate precipitation of soluble proteins generated fraction I (lane 4). Fraction II (lane 5) consisted of pooled, dialyzed fractions obtained by gel filtration chromatography of fraction I. Fraction III (lane 6) consisted of pooled, dialyzed fractions obtained from the chromatography of fraction II on hydroxylapatite. The size of molecular weight markers (lane 1) are shown in the left margin (kDa) and the arrow in the right margin points at p26.

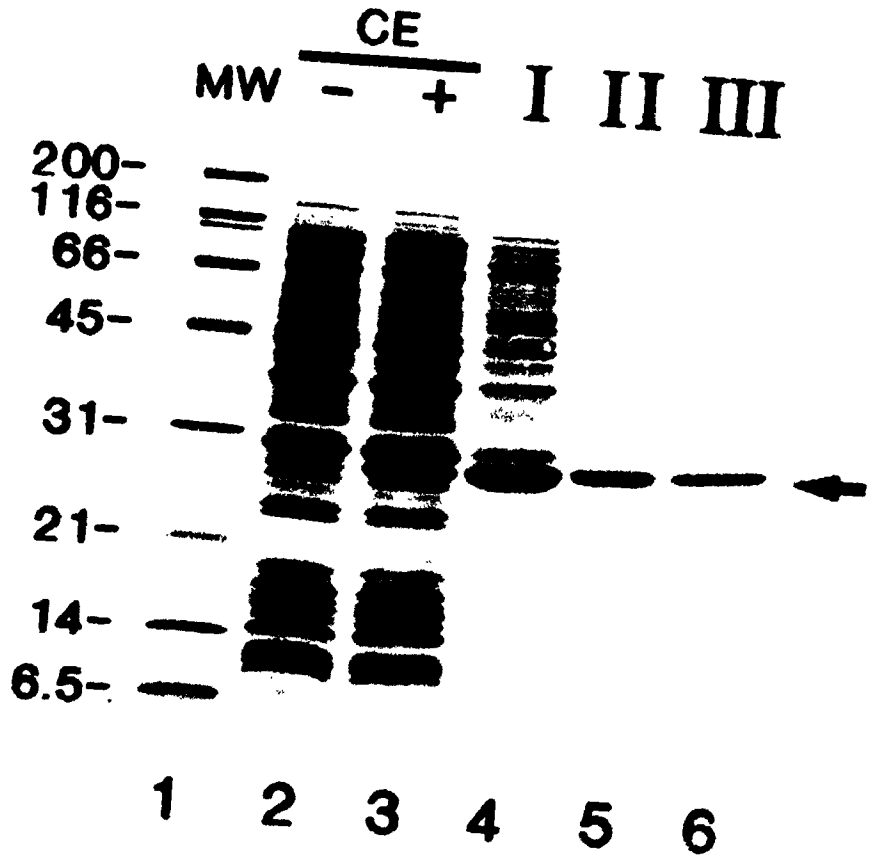
CE
MW
-
+
I
II
III
200-
116-
66-
45-
31-
21-
14-
6.5-
1
2
3
4
5
6

lane 3) but not in the culture of MR1 (Fig. 4.2, lane 2). The size of the novel polypeptide is consistent with it being p26. The identity of the overexpressed protein was nonetheless confirmed by an analysis of its amino acid composition (Table 4.1). The composition of the bacterially expressed protein was comparable with that of p26, deduced from its sequence. For a few amino acids, the values slightly differed, likely due to the slower hydrolysis of some peptide bonds (i.e. those involving Val or Ile; Ozols, 1990), because of contamination from the gel slice itself, such as from the running buffer (Gly; see section 4.2.6).

Lysis of the MR2 cells released a large proportion of p26 into the soluble fraction. It was quantitatively precipitated from the soluble fraction by 33% $(NH_4)_2SO_4$ to generate fraction I, significantly enriched in p26 (Fig. 4.2, lane 4). Further fractionation of the protein from bacterial contaminants was achieved by size exclusion chromatography (exclusion limit: 500 kDa) as described in section 4.2.3. The efficiency of this step was optimized by maintaining the NaCl concentration of fraction I above 200 mM to reduce the level of aggregation of p26 with the contaminating polypeptides. Even under these conditions, most of the protein still eluted in the void volume of the column (Fig. 4.3). Fractions containing p26 were pooled to produce fraction II (Fig. 4.2, lane 5) which was fractionated further on hydroxylapatite equilibrated in 1 mM NaCl. Most of the viral protein eluted in the 100 mM Na phosphate elution step. The fractions containing p26 were pooled to generate fraction III (Fig. 4.2, lane 6). In some experiments, proteins of bacterial origin co-eluted with p26 during the hydroxylapatite chromatography and are faintly visible in some preparations of fraction III (see below). The abundance of these contaminants varied among preparations, but the purity of the

Table 4.1 Analysis of the amino acid composition[1] of the protein expressed in *E. coli*: comparison with the predicted composition of p26.

	Mole percent[2]	
Amino acid[3]	experimental[4]	calculated[5]
Ala	9.4	8.9
Arg	6.6	6.8
Asp + Asn[6]	7.0	6.7
Glu + Gln[6]	11.5	9.7
Gly[7]	8.3	7.2
His	5.0	5.5
Ile[8]	3.3	4.2
Leu	10.7	10.1
Lys	4.1	3.4
Phe	3.1	3.4
Pro	5.2	5.1
Ser	4.3	4.2
Thr	10.9	10.2
Tyr	4.5	4.6
Val	6.1	6.8

[1] Determined by hydrolysis of the bacterially expressed protein in 6 N HCl, 0.25 % ß-mercaptoethanol, 72 hrs, 110°C.
[2] Values represent molar proportions expressed as a percentage. A difference of ± 0.5 % between the experimental and calculated values represents a 1 amino acid difference since p26 is 236 amino acids long.
[3] Met, Cys and Trp were not determined.
[4] Relative amounts of amino acids were determined by post-column derivatization with ninhydrin (section 4.2.6).
[5] Calculated from the amino acid sequence which was deduced from the nucleotide sequence of ORF2 (section 2.3.1).
[6] Asn and Gln are hydrolyzed quantitatively to Asp and Glu respectively.
[7] The difference between experimental and calculated values is due to the large Gly contamination in the running buffer used for the gel electrophoresis (Laemmli, 1970).
[8] Several Ile-X, X-Ile, Val-X and X-Val peptide bonds are slowly hydrolyzed (Ozols, 1990), resulting in a lower experimental than calculated values.

Figure 4.3 Profile of the p26 elution pattern during size exclusion chromatography.

Proteins from fraction I (prepared from cultures of MR2) containing 400 mM NaCl were separated on a Bio-Gel A0.5m column (1 cm x 40 cm) at a flow rate of 2.8 cm/hr. Fractions (1.0 ml) were collected and analyzed for protein concentrations as described in sections 4.2.3 and 4.2.4. The relative concentration of p26 in each fraction was estimated from a Coomassie blue-stained gel of the fractions. The column was calibrated prior to the chromatography of fraction I with the following molecular weight standards: bovine serum albumin (BSA), 66 kDa, ovalbumin (OVA), 45 kDa and lysozyme (LYS), 14 kDa. The void volume (V_o) was determined using blue dextran 2000. Arrows indicate the fractions containing the peak of each standard.

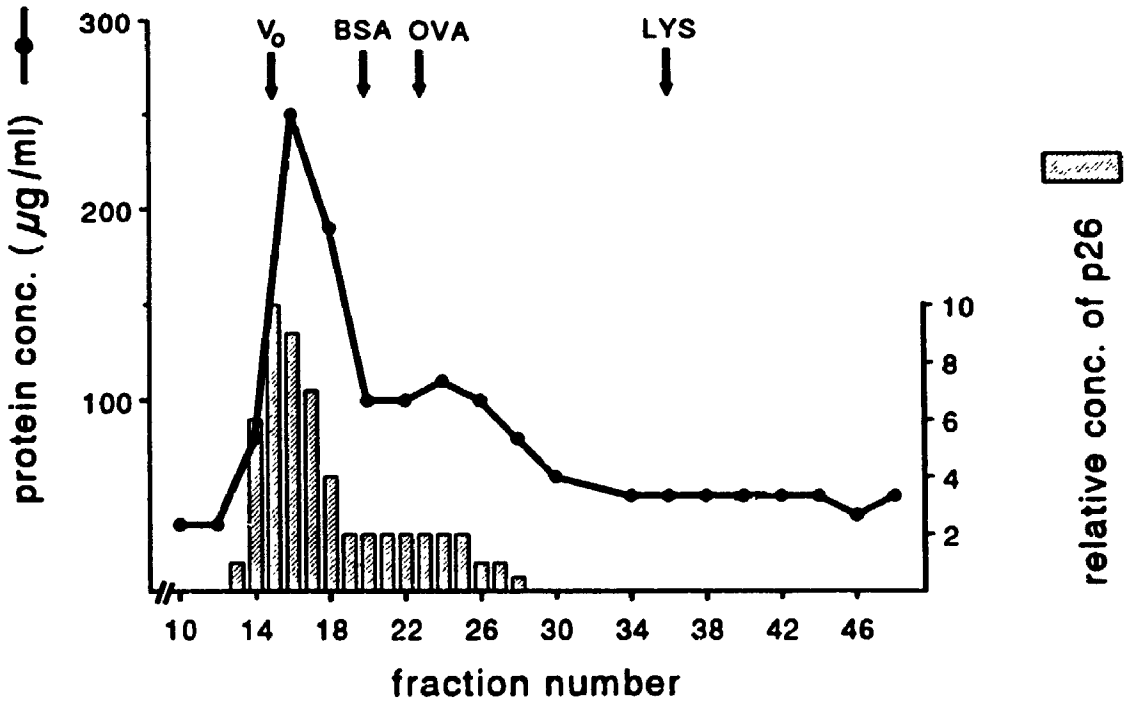
300
200
100
protein conc. (μg/ml)
Vo
BSA
OVA
LYS
10
8
6
4
2
relative conc. of p26
10
14
18
22
26
30
34
38
42
46
fraction number

p26 in fraction III, evaluated by scanning Coomassie blue-stained SDS-polyacrylamide gels, was greater than 90% in all preparations obtained. We estimated that approximately 200 μg of the viral protein is purified from a 200 ml culture of MR2.

2. Nucleotide binding activity of p26.

The ability of the bacterially expressed p26 to interact directly with nucleotides, suggested by the presence of the NTP-binding helicase motif in its amino acid sequence, was tested by photochemical crosslinking. Fraction I prepared from cultures of MR1 or MR2 was incubated with [α-^{32}P]-labeled ATP, CTP or GTP. Covalent nucleotide-protein interactions were generated by UV irradiation of the reaction mixtures and labeled proteins were analyzed by SDS-PAGE. The results of such an experiment are shown in Figure 4.4. A labeled protein band with mobility identical to that of p26 is detected in fraction I prepared from a culture of MR2 incubated with CTP (Fig. 4.4, lane 3) and ATP (Fig. 4.4, lane 6). This labeled protein band is not produced when the same reaction mixtures are not UV irradiated (Fig. 4.4, lanes 2 and 5) or when the nucleotides are incubated with fraction I prepared from a culture of MR1, expressing only the parental vector (Fig. 4.4, lanes 1 and 4). Similarly, little labelling was detected when fraction I obtained from a culture of MR2 was incubated and UV irradiated in the presence of [α-^{32}P] labeled GTP (Fig. 4.4, lane 9). These results indicate that p26 binds CTP and ATP well but not GTP. The binding of CTP and ATP was strictly dependent on the presence of divalent metal ions (Fig. 4.4, lane 7). Optimal binding occurs at Mg^{2+} concentrations of 5 mM. Mn^{2+}, but neither Ca^{2+} nor Zn^{2+}, could substitute for Mg^{2+} in promoting binding (data not shown).

Figure 4.4 Nucleoside triphosphate binding activity of p26.

Autoradiograph of SDS-polyacrylamide (15%) gels containing fractions I from cultures of MR1 (—; lanes 1, 4) or MR2 (+; lanes 2, 3, 5-9) incubated in the presence of [^{32}P]-labeled CTP (lanes 1-3), ATP (lanes 4-8) or GTP (lane 9) and subjected to UV light (see section 4.2.7). The UV irradiation treatment was omitted in samples shown in lanes 2 and 5. Mg^{2+} was absent in the reaction mixture shown in lane 7. In lane 8, the sample was treated with proteinase K prior to analysis on the gel. The mobility of molecular weight markers (in kDa) and of p26 (arrow) is indicated in the right margin.

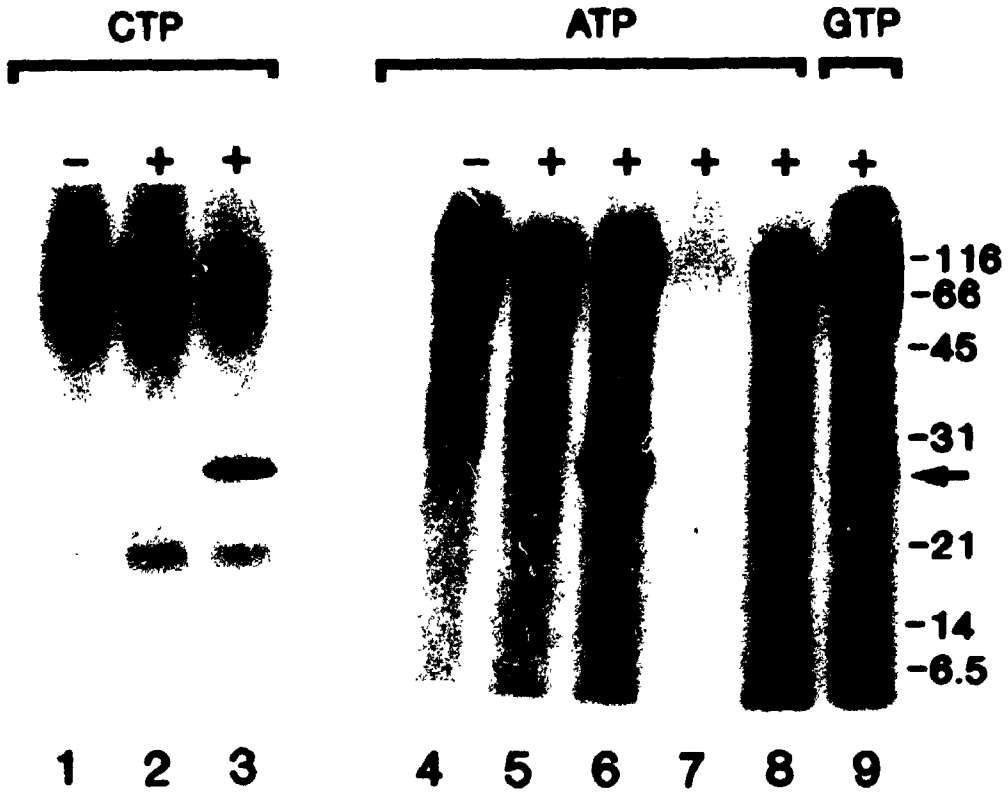
CTP
ATP
GTP
- + +
- + + + + +
-116
-66
-45
-31
-21
-14
-6.5
1 2 3
4 5 6 7 8 9

3. NTPase activity of p26.

In a preliminary assay, ATP and CTP hydrolysis was detected in fraction I prepared from cultures of both MR1 and MR2 (Fig. 4.5, lanes 2, 3, 6, 7). The CTPase activity was not present in fraction II (Fig. 4.5, lane 8), indicating that it was not associated with p26 but rather with a bacterial contaminant(s) which was eliminated during gel filtration chromatography. In order to determine if p26 contributed to the observed ATPase activity, we analyzed selected fractions obtained by hydroxylapatite chromatography of fraction II for their protein content by SDS-PAGE (Fig. 4.6A) and for their ability to hydrolyze [α-^{32}P]-labeled ATP. Products from the ATPase assays were separated by thin layer chromatography (Fig. 4.6B). The elution pattern of the ATPase activity closely matched that of p26 rather than the elution of any of the visible bacterial protein contaminants. Moreover, fraction III of p26 shown in Fig. 4.2 (lane 6), which lacks detectable contaminants, also exhibits significant ATPase activity. The specific activities of fraction III shown in Fig. 4.2 and of pooled material (fractions 54 to 66 in Fig. 4.6) were calculated and found to be comparable within the limits of the assay. On the basis of these results and of those of the preceding section, it is likely that p26 contributes to the ATPase activity detected in fraction III. However, we cannot exclude the possibility that some of the ATPase activity in fractions 54 to 85 (Fig. 4.6B) is due to contaminating proteins.

The ATPase activity was dependent on the presence of Mg^{2+} ions and optimal conditions consisted of 2.5-5.0 mM $MgCl_2$, pH 7.5 (in HEPES buffer) at 37°C. Mn^{2+}, Ca^{2+} or Zn^{2+} could not efficiently replace Mg^{2+} (data not shown). Bearing in mind that p26 may be a helicase, we also tested the effect of RNA on the ATPase activity of

Figure 4.5 ATPase and CTPase activities of fractions prepared from cultures of MR1 and MR2.

Fraction I from a culture of MR1 (—; lanes 2, 6) or MR2 (+; lanes 3, 7), or fraction II from a culture of MR2 (+; lanes 4, 8) were incubated in the presence of [α-^{32}P] ATP (lanes 2-4) or [α-^{32}P] CTP (lanes 6-8) as described in section 4.2.8. The products were resolved by thin layer chromatography and autoradiography. [α-^{32}P]ATP and [α-^{32}P]CTP incubated in reaction buffer alone were resolved in lanes 1 and 5 respectively. The mobility of the nucleotides is indicated in the right margins.

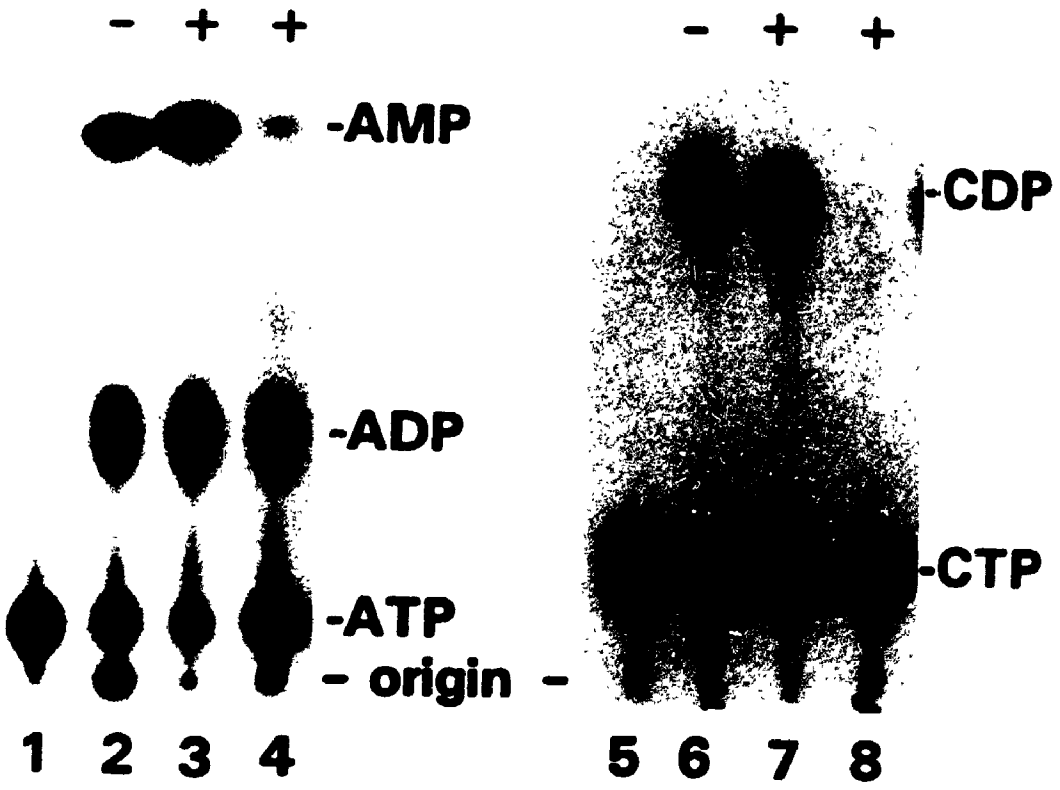
- + +
- + +
-AMP
-CDP
-ADP
-CTP
-ATP
- origin -
1 2 3 4
5 6 7 8

Figure 4.6 Protein content and ATPase activity of fractions from hydroxylapatite chromatography of fraction II.

(A) Coomassie blue stained 15% SDS-polyacrylamide gel of hydroxylapatite fractions (section 4.2.3). The numbers of the fractions analyzed are shown below the lanes. The arrow points at p26 and the mobility of molecular weight standards (kDa) is shown.

(B) Autoradiograph of ATPase products generated by the corresponding fractions. Products resulting from the incubation of [α-^{32}P] ATP in a reaction buffer lacking (—) or containing a sample from the fractions analyzed were resolved by thin layer chromatography (TLC) (section 4.2.8). The mobility of ATP and ADP is shown in the right margin.

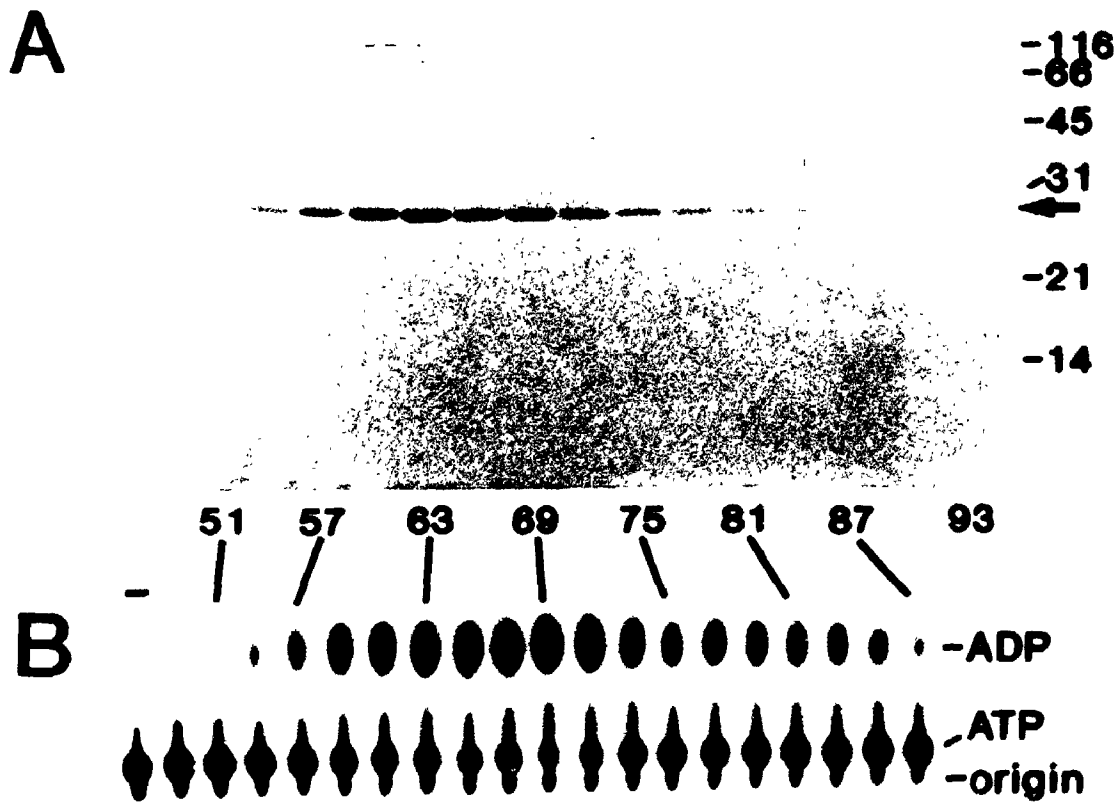
A
-116
-66
-45
-31
-21
-14
51
57
63
69
75
81
87
93
B
-ADP
ATP
-origin

fraction III. However, ATP hydrolysis was not stimulated by poly(A) RNA, by RNA transcripts of viral sequences or by highly structured RNA molecules such as *E. coli* 9S RNA (a precursor to 5S rRNA) (data not shown).

4. RNA binding activity of p26.

Photochemical crosslinking was also used to test the RNA binding activity of the viral protein. Fraction I obtained from cultures of MR1 or MR2 was incubated in the presence of ^{32}P-labeled RNA transcripts and was subjected to UV irradiation. Excess RNA was degraded by RNAse A and proteins were analyzed by SDS-PAGE. RNA transcripts of three different sequences were tested: a transcript of FMV viral sequences [(+) strand], one of sequences complementary to that of the viral genome [(—) strand] and one of a transcribed region of the vector pSP64 which is unrelated to the viral genome sequence. Similar results were obtained with the three transcripts (Fig. 4.7A). The radioactive label was transferred to three distinct proteins: two of them, with MW of ~65 kDa, are common to fraction I prepared from cultures of either MR1 or MR2 (Fig. 4.7A, lanes 1, 2, 5-8), indicating their bacterial origin, while a labeled protein with a MW of ~27 kDa is detected only in extracts of MR2 (Fig. 4.7A, lanes 2, 6, 8). The mobility of this protein and its absence from extracts of MR1 strongly suggest that it is the p26 protein. In addition, a similar labeled protein band was generated when a sample of fraction III was used in the incubation mixture (Fig. 4.7A, lane 9). The slightly slower mobility of the labeled band relative to p26 is likely to result from the few nucleotides which remain covalently attached to p26 following the RNase treatment. Since similar RNA-protein complexes are formed with the three transcripts tested and efficient competition can be achieved using yeast RNA (Fig. 4.7A, lane 4), we conclude that p26

Figure 4.7 RNA binding activity of p26.

(A) Autoradiograph of an SDS-polyacrylamide (15%) gel containing fraction I from cultures of MR1 (—; lanes 1, 5, 7) or MR2 (+; lanes 2, 3, 4, 6, 8) or fraction III from cultures of MR2 (lane 9). Fractions were incubated in the presence of the [^{32}P]-labeled RNA transcript indicated above the lane and subjected to UV light followed by treatment with RNase A as described in section 4.2.7. In lane 3, the sample was treated with proteinase K prior to analysis. The reaction mixture analyzed in lane 4 was supplemented with 5 μg (1000 fold excess) of competitor yeast RNA. The mobility of molecular weight markers (kDa) and of p26 (arrow) are indicated in the right margin.

(B) Effect of increasing the NaCl concentration on the stability of RNA-p26 complexes. Complexes were formed and analyzed as in (A) in the presence of NaCl at molar concentrations indicated above the lanes.

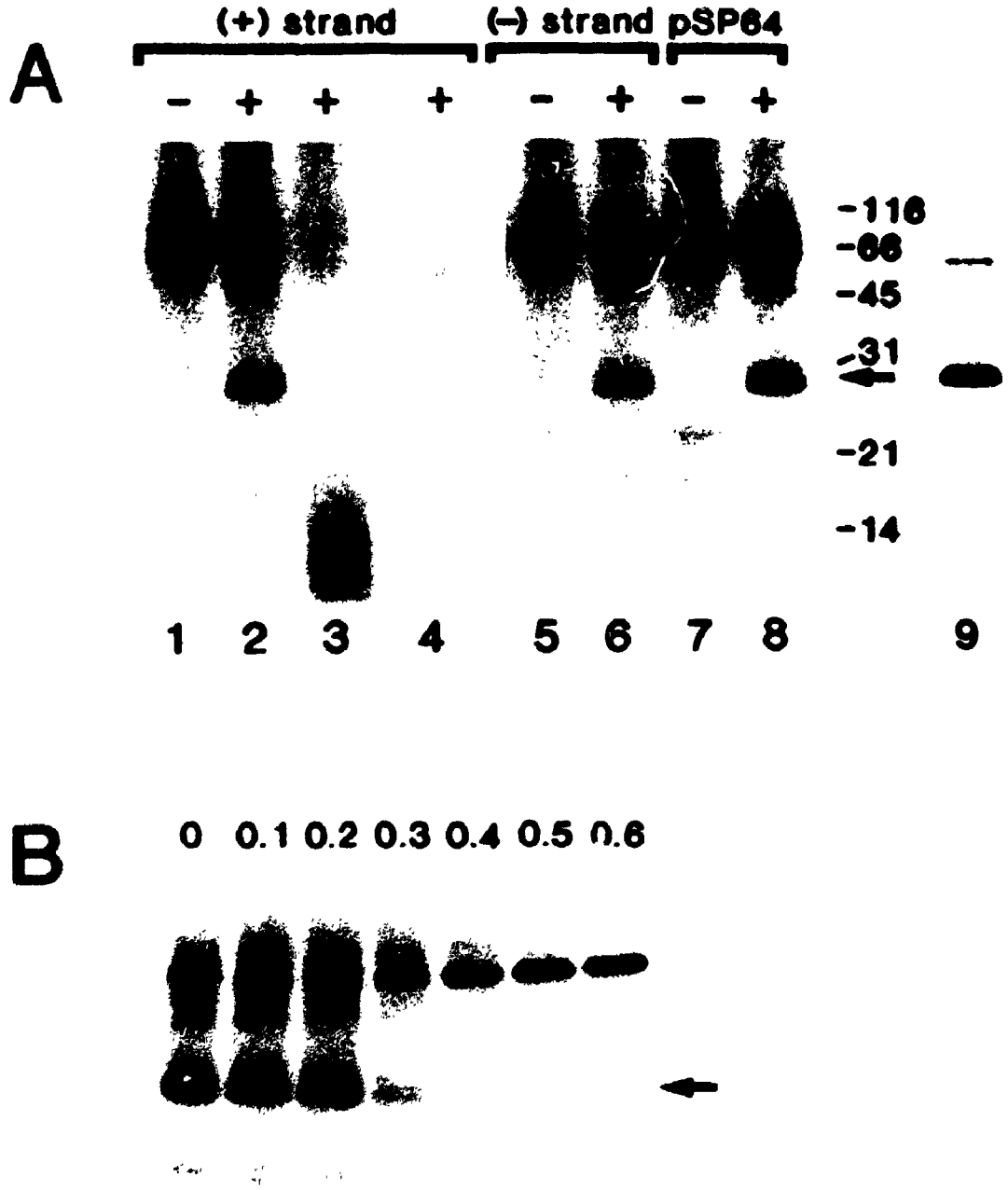
A
(+) strand
(-) strand
pSP64
- + + + - + - +
-116
-66
-45
-31
-21
-14
1 2 3 4 5 6 7 8 9
B
0 0.1 0.2 0.3 0.4 0.5 0.6

is an RNA-binding protein lacking sequence specificity. The binding of RNA by the viral protein was dependent on the presence of Mg^{2+} ions, concentrations of 1-10 mM giving similar levels of p26-RNA complex formation. We routinely performed our assays at 2-5 mM $MgCl_2$ which was also optimal for the other activities of p26.

The strength of protein-RNA interactions has been often evaluated on the basis of the stability of the complexes to increasing salt concentrations (Citovsky *et al.*, 1990; 1991; Osman *et al.*, 1992; Schoumacher *et al.*, 1992). The presence of NaCl at concentrations greater than 0.2 M in our assay mixtures resulted in reduced levels of RNA-p26 complex formation (Fig. 4.7B). The stability of the complex was independent of the sequence of the RNA used, similar levels of complex formation being observed with RNA transcripts of viral or unrelated sequences (data not shown). Previously characterized RNA-binding proteins from plant viruses do not appear to require Mg^{2+} ions for binding. The reason for this is not understood. The stability of p26-RNA complexes observed lies in a range similar to that reported for other plant virus RNA-binding proteins. It is greater than that formed with alfalfa mosaic virus P3 (Schoumacher *et al.*, 1992) and with cauliflower mosaic virus gene I protein (Citovsky *et al.*, 1991) which show decreased binding at 0.2 M NaCl. However, it is not as stable as complexes formed with the movement proteins of red clover necrotic mosaic virus (Osman *et al.*, 1992) and TMV (Citovsky *et al.*, 1990) which are stable at 0.4 and 0.6 M NaCl, respectively.

5. Expression and localization of p26 in FMV-infected plants.

The rabbit anti-serum raised against the bacterially produced p26 allowed an investigation of the kinetics of appearance of the viral protein following inoculation as

well as of its subcellular localization in two FMV infected hosts, *Chenopodium quinoa* and barley. On Western blots, the rabbit anti-serum reacted with only one polypeptide, whether in fraction I prepared from MR2 or in a homogenate from FMV-infected *C. quinoa* (Fig. 4.8, lanes 2 and 4, respectively) while no proteins were immunoreactive in fraction I from a culture of MR1 or in mock-inoculated plant homogenates (Fig. 4.8, lanes 1 and 3, respectively). Therefore, the anti-serum specifically reacts with p26 synthesized in *E. coli* and in infected plants. No difference could be detected between the mobility of the p26 produced in *E. coli* or infected plants (Fig. 4.8, compare lanes 4 and 5), suggesting that p26 does not undergo major post-translational modifications in plants.

Leaf homogenates from the systemic host barley and from the local lesion host *C. quinoa* were prepared at different times following inoculation with FMV and were analyzed by Western blotting using the anti-p26 serum. The temporal expression of p26 was monitored (Fig. 4.9 A and B) using the extracts previously assayed for the presence of p152, viral RNA synthesis and virus titres (sections 3.3.1 and 3.3.2), allowing a comparison of the accumulation of each component during infection. In order to extend the comparison of the expression of the viral components further, the presence of the coat protein (CP) in the same plant extracts was monitored (Fig. 4.9 C and D). In the local lesion host, p26 was first detected 2 days following inoculation and maximal levels of the protein were observed 6 days post-inoculation (p.i.) (Fig. 4.9A) while symptoms of the infection were visible by day 3 p.i. Significant levels of p26 were also detected for 6 additional days (Fig. 4.9A), at which time the experiment was terminated. The pattern of expression of the CP in *C. quinoa* paralleled that of p26. It was first detected 2 days p.i., peaked at day 6 p.i. and remained at a high and constant level following its

Figure 4.8 Comparison of the p26 anti-serum reaction with p26 expressed in *E. coli* and in infected-*C. quinoa* by Western blotting.

Proteins to be analyzed were separated by SDS-PAGE, electroblotted to nitrocellulose and immunoreacted with p26 anti-serum as described in section 4.2.4. Fractions I (0.4 μg proteins) from cultures of MR1 (—; lane 1) or MR2 (+; lanes 2, 5) or total cell homogenates corresponding to 3.6 mg of fresh tissue from mock-inoculated (M; lane 3) or 4-day-FMV-infected (I; lane 4) *C. quinoa* were analyzed. The mobility of molecular weight markers (kDa) is indicated in the left margin.

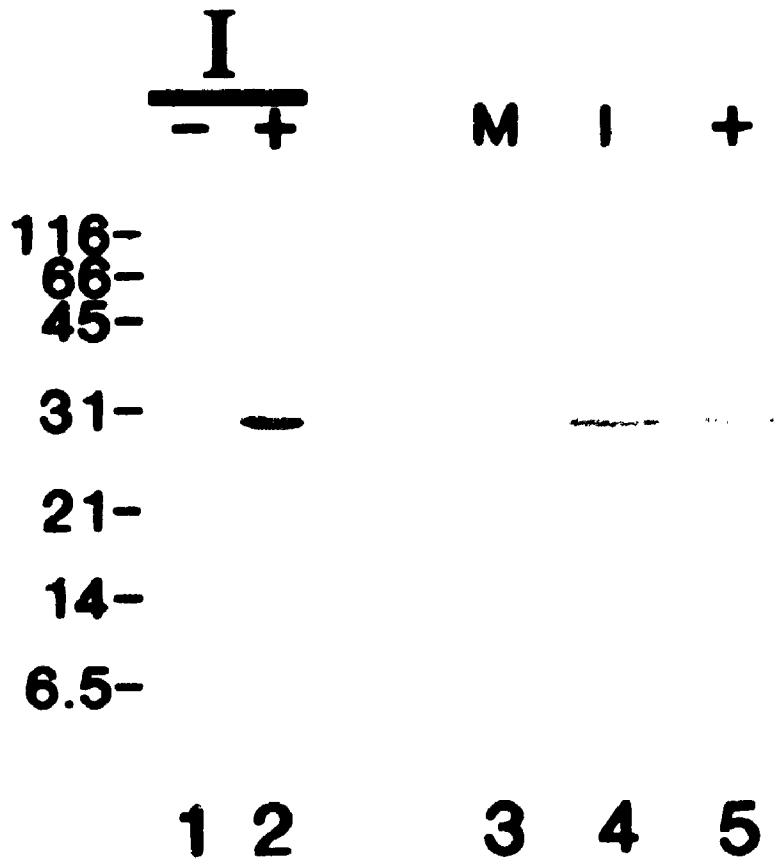
I
- +
M I +
116-
66-
45-
31-
21-
14-
6.5-
1 2
3 4 5

Figure 4.9 Expression of p26 and coat protein in *C. quinoa* and barley.

Proteins to be analyzed were separated by SDS-PAGE, electroblotted to PVDF membranes and immunoreacted with p26 anti-serum (A, B) or FMV anti-serum (C, D) as described in section 4.2.4.

(A) Time-course of appearance of p26 in *C. quinoa*. Leaf homogenates from mock-inoculated plants (lane M) or from plants 2, 4, 6, 8, 10 and 12 days post-inoculation (see section 4.2.9) were analyzed, using protein samples corresponding to 3.6 mg of fresh tissue for each lane. The arrow points at the p26 protein.

(B) Time-course of appearance of p26 in barley. Leaf homogenates from mock-inoculated plants (lane M) or from plants 6, 8, 10, 11, 12, 13, 14, 17 and 19 days post-inoculation were analyzed using protein samples equivalent to 4.3 mg of fresh tissue in each lane. The arrow points at the p26 protein.

(C) Time-course of appearance of the coat protein in *C. quinoa*. The protein blot was prepared as in (A). The arrow points at the coat protein and the arrowhead points at a degradation product of the coat protein.

(D) Time-course of appearance of the coat protein in barley. The protein blot was prepared as in (B). The arrow points at the coat protein and the arrowhead points at a degradation product of the coat protein.

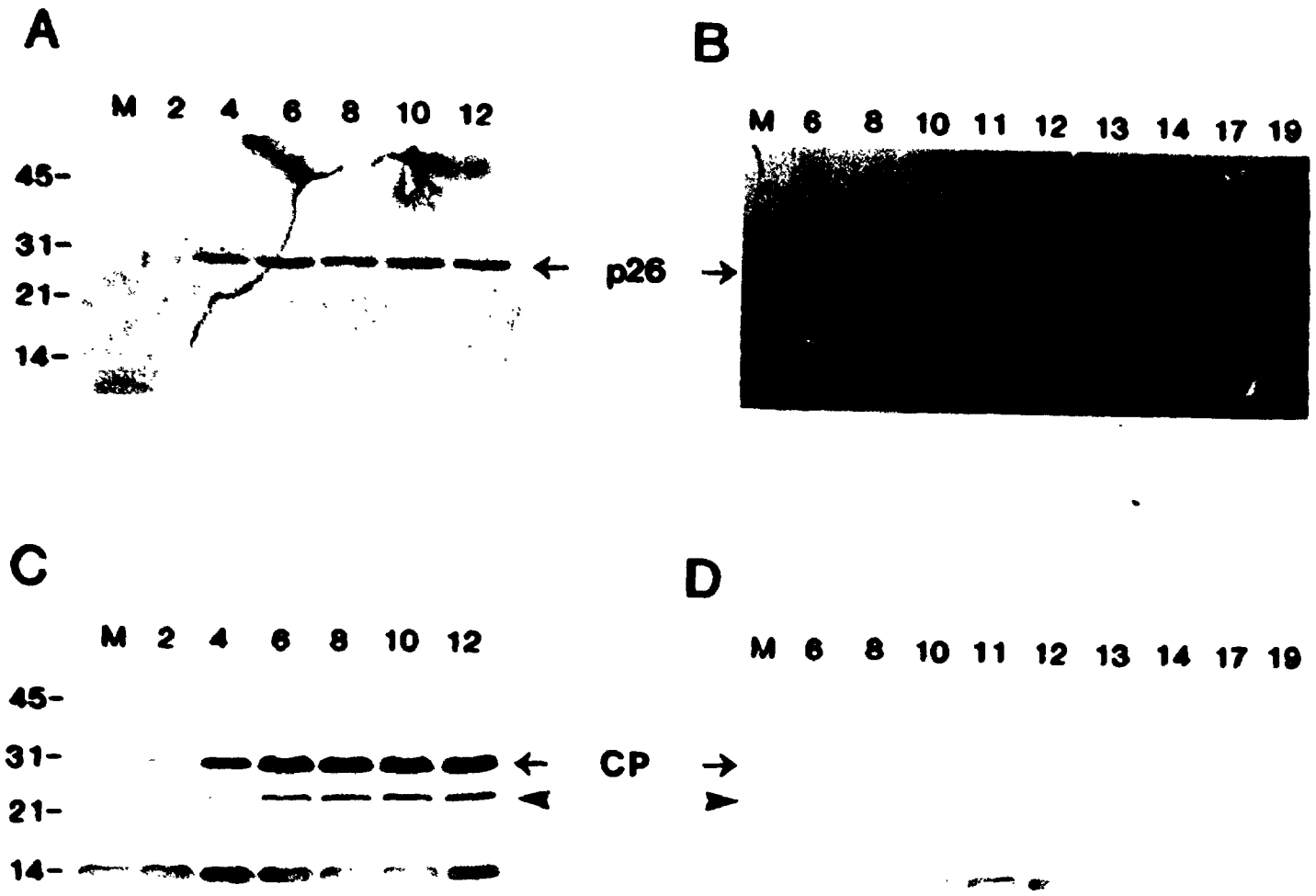
A
M 2 4 6 8 10 12
45-
31-
21-
14-
p26
B
M 6 8 10 11 12 13 14 17 19
C
M 2 4 6 8 10 12
45-
31-
21-
14-
CP
D
M 6 8 10 11 12 13 14 17 19

peak (Fig. 4.9C). Levels of p152 and virus titres were also maximal at day 6 p.i. (Fig. 3.4C and 3.3B, respectively), while the RNA-dependent RNA polymerase (RdRp) activity peaked at day 4 p.i. (Fig. 3.3A). The levels of RdRp activity and p152 differed from those of p26 and CP in that they declined slowly subsequent to their peak (Fig. 3.3A and 3.4C, respectively). These comparisons are summarized in Figure 6.1A (Chapter 6). A slower pattern of expression was detected in the systemic host. p26 was first detected 6-8 days p.i. when symptoms were just appearing on secondary leaves and reached maximal levels 13 days p.i. (Fig. 4.9B). Again, relatively high levels of p26 were maintained in barley for at least 6 more days (Fig. 4.9B). CP was also first detected in samples from 6-8 days p.i. but it only reached maximal levels 17-19 days p.i. (Fig. 4.9D). Maximal levels of p152, RdRp activity and virus titres were found at days 11, 12 and 15 p.i., respectively (Fig. 3.3C, D and 3.4D). Again, p152 and RdRp activity differed from p26 and CP in that their levels declined subsequent to the peak (Fig. 3.3C and 3.4D).

Infected leaves from *C. quinoa* and barley were fractionated by differential centrifugation to produce a cell wall (CW), 1000 *x g* pellet (P1), 30 000 *x g* pellet (P30) and soluble (S30) fractions and were then analyzed by Western blotting for their content in p26 and CP. The distribution of p26 was similar in fractions from *C. quinoa* and barley (Fig. 4.10A and B). Immunodetection revealed that p26 is found predominantly in the S30 fraction (Fig. 4.9A and B, lanes S), although low but significant amounts were also present in the other fractions analyzed, particularly in the CW fractions (Fig. 4.9 A and B, lanes CW). However, since the leaf protein equivalents analyzed were five times smaller for S30 than for CW, P1 and P30 fractions (see legends, Fig. 4.10), it is

Figure 4.10 Distribution of p26 and coat protein in *C. quinoa* and barley.

Proteins to be analyzed were separated by SDS-PAGE, electroblotted to PVDF membranes and immunoreacted with p26 anti-serum (A, B) or FMV anti-serum (C, D) as described in section 4.2.4.

(A) Subcellular localization of p26 in infected *C. quinoa* tissues. A leaf homogenate from 4 day-infected *C. quinoa* was fractionated into cell wall (CW), 1000 *x g* pellet (P1), 30 000 *x g* pellet (P30) and soluble protein (S30) fractions as described in section 4.2.9 and their content of p26 was analyzed. For fractions CW, P1 and P30, proteins equivalent to 12.5 mg of leaves were analyzed while for S30, proteins equivalent to 2.5 mg of leaves were used. The arrow points at the p26 protein.

(B) Subcellular localization of p26 in infected barley tissues. Samples were prepared as described in (A) from 14 day-infected barley. Proteins equivalent to 10 mg of fresh tissue were analyzed for CW, P1 and P30 fractions. Proteins corresponding to 2 mg of barley leaves were used for the S30 fraction. The arrow points at the p26 protein.

(C) Subcellular localization of coat protein in *C. quinoa*. The protein blot was prepared as in (A). The arrow points at the coat protein and the arrowhead points at a degradation product of the coat protein.

(D) Subcellular localization of coat protein in barley. The protein blot was prepared as in (B). The arrow points at the coat protein and the arrowhead points at a degradation product of the coat protein.

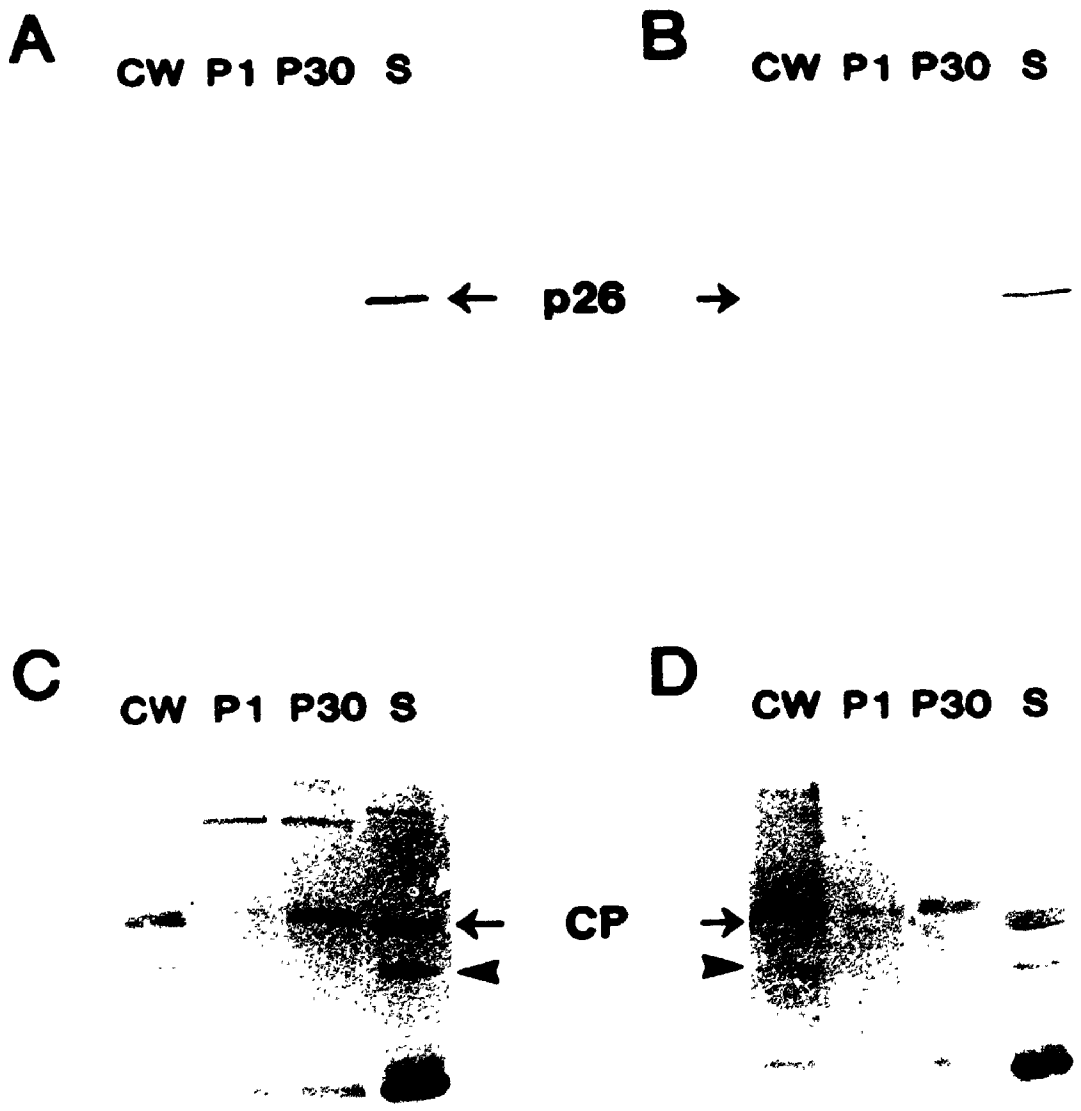
A
CW P1 P30 S
B
CW P1 P30 S
p26
C
CW P1 P30 S
CP
D
CW P1 P30 S

clear that p26 mainly partitioned into the soluble fraction. The distribution of the CP paralleled that of p26, in both *C. quinoa* (compare Fig. 4.10C with 4.10A) and barley (compare Fig. 4.10D with 4.10B). It was found predominantly in the S30 fraction (Fig 4.9C and D, lanes S) but in significant amounts in the other fractions as well. This distribution of the p26 and CP differs from that of p152 and RdRp activity which were detected predominantly in the P30 fraction (sections 3.3.1 and 3.3.2). Although it is not critical to this analysis, the mobility of the CP in the samples CW, P1 and P30 is slightly retarded relative to that in the S30 sample (Fig. 4.10C and 4.10D, compare lanes S with other lanes). This is possibly due to the use of ESB sample buffer (which contains 9 M urea and 4.5 % SDS) in the preparation of the CW, P1 and P30 fractions (but not of S30). The coat protein of FMV typically displays an anomalous behavior during electrophoresis in SDS-PAGE. Its mobility usually corresponds to a molecular weight of 31 kDa rather than the 24 kDa predicted from its amino acid sequence (section 2.3.1) perhaps due to associated glycosides (see section 2.3.1; Tozzini *et al.*, 1994), and may be sensitive to conditions of preparation or storage.

6. Immunocytochemical localization of p26.

To investigate further the location of p26 *in planta*, ultrathin sections of mock-inoculated and 4-day-infected *C. quinoa* leaves were immunogold labeled using the anti-p26 serum and visualized by electron microscopy (Fig. 4.11-4.17). In sections of infected tissue, the p26 anti-serum specifically decorated distinct cytoplasmic areas which often exhibited a fibrillar appearance (Fig. 4.13, 4.14, 4.15). These cytoplasmic inclusions were clearly distinguishable from virus particles, which were not labeled by the antibodies (Fig. 4.12B, 4.13-4.16A). Specific labeling by the anti-p26 serum was found

Figures 4.11-4.17: Localization of p26 in *C. quinoa* leaf tissues using anti-p26 and gold-conjugated antibodies as described in section 4.2.10. Infected tissues were harvested 4 days following inoculation.

Figure 4.11 Low magnification electron micrograph of FMV-infected *C. quinoa* cells.

Epidermal (E) and mesophyll (M) cells contain numerous aggregates of viral particles (arrowheads) and p26 inclusions (arrows). The boxed area is shown at higher magnifications in Fig. 4.12. Bar represents 2 μm.


M
M

Figure 4.12 Virus aggregates and p26 inclusions in a mesophyll cell.

(A) Clusters of virus particles (arrowheads) occupy a large area of the cytoplasm. The area containing the gold-labeled p26 inclusion is boxed. An enlarged view of the boxed area is shown in (B). cw: cell wall; Va: vacuole. Bar represents 400 nm.

(B) Gold-labeled p26 inclusion next to virus particles (V). Arrowheads specify the edges of the inclusion. Bar represents 200 nm.

Figure 4.13 Distribution of p26 inclusions in infected cells.

(A) Lower magnification micrograph of a gold-labeled, elongated p26 inclusion adjacent to aggregates of virus particles viewed transversely (V_t) or longitudinally (V). Bar represents 400 nm.

(B) Large gold-labeled p26 inclusion next to virus particles (V).

The diameter of gold particles is 30 nm (A) or 10 nm (B). Bar represents 200 nm.

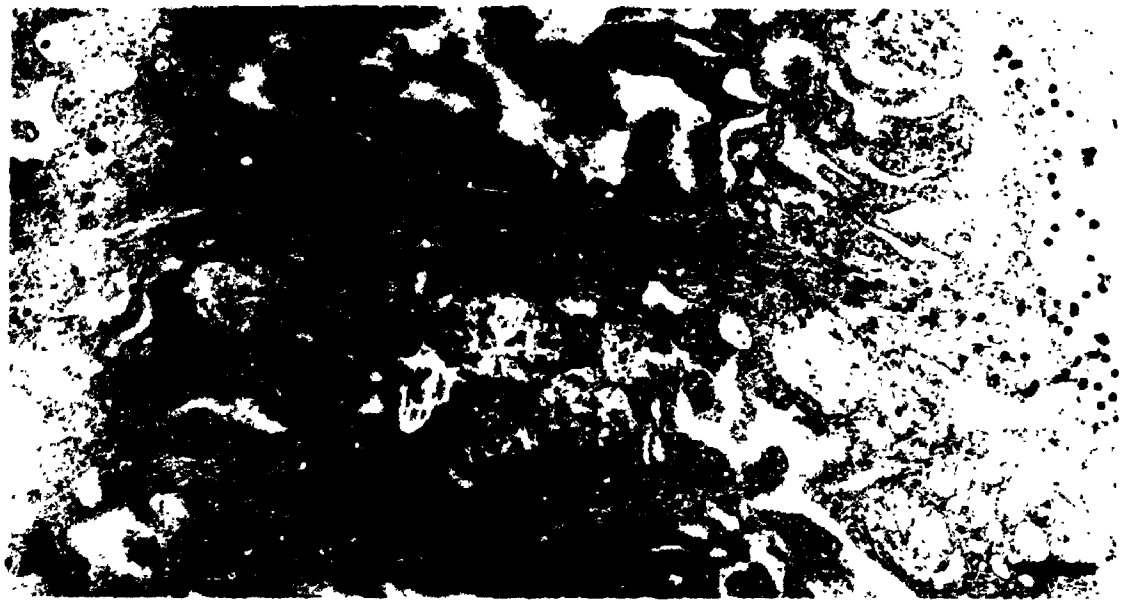

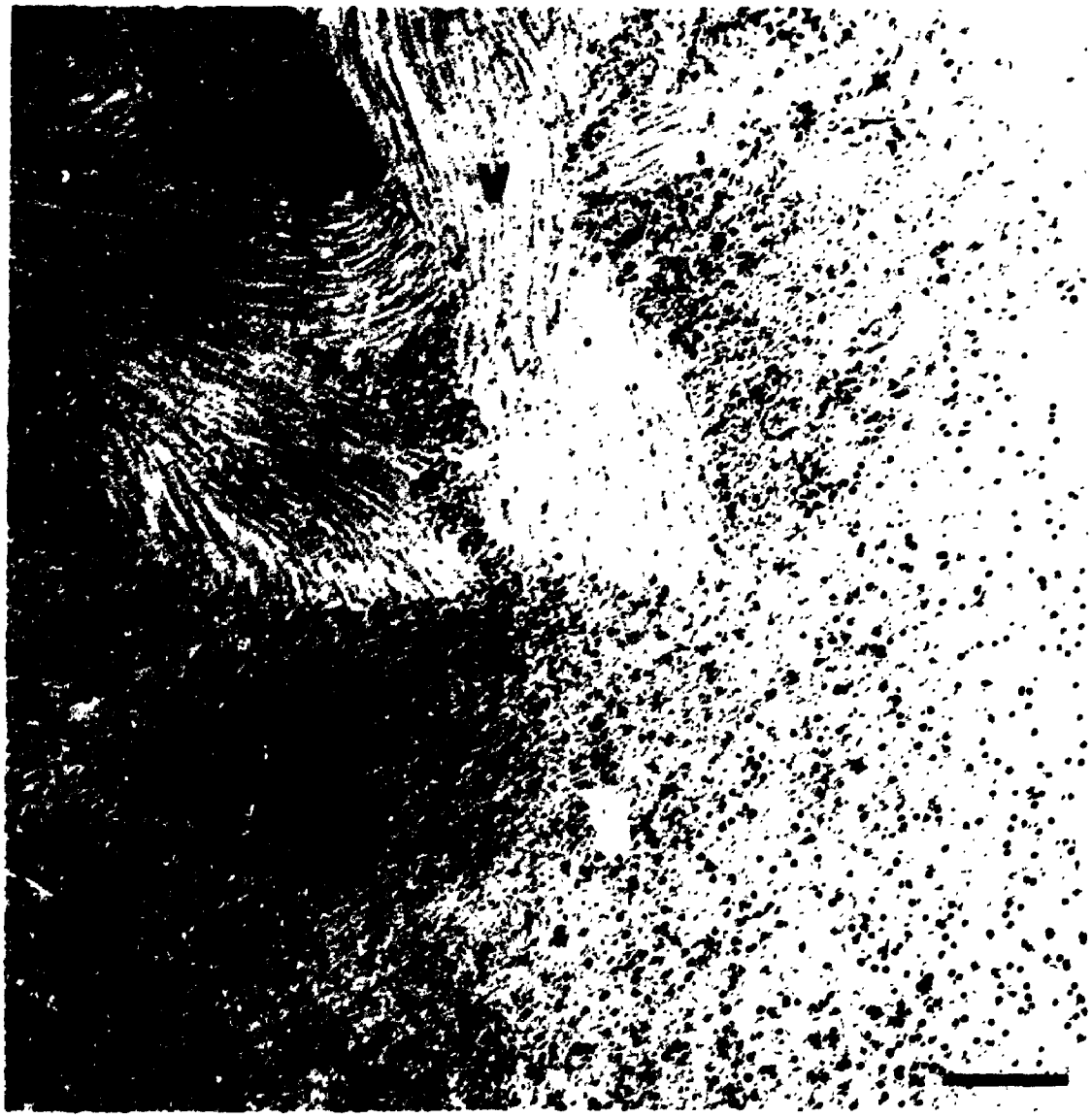

Figure 4.14 Small gold-labeled p26 inclusion adjacent to virus particles.

The fibrillar appearance of the labeled area is clearly seen. The arrowheads specify the lower edge of the inclusion. Mitochondria (m), cell wa: (CW) and virus particles (V) are indicated. Bar represents 200 nm.

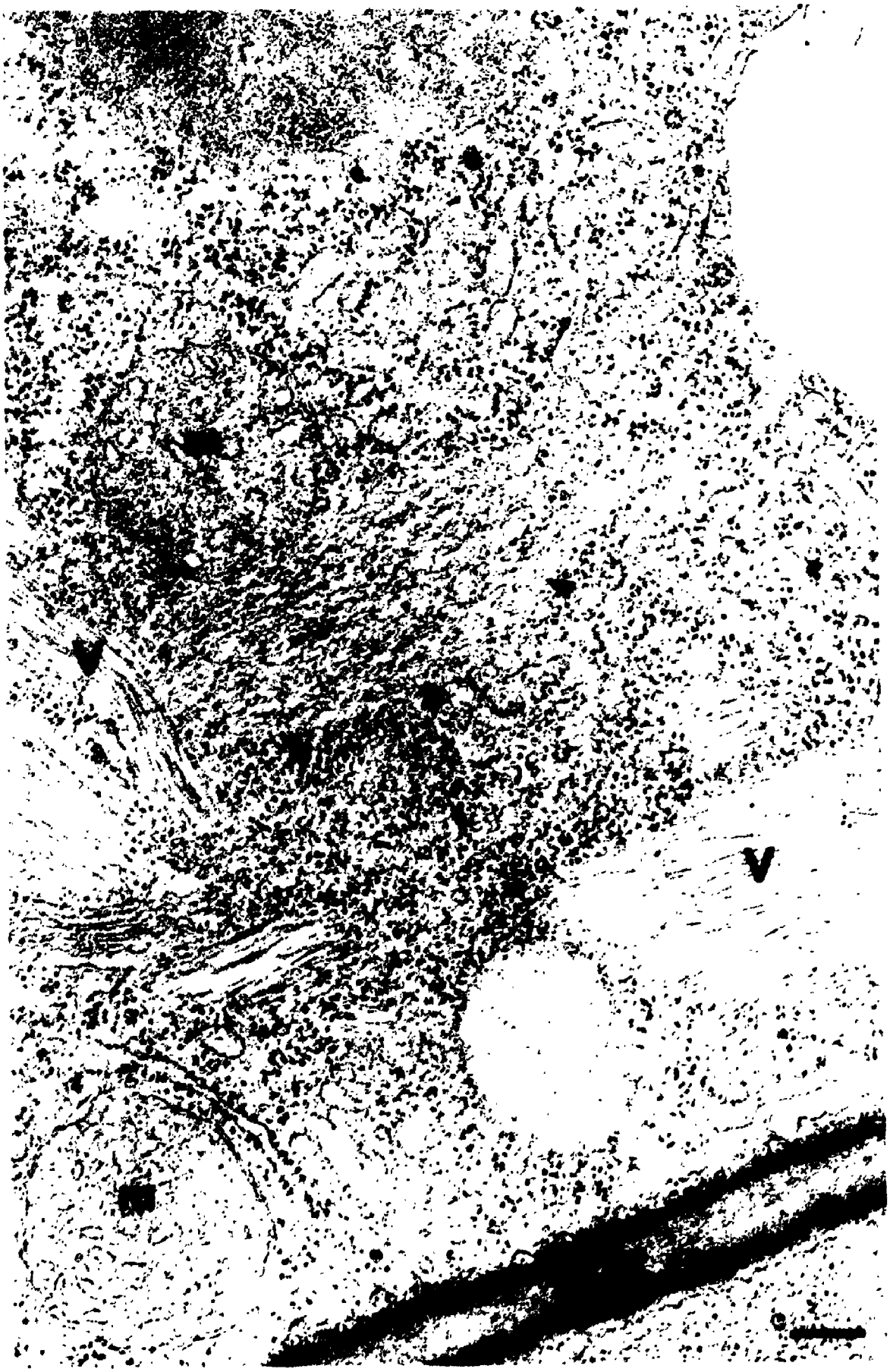
V
V

Figure 4.15 Small p26 inclusion adjacent to viral particles.

The filamentous organization of the p26 inclusion is in continuity with but distinct from the virus particles (V). The two structures do not blend. The junction between the particles and the p26-associated fibrillar structures is indicated by arrows. The cytoplasm, vacuole (Va) and mitochondria (m) are not labeled. 30 nm diameter gold particles were used. Bar represents 200 nm.


Va

Figure 4.16 Plasmodesmata of infected tissues and samples from mock-inoculated tissues.

(A) Plasmodesma (p) adjacent to aggregates of virus particles (V) and gold-labeled p26 inclusion is not labeled by p26 antibodies. Bar represents 200 nm.

(B) Mock-inoculated *C. quinoa* tissues are not decorated by the p26 antiserum. Bar represents 300 nm.


V
A

Figure 4.17 Virions and gold-labeled p26 inclusion in the vicinity of a nucleus.

Aggregates of virus particles (v) and a p26 inclusion (open arrows) accumulate next to the nuclear membrane (arrowheads) but not within the nucleus or nucleolus (Nu). Bar represents 300 nm.

only in the cytoplasm of cells examined. Inspection of 32 plasmodesmata (Fig. 4.16A) and 23 nuclei (Fig. 4.17) in infected cells failed to reveal any labeling. Low numbers of gold particles were detected on the cell wall of cells in both FMV-infected and mock-inoculated leaf sections but no other areas of mock-inoculated tissues were significantly labeled by the anti-p26 serum (Fig. 4.16B).

In *C. quinoa*, the aggregates of virus particles and the cytoplasmic inclusions were distributed primarily in epidermal and mesophyl' cells (Fig. 4.11). The "p26 inclusions" were present only in cells containing aggregates of virus particles and were generally located close to them (Fig. 4.11-4.17). The inclusions varied in size and shape (Fig. 4.12B, 4.13-4.15) perhaps as a function of the cutting angle. Although they were not enclosed by a membrane, the inclusions had a defined outline and did not mix with other cytoplasmic components (Fig. 4.13A, 4.14, 4.15). Within each inclusion, the decorated structures often appeared as an array of parallel intertwined fine filaments (Fig. 4.13A, 4.14, 4.15). The orientation of these filaments was independent of that of viral particles in separate neighbouring cluster(s) and did not blend with them (Fig. 4.13-4.15).

We have also investigated the distribution of p26 in *E. coli* cells from cultures of MR2 which were induced for the expression of the viral protein (Fig. 4.18-4.19A). Interestingly, p26 was localized discrete areas of the bacterial cells rather than being distributed evenly throughout the cytoplasm (Fig. 4.18-4.19A). The reason for this is not clear. Mostly, p26 was present at one extremity of the bacterial cell (Fig. 4.19A) and/or in elongated, tubular shaped structures which were located in various areas of the cell (Fig. 4.18-4.19A). The tubular shaped aggregates often appeared to span the nascent septum of dividing bacterial cells (Fig. 4.18-4.19A). The structural organization of the

Figure 4.18 Distribution of p26 in recombinant *E. coli* cells.

Sections of *E. coli* cells from a culture of MR2 induced for 3 hrs with IPTG were analyzed for the localization of p26 by immuno-electron microscopy as described in section 4.2.10. The gold label is distributed over a tubular shaped inclusion which spans the dividing cell. Bar represents 100 nm.

Figure 4.19 Distribution of p26 in recombinant *E. coli* cells. *E. coli* cells from a culture of MR2 (A) or MR1 (B) induced for 3 hrs with IPTG were analyzed for the localization of p26 by immuno-electron microscopy.

(A) In MR2 cells, the gold-labeled p26 is associated with tubular and globular shaped inclusions in defined areas of the bacterial cells.

(B) The MR1 cells do not contain similar inclusions and are not labeled by the p26 anti-serum.

Bars represent 200 nm.

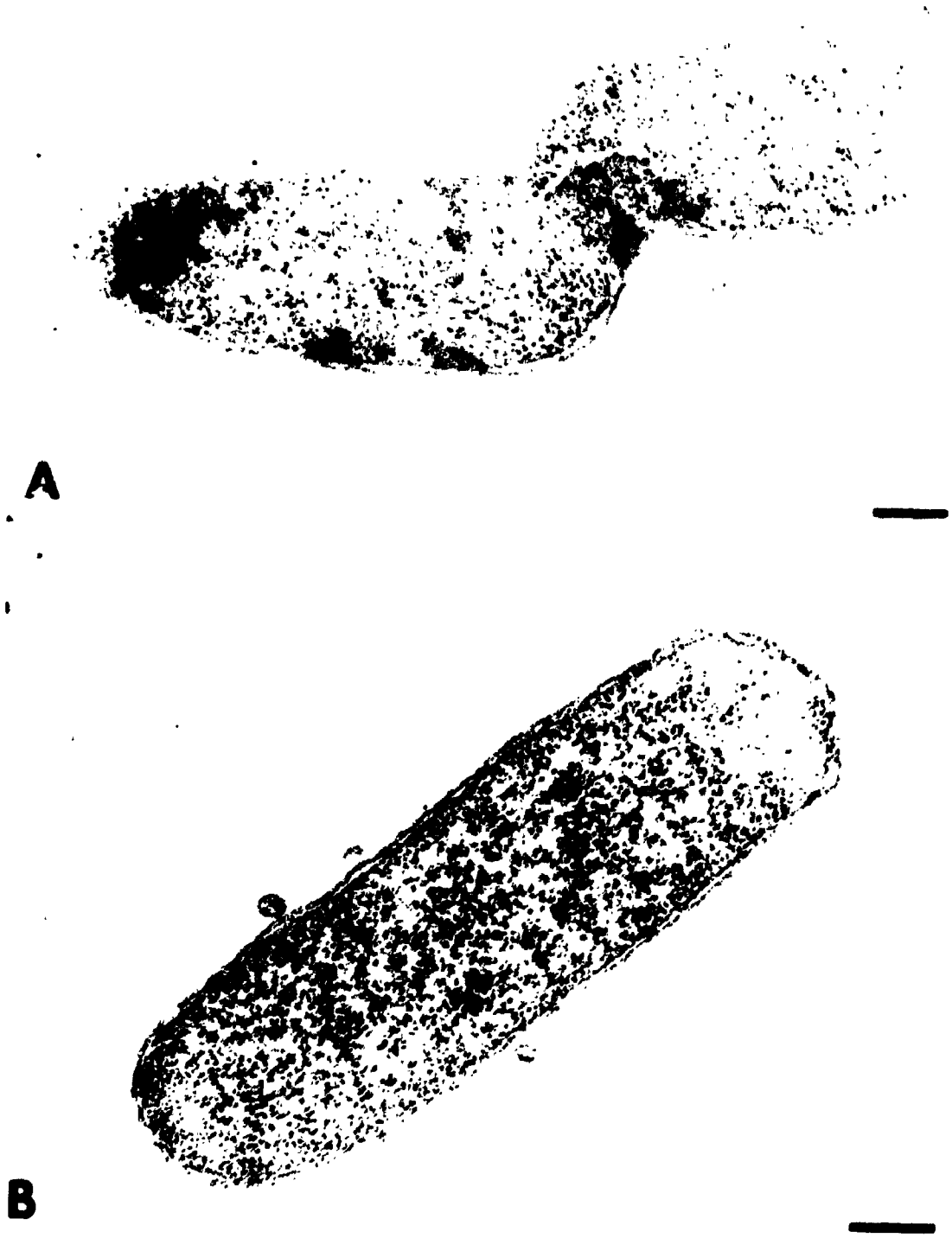
A
B

areas labeled by the p26 anti-serum could not be clearly distinguished. Moreover, it did not obviously resemble that of the p26 inclusions formed in infected plant tissues. *E. coli* cells from a culture of MR1 (expressing only the parental vector) did not contain any structures which could resemble the tubular or globular shaped aggregates. Moreover, the p26 anti-serum did not label any area of the control cells (Fig. 4.19B).

4.4 DISCUSSION

The functional properties of p26 demonstrated in this study are consistent with the requirement of this protein for the post-replicative metabolism of FMV genomic RNA leading to cell-to-cell movement of the virus. First, the RNA binding activity of p26 may be necessary to tag or sequester viral RNA molecules for their subsequent transport to neighbouring cells. Because of the lack of sequence specificity in binding displayed by p26, we cannot exclude the possibility that the viral protein may also interact with host RNAs. This lack of specificity of the FMV protein is also true for the movement proteins of TMV (Citovsky *et al.*, 1990), red clover necrotic mosaic virus (Osman *et al.*, 1992), cauliflower mosaic virus (Citovsky *et al.*, 1991) and alfalfa mosaic virus (Schoumacher *et al.*, 1992). However, specificity in RNA recognition by movement proteins may be provided by the compartmentalization of viral processes such as RNA synthesis and translation and/or by the involvement of other protein factors, such as, for potexviruses, the products of ORF3 and ORF4 (Beck *et al.*, 1991) and possibly the viral coat protein (Chapman *et al.*, 1992a, 1992b; Forster *et al.*, 1992). Second, since viral movement is an active process, it is conceivable that it may involve an energy-dependent transformation of the viral RNA or particles prior to transport. Our results suggest that

p26 could participate in such a process, perhaps using energy provided by ATP hydrolysis. Although it is tempting to speculate that p26 is an ATP-dependent RNA helicase, we did not detect any stimulation of the ATPase activity in the presence of RNA molecules. This, indeed, contrasts with the significant stimulatory effect of single-stranded RNA on other viral ATPases (Laín *et al.*, 1991: Tamura *et al.*, 1993; Warrener *et al.*, 1993) but resembles the poliovirus 2C ATPase activity (Mirzayan and Wimmer, 1994). Based on amino acid sequences flanking the core NTP-binding motif, proteins carrying this motif have been classified in three groups: sindbisvirus-like, picornavirus-like and flavi-pesti-potyvirus NTPases (Gorbalenya *et al.*, 1989). The stimulation of the NTPase activity by single-stranded RNA has so far been observed only for proteins of the latter group and may be another characteristic of these NTPases, which is not shared with the picornavirus-like (poliovirus 2C protein) and sindbisvirus-like (FMV p26) ATPases.

Our analysis of the temporal accumulation and distribution of p26 in FMV-infected systemic and local lesion hosts indicates that it is a stable protein which is predominantly found in the soluble fraction of infected plants. These findings generally agree with those recently published on the corresponding ORF2 product of potato virus X (PVX), the type member of the potexviruses (Davies *et al.*, 1993). The PVX homologue is found in all of the infected leaf fractions analyzed but is most prominent in the low speed pellet (P1), from which it is easily released by washes in the initial grinding buffer. In our study, the P1 and P30 fractions analyzed consisted of washed fractions (see section 4.2.9). We indeed detected significant amounts of p26 on Western blots in both washing solutions (data not shown), but the level of p26 observed did not

exceed that found in the S30 fraction. We cannot, accordingly, determine whether the association of the ORF2 product with the pellet fractions is biologically significant. However, the laminated inclusion components (LICs) with which the PVX 25-kDa protein is associated, are characteristic of and unique to PVX infections (Lesemann, 1985) and may contribute to the more abundant partition of the PVX 25-kDa protein to P1.

The cytoplasmic inclusions detected in FMV-infected tissue by the anti-p26 antibodies have not been reported in previous descriptions of FMV-related cytopathological effects (Short, 1983; Lesemann, 1985). Presumably, they escaped detection because their electron density renders them difficult to distinguish from other cytoplasmic material. The FMV "p26 inclusions" are structurally distinct from the LICs, often appearing as a homogenous mixture of intertwined fine filaments rather than the beaded structures forming LICs. Since our immunocytochemical analysis of p26 was restricted to infected cells of primary lesions on *C. quinoa* leaves, we cannot exclude the possibility that p26 may be associated with LIC-like structures in cells systemically infected by FMV. However, observation of systemically infected barley tissue by electron microscopy has failed to reveal any structures which resemble LICs. No p26 inclusions were found in the nuclei of 23 FMV-infected cells whereas 3/20 nuclei in cells infected with PVX contained LICs (Davies *et al.*, 1993). Although we cannot exclude that some FMV p26 inclusions may be found in nuclei at a later stage of infection, it is clear that p26 is most abundant in the cytoplasm of infected cells whereas TMV (Tomenius *et al.*, 1987) and "tubule-forming" (see section 4 1) movement proteins are found almost exclusively in plasmodesmata of infected cells.

During the viral infection, levels of the FMV 26-kDa protein reach a steady-state after the initial growth period which contrasts with the transient expression of the TMV movement protein in early infection, both in protoplasts (Watanabe *et al.*, 1984) and in synchronized leaf infections (Lehto *et al.*, 1990). The expression and subcellular localization of triple gene block homologous proteins of other plant viruses which carry the NTP-binding helicase motif also seem to differ from that of the potexviral 26-kDa protein. The BNYVV p42 protein, which is stably maintained at high levels in infected plants, partitions almost exclusively to the P30 fraction (Niesbach-Klösgen *et al.*, 1990). The BSMV $ß_b$ protein, which reaches high levels early in the infection but subsequently declines, is abundant in both soluble and cell wall fractions (Donald *et al.*, 1993). Interestingly, $ß_b$ is likely the BSMV-encoded protein which complexes with the unencapsidated viral RNA in early stages of infections *in vivo* and which appears to be uniformly distributed in the cytoplasm of infected cells (Brakke *et al.*, 1988). Complementation studies involving BSMV and PVX have demonstrated that each virus can act as a helper for the infection of the other in a normally non-host plant (Malyshenko *et al.*, 1989; Prody and Jackson, 1993). Therefore, although the triple gene block homologous proteins may accumulate in somewhat different cellular locations, it is possible that they exert similar functions in movement.

In view of the putative role of p26 in cell-to-cell transport, the reason for the formation of inclusions and for the apparent abundance of the protein, suggested by the size and number of these inclusions, is unknown. Davies *et al.* (1993) postulated that the PVX inclusions might consist of an inactive pool of the ORF2-encoded protein, the active proteins being located in other cellular areas and escaping detection due to their low

concentration. This could also be true for the p26 inclusions after adjacent cells become infected, unless the transfer process continues regardless of their being infected. However, there is no reason to exclude the possibility that the cytoplasmic inclusions may actually constitute the active site where specific processing reactions take place, leading to successful invasion of neighbouring cells by the virus. This could also involve the products of ORF3 and ORF4 and possibly the coat protein which collectively would perform functions similar to the TMV movement protein. Since p26 is an RNA-binding protein, it is conceivable that the p26 inclusions contain viral RNA sequestered and possibly modified for subsequent transport or assembly. This could be tested, in the future, by *in situ* hybridization. Despite their structural differences, a common feature of the cytoplasmic PVX inclusions and FMV p26 inclusions is their proximity to aggregates of virus particles, *in planta* (Shalla and Shepard, 1972; Davies *et al.*, 1993), and this may be related to particle processing prior to movement.

CHAPTER 5

SUBCELLULAR IMMUNOLOCALIZATION OF FOXTAIL MOSAIC VIRUS AND CACTUS VIRUS X IN INFECTED *C.QUINOA*

5.1 INTRODUCTION

The short distance movement of plant viruses involves passage from one cell to adjacent ones through intercellular connections, the plasmodesmata (reviewed by Maule, 1991; Deom *et al.*, 1992). Plant virus genomes code for protein(s) which facilitate cell-to-cell transport. Two mechanisms by which these movement proteins promote virus transport have so far been described, both involving structural alterations of the plasmodesmatal channel. The movement proteins of tobacco mosaic tobamovirus (TMV) and red clover necrotic mosaic dianthovirus (RCNMV) are single-stranded RNA binding proteins (Citovsky *et al.*, 1990; Osman *et al.*, 1992) which can also induce an increase in the plasmodesmatal space available for passage of molecules (Wolf *et al.*, 1989; Lommel *et al.*, 1994). In contrast, the movement proteins of cowpea mosaic comovirus (CPMV), cauliflower mosaic caulimovirus (CaMV) and tomato ringspot nepovirus (TomRSV) participate in the formation of tubular structures which extend from plasmodesmatal channels (van Lent *et al.*, 1990; Linstead *et al.*, 1988; Wieczorek and Sanfaçon, 1993). Other mechanisms by which viral proteins can facilitate cell-to-cell spread are conceivable. For example, the movement protein of alfalfa mosaic virus is found in middle lamellae of cell walls rather than the plasmodesmata (Stussi-Garaud *et al.*, 1987). Similarly, one of the three movement proteins of the potexviruses, encoded by ORF2 (p26 of FMV), is aggregated in inclusions in the cytoplasm of infected cells and is not present in plasmodesmata (Davies *et al.*, 1993; this thesis, Chapter 4).

In addition to different modes of action of movement proteins, viruses themselves move from cell to cell in various forms. The production of coat protein during infection has been prevented by suitable mutagenesis of the genomes of TMV (Dawson *et al.*,

1988), RCNMV (Xiong *et al.*, 1993), tobacco rattle tobravirus (Hamilton and Baulcombe, 1989), tomato bushy stunt tombusvirus (Scholthof *et al.*, 1993), turnip crinckle carmovirus (Hacker *et al.*, 1992) and barley stripe mosaic hordeivirus (Petty and Jackson, 1990). Nonetheless, these viruses continue to exhibit short distance movement. This indicates that they do not move as virions and that unpolymerized protein is not required for their movement. In contrast, CPMV, CaMV and TomRSV move in their encapsidated form and viral particles can be detected in the modified plasmodesmata (van Lent *et al.*, 1990; Linstead *et al.*, 1988; Wieczorek and Sanfaçon, 1993). Alfalfa mosaic virus (AlMV), potyviruses and potexviruses also require coat protein for cell-to-cell movement, although the need for encapsidation has not been clearly established from mutational analyses (Chapman *et al.*, 1992a, 1992b; Forster *et al.*, 1992; Sit and AbouHaidar, 1993; van der Vossen *et al.*, 1994; Dolja *et al.*, 1994). No virus particles can be isolated from plants infected with an AlMV coat protein mutant which can, nonetheless, spread from cell to cell. This suggests that although this mutant AlMV apparently cannot form stable virions, its short distance movement is not impaired. This is possibly because unpolymerized mutant coat protein is still present in infected cells since an AlMV mutant which cannot produce any coat protein will not spread (van der Vossen *et al.*, 1994). In contrast, tobacco etch potyvirus and potexviruses potato virus X (PVX) and white clover mosaic virus (WClMV) mutated in their coat protein coding sequence were unable to spread to adjacent cells although they could form virions in infected plants. This suggests that virion assembly is not the only role of the poty- and potexviral coat proteins in cell-to-cell movement and that coat protein might have different domains —some involved with assembly and others with transport in

conjunction with the other movement proteins produced by potexviruses (Chapman *et al.*, 1992b; Forster *et al.*, 1992; Dolja *et al.*, 1994). An ultrastructural analysis of tissues infected with potato virus Y (the prototype potyvirus) has suggested that electron dense, elongated particles resembling virions can be seen in plasmodesmata (Weintraub *et al.*, 1974) but this observation has not been verified.

In an effort to characterize the movement function of potexviruses further and to obtain more insight into the possible implications of virus particles and/or of the coat proteins in transport, we have monitored the distribution of foxtail mosaic virus (FMV) and cactus virus X (CVX) in infected *Chenopodium quinoa* by immunocytochemistry.

5.2 MATERIALS AND METHODS

1. Enzymes and Chemicals.

The various products used in this study have been described in section 4.2.1.

2. Anti-sera.

Anti-sera against FMV and CVX were obtained from J.B. Bancroft. The production of the FMV anti-serum was described in section 4.2.5. A serum against CVX was prepared similarly, using virions isolated from *C. quinoa* as antigen.

3. Plants and viruses.

C. quinoa plants approximately 12 inches tall were dusted with aluminum oxide and inoculated as described in section 3.2.2. Purified "barrel cactus virus", a strain of CVX (Attathom *et al.*, 1978), was used to inoculate *C. quinoa* plants. The CVX infection was developed by growing plants in a greenhouse at 24-28°C.

4. Embedding of *C. quinoa* for electron microscopy and immunocytochemical analysis.

Leaves of *C. quinoa* bearing primary chlorotic lesions 4 or 11 days following inoculation with FMV or CVX, respectively, were harvested and processed immediately for embedding. Leaf discs were cut out of the chlorotic lesions or of equivalent areas of mock-inoculated leaves and were embedded in Epon/Araldite epoxy resin as described in section 4.2.10. Ultrathin sections were prepared and treated with anti-sera as described in section 4.2.10. Anti-FMV and anti-CVX sera were diluted in phosphate buffered saline (pH 7.0) containing 0.1 % bovine serum albumin to 1:5000 and 1:2500, respectively. The 10 nm gold-conjugated goat anti-rabbit IgG antibodies were used at a dilution of 1:50.

5.3 RESULTS

1. Distribution of viral particles in FMV-infected *C. quinoa* cells.

Initially, sections of infected tissues were examined to determine the distribution of viral particles. Most of the epidermal and mesophyll cells examined contained aggregates of viral particles (Fig. 5.1-5.3). A few vascular parenchyma cells were also infected but not the tracheary or sieve elements (not shown). Viral particles were organized in parallel but curved arrays in the cytoplasm of infected cells (Fig. 5.1-5.3). These relatively compact fibrous aggregates of particles varied in size and could occupy a large proportion of the cytoplasm (Fig. 5.1, 5.2).

Subsequently, an FMV anti-serum was used in immunogold labeling experiments to evaluate the distribution of the coat protein antigens. As expected, the viral particles

Figures 5.1-5.7B: Distribution of FMV in FMV-infected *C. quinoa* cells 4 days following inoculation. Unless otherwise stated, the tissues were labeled with FMV antibodies.

Figure 5.1 Immunodetection of FMV in a mesophyll cell.

The gold-labeled virus particles (arrowheads) are clustered in curved arrays in the cytoplasm but not in the vacuole (Va) of the mesophyll cell. Mitochondria (m), chloroplast (Ch) and the cell walls (CW) are not labeled. Bar represents 400 nm.

Figure 5.2 Aggregates of viral particles in a mesophyll cell.

Higher magnification view of gold-labeled FMV virions (V) in the cytoplasm. A few gold-labeled virus particles are also seen in the vacuole (Va). The cell wall (CW), mitochondria (m) and areas of the cytoplasm filled with ribosomes (r) are not labeled by the FMV antibodies. Bar represents 200 nm.


Va

Figure 5.3 Control of the immunolabeling of FMV-infected *C. quinoa* cells.

The viral particles (arrowheads) in tissues incubated with a pre-immune (A) or with gold-conjugated goat anti-rabbit antibodies alone (B) are not labeled. Plasmodesmata (p) are also seen in (B). Bars represent 200 nm.

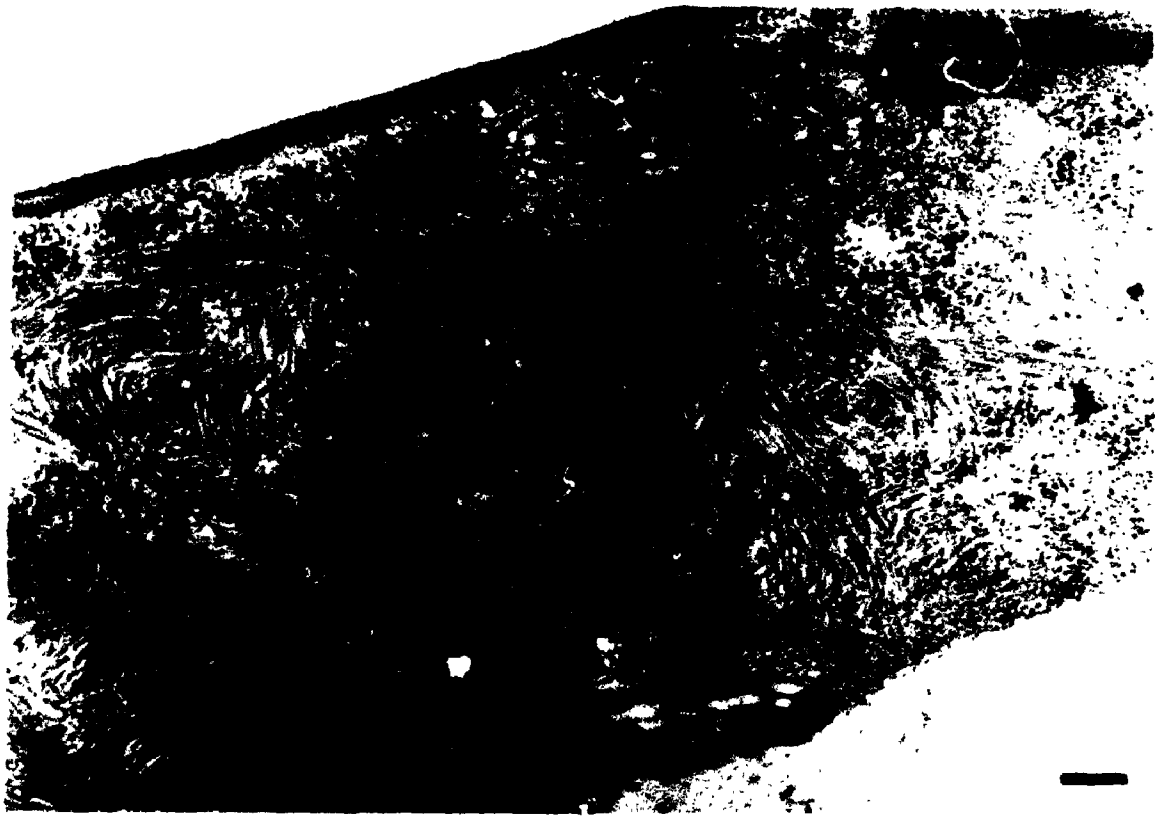

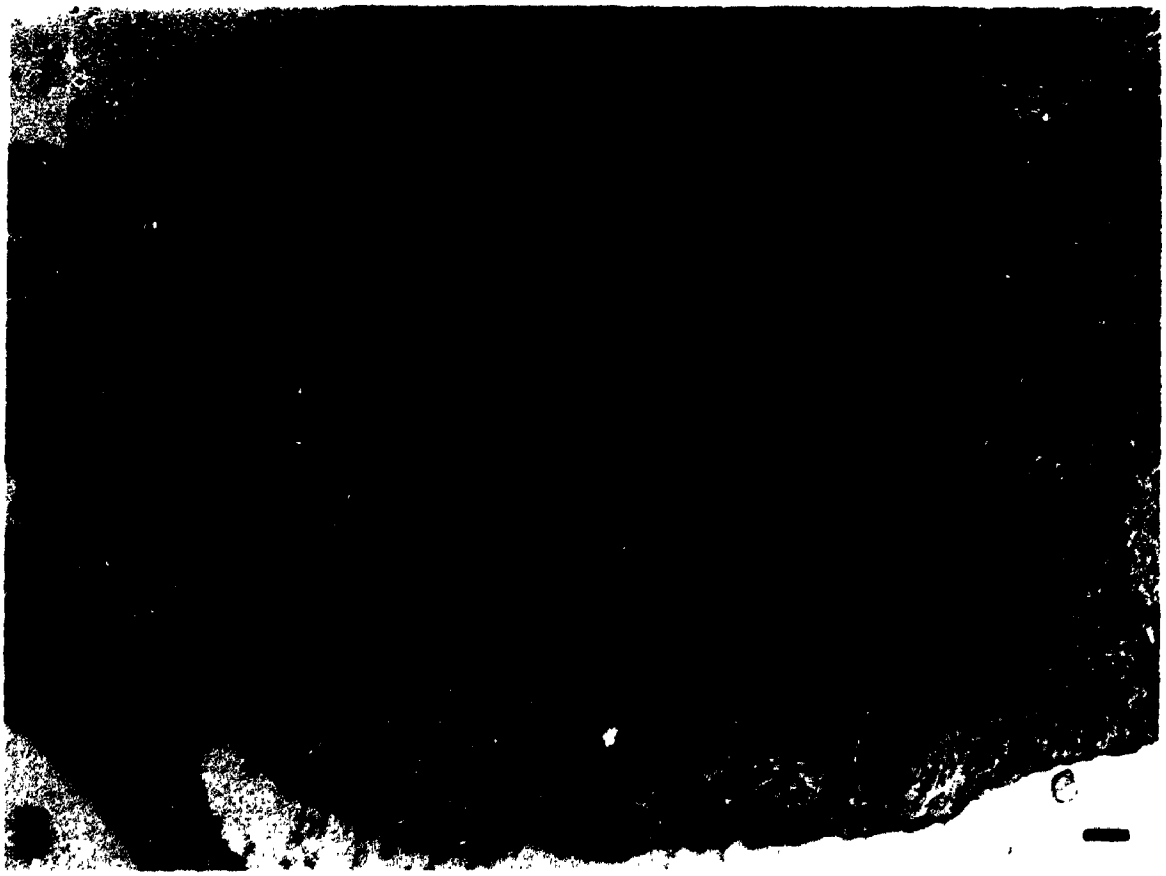

were labeled by the anti-FMV serum (Fig. 5.1, 5.2). No other cellular component was labeled by the same serum, including the nuclei of 32 infected cells (not shown), chloroplasts and mitochondria (Fig. 5.1, 5.2). This demonstrates not only the specificity of the labeling but also the absence of viral particles in the nucleus and cellular organelles. Moreover, neither mock-inoculated tissues incubated with the anti-FMV serum (Fig. 5.7C) nor FMV-infected tissue incubated with pre-immune serum (Fig. 5.3A), with anti-CVX serum (Fig. 5.7A, B) or with goat anti-rabbit antibodies alone (Fig. 5.3B) were decorated in any area.

Since coat proteins and/or viral particles are suspected to participate in the movement of potexviruses, cell wall and plasmodesmatal areas were examined for the presence of gold particles. Although it is difficult to obtain good sections throughout the plane of plasmodesmata, labeling was observed in or near a considerable number of them (Fig. 5.4-5.6). In several occasions, small clusters of viral particles were present next to plasmodesmata (Fig. 5.4A) and sometimes in continuity with them (Fig. 5.4B). These small clusters could also be noticed embedded in the cell wall although no plasmodesma were distinguishable (Fig. 5.4C). Moreover, several plasmodesmata were labeled even though clusters of viral particles were not seen adjacent to them (Fig. 5.5, 5.6). Although these plasmodesmata were only moderately labeled, the quantity of gold particles was significant when compared with control tissues (Table 5.1). Several lines of evidence suggest that the observed labeling did not result from a non-specific reaction of the serum with a plasmodesmatal component. First, not all plasmodesmata were labeled (Table 5.1). Labeled plasmodesmata were usually those connecting cells of which at least one was infected. Second, the anti-FMV serum did not decorate plasmodesmata in mock-inoculated

Figure 5.4 Plasmodesmata and small clusters of virus particles in mesophyll cells.

(A) Gold-labeled FMV particles are located next to a labeled plasmodesma (p). Virus particles cannot be seen in the plasmodesma.

(B) The cluster of gold-labeled virus is in continuity with a plasmodesmata (p) sectioned obliquely.

(C) Small cluster of compartmentalized labeled virus particles (arrowheads) embedded in the cell wall (CW) in an area where no plasmodesma is seen. Aggregates of gold-labeled virus particles (V) are seen in the adjacent cell.

Bars represent 200 nm.


A
B

Figure 5.5 Plasmodesmata decorated by the FMV anti-serum.

(A) View of labeled plasmodesmatal channels (p) connecting 2 cells containing virions (arrowheads).

(B) View of labeled plasmodesmata (p) sectioned transversely. The cell below the wall contains virions (V).

Bars represent 200 nm.

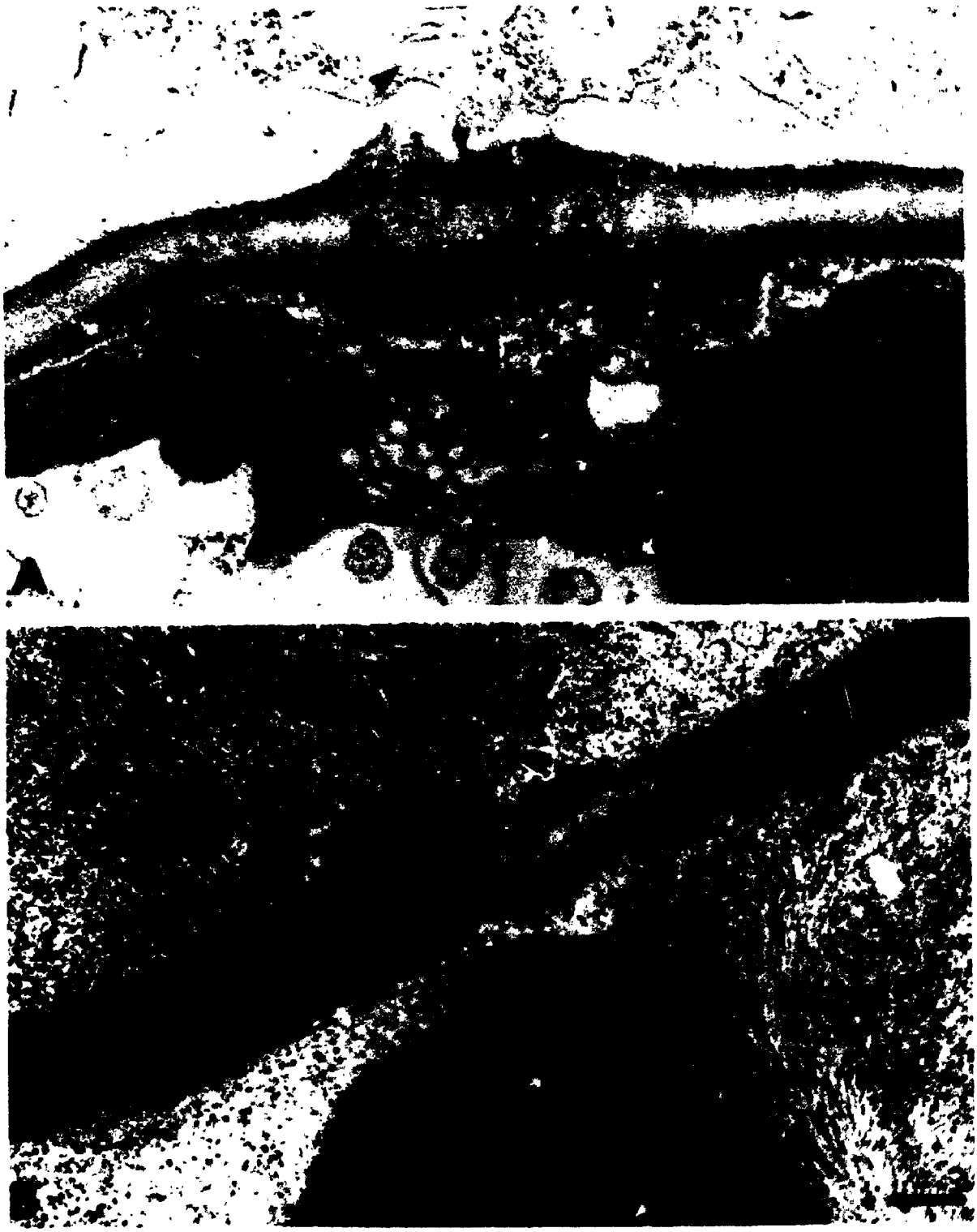

Figure 5.6 Higher magnification views of plasmodesmata, in FMV-infected cells, labeled by the FMV anti-serum. Bars represent 100 nm.

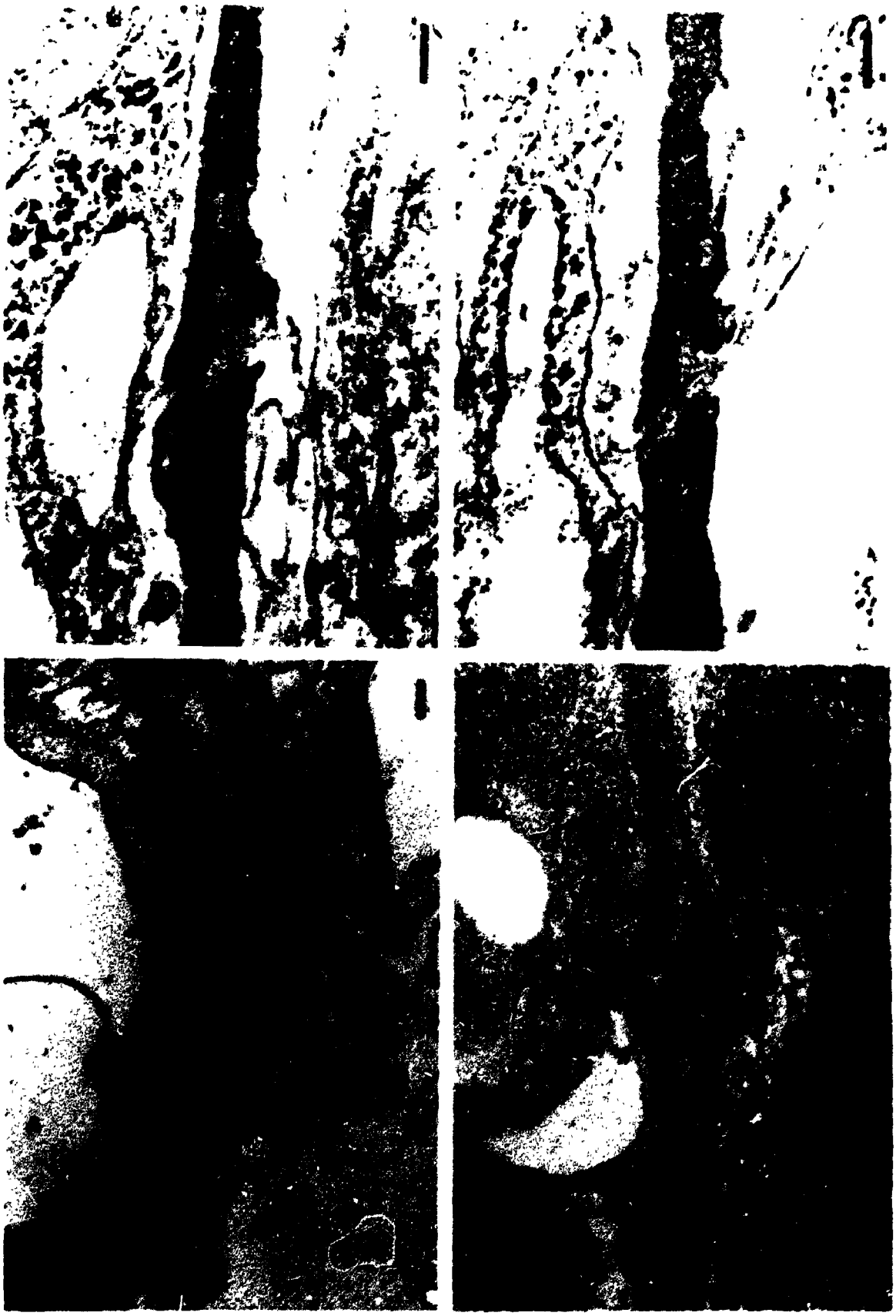

Figure 5.7 Control of the immunolabeling of cells in plasmodesmatal areas.

(A, B) FMV particles (arrowhead) and plasmodesmata (p) in FMV-infected tissues are not labeled by the CVX anti-serum.

(C) Transverse section of plasmodesmata (p) in mock-inoculated tissues which are not decorated by the FMV anti-serum.

Note that the electron dense material in the cytoplasm consists of ribosomes and not of gold particles. Bars represent 300 nm.

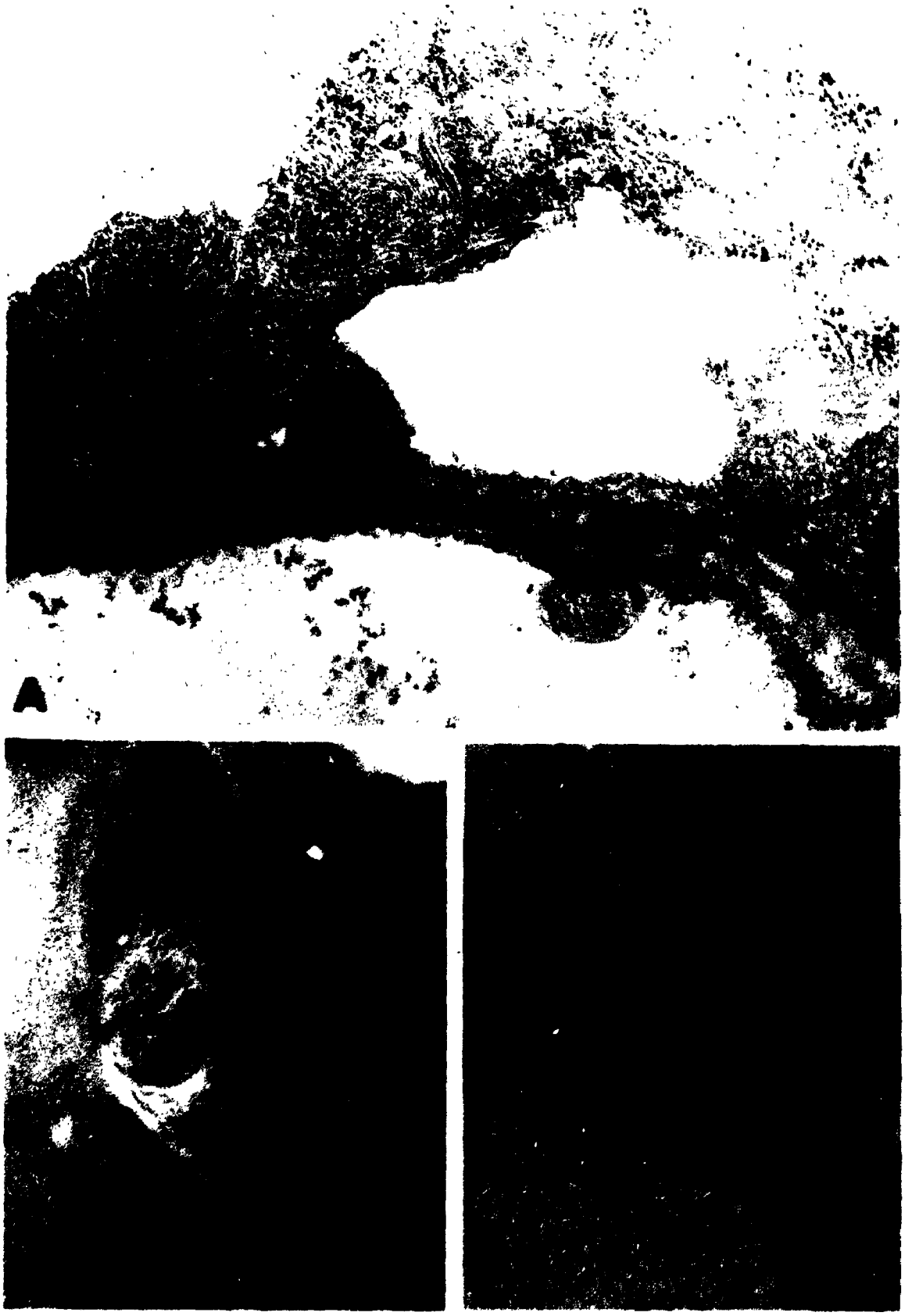
A

Table 5.1 Distribution of gold label within plasmodesmata of mock-inoculated and infected *C. quinoa* incubated with anti-FMV and anti-CVX sera.

serum	tissue	labeled plasmodesmata / observed plasmodesmata		average # gold particles per labeled plasmodes.
α-FMV	mock	1/42	(2.4 %)	2
	FMV-inf.	17/28	(60.7 %)	11
α-CVX	mock	0/31	(0 %)	-
	CVX-inf.	28/48	(58.3 %)	6

tissues (Fig. 5.7C; Table 5.1) or other regions of the cell wall (in infected and healthy tissues) (Fig. 5.1, 5.2, 5.4-5.6). Third, neither a pre-immune serum (data not shown) nor the anti-CVX serum (Fig. 5.7A, B) labeled plasmodesmata (or any other cellular structure) in FMV-infected *C. quinoa* sections. The result of the latter heterologous incubation largely eliminates the possibility that labeling of plasmodesmata results from the recognition of a host protein whose expression is induced during potexviral infections.

2. Distribution of viral particles in CVX-infected *C. quinoa* cells.

To extend our findings and to test their generality, we examined tissues infected with a second potexvirus, CVX. The distribution of CVX resembled that of FMV. CVX particles were mostly located within epidermal and mesophyll cells (Fig. 5.8, 5.9, 5.11, 5.12) and in a few vascular parenchyma cells (Fig. 5.13). CVX differed from FMV in that it was also present in close proximity to osmiophilic (lipid) globules present in some vascular parenchyma cells (Fig. 5.13). CVX particles sometimes had accumulated in aggregates larger than those formed by FMV particles (Fig. 5.8, 5.9, 5.11). Moreover, the parallel arrays of CVX particles were only slightly curved and generally were packed less tightly than FMV particles (compare Fig. 5.2 with 5.9 and 5.14) except in epidermal cells where CVX particles were aggregated in compact parallel arrays (Fig. 5.11). The tightness of the packing of the virus particles in epidermal cells can be particularly appreciated in aggregates of virions cut transversely (Fig. 5.12). Typical cytoplasmic material was almost completely excluded from the large areas occupied by the cytoplasmic aggregates of viral particles (Fig. 5.8, 5.9). On occasion, single viral particles could be observed in the vacuole of mesophyll cells, either alone or next to

Figures 5.8-5.15A, 5.16: Distribution of CVX in CVX-infected *C. quinoa* cells 11 days following inoculation. Unless otherwise stated, tissues were labeled with CVX antibodies.

Figure 5.8 Immunodetection of CVX in a mesophyll cell.

The gold-labeled virus particles (V) fill a large portion of the cytoplasm. Mitochondria (m), chloroplast (Ch) and cell walls (CW) are not labeled. The vacuole (Va) does not contain virus particles. Bar represents 400 nm.

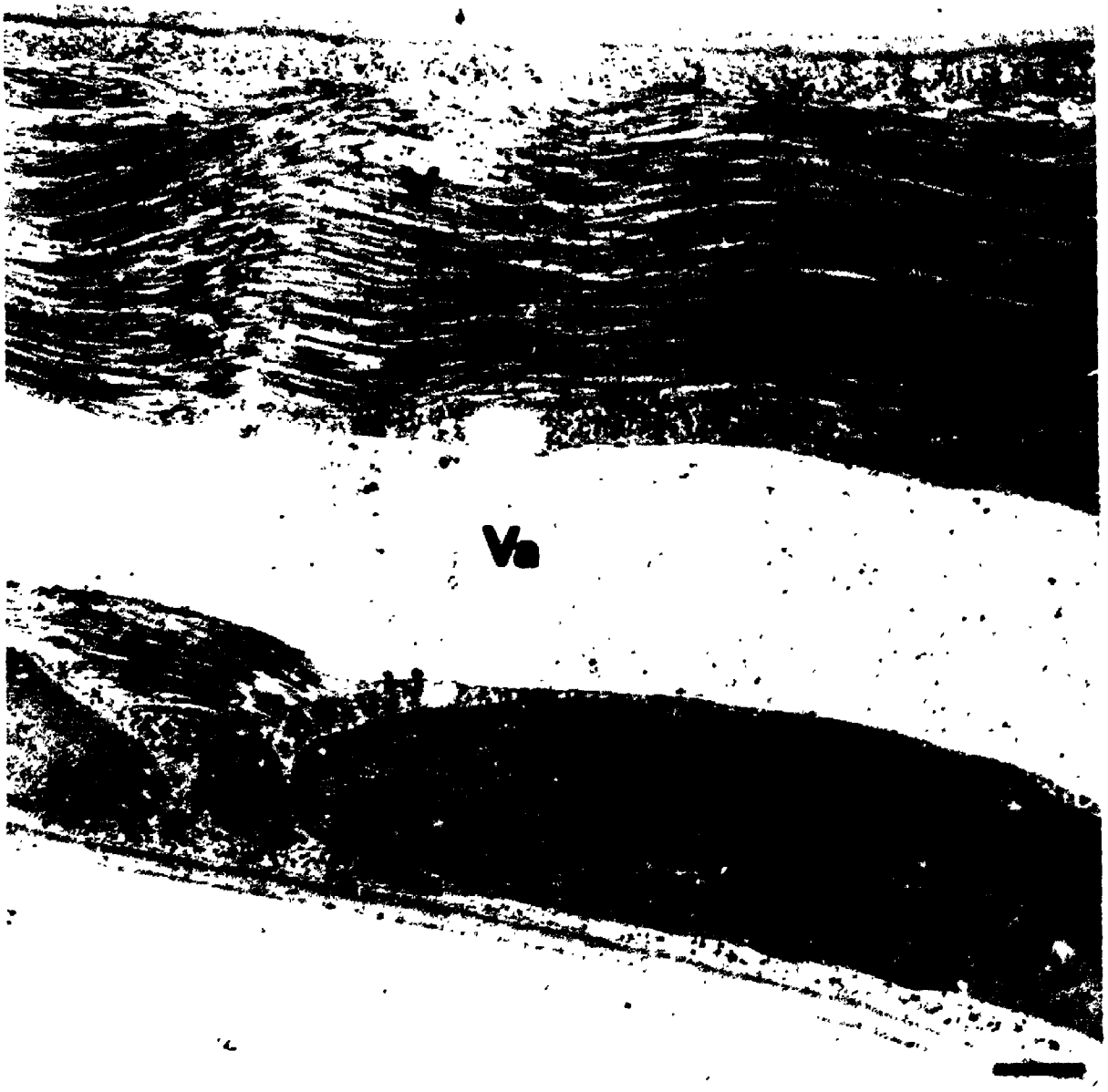
Va

Figure 5.9 Large aggregate of CVX particles in the cytoplasm of a mesophyll cell.

The virions in the aggregate are intensely labeled by the CVX anti-serum while mitochondria and chloroplast are not labeled. The cytoplasm filled with ribosomes (r) is almost completely excluded from the area containing virus. Bar represents 200 nm.

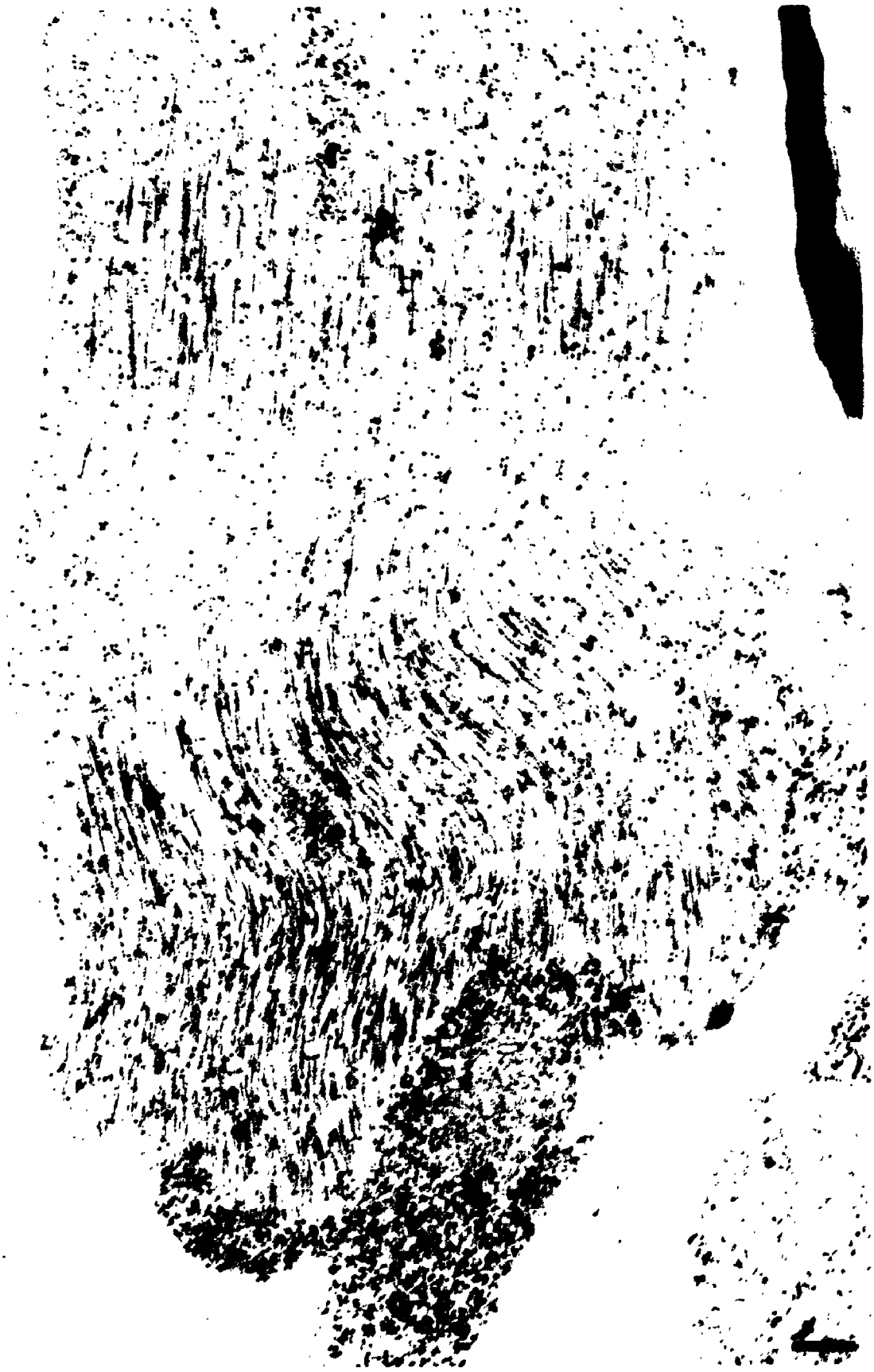

Figure 5.10 Single CVX particles located in the vacuole of a mesophyll cell.

The arrows point at particles which are probably complete. Most of the virus rods seen are shorter, probably due to the sectioning angle. A portion of an aggregate of virus (V) is also seen. Bar represents 200 nm.

Figure 5.11 Aggregate of CVX particles in an epidermal cell.

The gold-labeled viral particles are tightly packed in one area of the cytoplasm next to the cell wall (CW). Bar represents 200 nm.

Figure 5.12 View in cross-section of an aggregate of CVX particles in an epidermal cell.

Most of the virus particles are cut transversely and appear as small pinhead structures in the aggregate. Virus particles in the upper left of the aggregate are probably sectioned obliquely. The cell wall (CW) is not labeled by the CVX anti-serum. Bar represents 200 nm.

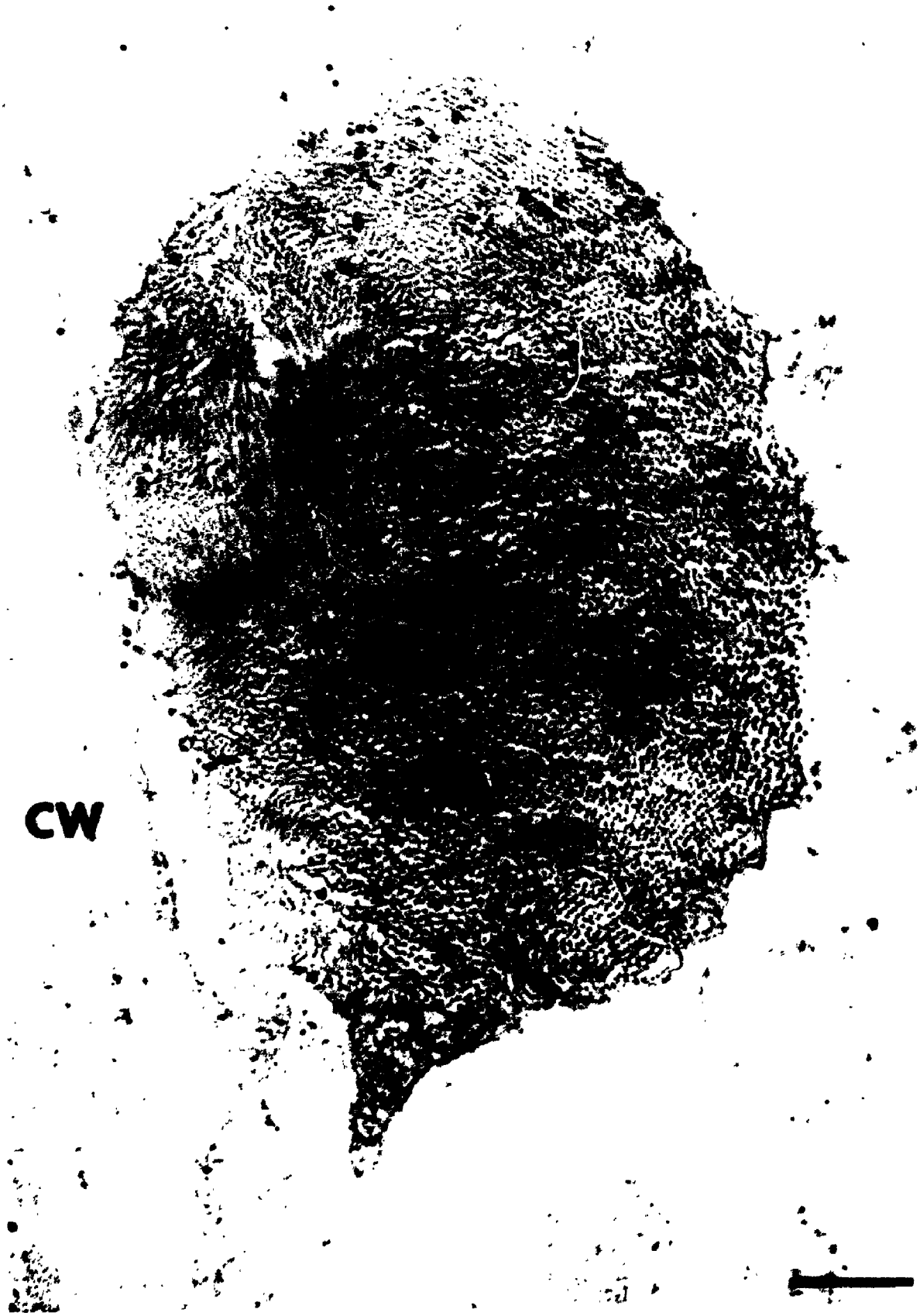
CW

Figure 5.13 CVX particles in a vascular parenchyma cell.

The gold-labeled viral particles are close to the osmiophilic globules (O). CVX appears associated with the lower right globule (arrowheads). The cytoplasm in the cell at the left of the thin cell wall is gold-labeled (arrow) although no viral particles are seen. Bar represents 200 nm.

Figure 5.14 CVX aggregates in a mesophyll cell.

CVX particles are packed in parallel aggregates which are labeled by the CVX anti-serum. The cytoplasm next to the virus aggregates is also labeled by the CVX anti-serum although viral particles are not seen. The cell wall, chloroplast and vacuole are not labeled. Bar represent 200 nm.

aggregates of virions (Fig. 5.10). This was also seen in FMV-infected tissues (not shown). The length of the loose rods appeared variable, with only a few being approximately 520 nm long, the normal length of CVX particles (Attathom *et al.*, 1978). This probably results from the cutting angle during the sectioning of tissues, since the loose virus particles were apparently oriented randomly.

The large aggregates of CVX particles were intensely labeled by CVX anti-serum (Fig. 5.8, 5.9, 5.11, 5.14). Interestingly, areas of the cytoplasm where viral particles could not be seen were also moderately labeled (Fig. 5.13, 5.14, 5.16A), suggesting that there were too few viral particles to be clearly seen or that unpolymerized coat protein was present. The labeling was specific to the cytoplasm. Chloroplasts, mitochondria and 18 nuclei within infected cells were not labeled (Fig. 5.8, 5.9, 5.13, 5.14). Moreover, tissue from mock-inoculated leaves was not decorated by anti-CVX serum (Fig. 5.15B, C) and a pre-immune serum did not label infected *C. quinoa* cells (Fig. 5.15A).

The anti-CVX serum also decorated plasmodesmata connecting a number of mesophyll cells (Fig. 5.16), at least one of which contained virions. The number of labeled plasmodesmata resembles that described for FMV-infected tissues although the intensity of labeling was lower in CVX-infected tissues (Table 5.1). Moreover, small clusters of CVX particles were not seen in the proximity of plasmodesmata or embedded in the cell wall as it was the case in FMV-infected *C. quinoa*. The anti-CVX serum did not label plasmodesmata of cells from mock-inoculated leaves (Fig. 5.15C) nor did pre-immune serum label plasmodesmata of CVX-infected cells (not shown), supporting the specificity of the labeling obtained with the CVX anti-serum. Moreover, CVX-infected *C. quinoa* incubated with anti-FMV serum did not result in the decoration of any area,

Figure 5.15 Control of the immunolabeling of CVX-infected and mock-inoculated *C. quinoa*.

(A) The pre-immune serum does not label CVX particles (V) or any other structures of an infected cell.

(B, C) The CVX anti-serum does not label any area of a mock-inoculated tissue, including the cytoplasm, chloroplast, cell wall or plasmodesmata (p).

Bars represent 200 nm.


C

Figure 5.16 Plasmodesmata labeled by the CV* anti-serum in CVX-infected *C. quinoa*.

(A) Plasmodesmata (p) connecting two cells containing the viral antigen (gold in the cytoplasm of the upper cell) and virions (arrowhead). One of the plasmodesmatal channels is gold-labeled.

(B) Labeled plasmodesma (p) connecting mesophyll cells. The cell above the wall contains a CVX aggregate (V).

Bars represent 200 nm.


B

including plasmodesmata (not shown).

5.4 DISCUSSION

This immunocytochemical study describes the distribution of viral particles and possibly of coat protein subunits in *C. quinoa* cells infected with the potexviruses FMV and CVX. The distribution of CVX differed from that of FMV only by its presence near lipid globules in vascular parenchyma cells. A similar observation has been described for beet yellows closterovirus (Esau and Hoefert, 1971). The lipid globules are also present in cells of healthy tissue (Esau and Hoefert, 1971; data not shown) indicating that they are not virus-induced structures. The reason for their proximity to CVX virions (and beet yellows virus) in infected tissues is not known. Although most of the viral antigen is assembled into virions in the cytoplasm of infected cells, small but significant amounts of both FMV and CVX antigens are associated with plasmodesmata. The latter observation has not been reported previously.

Mutational analysis of the coat protein in the genomes of PVX and WClMV demonstrated that the coat protein plays a role in the spread of the viruses in host plants (Chapman *et al.*, 1992a, 1992b; Forster *et al.*, 1992). However, because mutations in the coat protein also exerted an effect on the accumulation of the gRNA in infected plants, it could not be ruled out that the role of the coat protein in movement was indirect. This indirect role may be to reduce the level of gRNA produced or to affect the expression of the viral proteins involved in movement (encoded by ORFs 2, 3 and 4). The presence of gold label in plasmodesmata is consistent with the idea that the viral coat antigen, in some form, is directly involved in the cell-to-cell spread of the virus infection

in host plants. We could not clearly distinguish rod-shaped particles in the labeled plasmodesmata. Whether this is due to the absence of virions in the plasmodesmata or to the possible difficulty of resolving a few viral particles in this structure remains to be determined. A number of scenarios in which the coat protein could participate in the movement process of potexviruses can be envisaged. Since virions cannot be seen in plasmodesmata, ribonucleoprotein particles containing a few coat protein molecules may be involved in the translocation. Alternatively, the coat protein may alter the structure of the plasmodesma which in turn could facilitate the passage of a free viral RNA or of a viral RNA complexed with other proteins, a mechanism resembling that proposed for the movement protein of TMV (Deom *et al.*, 1992). These mechanisms are not mutually exclusive. We cannot exclude the possibility that targetting of the viral RNA to plasmodesmata occurs in its encapsidated form, a notion supported by the presence of clusters of viral particles adjacent to or in continuity with plasmodesmata in FMV-infected tissues. The subsequent translocation to adjacent cells could then occur in another form, as described above. If so, virions would have to be fully or partially stripped.

Similarities between potyviral and potexviral coat proteins have been documented previously. Poty- and potexviruses both have flexuous filamentous particles. The amino acid sequences of their coat proteins are significantly related (Dolja *et al.*, 1991). Moreover, like potexviruses, the cell-to-cell movement of potyviruses requires the coat protein, as demonstrated for tobacco etch potyvirus (Dolja *et al.*, 1994). Interestingly, an immunocytochemical study of wheat streak mosaic virus (another potyvirus) recently demonstrated the localization of the coat protein in plasmodesmata of infected cells

although the presence of viral particles could not be assessed (Elhassani *et al.*, 1994). Therefore, the coat protein of these two groups of filamentous viruses may share not only similar sequences but also similar functions.

CHAPTER 6

CONCLUSIONS AND PERSPECTIVES

Foxtail mosaic virus is a member of the potexvirus family which primarily infects monocotyledonous plants. Its flexuous filamentous particles are 500 nm long and consist of a messenger sense RNA encapsidated by a single type of coat protein. We have determined the nucleotide sequence of the FMV gRNA as well as the organization of its coding sequences. The gRNA is 6151 nucleotides long and contains five major open reading frames (ORF). The amino acid sequences of the putative proteins are closely related to homologous proteins of other sequenced potexviruses. The least similar of the proteins encoded by FMV to those of other potexviruses is the capsid protein, which nonetheless retains apparently critical consensus regions.

We have established a procedure for the partial purification of the RNA-dependent RNA polymerase from tissues infected with FMV. We determined that the enzyme isolated is template-independent, i.e. it could not copy added RNA templates. The products synthesized *in vitro* by the enzyme were double-stranded RNA molecules. Therefore, it appears that the FMV RdRp (and probably other potexviral RdRps) resembles many other RdRps previously isolated from unrelated viruses in that it is difficult to obtain an enzyme able to copy exogenous templates. So far, only the tricornaviridae (i.e. alfalfa mosaic, brome mosaic and cucumber mosaic viruses) and turnip yellow mosaic tymovirus have an RdRps which can be purified highly while retaining a significant template-dependent polymerase activity. Since the FMV RdRp probably consists of a quaternary protein complex, further attempts to purify it may be more likely to succeed with gentle separation procedures which are based on size fractionation (e.g. chromatography by size exclusion or density gradient centrifugation) rather than with fractionation procedures based on properties of such as charge or

hydrophobicity, which may promote the dissociation of components of the RdRp. The FMV RdRp, however, differed from other template-independent enzymes in that potexviral RNAs specifically inhibited the RNA synthesizing activity. At this stage, further characterization of the FMV enzyme could exploit this inhibitory aspect of potexviral RNAs on synthesizing activity. It has been suggested that inhibition results from a competition for the binding of essential component(s) of the RdRp (Chapter 3). Photochemical cross-linking using labeled inhibitory RNA transcripts could be used to initiate an investigation of potential proteins which can interact specifically with RNA of viral sequences and which may be part of the RdRp complex.

We have examined the temporal expression of various elements of the viral infection. The RdRp activity was followed by measuring the activity of plant extracts prepared at different days following inoculation of *C. quinoa* (in primary lesions) and barley (in systemically infected leaves) (Chapter 3). The levels of the virally-encoded proteins p152 (Chapter 3), p26 (Chapter 4) and coat protein (Chapter 4) were measured using the same plant extracts by Western blotting. In addition, relative virus titres were determined by local lesion assays of the sap from each time point on *C. quinoa* leaves. A summary of the kinetics of appearance determined for each parameter is presented in Figure 6.1. Maximal levels of RdRp activity preceded maximal levels of p26, coat protein and virus titres, in both hosts. The kinetics of appearance and accumulation of the RdRp activity also differed from that of p152. In *C. quinoa*, peak levels of RdRp activity preceded maximal levels of p152 (Fig. 6.1A) while in barley, the opposite was observed (Fig. 6.1B). Nonetheless, the levels of only RdRp activity and p152 declined significantly subsequent to their peak, whereas those of p26 and coat protein remained

Figure 6.1 Relative concentrations of parameters of the viral infection.

Relative concentrations were estimated visually from autoradiographs of RNA products synthesized (Fig. 3.3, RdRp) or from Western blots (Fig. 3.4, p152; Fig. 4.9, p26 and coat protein (CP)). For each protein, the maximal concentration was given a value of 100 and values at other time points are expressed relative to the maximal concentration. The infectivity of the sap [virus titres (VT)] at times of harvest is expressed relative to the infectivity of the sap at the last day of the experiment (section 3.2.3; Fig. 3.3).

(A) Infection in *C. quinoa*. Arrow indicates the day at which primary lesions were first detected. Lesions continued to expand as the infection progressed.

(B) Infection in barley. Arrow indicates the day at which symptoms were first detected on some secondary (non-inoculated) leaves.

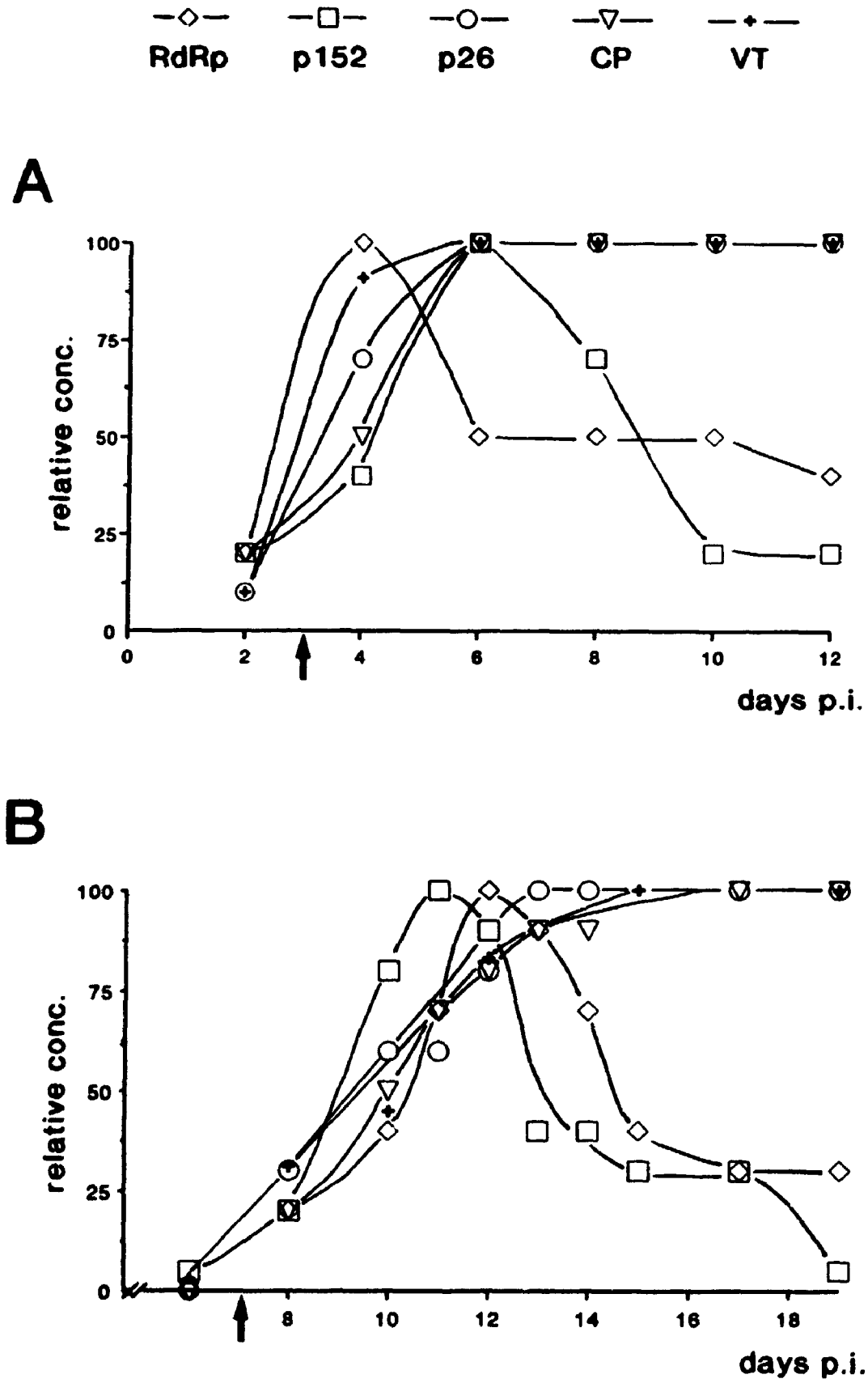
RdRp
p152
p26
CP
VT
A
relative conc.
100
75
50
25
0
0
2
4
6
8
10
12
days p.i.
B
relative conc.
100
75
50
25
0
8
10
12
14
16
18
days p.i.

high, reaching their maximum levels after those of RdRp and p152. Since the RdRp consists of a complex of proteins, the level of activity should be maximal only in the presence of the optimal concentration of each of the components forming the complex. One of these could be p152. Therefore, the general trends of the levels of the activity and of the protein are consistent with the hypothesis that p152 is associated with the RdRp activity. This is also supported by the presence of p152 in all of the active RdRp fractions obtained during the purification procedure (Chapter 3, section 3.3.2).

The accumulation of the viral indicators (i.e. RdRp activity, p152, p26 and virus titres) followed similar trends in both plant hosts, although it was slower in the systemic host barley than in *C. quinoa*. The levels measured in barley represent the average levels found in the leaves infected to different extents since infection continues to spread to new cells and leaves throughout the course of the experiment. Ideally, the kinetics of appearance of the indicators should be measured during a synchronous infection, thereby allowing measurements of true steady state levels. In this regard, *C. quinoa* provides a better system than barley, since during the formation of primary lesions, the infection is approximately at the same stage in each lesion. However, since each lesion consists of more than one cell, the correlation of the appearance of the various indicators may vary slightly with that obtained with a true synchronous infection, which can be generated using protoplasts.

The p26 protein of FMV, encoded by ORF2, possesses ATP, CTP and RNA binding activities as well as an ATP hydrolysis activity. These properties may all be required for the cell-to-cell spread of FMV in plants, a process in which p26 is believed to participate. We found that p26 is located in the cytoplasm of infected cells ather than

in plasmodesmata, unlike the movement proteins of most other plant viruses. p26 was associated almost exclusively with inclusions having the appearance of fine intertwined filaments. These inclusions were generally situated adjacent to aggregates of virus particles. In contrast, the immunocytochemical study of the distribution of the coat protein antigen in infected tissues indicated that small amounts of coat protein antigens are present in plasmodesmata. This finding agrees with those found previously from mutational analyses of the potexviral genome and, taken together, supports a direct role for the coat protein in the cell-to-cell spread of potexviruses. Furthermore, these observations point to the multiplicity of potexviral coat protein functions. The coat proteins interact not only with viral RNA and with each other, but also with plasmodesmata.

Clearly, there is no universal mechanism for the cell-to-cell movement of viruses in plants. Unlike TMV and several other viruses so far characterized which encode a single movement protein, potexviruses probably require four virally-encoded products for efficient cell-to-cell transport (i.e. the triple gene block proteins and the coat protein). The specific role played by each protein as well as the interactions among them necessary for an efficient process remain to be determined. We have proposed (Chapter 4) that p26 is involved in particle or RNA processing for transport rather than acting at the plasmodesmata, since it is located exclusively in the cytoplasm of infected cells. Since p26 is an RNA binding protein and since the inclusions with which it is associated are generally adjacent to virus particles, perhaps the inclusions consist of a pool of RNA or of ribonucleoprotein particles which are at a specific stage of the viral maturation. Indeed, it may be necessary to sequester these (immature) viral entities in a particular

area of the cell in order to reach a specific threshold sufficient for subsequent movement to occur. The quantity of viral entities (i.e. RNA, immature particles or completed virus) required over short time periods so that some molecules would be in proximity of a plasmodesmata is probably necessarily large, even if the process is more directed than that found in a random walk. This is an aspect of virus movement which is yet to be addressed.

The potexviral entity that traverses plasmodesmata has not been identified. As a next step to elucidate the movement process of potexviruses, future work should determine whether the virions, RNA or non-virion ribonucleoprotein particles are transported to adjacent cells. Additional mutagenesis of the coat protein coding sequence in the potexviral genome should indicate whether encapsidation and movement are separable activities of the coat protein, i.e. whether coat protein mutants which are unable to encapsidate RNA can still promote cell-to-cell spread of the infection. This would show whether virus moves as an encapsidated or as a non-virion entity. Immunocytochemical analyses of tissues infected by mutants would also contribute in defining the role of the coat protein in the movement process.

The proteins encoded by ORF3 and ORF4 both contain stretches of hydrophobic amino acids bordered by charged ones, a motif characteristic of a transmembrane domain. Expression of these proteins *in vitro* using a membrane-enriched Krebs-2 cell extract to translate synthetic RNAs provided experimental support to the predicted membrane-bound properties of both proteins (Morozov *et al.*, 1990). Further characterization of the subcellular location of these proteins in infected tissues should give more insight into their potential roles in movement.

REFERENCES

AbouHaidar, M.G., and Bancroft, J.B. (1978) The initiation of papaya mosaic virus assembly. *Virology* **90**, 54-59.

AbouHaidar, M.G. (1983) The structure at the 5' and 3' ends of clover yellow mosaic virus RNA. *Can. J. Microbiol.* **29**, 151-156.

AbouHaidar, M.G., and Erickson, J.W. (1985) Structure and *in vitro* assembly of papaya mosaic virus. In *Molecular plant virology*, Vol. I, Davies, J.W. ed., CRC Press, Boca Raton, Florida, pp. 85-121.

AbouHaidar, M.G. (1988) Nucleotide sequence of the capsid protein gene and 3' non-coding region of papaya mosaic virus RNA. *J. Gen. Virol.* **69**, 219-226.

Ahlquist, P., and Janda, M. (1984) cDNA cloning and *in vitro* transcription of the complete brome mosaic virus genome. *Mol. Cell. Biol.* **4**, 2876-2882.

Allison, R.F., Janda, M., and Ahlquist, P. (1988) Infectious *in vitro* transcripts from cowpea chlorotic mottle virus cDNA clones and exchange of individual RNA components with brome mosaic virus. *J. Virol.* **62**, 3581-3588.

Altshuh, D., Lesk, A.M., Bloomer, A.C., and Klug, A. (1987) Correlation of co-ordinated amino acid substitutions with function in viruses related to tobacco mosaic virus. *J. Mol. Biol.* **193**, 693-707.

Argos, P. (1988) A sequence motif in many polymerases. *Nucleic Acids Res.* **16**, 9909-9916.

Atabekov, J.G., and Taliansky, M.E. (1990) Expression of a plant virus-coded transport function by different viral genomes. *Adv. Vir. Res.* **38**, 201-248.

Attathom, S., Weathers, L.G., and Gumpf, D.J. (1978) Identification and characterization of a potexvirus from california barrel cactus. *Phytopathol.* **68**, 1401-1406.

Bancroft, J.B., Hiebert, E., Rees, M.W., and Markham, R. (1968) Properties of cowpea chlorotic mottle virus, its protein and nucleic acid. *Virology* **34**, 224-239.

Bancroft, J.B., AbouHaidar, M.G., and Erickson, J.W. (1979) The assembly of clover yellow mosaic virus and its protein. *Virology* **98**, 121-130.

Bancroft, J.B., Rouleau, M., Johnson, R., Prins, L., and Mackie, G.A. (1991) The complete nucleotide sequence of foxtail mosaic virus RNA. *J. Gen. Virol.* **72**, 2173-2181.

Baratova, L.A., Grebenshchikov, N.I., Dobrov, E.N., Gedrovich, A.V., Kashirin, I.A., Shishkov, A.V., Efimov, A.V., Järvdkülg, L., Radavsky, Yu.L., and Saarma, M. (1992a) The organization of potato virus X coat proteins in virus particles studied by tritium planigraphy and model building. *Virology* **188**, 175-180.

Baratova, L.A., Grebenshchikov, N.I., Shishkov, A.V., Radavsky, Yu.L., Järvekülg, L., and Saarma, M. (1992b) The topography of the surface of potato virus X: tritium planigraphy and immunological analysis. *J. Gen. Virol.* **73**, 229-235.

Beck, D.L., Forster, R.L.S., Bevan, M.W., Boxen, K.A., and Lowe, S.C. (1990) Infectious transcripts and nucleotide sequence of cloned cDNA of the potexvirus white clover mosaic virus. *Virology* **177**, 152-158.

Beck, D.L., Guilford, P.J., Voot, D.M., Andersen, M.T., Forster, R.L.S. (1991) Triple gene block proteins of white clover mosaic potexvirus are required for transport. *Virology* **183**, 695-702.

Bendena, W.G., AbouHaidar, M.G., and Mackie, G.A. (1985) Synthesis *in vitro* of the coat protein of papaya mosaic virus. *Virology* **140**, 257-268.

Bendena, W.G., and Mackie, G.A. (1986) Translational strategies in potexviruses: products encoded by clover yellow mosaic virus, foxtail mosaic virus, and viola mottle virus RNAs *in vitro*. *Virology* **153**, 220-229.

Bendena, W.G., Bancroft, J.B., and Mackie, G.A. (1987) Molecular cloning of clover yellow mosaic virus RNA: identification of coat protein coding sequences *in vivo* and *in vitro*. *Virology*, **157**, 276-284.

Birnboim, H.C., and Doly, J. (1979) A rapid alkaline extraction procedure for screening recombinant plasmid DNA. *Nucleic Acids Res.* **7**, 1513.

Blumenthal, T. (1980) Interaction of host-coded and virus-coded polypeptides in RNA phage replication. *Proc. R. Soc. Lond.* **B210**, 321-335.

Bos, L. (1982) Crop losses caused by viruses. *Crop Prot.* **1**, 263-282.

Bradford, M.M. (1976) A rapid and sensitive method for the quantitation of microgram quantities of protein utilizing the principle of protein-dye binding. *Anal. Biochem.* **72**, 248-254.

Bradley, D.W., and Zaitlin, M. (1971) Replication of tobacco mosaic virus II. The *in vitro* synthesis of high molecular weight virus-specific RNAs. *Virology* **45**, 192-199.

Brakke, M.K., Ball, E.M., and Langenberg, W.G. (1988) A non-capsid protein associated with unencapsidated virus RNA in barley infected with barley stripe mosaic virus. *J. Gen. Virol.* **69**, 481-491.

Bujarski, J.J., Hardy, S.F., Miller, W.A., and Hall, T.C. (1982) Use of dodecyl-ß-D-maltoside in the purification and the stabilization of RNA polymerase from brome mosaic virus-infected barley. *Virology* **119**, 465-473.

Bundin, V.S., Vishnyakova, O.A., Zakharyev, V.M., Morozov, S.Yu., Atabekov, J.G., and Skryabin, K.G. (1986) Comparative studies of potexvirus genomes: homology between the primary structures of coat protein genes. *Dokl. Akad. Nau. S.S.S.R* **290**, 728-733.

Chapman, S., Hills, G., Watts, J., and Baulcombe, D. (1992a) Mutational analysis of the coat protein gene of potato virus X: effects on virion morphology and viral pathogenicity. *Virology* **191**, 223-230.

Chapman, S., Kavanagh, T., and Baulcombe, D. (1992b) Potato virus X as a vector for gene expression in plants. *Plant J.* **2**, 549-557.

Citovsky, V., Knorr, D., Schuster, G., and Zambrisky, P. (1990) The P30 movement protein of tobacco mosaic virus is a single-strand nucleic acid binding protein. *Cell* **60**, 637-647.

Citovsky, V., Knorr, D., and Zambryski, P. (1991) Gene I, a potential cell-to-cell movement locus of cauliflower mosaic virus, encodes an RNA-binding protein. *Proc. Natl. Acad. Sci. USA* **88**, 2476-2480.

Citovsky, V., Wong, M.L., Shaw, A.L., Prasad, B.V.V., and Zambrisky, P. (1992) Visualization and characterization of tobacco mosaic virus movement protein binding to single-stranded nucleic acids. *Plant Cell* **4**, 397-411.

Cormack, R.S., and Mackie, G.A. (1992) Structural requirements for the processing of *Escherichia coli* 5S ribosomal RNA by RNase E *in vitro*. *J. Mol. Biol.* **228**, 1078-1090.

Costa, A.S., and Kitajima, E.W. (1972) Cassava common mosaic virus. *CMI/AAB Descriptions of Plant Viruses*, N° 90.

Damirdagh, I.S., and Ross, A.F. (1967) A marked synergistic interaction of potato viruses X and Y in inoculated leaves of tobacco. *Virology* **31**, 296-307.

Davies, C., Hills, G., and Baulcombe, D.C. (1993) Sub-cellular localization of the 25-kDa protein encoded in the triple gene block of potato virus X. *Virology* **197**, 166-175.

Dawson, W.O., Bubrick, P., and Grantham, G.L. (1988) Modifications of the tobacco mosaic virus coat protein gene affecting replication, movement, and symptomathology. *Phytopathol.* **78**, 783-789.

Deom, C.M., Lapidot, M., and Beachy, R.N. (1992) Plant virus movement proteins. *Cell* **69**, 221-224.

Devereux, J., Haeberli, P., and Smithies, O. (1984) A comprehensive set of sequence analysis programs for the VAX. *Nucleic Acids Res.* **12**, 387-395.

Dolja, V.V., Grama, D.P., Morozov, S.Yu., and Atabekov, J.G. (1987) Potato virus X-related single- and double-stranded RNAs. *FEBS Lett.* **214**, 308-312.

Dolja, V.V., Boyko, V.P., Agranovsky, A.A., and Koonin, E.V. (1991) Phylogeny of capsid proteins of rod-shaped and filamentous RNA plant viruses: two families with distinct patterns of sequence and probably structure conservation. *Virology* **184**, 79-86.

Dolja, V.V., Haldeman, R., Robertson, N.L., Dougherty, W.G., and Carrington, J.C. (1994) Distinct functions of capsid protein in assembly and movement of tobacco etch potyvirus in plants. *EMBO J.* **13**, 1482-1491.

Donald, R.G.K., Zhou, H., and Jackson, A.O. (1993) Serological analysis of barley stripe mosaic virus-encoded proteins in infected barley. *Virology* **195**, 659-668.

Dorssers, L., van der Krol, S., van der Meer, J., van Kammen, A., and Zabel, P. (1984) Purification of cowpea mosaic virus RNA replication complex: Identification of a virus-encoded 110,000-dalton polypeptide responsible for RNA chain elongation. *Proc. Natl. Acad. Sci. USA* **81**, 1951-1955.

Dreher, T.W., Rao, A.L.N., and Hall, T.C. (1989) Replication *in vivo* of mutant brome mosaic virus RNAs defective in aminoacylation. *J. Mol. Biol.* **206**, 425-438.

Dunn, S.D. (1986) Effects of the modification of transfer buffer composition and the renaturation of proteins in gels on the recognition of proteins on Western blots by monoclonal antibodies. *Anal. Biochem.* **157**, 144-153.

Elhassani, I., Gao, J.-G., and Nassuth, A. (1994) The expression and distribution of wheat streak mosaic virus coat protein during the infection process. Abstract P1-22. 13th annual meeting of the American Society for Virology, Madison, WI.

Erickson, J.W., and Bancroft, J.B. (1978) The self-assembly of papaya mosaic virus. *Virology* **90**, 36-46.

Esau, K., and Hoefert, L.L. (1971) Cytology of beet yellows virus infection in *Tetragonia*. I. Parenchyma cells in infected leaf. *Protoplasma* **72**, 255-273.

Fichot, O., and Girard, M. (1990) An improved method for sequencing of RNA templates. *Nucleic Acids Res.* **18**, 6162.

Forster, R.L.S., Bevan, M.W., Harbison, S.-A., and Gardner, R.C. (1988) The complete nucleotide sequence of the potexvirus white clover mosaic virus. *Nucleic Acids Res.* **16**, 291-303.

Forster, R.L.S., Beck, D.L., Guilford, P.J., Voot, D.M., van Dolleweerd, C.J., and Andersen, M.T. (1992) The coat protein of white clover mosaic potexvirus has a role in facilitating cell-to-cell transport in plants. *Virology* **191**, 480-484.

Forster, R.L.S., Beck, D.L., and Voot, D.M. (1993) The triple gene block proteins of white clover mosaic potexvirus are expressed *in vitro* from a single RNA transcript. Abstract P61-11, IXth International Congress of Virology, Glasgow, Scotland.

Foster, G.D. (1992) The structure and expression of the genome of carlaviruses. *Res. Virol.* **143**, 103-112.

Franssen, H., Leunissen, J., Goldbach, R., Lomonossoff, G., and Zimmern, D. (1984) Homologous sequences in non-structural proteins from cowpea mosaic virus and picornaviruses. *EMBO J.* **3**, 855-861.

French, R., and Ahlquist, P. (1987) Intercistronic as well as terminal sequences are required for efficient amplification of brome mosaic virus RNA3. *J. Virol.* **61**, 1457-1465.

French, R., and Ahlquist, P. (1988) Characterization and engineering of sequences controlling *in vivo* synthesis of brome mosaic virus subgenomic RNA. *J. Virol.* **62**, 2411-2420.

Garnier, M., Mamoun, R., and Bové, J.M. (1980) TYMV RNA replication *in vivo*: replication intermediate is mainly single-stranded. *Virology* **104**, 357-374.

Garnier, M., Candresse, T., and Bové, J.M. (1986) Immunocytochemical localization of TYMV-coded structural and non-structural proteins by the protein A-gold technique. *Virology* **151**, 100-109.

Gibbs, A. (1976) Viruses and plasmodesmata. In *Intercellular communication in plants: studies on plasmodesmata*, Gunning, B.E.S. and Robards, A.W. eds, Springer Verlag, Berlin, pp. 149-164.

Gilmer, D., Bouzoubaa, S., Hehn, A., Guilley, H., Richards, K., and Jonard, G. (1992). Efficient cell-to-cell movement of beet necrotic yellow vein virus requires 3' proximal genes located on RNA2. *Virology* **189**, 40-47.

Godefroy-Colburn, T., Gagey, M.-J., Berna, A., and Stussi-Garaud, C. (1986) A non-structural protein of alfalfa mosaic virus in the walls of infected tobacco cells. *J. Gen. Virol.* **67**, 2233-2239.

Goldbach, R.W. (1986) Molecular evolution of plant RNA viruses. *Ann. Rev. Phytopathol.* **24**, 289-310.

Goldbach, R.W. (1990) Genome similarities between positive-strand RNA viruses from plants and animals. In *New aspects of positive-strand RNA viruses*, Brinton, M.A. and Heinz, F.X. eds, American society for microbiology, Washington, pp. 3-11.

Gorbalenya, A.E., Koonin, E.V., Donchenko, A.P., and Blinov, V.M. (1988) A novel superfamily of nucleoside triphosphate-binding motif containing proteins which are probably involved in duplex unwinding in DNA and RNA replication and recombination. *FEBS Lett.* **235**, 16-24.

Gorbalenya, A.E., Blinov, V.M., Donchenko, A.P., and Koonin, E.V. (1989) An NTP-binding motif is the most conserved sequence in a highly diverged monophyletic group of proteins involved in positive strand RNA viral replication. *J. Mol. Evol.* **28**, 256-268.

Gorbalenya, A.E., and Koonin, E.V. (1989) Viral proteins containing the purine NTP-binding sequence pattern. *Nucleic Acid Res.* **17**, 8413-8440.

Goth, R.W. (1962) Aphid transmission of white clover mosaic virus. *Phytopathol.* **52**, 1228.

Guilford, P.J., and Forster, R.L.S. (1986) Detection of polyadenylated subgenomic RNAs in leaves infected with the potexvirus daphne virus X. *J. Gen. Virol.* **67**, 83-90.

Guilford, P.J., Beck, D.L., and Forster, R.L.S. (1991) Influence of the poly(A) tail and putative polyadenylation signal on the infectivity of white clover mosaic potexvirus. *Virology* **182**, 61-67.

Habili, N., and Symons, R.H. (1989) Evolutionary relationship between luteoviruses and other RNA plant viruses based on sequence motifs in their putative RNA polymerases and nucleic acid helicases. *Nucleic Acids Res.* **17**, 9543-9555.

Hacker, D.L., Petty, I.T.D., Wei, N., and Morris, T.J. (1992) Turnip crinkle virus genes required for RNA replication and virus movement. *Virology* **186**, 1-8.

Hamilton, W.D.O., and Baulcombe, D.C. (1989) Infectious RNA produced by *in vitro* transcription of a full-length tobacco rattle virus RNA-1 cDNA. *J. Gen. Virol.* **70**, 963-968.

Harrison, B.D., and Robinson, D.J. (1986) Tobraviruses. In *Plant viruses*, Vol. 2, van Regenmortel, M.H.V. and Fraenkel-Conrat, H. eds, Plenum Press, New-York, pp. 339-369.

Haseloff, J., Goelet, P., Zimmern, D., Ahlquist, P., Dasgupta, R., and Kaesberg, P. (1984) Striking similarities in amino acid sequences among non-structural proteins encoded by RNA viruses that have dissimilar genomic organization. *Proc. Natl. Acad. Sci. U.S.A.* **81**, 4358-4362.

Hayes, R.J., and Buck, K.W. (1990) Complete replication of a eukaryotic virus RNA *in vitro* by a purified RNA-dependent RNA polymerase. *Cell* **63**, 363-368.

Hefferon, K.L., Fakhrai, H., and AbouHaidar, M.G. (1994) Initiation of translation of the potato virus X coat protein in transgenic potato plants by internal ribosome binding. Abstract W16-1, 13th annual meeting of the American Society for Virology, Madison, Wisconsin.

Hemenway, C., Weiss, J., O'Connell, K., and Tumer, N. E. (1990) Characterization of infectious transcripts from a potato virus X cDNA clone. *Virology* **175**, 365-371.

Hills, G.J., Plaskitt, K.A., Young, N.D., Dunigan, D.D., Watts, J.W., Wilson, T.M.A., and Zaitlin, M. (1987) Immunogold localization of the intracellular sites of structural and non-structural tobacco mosaic virus proteins. *Virology* **161**, 488-496.

Hodgman, T. C. (1988) A new superfamily of replicative proteins. *Nature* **333**, 22-23.

Holy, S., and AbouHaidar, M.G. (1993) Production of infectious *in vitro* transcripts from a full-lenght clover yellow mosaic virus cDNA clone. *J. Gen. Virol.* **74**, 781-784.

Houwing, C.J., and Jaspars, E.M.J. (1986) Coat protein blocks the *in vitro* transcription of the virion RNAs of alfalfa mosaic virus. *FEBS Lett.* **209**, 284-288.

Huisman, M.J., Linthorst, H.J.M., Bol, J.F., and Cornelissen, B.J.C. (1988) The complete nucleotide sequence of potato virus X and its homologies at the amino acid level with various plus-stranded RNA viruses. *J. Gen. Virol.* **69**, 1789-1798.

Hull, R. (1989) The movement of viruses in plants. *Annu. Rev. Phytopathol.* **27**, 213-240.

Inokuchi, Y., and Hirashima, A. (1987) Interference with viral infection by defective RNA replicase. *J. Virol.* **61**, 3946-3949.

Jackson, A.O., Mitchell, D.M., and Siegel, A. (1971) Replication of tobacco mosaic virus. I. Isolation and characterization of double-stranded forms of ribonucleic acids. *Virology* **45**, 182-191.

Janda, M., and Ahlquist, P. (1993) RNA-dependent replication, transcription, and persistence of brome mosaic virus RNA replicons in *S. cerevisiae*. *Cell* **72**, 961-970.

Jelkmann, W., Martin, R.R., Lesemann, D.-E., Vetten, H.J., and Skelton, F. (1990) A new potexvirus associated with strawberry mild yellow edge disease. *J. Gen. Virol.* **71**, 1251-1258.

Jelkmann, W., Maiss, E., and Martin, R.R. (1992) The nucleotide sequence and genome organization of strawberry mild yellow edge-associated potexvirus. *J. Gen. Virol.* **73**, 475-479.

Joshi, C.P. (1987) Putative polyadenylation signals in nuclear genes of higher plants: a compilation and analysis. *Nucleic Acids Res.* **15**, 9627-9640.

Joshi, R.L., Joshi, V., and Ow, D.W. (1990) BSMV genome-mediated expression of a foreign gene in dicot and monocot plant cells. *EMBO J.* **9**, 2663-2669.

Jupin, I., Richards, K., Jonard, G., Guilley, H., and Pleij, C.W.A. (1990) Mapping sequences required for productive replication of beet necrotic yellow vein virus RNA3. *Virology* **178**, 273-280.

Kamen, R.I. (1975) Structures and function of the Qß replicase. In *RNA phages*, Zinder, N.D. ed., Cold Spring Harbor Laboratory, Cold Spring Harbor, New-York, pp.203-234.

Kamer, G., and Argos, P. (1984) Primary structural comparison of RNA-dependent polymerases from plant, animal and bacterial viruses. *Nucleic Acids Res.* **12**, 7269-7282.

Kao, C.C., Quadt, R., Hershberger, P., and Ahlquist, P. (1992) Brome mosaic virus RNA replication proteins 1a and 2a form a complex *in vitro*. *J. Virol.* **66**, 6322-6329.

Koenig, R. (1972) Anomalous behaviour of the coat proteins of potato virus X and cactus virus X during electrophoresis in dodecyl sulfate-containing polyacrylamide gels. *Virology* **50**, 263-266.

Koenig, R., and Lesemann, D.-E. (1989) Potato virus X. *CMI/AAB Descriptions of Plant Viruses*, N° 354.

Kozak, M. (1989) The scanning model for translation: an update. *J. Cell Biol.* **108**, 229-241.

Laemmli, U.K. (1970) Cleavage of structural proteins during the assembly of the head of bacteriophage T4. *Nature* **227**, 680-685.

Laín, S., Martín, M.T., Riechmann, J.L., and García, J.A. (1991) Novel catalytic activity associated with positive-strand RNA virus infection: nucleic acid-stimulated ATPase activity of the plum pox potyvirus helicaselike protein. *J. Virol.* **65**, 1-6.

Laín, S., Riechman, J.L., and García, J.A. (1990) RNA helicase: a novel activity associated with a protein encoded by a positive strand RNA virus. *Nucleic Acids Res.* **18**, 7003-7006.

Lehto, K., Bubrick, P., and Dawson, W.O. (1990) Time course of TMV 30K protein accumulation in intact leaves. *Virology* **174**, 290-293.

Lesemann, D.-E. (1985) Cytopathology. In *The plant viruses*, Vol. 4., Milne, R.G., ed., Plenum Press, New-York, pp. 179-235.

Lesemann, D.-E., and Koenig, R. (1977) Potexvirus group. In *Atlas of insect and plant viruses*, Maramorosch, K., ed., New-York, Academic Press, pp. 331-339.

Lin, N.-S., and Chen, C.C. (1991) Association of bamboo mosaic virus (BoMV) and BoMV-specific electron-dense crystalline bodies with chloroplasts. *Phytopathol.* **81**, 1551-1555.

Lin, N.-S., Lin, F.-Z., Huang, T.-Y., and Hsu, Y.-H. (1992) Genome properties of bamboo mosaic virus. *Phytopathol.* **82**, 731-734.

Lin, N.-S., Lin, B.Y., Lo, N.W., Hu, C.C., Chow, T.Y., and Hsu, Y.H. (1994) Nucleotide sequence of the gRNA of bamboo mosaic potexvirus. *J. Gen. Virol.* (in press).

Linstead, P.J., Hills, G.J., Plaskitt, K.A., Wilson, I.G., Harker, C.L., and Maule, A.J. (1988) The subcellular location of the gene 1 product of cauliflower mosaic virus is consistent with a function associated with virus spread. *J. Gen. Virol.* **69**, 1809-1818.

Lommel, S.A., Fujiwara, T., Giesman-Cookmeyer, D., Ding, B., and Lucas, W.J. (1994) RCNMV movement protein potentiates its own movement as well as the movement of viral RNA from cell-to-cell. Abstract W12-3, 13th annual meeting of the American Society for Virology, Madison, Wisconsin.

Longstaff, M., Brigneti, G., Boccard, F., Chapman, S., and Baulcombe, D. (1993) Extreme resistance to potato virus X infection in plants expressing a modified component of the putative viral replicase. *EMBO J.* **12**, 379-386.

Lütcke, H.A., Chow, K.C., Mickel, F.S., Moss, K.A., Kern, H.F., and Scheele, G.A. (1987) Selection of AUG initiation codon differs in plants and animals. *EMBO J.* **6**, 43-48.

Mackie, G.A., and Bancroft, J.B. (1986) The longer RNA species in narcissus mosaic virus encodes all viral functions. *Virology* **153**, 215-219.

Mackie, G.A., Johnston, R., and Bancroft, J.B. (1988) Single- and double-stranded viral RNAs in plants infected with the potexviruses papaya mosaic virus and foxtail mosaic virus. *Intervirol.* **29**, 170-177.

Malyshenko, S.I., Kondakova, O.A., Taliansky, M.E., and Atabekov, J.G. (1989) Plant virus transport function: complementation by helper viruses is non-specific. *J. Gen. Virol.* **70**, 2751-2757.

Marsh, L., Dreher, T.W., Hall, T.C. (1988) Mutational analysis of the core and modulator sequences of the brome mosaic virus RNA3 subgenomic RNA promoter. *Nucleic Acids Res.* **16**, 981-995.

Matthews, R.E.F. (1991) *Plant virology*, 3rd edition, Academic press, San Diego, California.

Maule, A.J. (1991) Virus movement in infected plants. *Crit. Rev. Plant Sci.* **9**, 457-473.

McMaster, G.K., and Carmichael, G.G. (1977) Analysis of single- and double-stranded nucleic acids on polyacrylamide and agarose gels by using glyoxal and acridine orange. *Proc. Natl. Acad. Sci. USA* **74**, 4835-4838.

Mead, D.A., Szczesna-Skorupa, E., and Kemper, B. (1986) Single-stranded DNA "blue" T7 promoter plasmids: a versatile tandem promoter system for cloning and protein engineering. *Prot. Eng.* **1**, 67-74.

Melton, D.A., Krieg, P.A., Rebagliati, M.R., Maniatis T., Zinn, K., and Green, M.R. (1984) Efficient *in vitro* synthesis of biologically active RNA and RNA hybridization probe fron. plasmids containing a bacteriophage SP6 promoter. *Nucleic Acids Res.* **12**, 7035-7056.

Memelink, J., van der Vlugt, C.I.M., Linthorst, H.J.M., Derks, A.F.L.M., Asjes, C.J., and Bol, J.F. (1990) Homologies between the genomes of a carlavirus (lily symptomless virus) and a potexvirus (lily virus X) from lily plants. *J. Gen. Virol.* **71**, 917-924.

Miki, T., and Knight, C.A. (1968) The protein subunit of potato virus X. *Virology* **36**, 168-173.

Miller, W.A., Dreher, T.W., and Hall, T.C. (1985) Synthesis of brome mosaic virus subgenomic RNA *in vitro* by internal initiation on (—)-sense genomic RNA. *Nature* **313**, 68-70.

Mirzayan, C., and Wimmer, E. (1994) Biochemical studies on poliovirus polypeptide 2C: evidence for ATPase activity. *Virology* **199**, 176-187.

Morch, M.D., Joshi, R.L., Denial, T.M., and Haenni, A.L. (1987) A new "sense" RNA approach to block viral RNA replication *in vitro*. *Nucleic Acids Res.* **15**, 4123-4130.

Morozov, S.Yu., Gorbulev, V.G., Novikov, V.K., Agranovsky, A.A., Kozlov, Y.V., Atabekov, J.G., and Baeyv, A.A. (1981) The primary structure of the 5'- and 3'-terminal regions of the RNA of potato virus X. *Dokl. Akad. Nau. S.S.S.R.* **259**, 723-725.

Morozov, S.Yu., Lukasheva, L.I., Chernov, B.K., Skryabin, K.G., and Atabekov, J.G. (1987). Nucleotide sequence of the open reading frames adjacent to the coat protein cistron in potato virus X genome. *FEBS Lett.* **213**, 438-442.

Morozov, S.Yu., Dolja, V.V., and Atabekov, J.G. (1989) Probable reassortment of genomic elements among elongated RNA-containing plant viruses. *J. Mol. Evol.* **29**, 52-62.

Morozov, S.Yu., Miroshnichenko, N.A., Zelenina, D.A., Fedorkin, O.N., Solovyev, A.G., Lukasheva, L.I., Atabekov, J.C. (1990) Expression of RNA transcripts of potato virus X full-length and subgenomic cDNAs. *Biochimie* **72**, 677-684.

Morozov, S.Yu., Miroshnichenko, N.A., Solovyev, A.G., Fedorkin, O.N., Zelenina, D.A., Lukasheva, L.I., Karassev, A.V., Dolja, V.V., and Atabekov, J.G. (1991) Expression strategy of the potato virus X triple gene block. *J. Gen. Virol.* **72**, 2039-2042.

Mouchès, C., Bové, C., and Bové, J.M. (1974) Turnip yellow mosaic virus RNA replicase: Partial purification of the enzyme from the solubilized enzyme-template complex. *Virology* **58**, 409-423.

Nassuth, A., and Bol, J.F. (1983) Altered balance of the synthesis of plus- and minus-strand RNAs induced by RNAs 1 and 2 of alfalfa mosaic virus in the absence of RNA3. *Virology* **24**, 75-85.

Neo, K.-K., Wong, S.-M., and Wu, M. (1993) Nucleotide sequence and *in vitro* translation of the coat protein gene of cymbidium mosaic virus. *Virus genes* **7**, 157-170.

Niesbach-Klösgen, U., Guilley, H., Jonard, G., and Richards, K. (1990) Immunodetection *in vivo* of beet necrotic yellow vein virus-encoded proteins. *Virology* **178**, 52-61.

Niesters, H.G.M., and Strauss, J.H. (1990) Mutagenesis of the conserved 51 nucleotide region of sindbis virus. *J. Virol.* **64**, 1639-1647.

Nilsson-Tillgren, T. (1970) Studies on the biosynthesis of TMV. III. Isolation and characterization of the replicative form and replicative intermediate RNAs. *Molec. Gen. Genet.* **109**, 246-256.

Orman, B.E., Celnik, R.M., Mandel, A.M., Torres, H.N., and Mentaberry, A.N. (1990) Complete cDNA sequence of a South American isolate of potato virus X. *Virus Res.* **16**, 293-306.

Osman, T.A.M., Hayes, R.J., and Buck, K.W. (1992) Cooperative binding of the red clover necrotic mosaic virus movement protein to single-stranded nucleic acids. *J. Gen. Virol.* **73**, 223-227.

Ozols, J. (1990) Amino acid analysis. In *Guide to protein purification*, Deutscher, M.P. ed., Academic Press Inc., San Diego, California, pp. 587-601.

Palukaitis, P., and Zaitlin, M. (1986) Tobacco mosaic virus: infectivity and replication. In *Plant viruses*, Vol. 2, van Regenmortel, M.H.V., and Fraenkel-Conrat, H. eds., New-York, Plenum Press, pp. 105-131.

Paulsen, A.Q., and Niblett, C.L. (1977) Purification and properties of foxtail mosaic virus. *Phytopathol.* **67**, 1346-1351.

Petty, I.T.D., and Jackson, A.O. (1990) Mutational analysis of barley stripe mosaic virus RNA ß. *Virology* **179**, 712-718.

Pognonec, P., Kato, H., Sumimoto, H., Kretzschmar, M., and Roeder, R.G. (1991) A quick procedure for purification of functional recombinant proteins over-expressed in *E. coli*. *Nucleic Acids Res.* **19**, 6650.

Pogue, G.P., Marsh, L.E., and Hall,, T.C. (1990) Point mutations in the ICR2 motif of brome mosaic virus RNAs debilitate (+)-strand replication. *Virology* **178**, 152-160.

Pogue, G.P., and Hall, T.C. (1992) The requirement for a 5' stem-loop structure in brome mosaic virus replication supports a new model for viral positive-strand RNA initiation. *J. Virol.* **66**, 674-684.

Poirson, A., Turner, A.P., Giovane, C., Berna, A., Roberts, K., and Godefroy-Colburn, T. (1993) Effect of the alfalfa mosaic virus movement protein expressed in transgenic plants on the permeability of the plasmodesmata. *J. Gen. Virol.* **74**, 2459-2461.

Price, M. (1992) Examination of potato virus proteins synthesized in infected tobacco plants. *J. Virol.* **66**, 5658-5661.

Prody, G.A., and Jackson, A.O. (1993) Movement of barley stripe mosaic virus in a non-host plant is potentiated by potato virus X. Abstract P63-8, IXth International Congress of Virology, Glasgow, Scotland.

Quadt, R., and Jaspars, E.M.J. (1989) RNA polymerases of plus-strand RNA viruses of plants. *Mol. Plant-Microbe Interact.* **2**, 219-223.

Quadt, R., and Jaspars, E.M.J. (1990) Purification and characterization of brome mosaic virus RNA-dependent RNA polymerase. *Virology* **178**, 189-194.

Quadt, R., Rosdorff, H.J.M., Hunt, T.W., and Jaspars, E.M.J. (1991) Analysis of the protein composition of alfalfa mosaic virus RNA-dependent RNA polymerase. *Virology* **182**, 309-315.

Quadt, R., Kao, C.C., Browning, K.S., Hershberger, P., and Ahlquist, P. (1993) Characterization of a host protein associated with brome mosaic virus RNA-dependent RNA polymerase. *Proc. Natl. Acad. Sci. U.S.A.* **90**, 1498-1502.

Querci, M., van der Vlugt, R., Goldbach, R., and Salazar, L.F. (1993) RNA sequence of potato virus X strain HB. *J. Gen. Virol.* **74**, 2251-2255.

Ribas, J.C., and Wickner, R.B. (1992) RNA-dependent RNA polymerase consensus sequence of the L-A double-stranded RNA virus: definition of essential domains. *Proc. Natl. Acad. Sci. U.S.A.* **89**, 2185-2189.

Richardson, J.F., Tollin, P., and Bancroft, J.B. (1981) The architecture of the potexviruses. *Virology* **112**, 34-39.

Robards, A.W., and Lucas, W.J. (1990) Plasmodesmata. *Annu. Rev. Plant Physiol. Plant Mol. Biol.* **41**, 369-419.

Rodriguez, P.L., and Carrasco, L. (1993) Poliovirus protein 2C has ATPase and GTPase activities. *J. Biol. Chem.* **268**, 8105-8110.

Rohozinski, J., Francki, R.I.B., and Chu, P.W.G. (1986) The *in vitro* synthesis of velvet tobacco mottle virus-specific double-stranded RNA by a soluble fraction in extracts from infected *Nicotiana clevelandii* leaves. *Virology* **155**, 27-38.

Rouleau, M., Bancroft, J.B., and Mackie, G.A. (1993) Partial purification and characterization of foxtail mosaic potexvirus RNA-dependent RNA polymerase. *Virology* **197**, 695-703.

Rouleau, M., Bancroft, J.B., and Mackie, G.A. (1994) Purification, properties, and subcellular localization of foxtail mosaic potexvirus 26-kDa protein. *Virology* **204**, in press.

Rozanov, M.N., Koonin, E.V., and Gorbalenya, A.E. (1992) Conservation of the putative methyltransferase domain: a hallmark of the "sindbis-like" supergroup of positive-strand RNA viruses. *J. Gen. Virol.* **73**, 2129-2134.

Saito, T., Yamanaka, K., and Okada, Y. (1990) Long-distance movement and viral assembly of tobacco mosaic virus mutants. *Virology* **176**, 329-336.

Sambrook, J., Fritsch, E.F., and Maniatis, T. (1989) *Molecular cloning: A laboratory manual.* 2nd ed. Cold Spring Harbor Laboratory Press, Cold Spring Harbor, New York.

Sanger, F., Nicklen, S., and Coulson, A.R. (1977) DNA sequencing with chain-terminating inhibitors. *Proc. Natl. Acad. Sci. U.S.A.* **74**, 5463-5467.

Schlegel, D.E., and Delisle, D.E. (1971) Viral protein in early stages of clover yellow mosaic virus infection of *Vicia faba*. *Virology* **45**, 747-754.

Scholthof, H.B., Morris, T.J., and Jackson, A.O. (1993) The capsid protein gene of tomato bushy stunt virus is dispensable for systemic movement and can be replaced for localized expression of foreign genes. *Mol. Plant-Microbe Interac.* **6**, 309-322.

Schoumacher, F., Erny, C., Berna, A., Godefroy-Colburn, T., and Stussi-Garaud, C. (1992) Nucleic acid-binding properties of the alfalfa mosaic virus movement protein produced in yeast. *Virology* **188**, 896-899.

Shalla, T.A., and Shepard, J.F. (1972) The structure and antigenic analysis of amorphous inclusion bodies induced by potato virus X. *Virology* **49**, 654-667.

Shanks, M., Tomenius, K., Clapham, D., Huskison, N., Barker, P., Wilson, I.G., Maule, A.J., and Lomonossoff, G.P. (1989) Identification and subcellular localisation of a putative cell-to-cell transport protein from red clover mottle virus. *Virology* **173**, 400-407.

Short, M.N. (1983) Foxtail mosaic virus. *C.M.I./A.A.B. Descriptions of Plant Viruses*, N°. 264.

Short, M.N., and Davies, J.W. (1983) Narcissus mosaic virus: a potexvirus with an encapsidated subgenomic messenger RNA for coat protein. *BioSci. Rep.* **3**, 837-846.

Short, M.N., and Davies, J.W. (1987) Host ranges, symptoms and amino acid compositions of eight potexviruses. *Ann. Appl. Biol.* **110**, 213-219.

Simon Moffat, A. (1992) Putting the moves on plant viruses. *Science* **255**, 291.

Sit, T.L., White, K.A., Holy, S., Padmanabhan, U., Eweida, M., Hiebert, M., Mackie, G.A., and AbouHaidar, M.G. (1990) Complete nucleotide sequence of clover yellow mosaic virus RNA. *J. Gen. Virol.* **71**, 1913-1920.

Sit, T.L., AbouHaidar, M.G., and Holy, S. (1989) Nucleotide sequence of papaya mosaic virus RNA. *J. Gen. Virol.* **70**, 2325-2331.

Sit, T.L., and AbouHaidar, M.G. (1993) Infectious RNA transcripts derived from cloned cDNAs of papaya mosaic virus: effect of mutations to the capsid and polymerase proteins. *J. Gen. Virol.* **74**, 1133-1140.

Sit, T.L., Leclerc, D., and AbouHaidar, M.G. (1994) The minimal 5' sequence requirement for *in vitro* initiation of papaya mosaic potexvirus assembly. *Virology* **199**, 238-242.

Skryabin, K.G., Kraev, A.S., Morozov, S.Yu., Rosanov, M.N., Chernov, B.K., Lukasheva, L.I., and Atabekov, J.G. (1988a) The nucleotide sequence of potato virus X RNA. *Nucleic Acids Res.* **16**, 10929-10930.

Skryabin, K.G., Morozov, S. Yu., Kraev, A.S., Rozanov, M.N., Chernov, B.K., Lukasheva, L.I., and Atabekov, J.G. (1988b) Conserved and variable elements in RNA genomes of potexviruses. *FEBS Lett.* **240**, 33-40.

Smirnyagina, E.V., Morozov, S.Yu., Rodionova, N.P., Miroshnichenko, N.A., Solovyev, A.G., Fedorkin, O.N., and Atabekov, J.G. (1991) Translational efficiency and competitive ability of mRNAs with 5'-untranslated αß-leader of potato virus X RNA. *Biochimie* **73**, 587-598.

Solovyev, A.G., Novikov, V.K., Merits, A., Savenkov, E.I., Zelenina, D.A., Tyulkina, L.G., and Morozov, S.Yu. (1994) Genome characterization and taxonomy of *Plantago asiatica* mosaic potexvirus. *J. Gen. Virol.* **75**, 259-267.

Sonenberg, N., Shatkin, A.J., Riccardi, R.P., Rubin, M., and Goodman, R.M. (1978) Analysis of terminal structures of RNA from potato virus X. *Nucleic Acids Res.* **5**, 2501-2521.

Stone, O.M. (1980) Two new potexviruses from monocotyledons. *Acta Horticul.* **110**, 59-63.

Studier, F.W., Rosenberg, A.H., Dunn, J.J., and Dubendorff, J.W. (1990) Use of T7 RNA polymerase to direct expression of cloned genes. *Meth. Enzymol.* **185**, 60-89.

Stussi-Garaud, C., Garaud, J.C., Berna, A., and Godefroy-Colburn, T. (1987) *In situ* localization of an alfalfa mosaic virus non-structural protein in plant cell walls: correlation with virus transport. *J. Gen. Virol.* **68**, 1779-1784.

Tamura, J.K., Warrener, P., and Collett, M.S. (1993) RNA-stimulated NTPase activity associated with the p80 protein of the pestivirus bovine viral diarrhea virus. *Virology* **193**, 1-10.

Terry, B.R., and Robards, A.W. (1987) Hydrodynamic radius alone governs the mobility of molecules through plasmodesmata. *Planta* **171**, 145-157.

Tomenius, K., Clapham, D., and Meshi, T. (1987) Localization by immunogold cytochemistry of the virus-coded 30K protein in plasmodesmata of leaves infected with tobacco mosaic virus. *Virology* **160**, 363-371.

Tozzini, A.C., Ek, B., Palva, E.T., and Hopp, H.E. (1994) Potato virus X coat protein: a glycoprotein. *Virology* **202**, 651-658.

Traynor, P., Young, B.M., and Ahlquist, P. (1991) Deletion analysis of brome mosaic virus RNA 2a protein: effects on RNA replication and systemic spread. *J. Virol.* **65**, 2807-2815.

Tumer, N., Lodge, J., and Kaniewski, W. (1993) Broad spectrum virus resistance in transgenic plants expression pokeweed antiviral protein. Abstract W65-3, IXth International Congress of Virology, Glasgow, Scotland.

van der Kuyl, A.C., Neeleman, L., and Bol, J.F. (1991) Deletion analysis of cis- and trans-acting elements involved in replication of alfalfa mosaic virus RNA3 *in vivo*. *Virology* **183**, 687-694.

van der Vossen, E.A.G., Neeleman, L., and Bol, J.F. (1994) Early and late functions of alfalfa mosaic virus coat protein can be mutated separately. *Virology* **202**, 891-903.

van Lent, J., Wellink, J., and Goldbach, R. (1990) Evidence for the involvement of the 58K and 48K proteins in the inter-cellular movement of cowpea mosaic virus. *J. Gen. Virol.* **71**, 219-223.

van Vloten-Doting, L., Francki, R.I.N., Fulton, R.W., Kaper, J.M., and Lane, L.C. (1981) Tricornaviridae - a proposed family of plant viruses with tripartite, single-stranded RNA genomes. *Intervirology* **15**, 198-203.

Warrener, P., Tamura, J.K., and Collett, M.S. (1993) RNA-stimulated NTPase activity associated with yellow fever virus NS3 protein expressed in bacteria. *J. Virol.* **67**, 989-996.

Watanabe, Y., Emori, Y., Ooshika, I., Meshi, T., Ohno, T., and Okada, Y. (1984) Synthesis of TMV specific RNAs and proteins at the early stage of infection in tobacco protoplasts: transient expression of the 30K protein and its mRNA. *Virology* **133**, 18-24.

Weiland, J.J., and Dreher, T.W. (1989) Infectious TYMV RNA from cloned cDNA: effects *in vitro* and *in vivo* of point substitutions in the initiation codons of two extensively overlapping ORFs. *Nucleic Acids Res.* **17**, 4675-4687.

Weintraub, M., Ragetli, H.W.J., and Lo, E. (1974) Potato virus Y particles in plasmodesmata of tobacco leaf cells. *J. Ultrastr. Res.* **46**, 131-148.

Wengler, G., and Wengler, G. (1991) The carboxy-terminal part of the NS 3 protein of the West Nile flavivirus can be isolated as a soluble protein after proteolytic cleavage and represents an RNA-stimulated NTPase. *Virology* **184**, 707-715.

White, K.A., and Mackie, G.A. (1990) Control and expression of 3' open reading frames in clover yellow mosaic virus. *Virology* **179**, 576-584.

White, K.A., Bancroft, J.B., and Mackie, G.A. (1991) Defective RNAs of clover yellow mosaic virus encode non-structural/coat protein fusion products. *Virology* **183**, 479-486.

White, K.A. (1992) Genome organization, replication and defective RNAs of clover yellow mosaic virus. Ph.D. thesis, University of Western Ontario, Ontario, Canada.

White, K.A., Bancroft, J.B., and Mackie, G.A. (1992a) Coding capacity determines *in vivo* accumulation of a defective RNA of clover yellow mosaic virus. *J. Virol.* **66**, 3069-3076.

White, K.A., Bancroft, J.B., and Mackie, G.A. (1992b) Mutagenesis of a hexanucleotide sequence conserved in potexvirus RNAs. *Virology* **189**, 817-820.

Wickens, M. (1990) How the message got its tail: addition of poly(A) in the nucleus. *Trends Biochem. Sci.* **15**, 277-281.

Wieczorek, A., and Sanfaçon, H. (1993) Characterization and subcellular localization of tomato ringspot nepovirus putative movement protein. *Virology* **194**, 734-742.

Wilson, T.M.A. (1985) Nucleocapsid disassembly and early gene expression by positive-strand RNA viruses. *J. Gen. Virol.* **66**, 1201-1207.

Wilson, T.M.A., and Shaw, J.G. (1987) Cotranslational disassembly of filamentous plant virus nucleocapsid *in vitro* and *in vivo*. In *Positive strand RNA viruses*, UCLA Symposia on Molecular and Cellular Biology New Series, Vol. 54, Brinton, M.A. and Rueckert, R.R. eds., Alan R. Liss, New-York, pp. 159-181.

Wilson, T.M.A. (1993) Strategies to protect crop plants against viruses: Pathogen-derived resistance blossoms. *Proc. Natl. Acad. Sci. U.S.A.* **90**, 3134-3141.

Wolf, S., Deom, C.M., Beachy, R.N., and Lucas, W.J. (1989) Movement protein of tobacco mosaic virus modifies plasmodesmatal size exclusion limit. *Science* **246**, 377-379.

Xiong, Z., Kim, K.H., Giesman-Cookmeyer, D., and Lommel, S.A. (1993) The roles of the red clover necrotic mosaic virus capsid and cell-to-cell movement proteins in systemic infection. *Virology* **192**, 27-32.

Young, N.D., and Zaitlin, M. (1986) An analysis of tobacco mosaic virus replicative structures synthesized *in vitro*. *Plant Mol. Biol.* **6**, 455-465.

Zaitlin, M., and Hull, R. (1987) Plant virus-host interactions. *Annu. Rev. Plant Physiol.* **38**, 291-315.

Zuidema, D., Linthorst, H.J.M., Huisman, M.J., Asjes, C.J., and Bol, J.F. (1989) Nucleotide sequence of narcissus mosaic virus RNA. *J. Gen. Virol.* **70**, 267-276.

APPENDICES

Appendix I. Synthetic oligonucleotides used in this study.

Oligo-nucleotide	Sequence	coordinates[1]	
GM40	5' ACTGCCTCGATAGACATAGTG	76-96	(—)
MR2[2]	5' CGCGAATTCTAATACGACTCACTA-TAGAAAACTCTTCCGAAACCGAAACTG	1-25	(+)
MR8	5' TGAAGGGACTCCATTCT	633-649	(—)
MR413	5' ATCACTGAGGTGCCTCGATGA	5999-6019	(—)
MR418	5' ATAAGCGATGTGTGCATTCA	6132-6151	(—)
FMV1-1[3]	5' CGCGGATCCAGGAGGTTGAGATCA-tGCTTGACGAGGAAG	1511-1533	(+)
FMV1-2[3]	5' GAGGGATCCAGCCTCAATcTAGCCCCTG	2102-2120	(—)
FMV2-1[4]	5' CGCGGATCCAGGAGGTAATAACAA-TGGATAGTGAAAT	4125-4145	(+)
FMV2-2	5' CTGAGGATCCCTTTCGTGTTGTCAGGCGGAG	4863-4833	(—)

[1] Coordinates on the FMV genomic sequence. The oligonucleotides are either of sequence identical (+) or complementary (—) to the FMV sequence.

[2] The first 26 nucleotides do not correspond to FMV sequences.

[3] The lower case nucleotide indicates a mismatch with the FMV sequence.

[4] The first 16 nucleotides do not correspond to FMV sequences.

Appendix II. Local lesions on *C. quinoa* leaves infected with FMV.

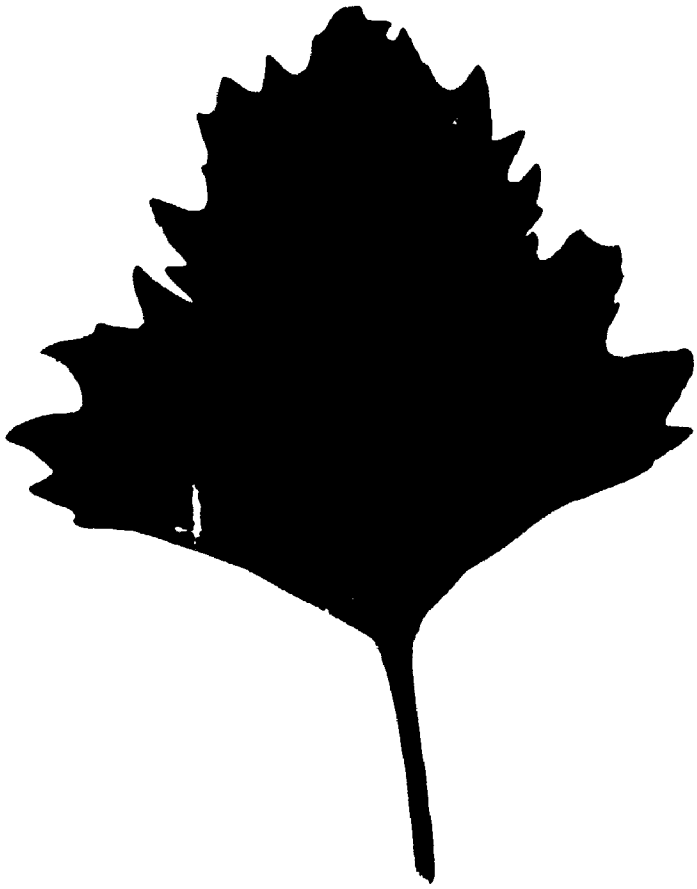

Appendix III. Purification of FMV RdRp from infected tissues: flow chart.